Central Events Precipitating Shock Following Severe Blood Loss

Daniel James Vagg

A thesis submitted to the University of Sydney in fulfilment of the requirements for the degree
Doctor of Philosophy

-Declaration-

The work presented in this thesis was undertaken in the Department of Anatomy and Histology, University of Sydney. To the best of my knowledge it contains no material previously published or written by another person except where due reference is made in the text.

Part(s) of the work included in this thesis have been published as a journal article. This publication is presented in the Appendix at the end of the thesis.

Daniel J. Vagg

July 2008

-Ethical Considerations-

All experiments conducted as part of this thesis conformed with the NHMRC/CSIRO/AAA "Code of Practice for the Care and Use of Animals in Research in Australia."

-Acknowledgements-

I would like to thank Associate Professor Kevin Keay for his tremendous guidance, encouragement, support and understanding over the many years I have spent working with him. Each day brought a new set of challenges, discussions and experiences that I doubt I would have ever had the opportunity to experience elsewhere. I have enjoyed every moment of the journey and look forward to continuing our friendship over the years to come.

I would like to thank Professor Richard Bandler for his continued enthusiasm and input into my work. I hope he is enjoying a relaxing retirement on the country property.

Thank you also to my laboratory colleagues who have each contributed enormously to my time in the laboratory. Especially Luke Henderson, Brendan Troy, Alison Bembrick and Karmina Sosa who have been a continual presence during my time in the lab, making each day an enjoyable one.

Finally, thank you to Eszter for your endless support and encouragement. It was amazing to know that no matter how difficult a day it has been I could soon expect to smile once we were together.

-Summary-

In humans and conscious animals progressive blood loss triggers a biphasic haemodynamic response. Initially, during moderate blood loss (up to 15% total blood volume), arterial pressure (AP) is maintained within a normal physiological range by a selective increase in sympathetic vasomotor tone in specific vascular beds (sympatho-excitation). This initial phase has been termed *compensation*. As blood loss progresses and becomes severe (i.e., loss of 30% total blood volume), a second *decompensatory* phase is triggered. Decompensation is characterised by a profound, life-threatening fall in AP driven by a rapid onset, centrally-mediated sympathoinhibition. Surprisingly, the neural circuitry underlying decompensation is yet to be identified.

The aim of the research described in this thesis was to identify the central afferent and efferent pathway(s) responsible for triggering decompensation. The ventrolateral column of the midbrain periaqueductal gray has recently been recognised as being a neural structure that integrates both the behavioural and cardiovascular components of the response to injury. Past findings have shown that the ventrolateral column of the PAG co-ordinates quiescence, hyporeactivity, hypotension and bradycardia in response to deep pain and haemorrhage, in addition to other inescapable stressors. This response has been classified as a *passive coping* strategy to injury and is an adaptive response essential for the survival of the individual. In addition, it has also been shown that: (i) hypotensive haemorrhage selectively evokes Fos-expression in the ventrolateral PAG; and (ii) haemorrhage-evoked decompensation is significantly attenuated following bilateral microinjection of the local anaesthetic lignocaine or cobalt chloride (an inhibitor of

synaptic transmission). Taken together, these data strongly suggest that the ventrolateral PAG mediates the decompensatory phase of haemorrhage. This region was therefore used as an entry point to begin to define the central circuits which mediate decompensation.

In an initial series of functional-anatomical experiments utilising immunohistochemistry for the protein product of the immediate early gene *c-fos*, it was revealed that a discrete midbrain region, the ventrolateral periaqueductal gray (vlPAG) contains a population of neurons which are selectively activated by severe blood loss. A second series of experiments combined retrograde tracing with immediate early gene expression to show that these neurons project to the caudal midline medulla (CMM), a medullary cardiovascular region whose integrity is critical for the expression of blood loss-evoked sympathoinhibition.

Further anatomical experiments aiming to identify the source of afferent drive onto the vlPAG showed that the vlPAG receives significant input from the A1 noradrenergic cell group. As well, it was revealed that: (i) almost all A1 noradrenergic neurons are activated by severe blood loss; and (ii) intra-vlPAG microinjections of phentolamine, the broad spectrum alpha adrenoreceptor antagonist, delay and attenuate the response to blood loss. These data suggest that ascending noradrenergic drive onto the vlPAG (arising from the A1 cell group) is responsible for triggering decompensation.

Having outlined both the central afferent and efferent pathways which likely mediate decompensation, a final series of experiments were performed to investigate the effect of

blockade of noradrenergic neurotransmission within the ventrolateral PAG under conditions of general (halothane) anaesthesia. Using microinjection of the both broad-spectrum alpha adrenoreceptor antagonist phentolamine it was revealed that blockade of noradrenergic neurotransmission within the ventrolateral PAG under conditions of general (halothane) anaesthesia resulted in a striking delay and attenuation of haemorrhage-evoked hypotension. A similar response was observed following administration of the selective alpha 2 adrenoreceptor antagonist yohimbine *but not* following the selective alpha 1 antagonist prazosin. Taken together, these data further support the hypothesis that decompensation is triggered by noradrenergic neurotransmission within the ventrolateral PAG and provide evidence that alpha 2 adrenoreceptors play a key role in this circuit.

Collectively, these data define a neural circuit which, in the conscious rat, is likely responsible for triggering the centrally-mediated sympathoinhibition and life-threatening hypotension evoked by severe blood loss (i.e., decompensation). In addition, these experiments have significantly advanced modern understanding of the central neural networks involved in cardiovascular regulation and provide a basis upon which future therapeutic strategies may be developed to prevent blood loss-evoked shock and ultimately death, especially under conditions of general anaesthesia.

-Table of Contents-

-Chapter 1-

Literature Review

1.1 Shock

Shock describes a condition in which acute circulatory failure occurs. There are various types of shock, all characterised by a profound hypotension. These include: (i) septic shock; precipitated by the release of endo- or exotoxins from bacteria into the bloodstream; (ii) cardiogenic shock; caused by acute myocardial infarction or chronic heart failure; (iii) anaphylactic shock; caused by an immediate immune-mediated hypersensitivity reaction to an exogenous substance; and (iv) hypovolemic shock; resulting from a reduction in blood volume (haemorrhage).

1.2 Hypovolaemic Shock

The signs of hypovolaemic shock were first described in 1867 by Edwin Morris. From this description, it is clear that acute blood loss not only evokes cardiovascular changes but also triggers changes in sensory and motor function;

a deathlike paleness, followed by sickness and vomiting, and afterwards succeeded by shakes and abundant perspiration, and the whole frame becomes shaken by a universal tremor. The pulse is small, feeble and slow. The patient is perfectly senseless and the respiration scarcely perceptible.

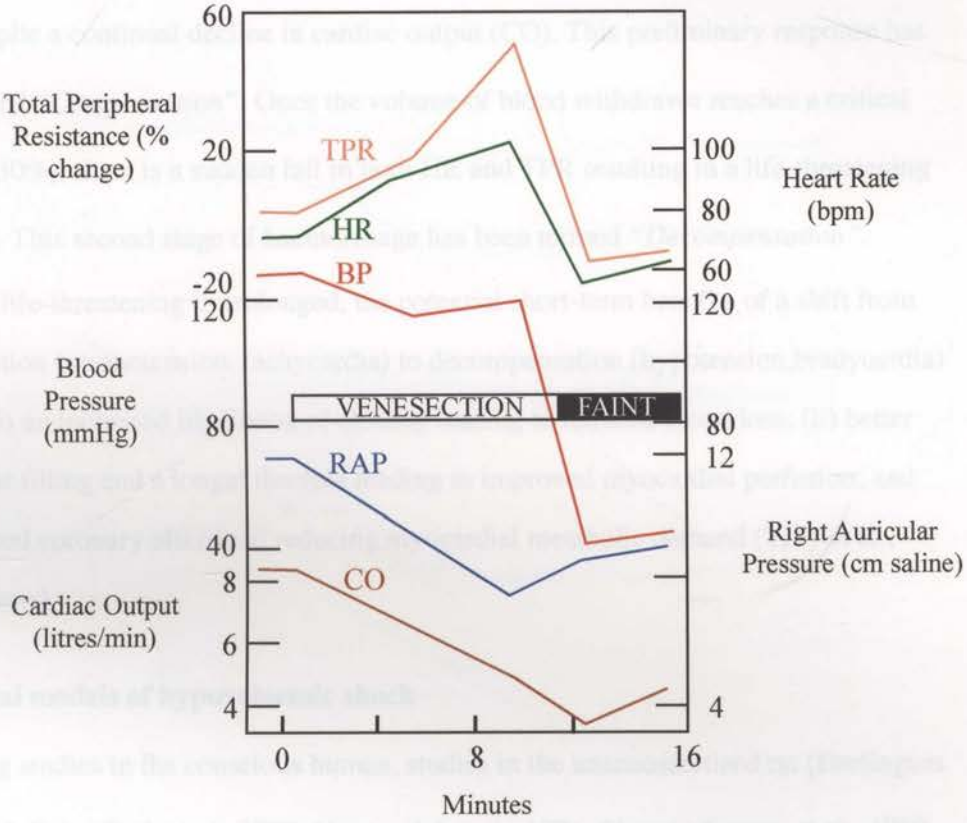

Figure 1.1
The haemodynamic response to blood loss induced by venosection in conscious humans. Initially as blood is withdrawn, increased HR and sympathetic nerve activity (as shown by an increase in TPR) maintain BP at normal levels despite the continual decline in CO. However, as blood loss continues both TPR and HR fall precipitously resulting in a life-threatening hypotension and the subject fainting. *CO, cardiac output; RAP, right auricular pressure; BP, blood pressure; HR, heart rate; TPR, total peripheral resistance.*

The first detailed measurements of the haemodynamic changes associated with hypovolemic shock were made during World War II on conscious human volunteers (Barcroft et al., 1944). These studies revealed that the response to acute blood loss occurs in two distinct phases (Figure 1). Initially as blood is withdrawn, a reflex increase in heart rate (HR) and total peripheral resistance (TPR) maintains arterial pressure (AP) at normal levels despite a continual decline in cardiac output (CO). This preliminary response has been termed *"Compensation"*. Once the volume of blood withdrawn reaches a critical level (15-30%), there is a sudden fall in both HR and TPR resulting in a life-threatening fall in AP. This second stage of haemorrhage has been termed *"Decompensation"*. Although life-threatening if prolonged, the potential short-term benefits of a shift from compensation (normotension, tachycardia) to decompensation (hypotension,bradycardia) include: (i) an increased likelihood of clotting leading to reduced blood loss; (ii) better ventricular filling and a longer diastole leading to improved myocardial perfusion; and (iii) reduced coronary after-load reducing myocardial metabolic demand (Troy et al., under review).

1.3 Animal models of hypovolaemic shock

Paralleling studies in the conscious human, studies in the unanaesthetised rat (Darlington et al., 1986, Fejes-Toth et al., 1988, Haggendal et al., 1986, Skarphedinsson et al., 1989, Troy et al., 2003), rabbit (Chalmers et al., 1967a, Chalmers et al., 1967b, Korner et al., 1990, Ludbrook et al., 1984, Neutze et al., 1968, Schadt et al., 1984, Yamashita et al., 1996), dog (Vatner et al., 1974, Shen et al., 1990, Morita et al., 1985, Hintze et al., 1982) and sheep have revealed a similar biphasic response to haemorrhage. Figure 1.2 shows representative traces of both pulsatile and mean AP, renal nerve activity (RNA) and mean RNA during haemorrhage (5ml/kg per minute) in the unanaesthetised rabbit. Following

Haemodynamic response to haemorrhage in the conscious rabbit

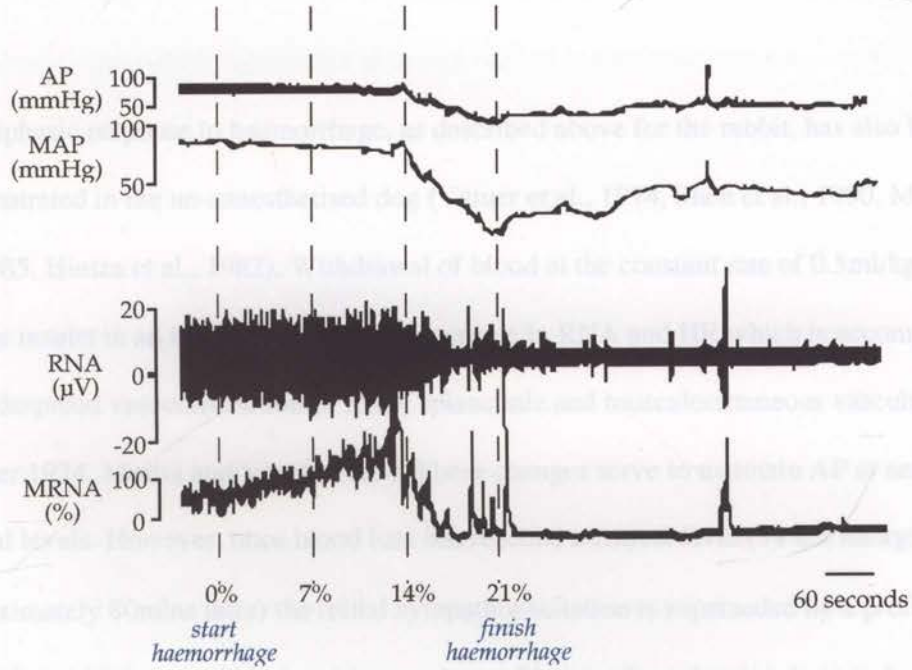

Figure 1.2
A representative trace showing pulsatile arterial pressure, mean arterial pressure, raw renal sympathetic nerve activity and mean renal sympathetic nerve activity during haemorrhage in the conscious rabbit. The percentages given throughout the haemorrhage period indicate the percent of total blood volume that has been removed at that point in time. Initially as blood is withdrawn, arterial pressure is maintained at normal levels (*compensation*) via an increase in sympathetic nerve activity (*sympathoexcitation*). Following removal of approximately 14% total blood volume, arterial pressure falls dramatically (*decompensation*) and a striking decrease in sympathetic nerve activity is observed (*sympathoinhibition*). *AP, arterial pressure; MAP, mean arterial pressure; RNA, renal sympathetic nerve activity; MRNA, mean renal sympathetic nerve activity.* Taken from Yamashita et al., 1996.

the removal of approximately 15% of total blood volume, AP is maintained at normal levels due to an increase in sympathetic nerve activity (sympathoexcitation; as illustrated by the concomitant increase in RNA). However, as blood is continually withdrawn there is a striking fall in RNA to below pre-haemorrhage levels. This decrease in RNA indicates a profound sympathoinhibition, which ultimately results in a precipitous fall in AP.

The biphasic response to haemorrhage, as described above for the rabbit, has also been demonstrated in the un-anaesthetised dog (Vatner et al., 1974, Shen et al., 1990, Morita et al., 1985, Hintze et al., 1982). Withdrawal of blood at the constant rate of 0.5ml/kg per minute results in an initial compensatory increase in RNA and HR which is accompanied by widespread vasoconstriction of renal, splanchnic and musculocutaneous vascular beds (Vatner 1974, Morita and Vatner 1985). These changes serve to maintain AP at near normal levels. However, once blood loss has reached a critical level (39 ± 2 ml/kg; approximately 80mins later) the initial sympathoexcitation is superseded by a profound sympathoinhibition resulting in widespread vasodilation of renal, splanchnic and musculocutaneous vascular beds (Vatner 1974). Consequently, AP is observed to fall precipitously to life-threatening levels (less than 50mmHg).

Interestingly, marked species differences with respect to the timing of the initial sympathoexcitatory phase have been reported in the literature. In contrast to the haemodynamic response observed in conscious dogs and rabbits, early experiments performed in the un-anaesthetised rat suggested that the initial compensatory phase of

haemorrhage (i.e., sympathoexcitation) was markedly reduced (Skoog et al., 1985, Thoren et al., 1988, Victor et al., 1989). When 20% total blood volume is withdrawn from the conscious rat at a rapid rate (over 1-3min), there is an immediate fall in AP, only a slight increase in HR and no increase in plasma norepinephrine spillover concentration suggesting no compensatory response occurs (Haggendal 1986, Darlington et al., 1986, Elam et al., 1985, Mansson et al., 1986, Skarphedinsson et al., 1986, Victor et al., 1989). Furthermore, these data suggest that decompensation in the conscious rat is evoked following removal of a smaller percentage of total blood volume compared to other species (c.f., the dog and rabbit).

However, further experiments aimed at characterising more thoroughly the cardiovascular and hormonal response to haemorrhage in the conscious rat later revealed that a comparable haemodynamic response to haemorrhage is evoked in the rat by altering the rate at which blood is withdrawn. When blood is withdrawn at a relatively slow rate (0.75% total body weight withdrawn over 5min once every half hour for 2hrs), AP is observed to remain at baseline levels due to a compensatory increase in HR and sympathetic nerve activity (Little et al., 1989, Fejes-Toth et al., 1988, Ohnishi et al., 1997). Once, however, a critical volume of blood has been lost there is a profound sympathoinhibition and precipitous fall in AP. Similar haemodynamic changes have been observed more recently by Troy et al., 2003 following removal of 30% total blood volume over a period of 20 minutes. Using this protocol AP and HR are maintained within 10% of baseline values until approximately 20% of total blood volume has been

removed. From this point onwards, AP and HR fall precipitously to a life-threatening level approximately 50% below pre-haemorrhage baseline (Troy et al., 2003).

Consistent with Morris' description of shock in humans, profound alterations in behavioural state following haemorrhage in the conscious rat have been reported. These changes are characterised by reduced exploratory locomotor activity and disengagement from the animals' environmental surroundings (Persson and Svensson 1981).

In summary, the haemodynamic response to haemorrhage in the conscious, un-anaesthetised rat, rabbit and dog is characterised by two successive phases: (i) an initial compensatory phase during which AP is maintained at normal levels via a reflex sympathoexcitation; and (ii) a subsequent decompensatory phase during which AP falls precipitously to life-threatening levels due to a profound sympathoexcitation. Accompanying the haemodynamic changes associated with severe blood loss are striking alterations in the behavioural state of the animal.

1.4 General anaesthesia alters the haemodynamic response to haemorrhage

It has been reported that the haemodynamic response to blood loss is profoundly altered by general anaesthesia. Experiments performed in the anaesthetised rat have demonstrated that when blood is withdrawn there is an immediate reduction in both AP and HR to below pre-haemorrhage levels. However, when blood is withdrawn at the identical rate in the conscious, un-anaesthetised rat no change in either AP or HR is observed (Samar et al., 1979, Seyde et al., 1985).

Underlying the haemodynamic differences observed in anaesthetised animals following hypotensive haemorrhage compared to that seen in the un-anaesthetised animal are marked differences in the degree of sympathetic drive evoked under each experimental preparation. When cardiac output falls at a constant rate of 8.5% per minute in the conscious rabbit, the normal biphasic response to blood loss is observed. That is, there is an initial increase in sympathetic nerve activity and consequent maintenance of AP at normal levels. However, it has been demonstrated in halothane, ketamine and propofol anaesthetised rabbits that the same fall in cardiac output (8.5% per minute) results in markedly reduced levels of renal sympathetic nerve activity to below pre-haemorrhage levels. Consequently, AP is observed to fall precipitously from the onset of blood loss presumably due to vasodilation of peripheral vascular beds (Van Leeuwen et al., 1990, Blake et al., 1995, see also Ruta and Mutch 1989, Warren and Ledingham 1978, Yates and Fentem 1975). Interestingly, a similar monophasic response has been described in halothane-anaesthetised humans subject to lower body negative pressure (Ebert et al., 1985).

In summary: The haemodynamic response to haemorrhage is altered by general anaesthesia. Unlike the biphasic response evoked by blood loss in conscious animals and humans, haemorrhage performed under conditions of anaesthesia evokes a monophasic response characterised by a premature centrally-mediated sympathoinhibition and consequent reduction in AP to below pre-haemorrhage levels. These findings suggest that under conditions of anaesthesia even *moderate* hypovolaemia may lead to shock and ultimately death (Caplan et al., 1988, Vatner 1978) and raise the possibility that

halogenated anaesthetics interact with the central neural circuitry underlying hypovolaemic shock.

1.5 Phase 1: Compensation

Extensive studies among various species have shown that the initial sympathoexcitatory phase of haemorrhage is mediated chiefly by the baroreceptor reflex. Following sinoaortic barodenervation in the conscious dog, rat, rabbit and monkey, AP decreases progressively from the onset of blood loss (Shen et al., 1989, Koyama et al., 1992, Rentero et al., 1997, Cornish et al., 1988, Courneya 1996, Courneya and Korner 1991, Victor et al., 1989, Singh et al., 1991). A similar response has also been observed in the barodenervated rabbit and sheep following inflation of a cuff placed around the inferior vena cava (caval cuff occlusion), a manipulation used to lower AP (by restricting venous return) in a manner similar to that of haemorrhage (Ludbrook et al, 1996, Wood 1989).

1.5.1 Neural Circuitry of the Baroreflex

Three medullary nuclei subserve the baroreflex: (i) the nucleus of the solitary tract (NTS); (ii) a physiologically defined 'vasodepressor' region in the caudal ventrolateral medulla (CVLM); and (iii) the rostral ventrolateral medulla (RVLM), a medullary region that contains tonically active presympathetic neurons. The arterial baroreflex is initiated following distortion of stretch-sensitive receptors located in the carotid sinus and aortic arch. These so-called baroreceptors are innervated by branches of both the glossopharyngeal and vagus nerves (cranial nerves IX and X respectively) (Dampney 1994, Spyer 1994).

In the rat, baroreceptor afferent fibres travel through the ventral aspect of the spinal trigeminal nucleus (SpV) before turning dorsomedially to enter the region of the solitary tract approximately 2mm rostral to the Obex (Calamus Scriptorius). At this level, some axons terminate in the dorsal and medial subnuclei of the NTS while the majority travel ventrally to terminate at the level of Obex in the dorsolateral subnucleus. The remaining baroreceptor axons terminate in the ventrolateral and commissural subnuclei between 0.5mm to 1.0mm caudal to Obex (Ciriello 1983, Chan et al., 2000). At the site of termination, baro-sensitive afferents form excitatory synapses onto second order NTS neurons (Velley et al., 1991, Aicher et al., 1998), which in turn project to the CVLM (Cravo et al., 1991, Dampney 1994, Yu and Gorden 1996). The NTS to CVLM projection is reported to be excitatory, as suggested by data showing that blockade of glutamate receptors in the NTS with kynurenic acid results in abolition of the baroreflex (Guyenet et al., 1987, Kubo et al., 1995, Gatti et al., 1995).

The baro-recipient region of the CVLM is located adjacent to (but independent from) the A1 noradrenergic cell group (Aicher et al., 1995). Cells within this region are considered to be inhibitory interneurons located between baro-sensitive NTS neurons, which serve to excite them, and RVLM presympathetic vasomotor neurons, which they inhibit. Electrophysiological studies support this by showing that CVLM barosensitive neurons can be *antidromically* activated from the RVLM and *orthodromically* activated by baroreceptor stimulation (Jeske et al., 1995). In addition, ultrastructural evidence showing that CVLM neurons form symmetric (*inhibitory*) synapses with RVLM neurons suggests that CVLM neurons inhibit RVLM neurons through the release of GABA, a finding

supported by anatomical studies showing that barosensitive CVLM neurons are GABAergic (Aicher et al., 1995, Jeske et al., 1995, Chan and Sawchenko 1998, Minson et al., 1997, Schreihofer and Guyenet 2003).

Following activation of arterial baroreceptors, the firing rate of RVLM sympathetic premotor neurons is reduced due to the GABAergic projection from the CVLM. This in turn results in withdrawal of tonic excitatory input to sympathetic preganglionic neurons located in the intermediolateral cell column of the spinal cord (IML) (Dampney et al., 1988, Dampney 1994). Early electrophysiological studies suggested that many barosensitive neurons in the RVLM are part of the C1 adrenergic (PNMT containing) cell population (Schreihofer and Guyenet 1997). Selective destruction of C1 neurons following injection of anti-dopamine β-hydroxylase into the RVLM significantly decreases resting AP and attenuates the baroreflex in the conscious rat, although such changes are surprisingly small (Madden and Sved 2003). Furthermore, both anterograde tracing and ultrastructural studies show that RVLM efferents and adrenergic terminals form excitatory synapses with sympathetic preganglionic neurons in the IML (Milner et al., 1988, Morrison et al., 1991, Oshima et al., 2006). Taken together, these data indicate that *adrenergic* RVLM neurons are critical for the maintenance of both resting AP and baroreceptor-induced sympathoexcitation. It is worthy of note, however, that given such a small change in AP is noted following destruction of C1 neurons, it may be that non-C1 medullospinal neurons also play an important role in the maintenance of resting AP.

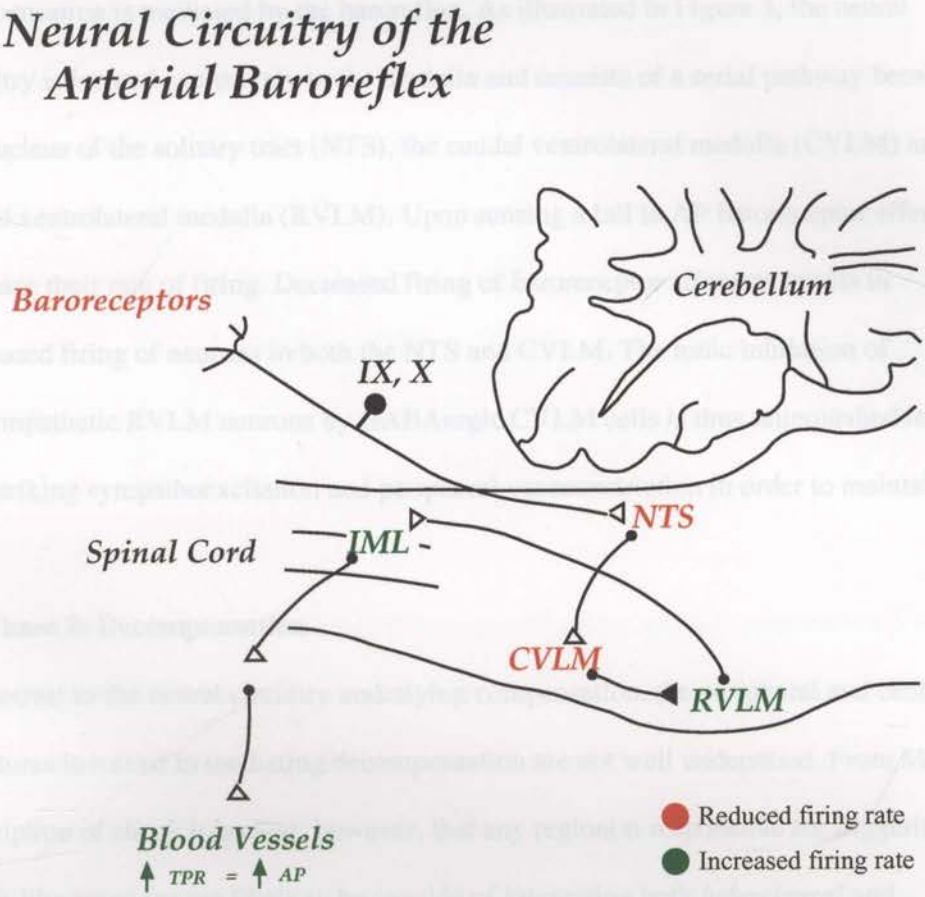

Figure 1.3
Schematic diagram illustrating the neural circuitry of the arterial baroreflex. An acute reduction in blood volume triggers a decrease in the rate of firing of tonically active baroreceptors located in the carotid sinus and aortic arch. Consequently barosensitive neurons in the NTS which project onto CVLM neurons decrease their rate of firing. This in turn results in disinhbition of RVLM pre-sympathetic neurons which, via an excitatory synapse in the IML, gives rise to an increase in sympathetic nerve activity. Arterial pressure is subsequently maintained at normal physiological levels as a result of increased total peripheral resistance (vasoconstriction). *IX, glossopharangeal nerve; X, vagus nerve; NTS, nucleus of the solitary tract; CVLM, caudal ventrolateral medulla; RVLM, rostral ventrolateral medulla; IML, intermediolateral cell column; TPR, total peripheral resistance; AP, arterial pressure.* (Figure adapted from Dampney 1994)

Summary

Compensation is mediated by the baroreflex. As illustrated in Figure 3, the neural circuitry is located exclusively in the medulla and consists of a serial pathway between the nucleus of the solitary tract (NTS), the caudal ventrolateral medulla (CVLM) and the rostral ventrolateral medulla (RVLM). Upon sensing a fall in AP baroreceptor afferents decrease their rate of firing. Decreased firing of baroreceptor afferents results in decreased firing of neurons in both the NTS and CVLM. The tonic inhibition of presympathetic RVLM neurons by GABAergic CVLM cells is thus relinquished leading to a striking sympathoexcitation and peripheral vasoconstriction in order to maintain AP.

1.6 Phase 2: Decompensation

In contrast to the neural circuitry underlying compensation, the peripheral and central structures involved in mediating decompensation are not well understood. From Morris' description of shock it is clear, however, that any region(s) responsible for triggering shock-like reactions are likely to be capable of integrating both *behavioural* and *physiological* changes.

1.6.1 Evidence that endogenous opiates play a role in triggering decompensation

Early studies aimed at delineating possible neural circuit(s) responsible for triggering decompensation focussed on the role of endogenous opiates. Endogenous opiates have been shown to function in a variety of physiological systems including the cardiovascular system (for recent discussion see Wang et al., 2007). Early experiments performed in the anaesthetised rat showed that intravenous administration of opioids evokes a significant

hypotension and bradycardia (Fennessy and Rattray 1971); a response that closely mirrors that evoked by severe blood loss. Strikingly, intravenous administration of the broad-spectrum opioid receptor antagonist naloxone has been reported to rapidly reverse the hypotension evoked by both hypovolaemic and endotoxic shock (Faden and Holaday 1979, Holaday and Faden 1978). Interestingly, the same dose of naloxone given to normotensive (i.e., unbled) animals had no effect on any element of the cardiovascular system (see also Gordon 1986, Morilak et al., 1990) suggesting that although opioidergic systems are *inactive* under normal circumstances, they likely play a significant role in triggering shock-like reactions.

Further experimental reports extended these early findings made in anaesthetised animals by showing that intravenous naloxone significantly increases AP following blood loss in the un-anaesthetised rabbit, rat and baboon (Schadt and York 1981, Rutter et al., 1986, Morita et al., 1988, Golanov et al., 1983, Faden and Holaday 1979, Feuerstein et al., 1981, Bennett and Gardiner 1982). Moreover, the restorative effect of intravenous naloxone on haemorrhage-evoked hypotension has been shown to occur as a result of increased peripheral vascular resistance (Schadt et al., 1984) making it likely that opioidergic mechanisms interact with the sympathetic nervous system in order to trigger decompensation (Schadt and Gaddis 1985). Further support for this hypothesis arises from data obtained in conscious rabbits showing that the prophylactic administration of naloxone (intravenous bolus given prior to removal of blood) significantly attenuates the fall in renal sympathetic nerve activity, peripheral vascular resistance and arterial

pressure evoked by haemorrhage (Burke and Dorward 1988, Ludbrook and Rutter 1988, Yamashita et al., 1996).

Although the experiments described above clearly indicate that opioidergic mechanisms play a critical role in triggering decompensation, the ability of naloxone to cross the blood brain barrier meant that it was unclear whether the effects of naloxone were mediated via central or peripheral opioid receptors. To clarify the site of drug action and thus further elucidate the role of opioidergic mechanisms in producing shock-like reactions, Yamishita et al., 1996 compared the effect of naloxone to methyl-naloxone (an analogue unable to cross the blood-brain barrier) on the changes in renal nerve activity and AP evoked by hypotensive haemorrhage. By showing that naloxone *but not* methyl-naloxone reversed the decrease in renal nerve activity and AP evoked by severe blood loss it was concluded that the sympathoinhibition and consequent hypotension evoked by severe blood loss is mediated via *central* opioid receptors (Yamashita et al., 1996).

1.6.2 Central δ–opioid receptors play a critical role in triggering decompensation

Consistent with the notion that central opioid receptors play a critical role in triggering decompensation, experiments performed in the un-anaesthetised rat have shown that low dose naloxone (10μg) microinjected into the lateral ventricle following hypotensive haemorrhage produces a large pressor response (Holaday et al., 1981). As well, the minimum fourth ventricular dose of naloxone necessary to prevent haemorrhage-evoked sympathoinhibition is reported to be 90-900 times less than the minimum required intravenous dose (Evans et al., 1989).

Although widely accepted that central opioid receptors are involved in triggering decompensation, the broad-spectrum action of naloxone meant that the receptor subtype(s) involved were poorly characterised. An early indication that the effects of naloxone may be mediated via interaction with δ-opioid receptors arose from the observation that high doses of intravenous naloxone (2-6mg/kg) were necessary to block decompensation. Naloxone is known to be a strong μ-receptor antagonist but only a weak δ-receptor antagonist; therefore, a larger dose was required in order to abolish opioidergic neurotransmission at δ-opioid receptors (Evans et al., 1989, see also D'Amato and Holaday 1984).

Further support for δ-opioid receptor involvement came when it was shown that small doses of the δ-opioid receptor antagonist naltrindole made in the fourth ventricle of conscious rabbits prevented decompensation (Evans et al., 1989, Ludbrook and Ventura 1993). Furthermore, in the same series of experiments the δ-opioid receptor agonist DPDPE was found to counteract the restorative effect of naloxone on AP (Evans et al., 1989). Taken together, these data suggest that central δ-opioid receptors play an integral role in mediating decompensation.

1.6.3 Central neural circuitry underlying decompensation

Despite providing a wealth of functional evidence suggesting that central δ-opioid receptors are a critical part of the neural circuitry which triggers decompensation, the experiments described above provide little anatomical information about possible neural loci responsible for producing a coordinated shock response (i.e., decompensation).

A striking finding arose when Evans and colleagues reported that decompensation as a result of simulated haemorrhage (60% fall in cardiac output evoked by caval cuff occlusion) was abolished following high mesencephalic decerebration in rabbits (Evans et al., 1991). Extending this finding, recent work has shown that decompensation is completely blocked in pre-trigeminal decerebrate rats (transection at the junction of midbrain and pons) but not in pre-collicular decerebrate rats (transection at the junction of midbrain and diencephalon) (Figure 4) (Troy et al., 2003). These data suggest that the integrity of *descending midbrain projections* are critical for triggering the decompensatory phase of severe blood loss.

Recent anatomical reports utilising autoradiographic, immunohistochemical and *in situ* hybridisation techniques have revealed that δ-opioid receptors are extensively located throughout the midbrain. In particular, δ-opioid receptor immunoreactive cells and fibres have been localised primarily within the midbrain periaqueductal gray (PAG) (Brodsky et al., 1995, Kalyuzhny and Wassendorf 1998). Specifically, within the PAG, varicose fibres and cells expressing δ-opioid receptor immunoreactivity are reported to be densely clustered throughout the ventrolateral subregion (Kalyuzhny et al., 1996, Mansour et al., 1995, Mansour et al., 1994). As well, accumulations of δ-opioid receptor immunoreactive varicosities have been found in both ventromedial and dorsolateral subregions of the PAG (Kalyuzhny et al., 1996, Mansour et al., 1995, Mansour et al., 1994, Commons et al., 2001, Commons et al., 2003).

In addition to containing δ-opioid receptor immunoreactive cells and fibres, the PAG is densely innervated by opioidergic neurons (Khachaturian et al., 1985, Martin-Schild et al., 1999) and known to contain relatively high amounts of β–endorphin and met–enkephalin; both of which act as endogenous ligands for δ-opioid receptors (Paterson et al., 1983). Strikingly, recent experiments performed in the un-anaesthetised rat have shown that preproenkephalin mRNA is significantly up-regulated in the periaqueductal gray following severe blood loss (Fan and McIntosh 1993), and that blockade of δ opioid receptors, specifically within the ventrolateral subregion of the PAG, significantly attenuates haemorrhage-evoked hypotension in the conscious rat (Cavun et al., 2001).

In summary, early decerebrate experiments suggested that descending midbrain projections are critical for triggering decompensation. As well, functional evidence shows that central δ-opioid receptors form a critical part of the neural circuitry underlying decompensation. The midbrain periaqueductal gray receives dense opioidergic input and contains numerous cells and varicosities immunoreactive for the δ-opioid receptor. Data showing that severe blood loss up-regulates preproenkephalin mRNA within the PAG makes it likely that the PAG is a pivotal neural locus which triggers decompensation via δ-opioid receptor dependent signalling pathways.

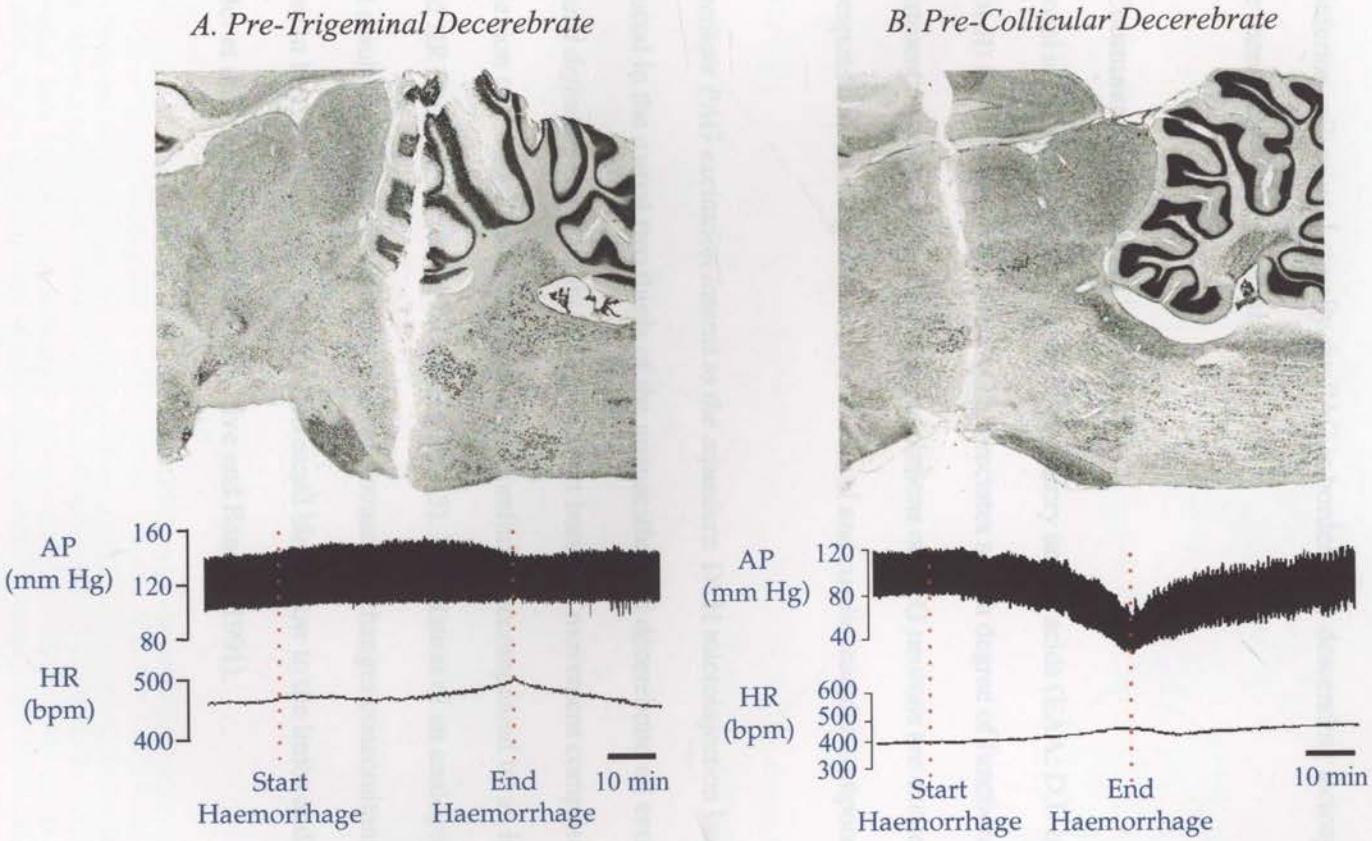

Figure 1.4
(A) Effect of pre-trigeminal decerebration (transection at midbrain-pontine junction) on the haemodynamic response to blood loss. Arterial pressure is maintained at normal levels whille blood is removed at a constant rate during the haemorrhage period. (B). Effect of pre-collicular decerebration (transection at junction of midbrain and diencephalon) on the haemodynamic response to blood loss. In striking contrast to pre-trigeminal decerebration, as blood is withdrawn AP is initially maintained at normal physiological levels (*compensation*). Upon removal of a critical volume of blood, AP precipitously falls to life-threatening levels (*decompensation*).

1.7 The Midbrain Periaqueductal Gray

The periaqueductal gray (PAG) is the cell dense region surrounding the midbrain aqueduct. In the rat, the PAG lies between 5.2 and 8.8mm caudal to Bregma, with the rostral two thirds lying ventral to the superior colliculus and the caudal one third ventral to the inferior colliculus. Laterally the PAG is bordered by descending tectospinal fibres and the mesencephalic trigeminal tract.

1.7.1 Columnar Organisation of the PAG

Functional studies utilising injections of excitatory amino acids (EAA; D,L-homocysteic acid, DLH) have revealed that the PAG appreciates a high degree of functional compartmentalisation. When different populations of PAG neurons are excited one of three responses consisting of both a *behavioural* and *cardiovascular* component occurs.

Intermediate PAG excitation lateral to the aqueduct: DLH microinjection lateral to the aqueductal in the rostral two thirds of the unanaesthetised decerebrate rat evokes *backward defensive* movements including short bursts of movement comprising dorsiflexion of the back and extension of the forelimbs, accompanied by an increase in AP and HR (Depaulis et al., 1992; see Figure 1.5). Stimulation of an analogous region in the cat results in similar behavioural and cardiovascular changes concomitant with an increase in blood flow to the head and decreased blood flow to the limbs and viscera (Bandler et al., 1991, Carrive 1991, Carrive and Bandler 1991).

A. Behavioural Effects:

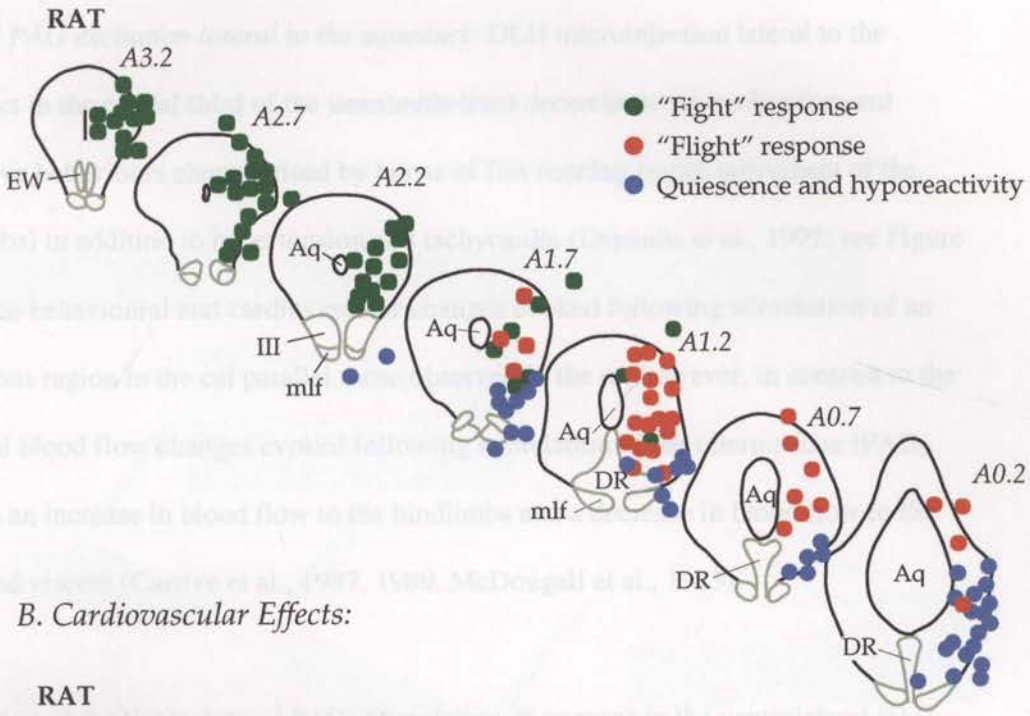

B. Cardiovascular Effects:

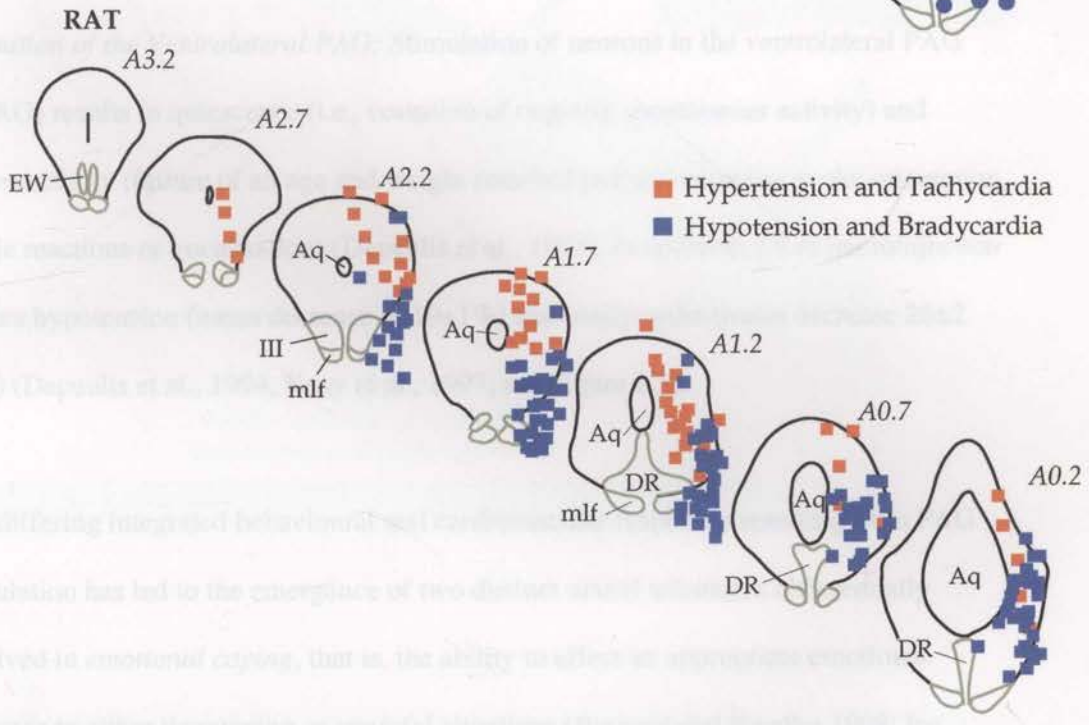

Figure 1.5

(A) A series of 7 representative coronal sections through the midbrain periaqueductal gray matter (PAG) of the rat showing sites at which excitatory amino acid (EAA) microinjections evoke behavioural changes. Note that active defensive behaviour was evoked from the region lateral to the aqueduct (red filled circles) (taken from Bandler et al, 1991), whereas passive behaviour was evoked from the region ventrolateral to the aqueduct (blue filled circles) (taken from Depaulis et al, 1994). (B) An identical series of seven PAG sections indicating sites where EAA microinjections evoke cardiovascular changes. Note that hypertension and tachycardia can be evoked from the region lateral to the aqueduct (red filled squares) (taken from Keay et al, 1990 and Depaulis et al, 1992), whereas hypotension and bradycardia is evoked from the region ventrolateral to the aqueduct (blue filled squares) (taken from Keay et al, 1997). *III; oculomotor nucleus; Aq; cerebral aqueduct; DR; dorsal raphe nucleus; EW; Edinger-Westphal nucleus; mlf, medial longitudinal fasciculus.*

Caudal PAG excitation lateral to the aqueduct: DLH microinjection lateral to the aqueduct in the caudal third of the unanaesthetised decerebrate rat evokes forward defensive behaviours characterised by bursts of fast running (rapid movement of the forelimbs) in addition to hypertension and tachycardia (Depaulis et al., 1992; see Figure 1.5). The behavioural and cardiovascular changes evoked following stimulation of an analogous region in the cat parallel those observed in the rat however, in contrast to the regional blood flow changes evoked following stimulation of the intermediate lPAG, there is an increase in blood flow to the hindlimbs and a decrease in blood flow to the head and viscera (Carrive et al., 1987, 1989, McDougall et al., 1985).

Excitation of the Ventrolateral PAG: Stimulation of neurons in the ventrolateral PAG (vlPAG) results in quiescence (i.e., cessation of ongoing spontaneous activity) and hyporeactivity (failure of an age and weight matched partner animal to evoke orientation, startle reactions or vocalisation) (Depaulis et al., 1994). In addition, DLH microinjection evokes hypotension (mean decrease of 19±1%) and bradycardia (mean decrease 26±2 bpm) (Depaulis et al., 1994, Keay et al., 1997; see Figure 1.5).

The differing integrated behavioural and cardiovascular responses resulting from PAG stimulation has led to the emergence of two distinct neural substrates differentially involved in *emotional coping*, that is, the ability to affect an appropriate emotional response to either threatening or stressful situations (Bernard and Bandler 1998; for summary see Figure 1.6). Lateral PAG excitation evokes *active emotional coping* characterised by environmental engagement (confrontation, fight-flight reactions) and

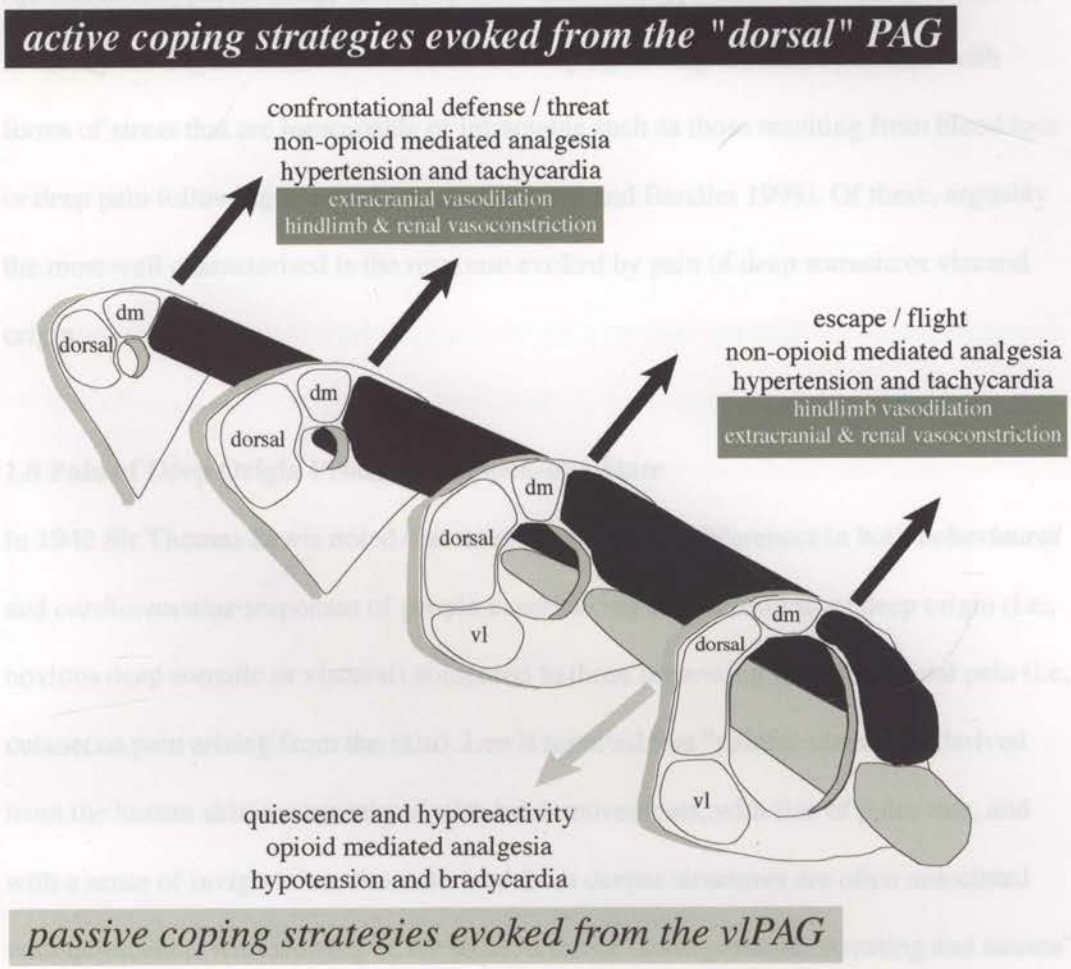

Figure 1.6
Illustration summarising the effects of excitatory amino acid (DLH) stimulation of both lateral and ventrolateral columns of the midbrain periaqueductal gray (PAG). Excitation of neurons in the rostral two thirds of the lateral PAG evokes confrontational defensive behaviour ("fight") and an increase in arterial pressure and heart rate. Excitation of neurons in the caudal third of the lateral PAG evokes forward defensive behaviour ("flight") coupled with an increase in arterial pressure and heart rate. In contrast, excitation of neurons in the ventrolateral PAG results in quiescence and hyporeactivity and a concommitant fall in arterial pressure and heart rate. *dm, dorsomedial column of PAG; dorsal, encompassing both dorsolateral and lateral PAG columns; vl, ventrolateral PAG column (Modified from Figure 1 of Keay and Bandler 2004).*

sympathoexcitation (hypertension, tachycardia, distribution of blood flow to vascular beds with high metabolic demands). In contrast, ventrolateral PAG activation evokes a *passive emotional coping* strategy characterised by environmental withdrawal (quiescence, hyporeactivity) and sympathoinhibition (hypotension and bradycardia; for summary see Figure 1.6). Passive emotional coping strategies function to cope with forms of stress that are inescapable or intractable such as those resulting from blood loss or deep pain following traumatic injury (Bernard and Bandler 1998). Of these, arguably the most well characterised is the response evoked by pain of deep somatic or visceral origin.

1.8 Pain of Deep Origin Produces a Shock-like State

In 1942 Sir Thomas Lewis noted that there were striking differences in both *behavioural* and *cardiovascular* responses of people experiencing pain arising from deep origin (i.e., noxious deep somatic or visceral) compared to those presenting with superficial pain (i.e., cutaneous pain arising from the skin). Lewis reported that "painful sensations derived from the human skin are associated with brisk movements, with rise of pulse rate, and with a sense of invigoration, those derived from deeper structures are often associated with quiescence, with slowing of the pulse, a fall of blood pressure, sweating and nausea" (Lewis 1942).

Lewis' clinical observations are supported by animal studies which demonstrate that both deep somatic (induced by bilateral injection of 5% formalin into the deep dorsal neck muscles) and noxious visceral (intraperitoneal injection of 3.5% acetic acid)

manipulations evoke a significant increase in hyporeactivity and quiescence (Keay et al., 1994). As well, both deep somatic (injection of formalin into gastrocnemius soleus muscle and/or injection of kaolin/carrageenan into knee joint) and noxious visceral (intravenous 5-HT and/or intraperitoneal acetic acid) manipulations evoke a substantial reduction in AP (15-45 mmHg) coupled with a bradycardia (75-100 bpm) (Clement et al., 1996).

Vigorous study throughout the past decade has shown that the midbrain periaqueductal gray contains distinct neuronal populations which mediate the differing responses to pain of deep versus superficial origin. In particular, the ventrolateral column of the periaqueductal gray (vlPAG) has been shown to integrate the *behavioural* and *cardiovascular* changes evoked by deep somatic and visceral pain (for recent review see Keay and Bandler 2005). Briefly, neurons of the vlPAG have been shown to be selectively 'activated' following: (i) noxious muscle stimulation (5% formalin into gastrocnemius soleus muscle); (ii) noxious joint stimulation (4% kaolin injected into knee joint); (iii) noxious cardiopulmonary and peritoneal stimulation (i.v. 5-HT and i.p. 3.5% acetic acid respectively); and (iv) urinary bladder inflammation (Clement et al., 1996, Clement et al., 2000, Keay and Bandler 1993, Rodella et al., 1998). That noxious stimuli known to trigger a passive coping response evokes neural activation within the ventrolateral PAG strongly suggests that the vlPAG forms a critical part of the neural circuitry required to affect a passive coping reaction in response to injury. Moreover, given that the reaction evoked by noxious deep somatic and visceral stimulation is so profoundly similar to decompensation lends additional support to the notion that the

ventrolateral PAG may also integrate the *behavioural* and *cardiovascular* changes evoked by severe blood loss.

1.9 Evidence that the ventrolateral PAG precipitates shock following blood loss

As discussed above, excitation of neurons in the ventrolateral column of the PAG with excitatory amino acids (EAA; DLH) results in cardiovascular (hypotension and bradycardia) and behavioural (quiescence, decreased vigilance, decreased reactivity) responses identical to those characteristic of decompensation. As well, intra-vlPAG microinjection of the δ-opioid receptor agonist DPDPE has been reported to evoke hypotension (mean decrease 17 ± 2.3%) and bradycardia (mean decrease 31 ± 5.5bpm; range 6-72bpm) (Keay et al., 1997).

Experiments utilising expression of the protein product (Fos) of the immediate early gene *c-fos* to identify the patterns (both spatial and temporal) of neuronal activation in response to various experimental manipulations have revealed that there is a selective increase in vlPAG Fos-expression following severe haemorrhage (removal of 25% total blood volume over 10 min) (Keay et al., 2002) in addition to pharmacologically induced hypotension of comparable magnitude (Murphy et al., 1995, Horiuchi et al., 1999, Potts et al., 2000, Li et al., 1994).

Still more powerful evidence to suggest that the vlPAG plays a critical role in the expression of decompensation has arisen from recent physiological experiments performed in the conscious rat and rabbit. Electrophysiological recordings made from

vlPAG neurons have revealed that a discrete population of vlPAG neurons show an abrupt increase in firing rate moments before the onset of haemorrhage-evoked hypotension (Schadt et al., 2006). As well, bilateral inactivation of vlPAG neurons (microinjection of intra-vlPAG lignocaine or the GABA receptor agonist muscimol) has been reported to significantly attenuate the hypotensive phase of severe haemorrhage and to abolish haemorrhage-evoked sympathoinhibition (Cavun and Millington 2001, Dean 2004). Further experiments substituting lignocaine with cobalt chloride, an inhibitor of synaptic transmission, have been shown to produce an even greater inhibitory response (Cavun and Millington 2001). These data strongly suggest that synaptic transmission within the vlPAG is responsible for co-ordinating the shock-like reaction precipitated by severe haemorrhage.

Summary

Stimulation of the ventrolateral column of the midbrain PAG produces a response strikingly similar to the shock-like reaction evoked by deep pain (somatic and/or visceral) and severe haemorrhage. Experimental evidence has shown that vlPAG neurons are "activated" by such events (deep somatic/visceral pain, severe haemorrhage), and that vlPAG inactivation abolishes the decompensatory phase of haemorrhage. These data provide powerful evidence that the integrity of the ventrolateral periaqueductal gray is critical for the expression of shock-like reaction(s) evoked by traumatic injury.

1.10 Output projections of the vlPAG – anatomical substrates for decompensation

To produce a co-ordinated shock-like response, the vlPAG must possess appropriate efferent pathways capable of modulating cardiovascular sympathetic outflow and affecting appropriate behavioural changes. Anterograde tracing studies have demonstrated that the PAG provides no direct input to sympathetic premotor neurons in the intermediolateral cell column (IML) (Mouton and Holstege 1994, Farkas et al., 1998). This suggests that the PAG modulates all sympathetic functions via indirect pathways, presumably involving synaptic relay(s) in medullary sympathetic premotor cell groups. Both anterograde and retrograde tracing studies show that the vlPAG projects to three main cardiovascular regulatory regions in the medulla: (i) the rostral ventrolateral medulla (RVLM) (Van Bockstaele et al., 1991, Keay et al., 2000, Farkas et al., 1998, Chen and Aston-Jones 1995, Chen and Aston Jones 1996, Verberne and Guyenet 1992); (ii) the caudal ventrolateral medulla (CVLM) (Henderson et al., 1998, Henderson et al., 2000, Chen and Aston Jones 1996); and (iii) the caudal midline medulla (CMM) encompassing the nucleus raphe obscurus (RPo) and raphe pallidus (RPa) (Henderson et al., 1998).

Rostral ventrolateral medulla: Neurons in the vlPAG have been shown to project to the sympathoexcitatory region of the RVLM (Carrive et al., 1989, Carrive and Bandler 1991, Van Bockstaele et al., 1991, Keay et al., 2000, Farkas et al., 1998, Chen and Aston-Jones 1995, Chen and Aston Jones 1996, Verberne and Guyenet 1992). Following microinjection of the anterograde tracer phaseolus vulgaris leucoagglutinin (PHA-L) into the vlPAG, labelled fibres and terminals are observed to be intermingled among

adrenergic neurons of the C1 cell group (as revealed by phenylethanolamine N-methyl transferase immunoreactivity) (Chen and Aston Jones 1995). However, given that only a small number of PHA-L varicosities and boutons have been observed in close apposition with catecholaminergic elements, and that only a small number of RVLM-projecting vlPAG neurons are double labelled with pseudorabies virus (PRV) retrogradely transported from the stellate ganglion (Farkas et al., 1998) suggests that only a small proportion of RVLM projecting vlPAG output neurons directly innervate C1 adrenergic cells.

It is well documented that the RVLM contains tonically active pre-sympathetic neurons. For the vlPAG to produce sympathoinhibition via the RVLM, logically it would need to inhibit the ongoing activity of these sympathetic vasomotor neurons. Electrophysiological studies have revealed that electrical stimulation of the vlPAG inhibits both spontaneous and DLH-induced activity of RVLM neurons (Wang and Lovick 1992, Wang and Lovick 1992, Wang and Lovick 1993). This effect has been shown to be reduced following systemic administration of the 5-HT receptor antagonist spiperone (Wang and Lovick 1992), and by direct iontophoretic application of the selective 5-HT_{1A} receptor antagonist WAY-100653 into the pressor region of the RVLM. These findings suggest that vlPAG-evoked sympathoinhibition may be mediated by 5-HT_{1A} receptors in the RVLM (Bago and Dean 2001).

Direct evidence for the involvement of the vlPAG to RVLM pathway in precipitating a shock-like state arose when it was reported that following intramuscular injection of 5%

formalin into the deep dorsal neck muscles, a significant number of "activated" neurons within the caudal vlPAG projected to the RVLM (approximately 25%) (Keay et al., 2000). This result suggests that vlPAG-dependent cardiovascular responses may be mediated (either wholly or in part) via a direct projection from the vlPAG to the RVLM.

Caudal ventrolateral medulla: The CVLM is located in the ventrolateral tegmentum of the medulla extending caudally from the level of Obex to the spinomedullary junction. Intermingled within this region are catecholaminergic neurons (predominantly noradrenergic) comprising the A1 cell group. EAA microinjection into the CVLM of the rat evokes a profound hypotension (mean fall of 29±3%) and bradycardia (mean fall 15±3%) (Henderson et al., 1998, Henderson et al., 2000).

Much attention has been given to the role of the CVLM in modulating acute cardiovascular perturbations (see baroreflex above). However, evidence also exists which suggests the CVLM is involved in producing "behaviourally coupled" responses. Following hypotensive haemorrhage a significant number of CVLM neurons are activated, including many neurons in the A1 catecholaminergic cell group (Dayas et al., 2001, Chan and Sawchenko 1994, Chan and Sawchenko 1998, Buller et al., 1999, Dun et al., 1993). Furthermore, following bilateral inactivation of the CVLM with cobalt chloride, the magnitude of the fall in both AP and HR is significantly attenuated following hypotensive haemorrhage (Henderson et al., 2000). These data suggest that the CVLM is not only involved in regulating acute "homeostatic" cardiovascular functions,

but may also be involved in mediating "behaviourally – coupled" cardiovascular changes (i.e., those associated with stimuli capable of producing a shock-like state).

Caudal midline medulla : Neurons within the caudal midline medulla (CMM) including portions of the raphe obscurus and raphe pallidus nuclei are known to influence sympathetic nerve activity (Larsen et al., 2000, Nakamura et al., 2004, Gilbey et al., 1981, McCall and Harris 1987, Morrison 1993, Cao and Morrison 2003, Morrison and Gebber 1982). Following EAA microinjection into a restricted *rostral* region of the CMM (approximately 1.5mm rostral to Obex), powerful sympathoinhibitory and vasodepressor responses have been observed (Henderson et al., 1998, Henderson et al., 2000, Heslop et al., 2002, Coleman and Dampney 1995, Coleman and Dampney 1998). Furthermore, it has been reported that under both halothane and urethane anaesthesia, the integrity of the rCMM is critical for the expression of the hypotensive phase (decompensation) of haemorrhage (Henderson et al., 2000, Henderson et al., 2002, Heslop et al., 2002). Specifically, inactivation of the rCMM with either lignocaine or cobalt chloride abolishes the hypotension and bradycardia evoked by severe haemorrhage (Henderson et al., 2000, 2002, Heslop et al., 2002).

In contrast to the ventrolateral medulla, the CMM appears to have no role in regulating homeostatic cardiovascular function. Blockade of the CMM neither alters resting AP and HR, nor has any effect on the hypotension and bradycardia evoked following baroreceptor unloading or activation of 5-HT_3 sensitive cardiopulmonary vagal afferents (Coleman and Dampney 1998, Henderson et al., 2000, McCall and Harris 1987).

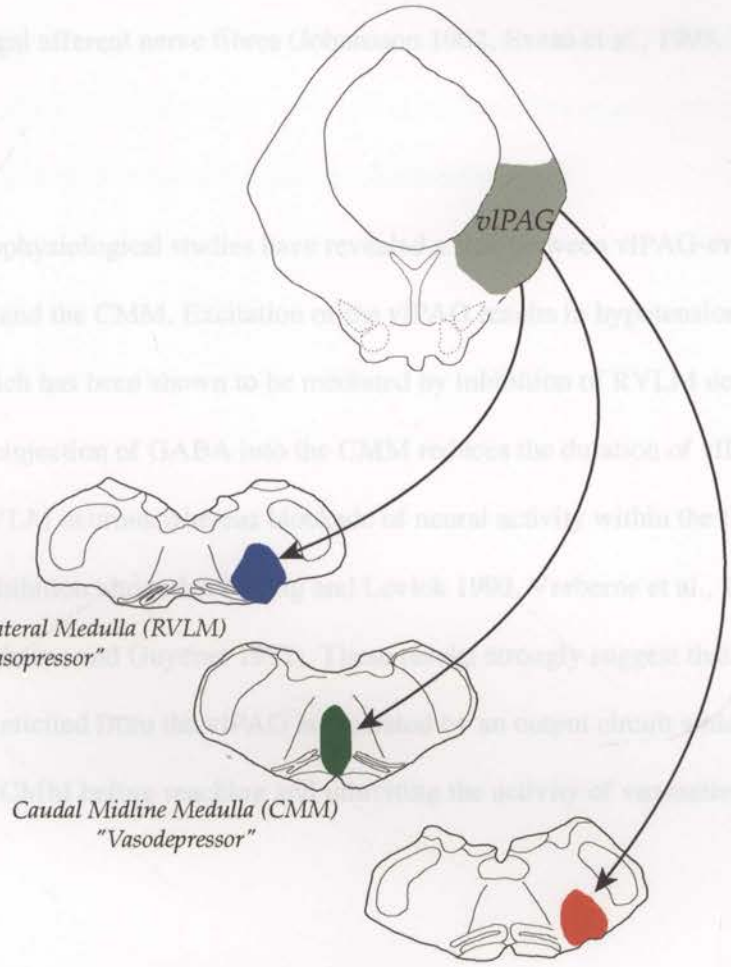

Figure 1.7
Schematic summary of the major descending output projections from the ventrolateral column of the PAG. The vlPAG projects to the "vasopressor" rostral ventrolateral medulla, the "vasodepressor" region of the caudal midline medulla, and the "vasodepressor" region of the caudal ventrolateral medulla. Projections to one or more of these areas may be responsible for mediating decompensation. *vlPAG, ventrolateral periaqueductal gray; RVLM, rostral ventrolateral medulla; CMM, caudal midline medulla; CVLM, caudal ventrolateral medulla.*

Consistent with these findings, it has been reported that lesions of the midline medulla blocks the hypotension and bradycardia evoked by electrical stimulation of nociceptive muscle afferents (Aδ and C-fibres originating in the sciatic nerve) but not following excitation of vagal afferent nerve fibres (Johansson 1962, Evans et al., 1993, McCall and Harris 1987).

Previous electrophysiological studies have revealed a link between vlPAG-evoked vasodepression and the CMM. Excitation of the vlPAG results in hypotension and bradycardia which has been shown to be mediated by inhibition of RVLM neurons. However, microinjection of GABA into the CMM reduces the duration of vlPAG-evoked inhibition of RVLM neurons whereas blockade of neural activity within the CMM abolishes the inhibition altogether (Wang and Lovick 1993, Verberne et al., 1999, Zhang et al., 1994, Verberne and Guyenet 1992). These results strongly suggest that vasodepression elicited from the vlPAG is mediated by an output circuit which first synapses in the CMM before reaching and inhibiting the activity of vasoactive neurons in the RVLM.

Summary

The ventrolateral PAG has no direct input to sympathetic preganglionic neurons of the IML indicating that it modulates sympathetic nerve activity via indirect pathways. The vlPAG projects heavily onto three important cardiovascular regulatory regions in the medulla: (i) the vasopressor region of the RVLM; and (ii) the vasodepressor regions of the caudal medulla; CVLM and CMM. The projection from vlPAG to RVLM has been

shown to form part of the circuit responsible for producing a shock-like state following noxious muscle stimulation while both the CVLM and CMM have been shown to be critical neural structures for the expression of decompensation. Delineating the functional-anatomical organization of output projections from the vlPAG to each of these medullary regions would undoubtedly provide a significant first step towards understanding the central events precipitating shock after injury.

HYPOTHESIS I

It is proposed that the ventrolateral PAG produces the cardiovascular changes evoked by haemorrhage (i.e., haemorrhage-evoked hypotension) via descending projections to one or more medullary cardiovascular regulatory regions – RVLM, CVLM, CMM.

To investigate this hypothesis an initial series of experiments were performed to confirm that the ventrolateral PAG contains a population of neurons which are selectively activated by severe blood loss. A second series of experiments aimed to identify the medullary projections of this population of neurons whose selective activation triggers decompensation.

1.11 Signals triggering decompensation

Early studies in the cat showing that haemorrhage-evoked hypotension was preceded by increased activity of left ventricular cardiac mechano-sensitive vagal afferents led to the hypothesis that decompensation is triggered by a combination of poor diastolic atrial filling, and subsequent contraction of the myocardium around poorly filled ventricles (Pearce and Henry 1955, Oberg and Thoren 1970, 1972, 1973). The notion that signals arising from cardiac vagal afferents were responsible for triggering decompensation gained further support when it was shown that bilateral cervical vagotomy delays the onset of decompensation in the unanaesthetised rabbit (Evans et al., 1994), and abolishes haemorrhage-evoked sympathoinhibition in the unanaesthetised rat (Skoog et al., 1985, Thoren et al., 1988, Togashi et al., 1990).

In contrast to early work which focussed on the contribution of cardiac vagal afferents in triggering decompensation, recent work provides compelling evidence to suggest that the critical signal may infact arise from cardiac *spinal* afferents. In contrast to bilateral vagotomy which delays the onset of blood loss induced sympathoinhibition, blockade of cardiac spinal afferents (in addition to cardiac vagal afferents) with pericardial procaine infusion *abolishes* decompensation altogether (Ludbrook and Ventura 1996). Evaluating the specific contributions of cardiac spinal versus cardiac vagal afferents in the unanaesthetised rat, Troy and colleagues have since reported that cardiac spinal deafferentation (achieved by bilateral stellate ganglionectomy) significantly delayed the onset of decompensation whereas selective cardiac vagal deafferentation (achieved by bilateral vagal sensory rhizotomy) neither delayed nor attenuated the onset of

decompensation (Troy et al., in press). Taken together, these findings indicate that in the conscious rat, haemorrhage-evoked hypotension is triggered by signals arising from the heart which are carried by *spinal* rather than vagal afferents.

The central projections of cardiac spinal and cardiac vagal afferents differ. Cardiac spinal afferents travel within the sympathetic nerves (superior, middle and inferior cardiac nerves) before terminating in the superficial dorsal horn of the thoracic spinal cord (lamina 1; T2-T6) (White 1933, Meller and Gebhart 1992). Ascending spinal projections to the brainstem have been shown to play an important role in initiating homeostatic control in response to a number of somato-sympathetic reflexes (Sato and Schmidt 1973). Anterograde tracing studies have revealed dense bilateral inputs arising from spinal cord lamina 1 to a restricted portion of the caudal ventrolateral medulla, a brainstem region uniquely positioned to subserve such responses (Craig and Kniffki 1985, Craig et al., 1995, Westlund and Craig 1996).

The caudal ventrolateral medulla (CVLM) contains neurons integral to cardio-respiratory function (for review see Dampney 1994). It also contains the A1 (noradrenergic) cell group which is known to be critical for eliciting appropriate neuro-endocrine responses to stressful stimulation (Blessing et al., 1980, Day and Sibbald 1990, Sawchenko et al., 1996). Previous double-label studies in the primate have shown that ascending neurons within the superficial dorsal horn (specifically lamina 1) form direct mono-synaptic connections onto A1 noradrenergic neurons (Westlund and Craig 1996). This finding suggests that signals arising from cardiac spinal afferents present within the myocardium

may ascend via lamina I projections and synapse onto A1 neurons within the caudal brainstem.

Previous reports show that A1 neurons are 'activated' (i.e., express Fos-IR) following severe hypotension (haemorrhage and/or graded caval occlusion) in both conscious and anaesthetised rats (Buller et al., 1999, Chan and Sawchenko 1994, Chan and Sawchenko 1998). As well, the PAG has been shown to receive significant input from the A1 cell group (Herbert and Saper 1992), and *in vitro* electrophysiological studies have shown that noradrenaline depolarises the vast majority of ventrolateral PAG neurons (Vaughan et al., 1994). Taken together these data suggest that the A1 cell group may play a critical role in relaying signals received from cardiac spinal afferents (or from other visceral sites) to the midbrain PAG, which are responsible for triggering decompensation.

The central termination pattern of vagal afferent fibres arising from the heart have been well characterised. They include: (i) myelinated mechanoreceptive Aδ fibres which form a complex network of flower-spray endings in atrial epicardial and endocardial connective tissue (Paintal 1963, Miller and Kasahara 1964, Quigg 1991, Cheng et al., 1997); and (ii) non-myelinated C-fibres which form a plexus in both atrial and ventricular endocardium. As well as responding to mechanical distortion of the ventricular myocardium, cardiac vagal C-fibres have been shown also to respond to chemical and nociceptive stimuli (Paintal 1963, Miller and Kasahara 1964, Quigg 1991, Cheng et al., 1997).

The central projections of cardiac vagal afferent fibres have been well characterised. Following intra-cardiac injection of HRP, transganglionic labelled fibres are observed to travel within the dorsomedial medulla before terminating within the nucleus of the solitary tract (NTS) (Kalia and Mesulam 1980, Xie et al., 1999, Corbett et al., 2005). It has long been recognised that the NTS is a central sensory relay nucleus critical for integrating multiple afferent inputs which contribute to autonomic function (Spyer 1994). NTS neurons have been shown to respond to electrical, chemical and mechanical stimulation of cardiac vagal afferent fibres (Bennet et al., 1985, Silva-Carvalho et al., 1998, Oshinara et al., 2006). As well, increased numbers of Fos-positive neurons have been found in the NTS following hypotensive haemorrhage (Badoer et al., 1993, Dun et al., 1993). Interestingly, many TH-immunoreactive NTS neurons (i.e., those belonging to the A2 cell group) have also been found to express Fos protein following hypotensive haemorrhage (Buller et al., 1999, Dun et al., 1993). These data suggest that NTS noradrenergic (i.e., A2) neurons may also form an important part of the ascending pathway responsible for triggering haemorrhage-evoked decompensation.

1.12 Other signals triggering decompensation:

In addition to the signals arising from the heart, two other potential signals that have been suggested as being critical for the expression of decompensation are: (i) signals arising from the kidney; and (ii) nociceptive signals arising from the viscera as a result of global ischaemia.

1.12.1 Signals arising from the kidneys: During the initial compensatory phase of haemorrhage, renal vasoconstriction results in a dramatic decrease in renal blood flow (up to 70%), which decreases even further with the onset of decompensation (up to 250%). The combined effect of this intense vasoconstriction has been shown to lead to renal ischaemia (Anderson and Szenasi 1994). Renal arteries and veins both contain mechanoreceptors and chemoreceptors, the latter of which may become activated by the ischaemia resulting from severe blood loss (Recordati et al., 1978, 1981). In the rat, electrical stimulation of the renal nerve results in a profound decrease in arterial pressure coupled with an increase in plasma vasopressin concentration (Ueda et al., 1967, Herman and Kostreva 1986, Lappe et al., 1985, Webb and Brody 1987, Simon et al., 1989, Stella and Zanchetti 1991).

Studies utilising transport of horseradish peroxidase from the cut end of the renal nerve have identified that renal afferents enter the dorsal horn of the spinal cord through the dorsal root ganglia of lower thoracic and upper lumbar segments (T_6 to L_2) (Ciriello and Calaresu 1983, Donovan et al., 1983, Ferguson et al., 1986). Renal afferent terminations in the spinal cord are localised to lamina I, III, IV, V and X where they synapse onto spinal cord neurons which also receive input from other deep visceral and somatic structures (Stella and Zanchetti 1991). However, lamina 1 neurons are unique and respond exclusively to stimulation of renal nerve fibres not to stimulation of other visceral structures (Knuepfer et al., 1988) suggesting that lamina I neurons, which receive renal afferent input, may be reserved for relaying signals to the brainstem when renal homeostasis becomes compromised such as during severe blood loss.

Afferent information carried from the kidney to the spinal cord originates from one of two sensory receptors: (i) renal mechanoreceptors sensitive to mechanical stimuli (i.e., changes in arterial, venous, or ureteral pressure); and (ii) renal chemoreceptors activated by renal ischemia, changes in ionic composition of the interstitium, or by noxious stimulation (Moss et al., 1990, Recordati et al., 1980, Recordati et al., 1978, Rogenes 1982). It is suggested that signals from the kidney which may be critical for the expression of decompensation arise from renal chemoreceptors given that these receptors become active only during conditions of impaired renal blood flow such a those resulting from clamping of the renal artery, prolonged renal vein occlusion, and systemic asphyxia (Recordati et al., 1978).

Functional-anatomical studies using occlusion of the renal artery to induce renal ischemia (and subsequent activation of renal chemoreceptors) have revealed that large numbers of c-Fos immunoreactive nuclei are expressed in the dorsolateral aspect of lamina I of the spinal cord (Rosas-Arellano et al., 1999). Furthermore, renal ischaemia has been shown to evoke large numbers of Fos-positive catecholaminergic neurons within the ventrolateral medulla (Ding 2001).

Experiments performed to identify the contribution renal afferents make toward triggering decompensation revealed that bilateral renal denervation in the conscious rat delays and attenuates the fall in AP evoked by severe haemorrhage (Kemal Ozsayin., Honours Thesis 2004). Interestingly, hypotensive haemorrhage following renal denervation produced a tachycardia of 25% relative to baseline values suggesting that the

attenuation in hypotension evoked by renal denervation may reflect a change in cardiac contractility. Further experiments showed that atropine administration prior to hypotensive haemorrhage results in an identical delay and attenuation of haemorrhage-evoked hypotension. It is therefore unlikely that renal afferents provide a significant contribution toward triggering decompensation; however likely play a role towards triggering haemorrhage-evoked bradycardia.

1.12.2 Nociceptive signals arising from deep somatic and visceral structures: It has been suggested that nociceptive signals of deep somatic or visceral origin contribute to triggering hypotension and bradycardia evoked by severe blood loss (Evans and Ludbrook 1991, Fitzpatrick et al., 1993, Ludbrook 1993, Evans et al., 1994). During the initial compensatory phase of blood loss, blood flow is redirected from selected vascular beds such as splanchnic, renal, cutaneous; in order to maintain perfusion to vital structures (brain, myocardium etc.) (Johnson 1994, Thoren et al., 1998, Vissing 1997). The redistribution of blood flow, in addition to intense vasoconstriction as a result of increased sympathetic drive and rapidly decreasing cardiac output, may be sufficient to produce severe ischaemia in many skeletal muscle and visceral vascular beds (Mudge et al., 1976, Skarphedinsson et al., 1986).

Ischaemic cells have been shown to release potassium ions, prostaglandins, and bradykinin, all of which are capable of depolarising nociceptive nerve fibres. Nociceptive signals are relayed to the central nervous system via either lightly myelinated (Aδ) or unmyelinated (C-fibre) afferent nerve fibres. Nociceptor activation following renal-pelvic

distension (Brasch and Zetler 1982), colo-rectal distension (Banner et al., 1995), distension of the small intestine (Skofitsch and Lembeck 1980) and noxious stimulation of the stomach, heart and peritoneum (Sabbatini et al., 2004, Meller and Gebhart 1992, Dawes 1947, Clement et al., 1996, Keay et al., 1994) has been shown to evoke a hypotension and bradycardia strikingly similar to that of haemorrhage.

The caudal VLM has been identified as a brainstem region critical for nociceptive-cardiovascular integration (Tavares et al., 1997). Stimulation of the caudal VLM results in a powerful inhibition of spinal cord dorsal horn nociceptive neurons (Morton et al., 1983, Janss and Gebhart 1988, Liu and Zhao 1992) as well as depression of nociceptive reflexes (Gebhart and Osipov 1986, Janss and Gebhart 1987). Furthermore, blockade of the caudal VLM abolishes the depressor response evoked by stimulation of greater splanchnic nerve afferent fibres, electrical stimulation of the tibial nerve, and the vasodepression evoked by activation of 5-HT_3 sensitive cardiopulmonary afferents (Peng et al., 2002, Verberne et al., 1989, Ruggeri et al., 1995). Thus, nociceptive signals arising from deep somatic or visceral structures as a result of the initial compensatory phase of haemorrhage are likely to be relayed to the caudal VLM where an appropriate *integrated* nociceptive-cardiovascular response is actioned.

It is interesting to note that in addition to releasing substances that activate nociceptors, ischaemic cells also release substances that have the capacity to activate chemoreceptors present on cardiac spinal afferents within the myocardium (Ludbrook 1990, Hainsworth 1991). There is much evidence to suggest that sympathetic afferent nerves arising from

the left ventricle exhibit chemo-sensitivity given that they respond to acetylcholine, sodium cyanide, histamine, veratridine, bradykinin and asphyxia (Nishi and Takenaka 1973, Staszewska-Woolley et al., 1986, 1988). The activity of cardiac sympathetic afferents has been shown to increase following coronary artery occlusion and injection of both bradykinin and capsaicin into the epicardium (Staszewska-Woolley et al., 19876, 1988, Pan et al., 2004). Moreover, Fos expression has been shown to increase in lamina I of the spinal cord, as well as within the ventrolateral medulla in response to activation of cardiac ischaemia-sensitive afferent neurons (Hua et al., 2004, 2003).

In summary: Early experimental reports suggested that haemorrhage-evoked hypotension is triggered by activation of left ventricular cardiac mechano-sensitive vagal afferents precipitated by a combination of poor atrial diastolic filling and subsequent contraction of the myocardium around poorly filled ventricles. However, recent evidence suggests that haemorrhage-evoked hypotension is triggered by activation of cardiac spinal afferents. The central patterns of termination differ; cardiac spinal afferents terminate within lamina I of the spinal cord before ascending to the ventrolateral medulla while cardiac vagal afferents terminate wholly within the NTS. Increased levels of Fos expression have been demonstrated in both the VLM and NTS, most notably within A1 and A2 cell groups suggesting that medullary catecholaminergic neurons (in particular noradrenergic neurons) may form a critical part of the central afferent responsible for triggering decompensation.

HYPOTHESIS II

It is proposed that the central afferent pathway responsible for relaying signals from the heart and/or ischaemic viscera in order to trigger decompensation involves a catecholaminergic projection arising from medullary catecholaminergic cell groups to the ventrolateral PAG.

To investigate this hypothesis an initial series of experiments were performed to quantify the patterns of haemorrhage-evoked neural activity in specific medullary catecholaminergic cell groups. A second series of anatomical experiments was then carried out to determine the distribution of medullary catecholaminergic projections to the ventrolateral PAG. A third and final series of physiological experiments confirmed that noradrenergic neurotransmission within the ventrolateral PAG plays a critical role in triggering decompensation.

1.13 Clinical Correlations: Hypotensive haemorrhage in the clinical setting

As discussed in section 1.4, the haemodynamic response to blood loss is profoundly altered by anaesthesia. Under conditions of general anaesthesia, even moderate hypovolaemia has been shown to precipitate a profound and premature centrally-mediated sympathoinhibition resulting in shock and ultimately death. Presently, the most widely used general anaesthetics in the clinical setting are halogenated (i.e., sevoflurane, isoflurane, halothane). Therefore, understanding the complex interaction(s) between halogenated anaesthetics and the central mechanism underlying hypovolaemia represents an important clinical issue.

The experiments performed in this thesis aiming to delineate the central afferent pathway responsible for triggering hypovolaemic shock (presented in chapters 4 and 5) revealed that the vlPAG receives dense ascending input from noradrenergic neurons in the ventrolateral medulla (the A1 cell group). Strikingly, the vast majority of these neurons are 'activated' following hypotensive haemorrhage suggesting that a noradrenergic mechanism within the vlPAG may trigger the hypotension evoked by severe blood loss. Further experiments showing that bilateral microinjections of phentolamine, a broad spectrum alpha receptor antagonist, made in the vlPAG significantly delayed and attenuated the magnitude of haemorrhage-evoked hypotension lend further support to the hypothesis that vlPAG noradrenergic neurotransmission is critical for the expression of decompensation.

Interestingly a past study has revealed that induction of halothane anaesthesia results in a striking increase in catecholamine concentration within the ventrolateral PAG (Roizen et al., 1976). As well, it has been reported that induction of halothane anaesthesia evokes Fos-expression in vlPAG-projecting, A1 noradrenergic neurons (Clement et al., 1998). The authors of this latter study suggested that activation of this pathway by halogenated anaesthetics may explain why decompensation is dramatically potentiated in anaesthetised animals (Ong et al., 1984, Ingwersen et al., 1987, Seyde and Longnecker 1984, Van Leeuwen et al., 1990), and why in humans, induction of general anaesthesia is usually associated with a significant hypotension (McKinney and Fee 1998, Kadam et al., 1993, Ebert et al., 1985).

HYPOTHESIS III

It is proposed that activation of ventrolateral PAG-projecting A1 noradrenergic neurons by halothane anaesthesia results in the premature expression and potentiation of the decompensatory response to severe blood loss in anaesthetised animals.

To address this issue, a final series of physiological experiments was carried out to determine whether blockade of noradrenergic neurotransmission within the ventrolateral PAG has any effect of the haemodynamic response to severe blood loss under conditions of halogenated anaesthesia.

-Chapter 2-

General Methods

All experiments were carried out following the guidelines of the NHMRC/CSIRO/AAA "Code and Practice for the Care and Use of Animals in Research in Australia" and were approved by the University of Sydney Animal Care Ethics Committee.

2.1 Animals

All surgical and experimental procedures were performed on adult male Sprague-Dawley rats. All rats were obtained from ARC Perth. Prior to experimentation the animals were housed in groups of six and were provided with food and water *ad libitum*. Room temperature was maintained at 22°C and the lights were kept on a 12 hour *on-off* cycle.

2.2 General Surgical Procedures

Prior to all surgical and/or experimental procedures, animals were removed from their home cage and weighed. All procedures were performed on rats weighing between 250 and 400 grams.

2.3 Anaesthesia

Ketamine: Each animal was placed in an air-tight perspex box. In order to initiate a brief period of CO_2 narcosis, carbon dioxide was introduced into the box for approximately five seconds via a hose connected to a CO_2 cylinder. During this time the animals

respiratory signs were closely monitored. Once unconscious, the animal was removed from the box, placed in the prone position and given an intramuscular injection of ketamine (75mg/kg) and xylazine (4mg/kg) into the biceps femoris muscle.

Halothane: Each animal was placed into an air-tight perspex box which had an outlet connected to a halothane vaporiser. Halothane (5%) mixed with 100% O_2 was introduced into the box at a rate of 1 litre/minute. Once unconscious, the animals were transferred to a custom built face mask consisting of two outlets; one connected to the halothane vaporiser, the other to an evacuation pump. The halothane concentration was subsequently reduced to 2% in 100%$_2$ and evacuated at a rate of 125cc/minute for the duration of the procedure.

Anaesthesia induced by either ketamine or halothane was considered to be at an acceptable surgical level if there was an absence of both hindlimb withdrawal and corneal blink reflexes.

2.4 Body temperature regulation

While under anaesthesia animals were placed on a homeothermic blanket. Body temperature was monitored via a thermo-sensitive probe which was connected to a homeothermic blanket control unit. The temperature of the blanket was maintained at 37 ± 1°C.

2.5 Chronic Arterial and Venous Cannulation

Arterial pressure (AP) was measured via a cannula inserted into the left common carotid artery. A venous cannula placed in the right jugular vein was used to facilitate blood withdrawal.

Common carotid arterial cannulation: Once under halothane anaesthesia, the animal was placed in the supine position and a superficial midline incision was made. The sternocleidomastoid muscle was retracted allowing the common carotid to be carefully dissected free from the carotid sheath and vagus nerve. Once free, the distal end of the artery was occluded with silk thread (4-0) and the proximal end temporarily occluded with a second silk thread. A small incision was made in the arterial wall allowing a polyethylene cannula (ID 0.58mm; OD 0.96mm) filled with heparinized saline to be inserted to the level of the aortic arch. The free end of the cannula was connected to a pressure transducer which was in turn connected to a recording amplifier. The raw signal was filtered through a Maclab and the pulsatile arterial pressure trace then displayed and recorded on a Macintosh computer running Chart 4.01.

Jugular vein cannulation: Once under halothane, the animal was placed in the supine position before an incision lateral to the midline at the level of the clavicle was made. The right jugular vein was exposed by blunt dissection. The distal end of the vessel was occluded with silk thread (4-0) and the proximal end temporarily occluded with a second silk thread. A small incision was made in the venous wall allowing a polyethylene cannula (ID 0.8mm; OD 1.2mm) filled with heparinized saline to be inserted to the level

of the superior vena cava. The cannula was then passed subcutaneously and exteriorised between the scapula. After cannulation, halothane anaesthesia was discontinued and the animal returned to its home cage. A twenty-four hour recovery period followed before any further experimental manipulations were performed.

2.6 Retrograde Tracer Injections

Medullary Microinjections: Following ketamine anaesthesia animals were transferred to a stereotaxic frame and placed in the flat skull position. Non penetrating ear bars positioned in the external acoustic meatus secured the animals head. The dorsal surface of the skull and the dorsal neck muscles were exposed with a scalpel incision. The three layers of dorsal neck muscles were displaced with forceps to expose the baso-occipital plate. A dental drill was then used to remove a small (approximately $5mm^2$) medial portion of the baso-occipital plate, exposing the cerebellum and dorsal surface of the medulla at the level of the obex.

Midbrain Microinjections: Following ketamine anaesthesia animals were transferred to a stereotaxic frame and placed in the flat skull position. The dorsal surface of the skull was exposed with a scalpel incision. An area of bone (approximately $25mm^2$) located approximately 12mm caudal to Bregma and 1.8mm lateral to the midline was removed with a dental drill. The underlying dura mater was removed with a 19-gauge needle to expose the dorsal surface of the cerebellum.

Pressure Injections

Microinjections were made using single barrel glass micropipettes connected to an automated air pressure injection system (Picospritzer II). The automated air pressure system was connected to a compressed air cylinder and applied brief pulses of air to the micropipette barrel via polyethylene tubing. Both the strength and duration of the air pulses were adjusted to suitable levels in order to control the injection volume. The volume of each injection was monitored by observing the meniscus of the injectate through a calibrated graticule eyepiece on a dissecting microscope.

2.7 Experimental Protocols

The experiments performed in this thesis aimed to identify the central circuit(s) mediating decompensation. Three experimental protocols were used:

Normotensive (10%) Haemorrhage: Following a 2hr habituation period to the environmental surroundings (i.e., level of lighting and ambient noise in the laboratory), 10% total blood volume was withdrawn via the venous cannula over a 10 minute period. Following blood withdrawal, the rat was left undisturbed for a further 110 minutes before being transcardially perfused. Ten percent total blood volume is equivalent to withdrawal of 8 ml/kg. This manipulation was used to control for the initial normotensive phase of haemorrhage (i.e., *compensation*).

Hypovolaemic (30%) Haemorrhage: Following a 2hr habituation to the environmental surroundings (i.e., level of lighting and ambient noise in the laboratory), 30% total blood

volume was withdrawn via the venous cannula over a 20 minute period (10% over 10 minutes, followed by the removal of an additional 20% over the subsequent 10 minutes). Following blood withdrawal, the rat was left undisturbed for a further 100 minutes before being transcardially perfused. Thirty percent total blood volume is equivalent to withdrawal of 24 ml/kg.

Euvolaemic Hypotension: Following a 2hr habituation to the environmental surroundings (i.e., level of lighting and ambient noise in the laboratory), the peripheral vasodilator sodium nitroprusside was infused at a rate of 30μl/min over 20 minutes. The rat was then left undisturbed for a further 100 minutes before being transcardially perfused.

2.8 Perfusion Procedure

Animals were placed in an airtight perspex box and exposed briefly to CO_2. Once unconscious the animal was removed and given a 1.0ml intra-peritoneal injection of sodium pentobarbitone (Nembutal; 60mg/ml). In experiments where the animal was cannulated, Nembutal was administered intravenously (0.5ml made up in 0.9% NaCl). Once unconscious the animal was placed in the supine position and three incisions made: one through the skin and muscles above the xyphoid process followed by an incision through both sides of the rib cage. The diaphragm was cut and the rib cage retracted to expose the thoracic cavity. The pericardium was gently teased away from heart and a perfusion needle connected to a peristaltic pump was inserted into the left ventricle. The right atrium was cut and 500ml of 0.9% isotonic saline followed by 500ml of cold (4°C) 4% paraformaldehyde (in borate-acetate buffer; pH 9.6) was pumped through the heart.

Following perfusion the animals skull was removed, the brain collected and post-fixed in 4% paraformaldehyde for 24 hours. Following post-fixation the brain was cut into three blocks: (i) a medullary block extending from the midbrain-pontine junction to the upper cervical spinal cord; (ii) a midbrain block extending from the midbrain-pontine junction to the optic chiasm; and (iii) the forebrain block extending from the optic chiasm to the olfactory bulbs. Each block was cryoprotected in 10% sucrose made up in 0.1M phosphate buffered saline for 2-4 days.

2.9 Mounting and Coverslipping

Once all immunohistochemical procedures had been completed each section was mounted onto twice dipped gelatinised (1%) glass slides and allowed to air dry overnight. Sections were then passed through an ascending series of alcohols (50%, 70%, 90%, 100%; 1min in each) before being cleared in Histoclear for approximately 10 minutes. Each slide was then coverslipped using medical coverslips and DPX mounting medium. Where sections contained fluorescent tracer, they were briefly dipped in 100% ethanol and Histoclear (approximately 1min each) before being coverslipped with medical coverslips and Fluromount mounting medium.

2.10 Microscopy

Non-fluorescent immunohistochemistry was analysed under the light microscope. Cells were considered to be Fos-immunoreactive if DAB reaction product was clearly visible in the nucleus at x40 magnification and could be distinguished from the background staining at x4 to x20 magnifications. The presence of retrograde label (Fast Blue or

Fluorogold) in neurons was determined under fluorescence illumination at x100 magnification. Double labelled neurons were identified by switching between illumination conditions.

-Chapter 3-

Hypovolaemic shock: critical involvement of a projection from the ventrolateral PAG to the caudal midline medulla

3.1 Introduction

In conscious mammals (including humans) progressive blood loss triggers a biphasic haemodynamic response. Initially, during moderate blood loss (up to15% total blood volume), arterial pressure is maintained within a normal range by a selective increase in sympathetic vasomotor tone in specific vascular beds (skeletal muscles, most viscera). The net effect of this *compensatory response* is to maintain, in the face of falling cardiac output, adequate vascular perfusion of critical structures (brain, heart) (Schadt and Ludbrook, 1991, Ludbrook, 1993). In behaving animals compensation is associated usually with increased vigilance and alertness (Persson and Svensson, 1981). Compensation is triggered by baroreceptor unloading, i.e., it is blocked by barodenervation (Evans and Ludbrook, 1991, Evans et al., 1994a).

If blood loss progresses and becomes severe (e.g., 15-30% total blood volume) a second or *decompensatory phase* (i.e., *shock*), is triggered. This phase is characterised by a large and sustained fall in arterial pressure mediated by a rapid-onset sympatho-inhibition and often a vagally-mediated bradycardia (Schadt and Ludbrook, 1991, Ludbrook, 1993). In behaving animals decompensation is associated with quiescence, decreased vigilance and decreased reactivity (Persson and Svensson, 1981).

Decompensation is thought to be triggered, at least in part, by cardiac mechanoreceptors and/or cardiac nociceptors detecting inadequate ventricular filling and/or myocardial perfusion (Oberg and Thoren, 1970, Oberg and Thoren, 1972, Oberg and Thoren, 1973, Skoog et al., 1985, Thoren et al., 1988, Victor et al., 1989, Togashi et al., 1990, Evans et al., 1994b).

Although it is well established that the baroreceptor circuitry contained within the lower brainstem (pons, medulla) is sufficient to mediate compensation (Schadt and Ludbrook, 1991), the neural structures mediating decompensation have yet to be identified. Recent experiments suggest that decompensation requires the integrity of the midbrain. That is, severe haemorrhage triggers decompensation in pre-collicular decerebrate rats (midbrain and lower brainstem intact), but not in rats decerebrated at the pre-trigeminal level (midbrain absent) (Evans et al., 1991, Troy et al., 2003). Additional data indicate that the critical midbrain region mediating decompensation is the ventrolateral column of the periaqueductal gray region (vlPAG). Specifically: (i) stimulation of the vlPAG with excitatory amino acids evokes cardiovascular (hypotension, bradycardia) and behavioural (quiescence, decreased vigilance and decreased reactivity) responses identical to those characteristic of decompensation (Zhang et al., 1990, Lovick, 1992a, Depaulis et al., 1994, Keay et al., 1997a);(ii) severe haemorrhage preferentially evokes immediate early gene (c-Fos) expression within the vlPAG column (Keay et al., 1997b, Keay et al., 2002) and (iii) synaptic blockade or reversible inactivation of the vlPAG significantly delays and/or attenuates the sympathoinhibition, hypotension and bradycardia evoked by severe haemorrhage (Cavun and Millington, 2001, Cavun et al., 2001, Dean, 2004).

The specific aim of this study was to identify the main descending pathway(s) via which vlPAG neurons trigger decompensation in response to severe blood loss. A first set of experiments confirmed that the vlPAG contains a population of vlPAG neurons

selectively activated by severe blood loss. Subsequent experiments used a combination of retrograde tracing and immediate early gene expression (i.e., double labeling) to identify the medullary projections of the population of vlPAG neurons whose selective activation triggers decompensation.

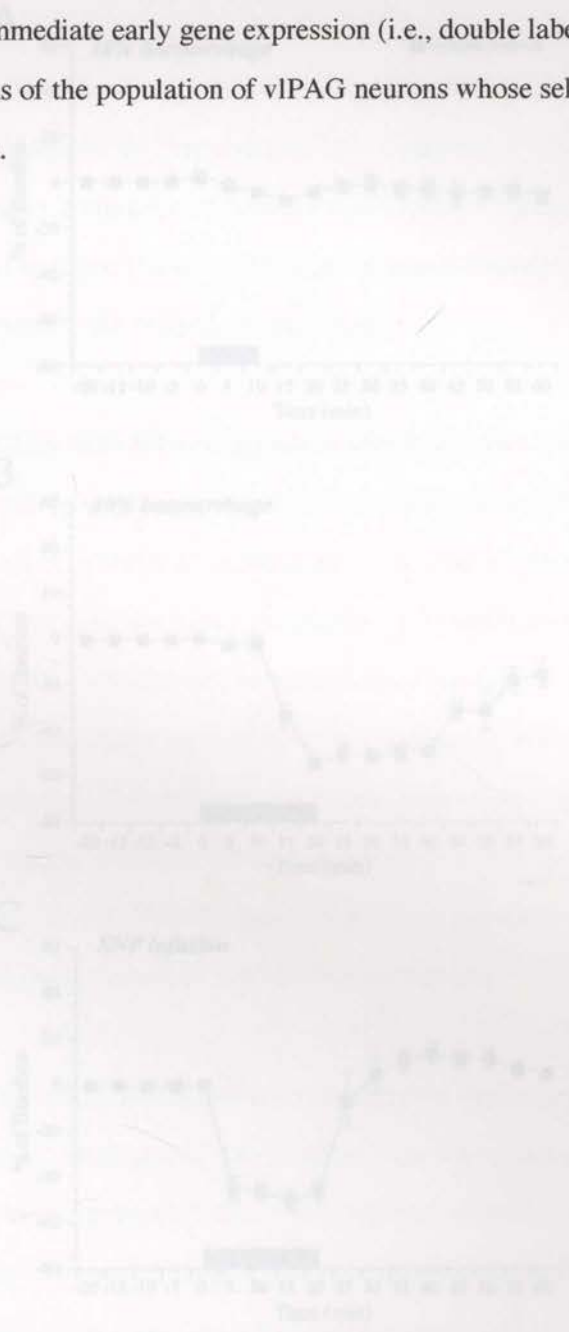

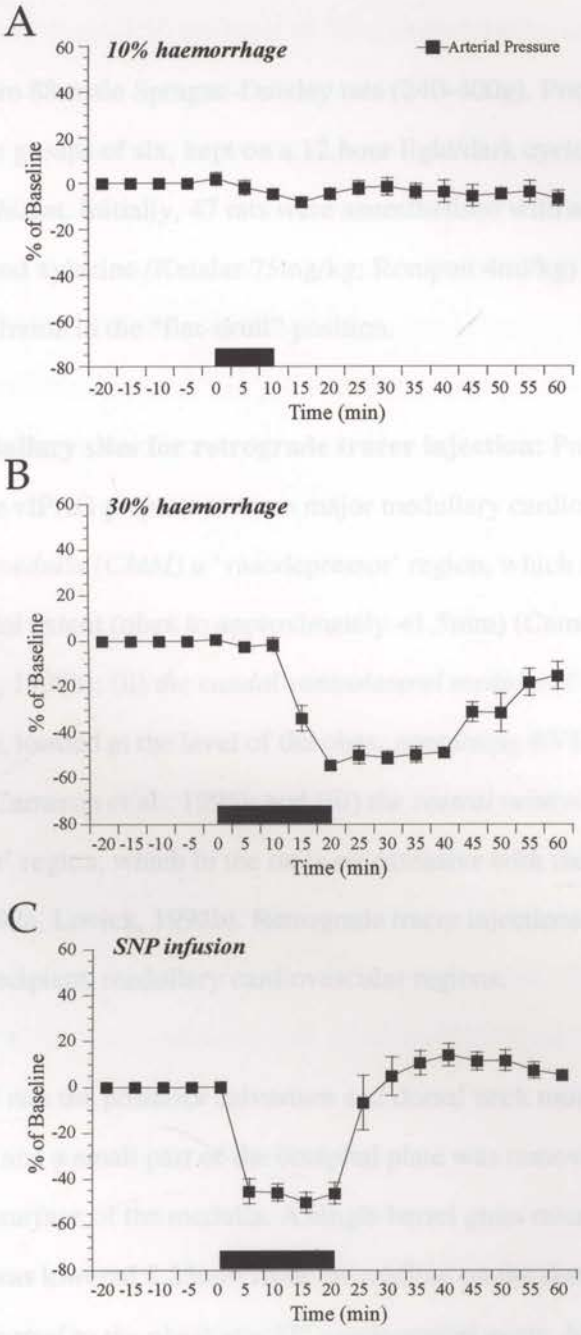

Figure 3.1
Graphs illustrating the mean (±SEM) changes in arterial pressure (AP) (percent of baseline) following either: **A** 10% (normotensive) haemorrhage; **B** 30% (hypotensive) haemorrhage; or **C** intravenous infusion of sodium nitroprusside (SNP 1mg/ml at 30µl/min). The black marker along the abscissa indicates the period of blood withdrawal (A&B) or infusion (C).

3.2 Materials and Methods

Data were obtained from 88 male Sprague-Dawley rats (240-400g). Prior to surgery all animals were housed in groups of six, kept on a 12 hour light/dark cycle, and had access to food and water *ad libitum*. Initially, 47 rats were anaesthetised with an intramuscular injection of ketamine and xylazine (Ketalar 75mg/kg; Rompun 4ml/kg) before being placed in a stereotaxic frame in the "flat-skull" position.

3.2.1 Selection of medullary sites for retrograde tracer injection: Previous anatomical studies indicate that the vlPAG projects to three major medullary cardiovascular regions: (i) *the caudal midline medulla (CMM)* a 'vasodepressor' region, which in the rat has a restricted rostro-caudal extent (obex to approximately +1.5mm) (Cameron et al., 1995, Henderson et al., 1998b); (ii) *the caudal ventrolateral medulla (CVLM)* a 'vasodepressor' region, located at the level of the obex, containing RVLM-projecting GABAergic neurons (Cameron et al., 1995); and (iii) *the rostral ventrolateral medulla (RVLM)* a 'vasopressor' region, which in the rat is co-extensive with the C1 (adrenergic) cell group (Lovick, 1992a, Lovick, 1992b). Retrograde tracer injections were aimed at each of these vlPAG-recipient, medullary cardiovascular regions.

CMM injections: In 29 rats the posterior calvarium and dorsal neck muscles were exposed and reflected, and a small part of the occipital plate was removed exposing the cerebellum and dorsal surface of the medulla. A single barrel glass micropipette (tip diameter 10 - 20mm) was lowered 2.25mm from the midline on the dorsal surface of the medulla (*0.5 -1.0mm rostral to the obex*) at a 23° caudo-rostral angle. Microinjections (50nl) of retrograde tracer (Fast Blue: N=7; Fluorogold: N=22) were made via an automated air-pressure system that applied brief air pulses (10 msec.) to the pipette barrel. The tracers Fast Blue (FB) and Fluorogold (FG) share similar uptake, spread and

labelling efficiencies (Richmond et al., 1994, Novikova et al., 1997, Choi et al., 2002). To determine the volume of injectate, the level of the meniscus in the micropipette was monitored via a calibrated graticule in a dissecting microscope. Each injection was made over a period of 10 minutes after which time the pipette remained *in situ* for a further 10 minutes. Following removal of the pipette, the rat was removed from the stereotaxic frame, the neck muscles sutured and the scalp incision closed. Subsequently, each animal was given fluids (2.0ml, 0.9% saline i.p.) before being returned to its home cage. The mobility, activity level, eating, drinking and grooming of each rat was closely observed each post-operative day. A period of seven days was allowed for transport of the tracer before further experimental procedures were undertaken.

RVLM and CVLM injections: In 18 rats, the dorsal surface of the cerebellum was exposed by a small craniotomy to allow injection of retrograde tracer to be made into either the rostral VLM (Fast Blue; N=5) or the caudal VLM (Fluorogold; N=13) using stereotaxic co-ordinates relative to anatomical landmarks (RVLM: *12.5mm caudal to bregma; 2.0mm lateral; 10.5mm below cerebellar surface;* and CVLM: *obex; 1.8mm lateral; 2.25mm below medullary surface*). Injection of retrograde tracer and the post-injection recovery period was as described above. A period of seven days was allowed for transport of the tracer before further experimental procedures were undertaken.

3.2.2 Cannulation Procedures: Each of the 47 rats injected with retrograde tracer, plus an additional 18 rats (no tracer injection) were cannulated for subsequent removal of blood. Each rat was anaesthetised with halothane (2%) and a cannula was placed into the right external jugular vein. The cannula (PE tubing, OD= 0.96mm, with a 32mm silastic tip OD= 1.19mm) was passed subcutaneously and exteriorised in the interscapular region. Following cannulation, anaesthesia was discontinued and each animal was given an injection of antibiotic (Norocillin, 150mg/kg, i.m.) and fluids (2ml, 0.9% saline i.p.) and

returned to its home cage. In another 17 rats, in addition to cannulation of the R external jugular vein, an additional cannula was placed in the L carotid artery to record pulsatile arterial pressure. These 17 animals were used to validate the cardiovascular responses to: (i) 10% haemorrhage; (ii) 30% haemorrhage; and iii) sodium nitroprusside infusion (see Figure 1).

3.2.3 Experimental Protocols: Twenty four hours following cannulation surgery rats were placed on their own bedding in an opaque plastic cage (30cm dia.) in a dimly lit experimental room and the venous cannula was connected via heparinized, PE 50 tubing to a 1ml plastic syringe. Each rat was then left undisturbed for 2 hours to habituate to the surroundings. Subsequently, each rat was subjected to one of four procedures:

(i) *Venous cannulation alone (no haemorrhage)*: following the habituation period rats were left for an additional 2 hours and then perfused.

(ii) *10% (normotensive) haemorrhage*: following habituation, 10% total blood volume (t.b.v.) was withdrawn over a 10 min period after which the rat was left undisturbed for an additional 110 min, followed by perfusion. Ten percent (10%) total blood volume is equivalent to withdrawal of 8ml/kg, the range of volumes removed was 1.84ml to 3.0ml. A 10% haemorrhage does not alter significantly resting arterial pressure (Figure 1A).

(iii) *30% (hypotensive) haemorrhage*: following habituation, 30% t.b.v. was withdrawn over 20 min (10% over 10 minutes, followed by the removal of an additional 20% over the subsequent 10min). Rats were then left undisturbed for an additional 100min, followed by perfusion. Thirty percent (30%) total blood volume is equivalent to 24ml/kg, the range of blood volumes removed

during a 30% haemorrhage was 6.72ml to 9.6ml. A 30% haemorrhage evokes a sustained hypotensive response (Figure 1B).

(iv) *Euvolaemic hypotension*: following habituation, sodium nitroprusside (SNP), a peripheral vasodilator (1mg/ml solution) was infused at a rate of 30µl/min over 20 min. Rats were then left undisturbed for an additional 100min, followed by perfusion. Infusion of sodium nitroprusside evokes a hypotensive response similar that evoked by 30% haemorrhage (c.f. Figures 1B and 1C).

(v) *Non-cannulated control*: 6 additional rats were taken from their home cage, placed in the opaque plastic cage in the experimental room and left undisturbed for the same duration as procedures (i) to (iv) above and then perfused.

3.2.4 Perfusion: each animal was deeply anaesthetised (sodium pentobarbital, 90mg/kg i.v.) and rapidly perfused transcardially with 500ml of 0.9% saline followed by 500ml of ice cold fixative (4% paraformaldehyde in borate-acetate buffer, pH 9.6). The brains were removed, post-fixed for 4 hours in the same fixative, then cryoprotected for at least 3 days in 10% sucrose in 0.1M phosphate buffer. Fifty micron frozen, serial coronal sections of the medulla were cut immediately in order to identify the location and extent of each retrograde tracer injection. Subsequently, frozen, 50µm serial, coronal sections of the midbrain were cut. Every second section was collected in 0.1M phosphate buffered 0.9% saline (PBS pH 7.4) for immunohistochemical processing.

3.2.5 Immunohistochemistry: Free-floating midbrain sections were washed in PBS, and incubated in polyclonal rabbit anti-c-Fos (Santa Cruz, sc-50:1:2000 for 24 hours at 4°C). Sections were then washed (PBS) and incubated in biotinylated goat anti-rabbit IgG (Vector Labs: 1:500, 2 hours at room temperature. The sections were washed again and incubated in Extr-Avidin peroxidase (Sigma: 1:1000, 2 hours at room temperature). Following a final wash in PBS, chromogenic detection of Fos protein with 3,3,-diaminobenzidine tetrahydrochloride (DAB) was performed. The sections were incubated for 20 minutes in "DAB mix" containing 10mg 3,3,-diaminobenzidine tetrahydrochloride, 0.2ml of 4% ammonium chloride in 0.1M PBS (pH 7.4), 0.2ml of 20% D-glucose in 0.1M PBS (pH 7.4), made up to 20ml with 0.1M PBS (pH 7.4). The sections were then placed in a fresh 20ml of "DAB mix" and 20_l of glucose oxidase (Sigma: 1000U/ml) was added to the solution to initiate the chromogenic reaction. The reaction was carried out over ice to control chromogenesis and the reaction stopped when the background staining became visible by rinsing the sections in several changes of 0.1M PBS (pH 7.4) (Clement et al., 1996). Sections were mounted onto gelatinised slides, air dried, rapidly dehydrated, cleared and coverslipped with Fluoromount (Gurr).

3.2.6 Analysis: The numbers of single-labelled (Fos-immunoreactive (IR) or retrogradely-labelled) and double-labelled (Fos-IR and retrogradely labelled) PAG neurons were counted in five equi-distant midbrain sections (-6.8, -7.3, -7.8, -8.3 and -8.8 mm caudal to bregma) (Paxinos and Watson, 1986). Fos-IR neurons were defined under light microscopic conditions by the presence of DAB reaction product clearly visible in the nucleus at 40x magnification (for details see (Clement et al., 1996). The presence of retrograde label (Fast Blue, Fluorogold) in neurons was determined under fluorescence illumination at 100x magnification. Double-labelled neurons were identified by switching between illumination conditions. The boundaries of each PAG column were defined using anatomical and functional criteria as described previously (Keay and Bandler,

2001, Keay and Bandler, 2004). The mean numbers of single-labelled and double-labelled neurons (±SEM) in each PAG column, under each experimental condition were compared using non-parametric statistics (Mann-Whitney U-test). Camera-lucida plots of the distribution of single- and double-labelled PAG neurons were drawn from representative animals.

3.3 Results

3.3.1 PAG Fos-Immunoreactivity (IR): control, venous cannulation and haemorrhage groups:

Figure 3.2 presents the mean numbers (±SEM) of Fos-IR cells observed in each PAG column in the following groups: control (basal Fos-IR), venous cannulation, normotensive haemorrhage (10% tbv removed) and hypotensive haemorrhage (30% tbv removed). Comparisons of the numbers of PAG Fos-IR cells in control versus venous cannulation animals revealed a significant increase in Fos-IR in the vlPAG of the venous cannulation group alone (control, 137.5 ± 14.8 *vs* v cann, 227.3 ± 27.1, $p<0.01$). Compare also Figs 3.3B and 3.3C and Figs 3.4B and 3.4C.

Compared to venous cannulation rats, normotensive haemorrhage increased the numbers of Fos-IR cells only in the dorsolateral (dlPAG) and lateral (lPAG) columns (dlPAG: v. cann 105.8± 9.9 vs 10% haem 173.3 ± 11.9, $p< 0.01$; lPAG: v. cann 151.7 ± 7.3 vs 10% haem 193.3 ± 13.6, $p< 0.05$; vlPAG: v cann 227.3 ± 27.1 vs 10% haem 226.7 ± 7.6, n.s.). Compare also Figs 33.C and 3.3D and Figs 3.4C and 3.4D. In contrast, when 30% tbv was withdrawn, i.e., a hypotensive haemorrhage, Fos-IR was increased only in the vlPAG (dlPAG: 10% haem 173.3 ± 11.9 vs 30% haem 163.7 ± 14.2, n.s.; lPAG: 10% haem 193.3 ± 13.6 vs 30% haem 191.0 ± 19.7, n.s.; vlPAG: 10% haem 226.7 ± 7.6 vs 30% haem 512.0 ± 32.9, $p< 0.001$). Compare also Figs 3.3D and 3.3E and Figs 3.4D and 3.4E.

To summarise, the sudden transition during progressive blood loss, from normotension to hypotension is associated with a selective and dramatic increase in Fos-IR only within the vlPAG.

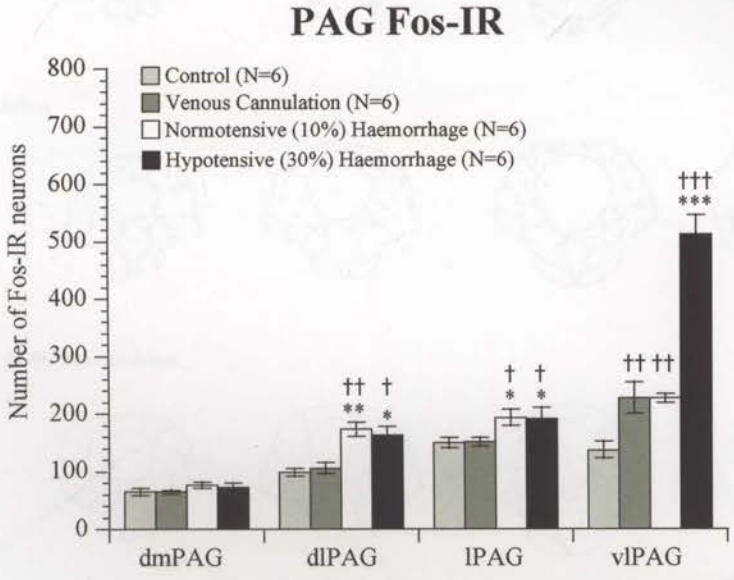

Figure 3.2
Bar graphs summarising the PAG columnar distribution of Fos-immunoreactive (IR) neurons. Each bar represents the mean number (±SEM) of Fos-IR cells in: (i) control rats (N=6), and following (ii) venous cannulation alone (N=6); (iii) 10% (normotensive) haemorrhage (N=6); and (iv) 30% (hypotensive) haemorrhage (N=6). Significance relative to control (Mann-Whitney U-test), †$p<0.05$, ††$p<0.01$, †††$p<0.005$. Significance relative to venous cannulation alone (Mann-Whitney U-test), *$p<0.05$, **$p<0.01$, ***$p<0.005$.

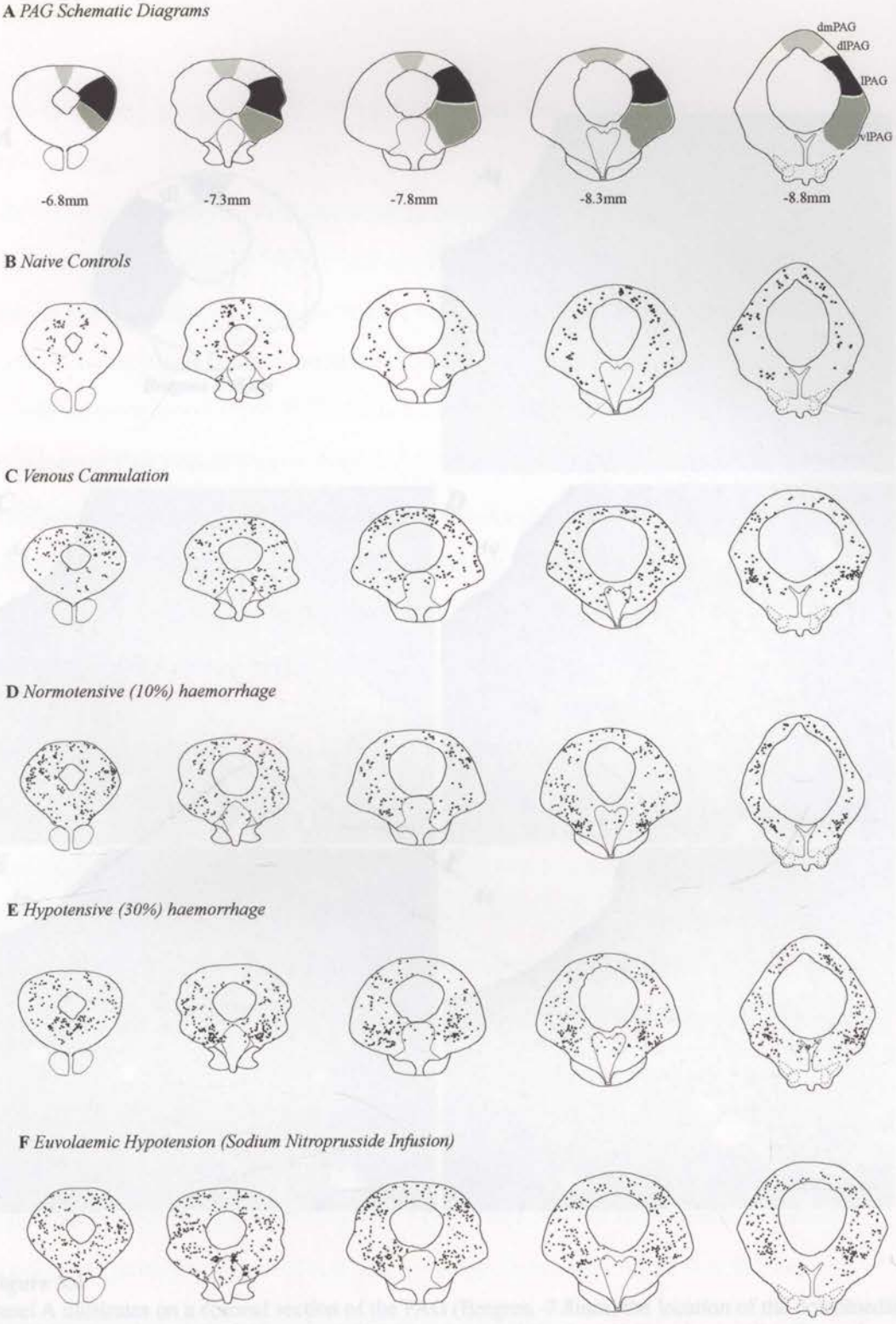

Figure 3.3

Panels A to F show camera lucida reconstructions of five, equi-distant PAG coronal sections (bregma -6.8mm to -8.8mm; rostral to left). Panel **A** shows the location of the dorsomedial (dmPAG), dorsolateral (dlPAG), lateral (lPAG) and ventrolateral (vlPAG) columns of the PAG as defined by earlier functional-anatomical studies (for review see Keay and Bandler 2004). Panels B to F show the location of Fos-IR neurons (black dots) evoked in **B** naive controls, and following **C** venous cannulation; **D** normotensive (10%) haemorrhage; **E** hypotensive (30%) haemorrhage; and **F** euvolaemic hypotension (sodium nitroprusside infusion; 1mg/ml).

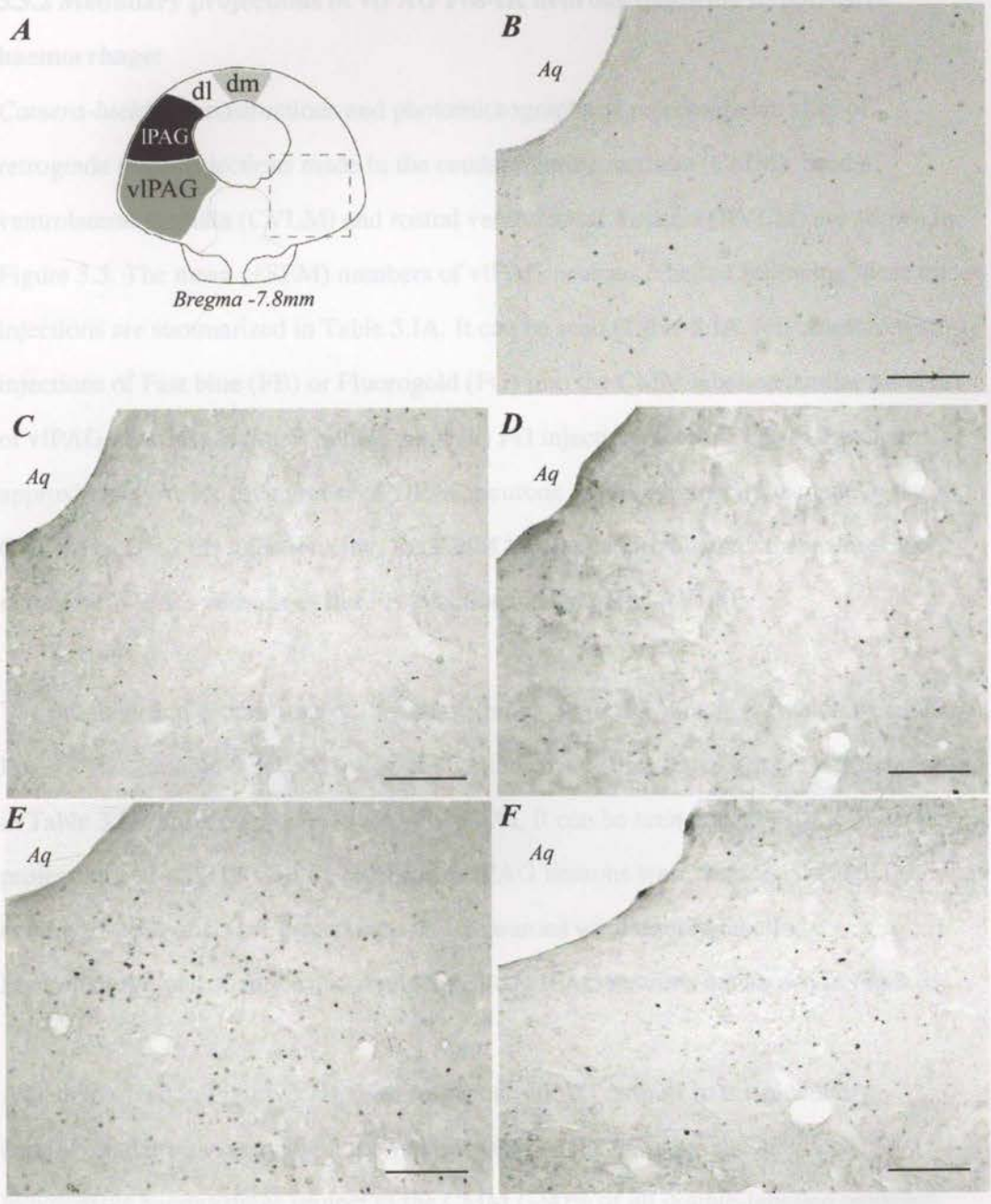

Figure 3.4
Panel A illustrates on a coronal section of the PAG (Bregma -7.8mm) the location of the dorsomedial (dmPAG), dorsolateral (dlPAG), lateral (lPAG) and ventrolateral (vlPAG) columns (Bandler and Shipley 1994, Keay and Bandler 2004). Panels B-F are low power photomicrographs illustrating Fos-IR in the vlPAG region indicated by the rectangle in: (B) control rats; and rats subjected to (C) venous cannulation alone; (D) 10% (normotensive) haemorrhage; (E) 30% (hypotensive) haemorrhage; or (F) euvolaemic hypotension (infusion of sodium nitroprusside: SNP). Scale bar represents 200um. *Aq, cerebral aqueduct.*

3.3.2 Medullary projections of vlPAG Fos-IR neurons following hypotensive haemorrhage:

Camera-lucida reconstructions and photomicrographs of representative sites of retrograde tracer injections made in the caudal midline medulla (CMM), caudal ventrolateral medulla (CVLM) and rostral ventrolateral medulla (RVLM) are shown in Figure 3.5. The mean (±SEM) numbers of vlPAG neurons labelled following these tracer injections are summarized in Table 3.IA. It can be seen (Table 3.IA, left column) that: (i) injections of Fast blue (FB) or Fluorogold (FG) into the CMM labelled similar numbers of vlPAG neurons (Mann-Whitney, n.s.); (ii) FG injections into the CMM labelled approximately twice the number of vlPAG neurons as did FG injections made in the CVLM; and (iii) FB injections into the CMM labelled approximately three times the number of vlPAG neurons as did FB injections made in the RVLM.

The numbers and proportions of medullary-projecting vlPAG neurons which were also Fos- IR (i.e., double-labelled) following hypotensive (30%) haemorrhage are summarised in Table 3.IA, right column (see also Fig 3.7A). It can be seen that ~1% of RVLM-projecting and ~5% of CVLM-projecting vlPAG neurons were double-labelled. In contrast, ~20% of CMM-projecting vlPAG neurons were double-labelled. Photomicrographs of single and doublelabelled vlPAG neurons are shown in Fig 3.6.

As summarized in Figure 3.7B, with respect to vlPAG outputs to the medullary cardiovascular regions studied, the vast majority of vlPAG neurons 'activated' by hypotensive haemorrhage project to the CMM (~90% of all double-labelled neurons). Many fewer double-labelled vlPAG neurons projected to the CVLM (~10%), and the RVLM-projecting vlPAG neurons were rarely activated.

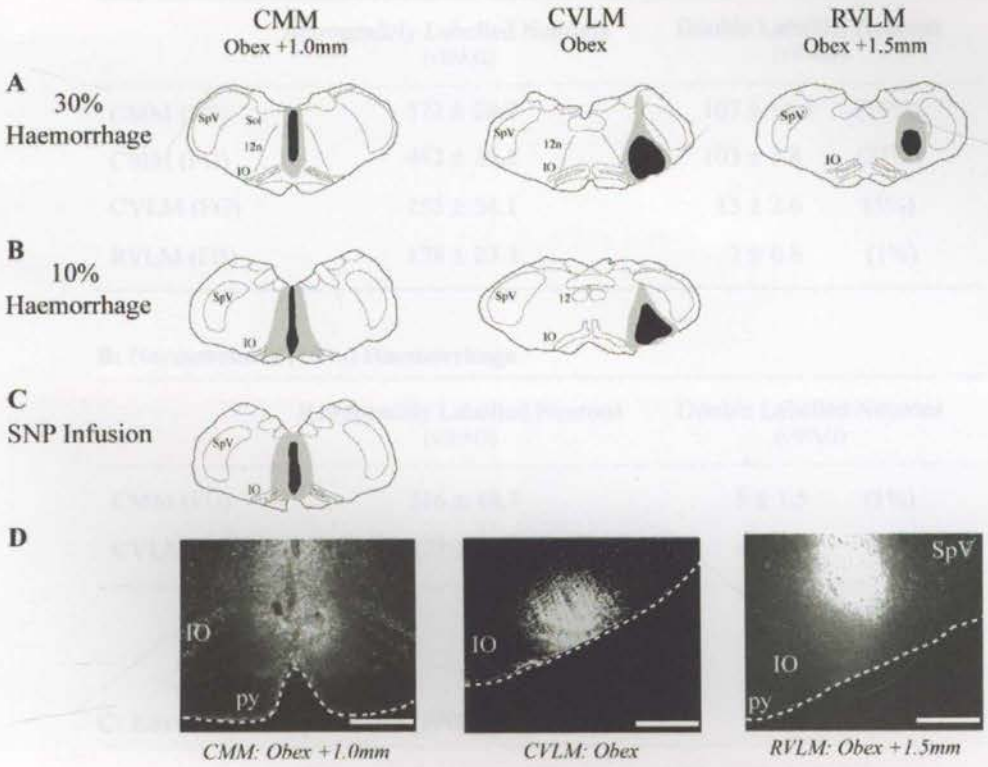

Figure 3.5
Rows A-C show camera lucida reconstructions of representative coronal sections of the medulla. A: representative sites of retrograde tracer injections made in CMM (FG), CVLM (FG) or RVLM (FB) of rats subjected to hypotensive (30%) haemorrhage. B: representative injection sites in CMM (FG) and CVLM (FG) of animals subjected to normotensive (10%) haemorrhage. C: representative injection site in the CMM (FG) of a rat subject to euvolaemic hypotension (SNP infusion). The sites of tracer injection are shown in black shading and the penumbra of spread in grey stippling. D: representative photomicrographs of retrograde tracer injections made in CMM (FG), CVLM (FG) or RVLM (FB). The scale bar indicates 1mm.

A: Hypotensive (30%) Haemorrhage

	Retrogradely Labelled Neurons (vlPAG)	Double Labelled Neurons (vlPAG)	
CMM (FB)	572 ± 28.2	107 ± 16.4	(19%)
CMM (FG)	482 ± 36.5	103 ± 7.8	(21%)
CVLM (FG)	255 ± 54.1	13 ± 2.6	(5%)
RVLM (FB)	178 ± 23.3	2 ± 0.8	(1%)

B: Normotensive (10%) Haemorrhage

	Retrogradely Labelled Neurons (vlPAG)	Double Labelled Neurons (vlPAG)	
CMM (FG)	516 ± 18.7	5 ± 1.5	(1%)
CVLM (FG)	237 ± 31.9	4 ± 1.3	(2%)

C: Euvolaemic Hypotension (SNP)

	Retrogradely Labelled Neurons (vlPAG)	Double Labelled Neurons (vlPAG)	
CMM (FG)	548 ± 22.6	14 ± 1.2	(3%)

Table 3.1
Summary of the proportions of double-labelled vlPAG neurons projecting to targetted medullary cardiovascular regions following: (i) hypotensive (30%) haemorrhage; (ii) normotensive (10%) haemorrhage; and (iii) euvolaemic hypotension (SNP infusion).

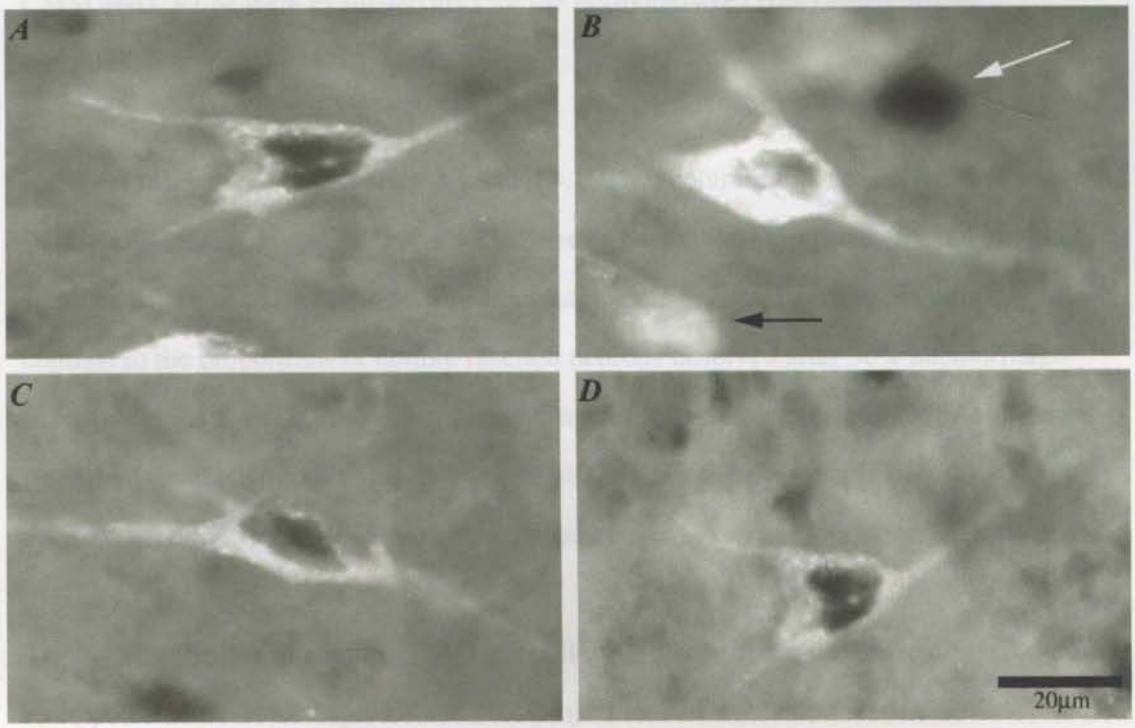

Figure 3.6
Photomicrographs A-D show vlPAG neurons in four individual animals. Fos-IR cells are identified by a darkly stained nucleus (nickel-enhanced diamino-benzidine). A single-labelled Fos-IR nucleus is indicated by the white arrow in plate B. CMM-projecting (retrogradely labelled) neurons are identified by their fluorescence under UV-light. The black arrow in plate B indicates a single labelled (CMM-projecting) vlPAG neuron. The scale bar in plate D shows 20um.

3.3.3 Medullary projections of vlPAG Fos-IR neurons following normotensive haemorrhage:

To determine whether the above patterns of double-label were specific to hypotensive haemorrhage, the numbers of double-labelled vlPAG neurons (FG/Fos) projecting to the CMM and CVLM were evaluated also for the normotensive (10%) haemorrhage condition.

Firstly, it can be seen (c.f., Tables 3.1A and 3.1B, left column) that the numbers of single (retrograde) labelled neurons in the normotensive haemorrhage experiments did not differ significantly from those in the 30% haemorrhage experiments. However, in striking contrast to the proportions of double-labelled neurons observed after 30% haemorrhage (c.f., Tables 3.1A and 3.1B, right column), very few medullary-projecting vlPAG neurons were double-labelled following 10% haemorrhage (CMM-projecting: hypotension, 21% vs normotension, 1%; CVLM-projecting: hypotension 5% vs normotension 2%).

To summarize, with respect to vlPAG (medullary-projecting) output neurons 'activated' by hypotensive haemorrhage, almost 90% project to the CMM and further the 'activation' of these neurons is specific to the decompensatory phase of the response. The relative contribution of CVLM-projecting vlPAG neurons is both smaller and less specific to decompensation.

3.3.4 Fos-IR in CMM-projecting vlPAG neurons following euvolemic versus hypovolemic hypotension:

In a final set of experiments the numbers of double-labelled neurons evoked by euvolemic (SNP infusion) versus hypovolemic hypotension were compared to determine the extent to which the 'activation' of CMM-projecting vlPAG neurons was a direct consequence of blood loss. A comparison of Figs 3.1B and 3.1C shows that the SNP

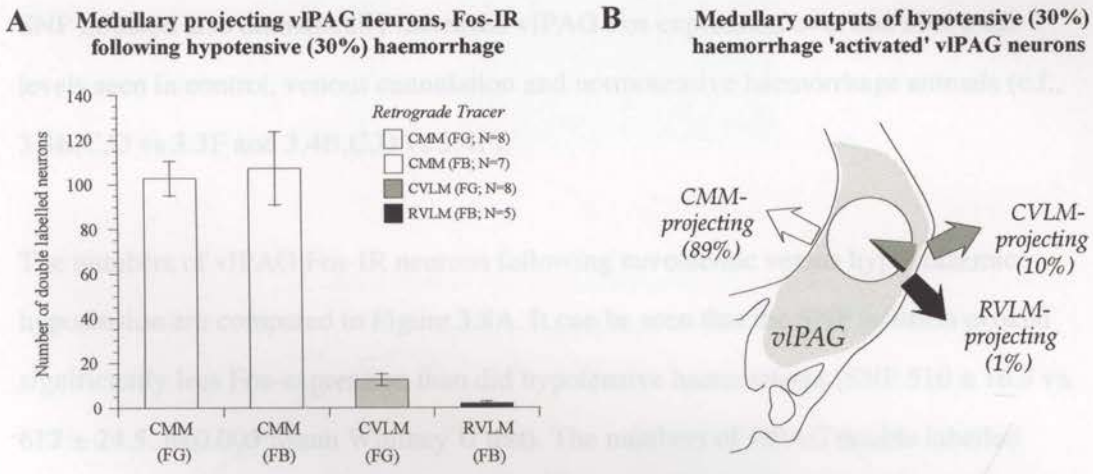

Figure 3.7

A: Bar graphs summarising the mean number (±SEM) of CMM- (FG: N=8, FB: N=7), CVLM- (FG: N=8) and RVLM- (FB: N=5) projecting vlPAG neurons which were also Fos-IR (i.e., double labelled) following 30% (hypotensive) haemorrhage. B: illustrates that the vast majority (89%) project to the caudal midline medulla (CMM).

infusion evoked a *maximal fall in AP* nearly identical in size (60.7±5 mmHg *vs* 62.5±2.7 mmHg) and duration (16.4±1.2 min *vs* 16.5±1.4 min) to that evoked by 30% haemorrhage.

Table 3.1C shows that the numbers of CMM-projecting vlPAG neurons were nearly identical to those of the previous experiments (c.f., Table 3.1A, 3.1B and 3.1C, left column). Figures 3.3 and 3.4 indicate that similar to hypotensive (30%) haemorrhage, SNP infusion also dramatically increased vlPAG Fos expression over and above the levels seen in control, venous cannulation and normotensive haemorrhage animals (c.f., 3.3B,C,D vs 3.3F and 3.4B,C,D vs 3.4F).

The numbers of vlPAG Fos-IR neurons following euvolaemic versus hypovolaemic hypotension are compared in Figure 3.8A. It can be seen that the SNP infusion evoked significantly less Fos-expression than did hypotensive haemorrhage (SNP 510 ± 16.3 vs. 612 ± 24.5. $p<0.005$ Mann Whitney U test). The numbers of vlPAG double labelled neurons are compared in Figure 3.8B. Note that in striking contrast to the large numbers of CMM-projecting vlPAG neurons double-labelled after a 30% haemorrhage, *very few CMM-projecting vlPAG neurons were double-labelled after SNP infusion*. In fact, the absolute difference in the numbers of double-labelled vlPAG neurons following 30% haemorrhage *versus* SNP infusion (103 ± 7.8 *vs* 14 ± 1.2; a *difference of 89 neurons*) (see Fig 3.8B and c.f., Table 3.1A and 3.1C, right columns) is remarkably similar to the difference in the numbers of Fos-IR vlPAG neurons following 30% haemorrhage *versus* SNP infusion (612 ± 24.5 *vs* 510.0 ± 16.3; a *difference of 102 neurons*) (see Figure 3.8A). In other words, compared to hypotension triggered by SNP infusion, the hypotension triggered by severe hypovolaemia (i.e., 30% tbv removal) *evoked Fos-expression in an additional group of vlPAG neurons (Figure 3.8A), ~90% of which project to the CMM* (Figure 3.8B).

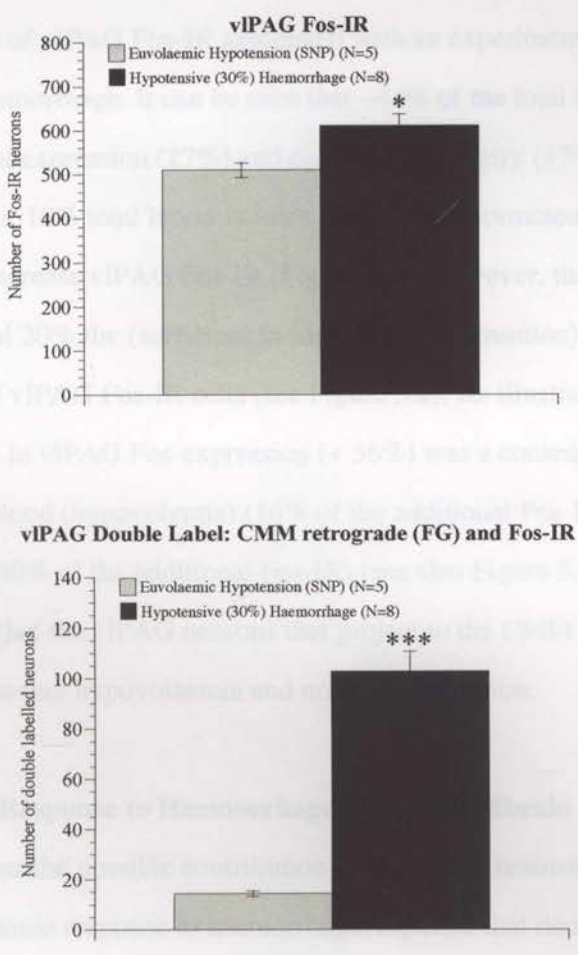

Figure 3.8
Bar graphs showing A: mean number (±SEM) of single labelled Fos-IR vlPAG neurons; and B: the mean number (±SEM) of double labelled (i.e., CMM-projecting, Fos-IR) neurons following euvolaemic hypotension evoked by SNP infusion (N=5) and 30% (hypotensive) haemorrhage(N=8). *p<0.05, ***p<0.005 (Mann-Whitney U-test).

3.4 Discussion

The major findings of this study are illustrated schematically in Figure 3.9. Figure 3.9A summarises the sources of vlPAG Fos-IR associated with an experimentally-induced, hypovolemic (30%) haemorrhage. It can be seen that ~44% of the total Fos-IR is due to the combination of basal expression (27%) and cannulation surgery (17%) (Figure 3.2). The initial withdrawal of 10% total blood volume (tbv) (i.e., a normotensive haemorrhage) did not increase vlPAG Fos-IR (Figure 3.2). However, the subsequent removal of an additional 20% tbv (sufficient to trigger decompensation) more than doubled the numbers of vlPAG Fos-IR cells (see Figure 3.2). As illustrated in Figure 3.9B this large increase in vlPAG Fos-expression (+ 56%) was a consequence of: (i) the removal of additional blood (hypovolemia) (16% of the additional Fos-IR); and (ii) the resultant hypotension (40% of the additional Fos-IR) (see also Figure 3.8A). Finally, Figure 3.9C illustrates that the vlPAG neurons that project to the CMM are activated almost exclusively by severe hypovolaemia and not by hypotension.

3.4.1 Haemodynamic Response to Haemorrhage: Role of Midbrain

The first study to address the possible contribution of the rostral brainstem/forebrain to the biphasic haemodynamic response to haemorrhage, reported that decompensation to a simulated haemorrhage (60% reduction in cardiac output evoked by gradual caval occlusion) in the rabbit, was blocked completely by a high mesencephalic decerebration (Evans et al., 1991). As the extent of midbrain damage was not evaluated histologically, the authors concluded cautiously that the integrity of a suprapontine site(s) was critical for haemorrhage-evoked decompensation. More recently (Troy et al., 2003) evaluated specifically the contribution of the midbrain by comparing the hemodynamic response to blood loss in precollicular decerebrate versus pre-trigeminal decerebrate rats. It was found that pre-trigeminal decerebration (removal of forebrain + midbrain) blocked the

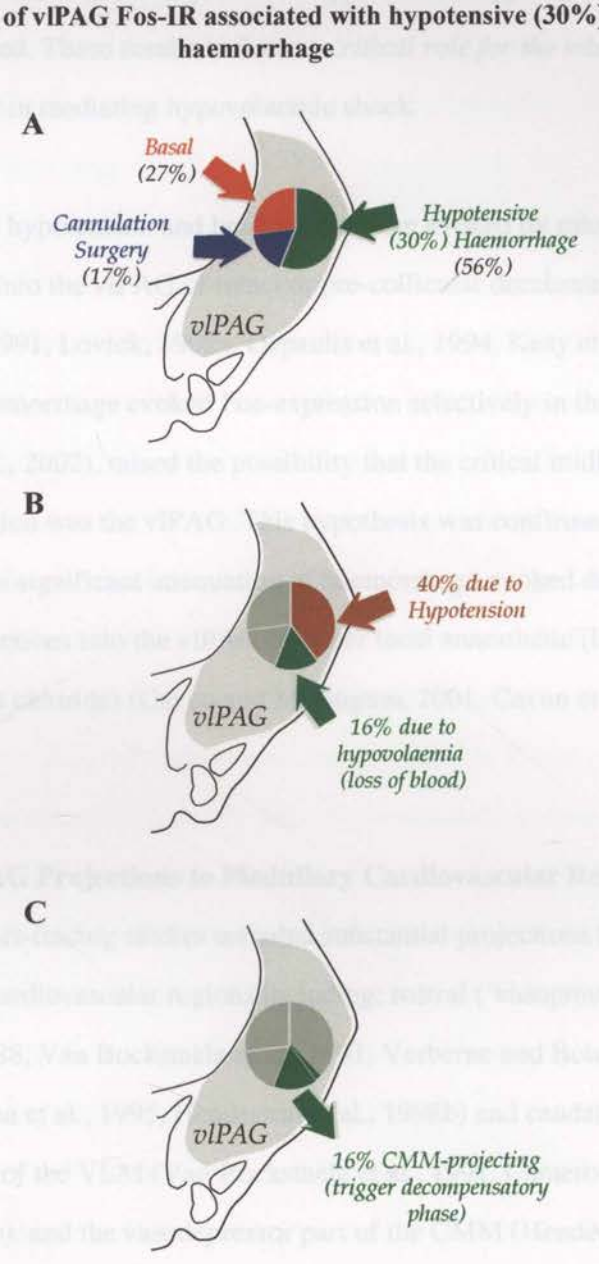

Figure 3.9
A: illustrates the sources of vlPAG Fos-IR associated with an experimentally-induced, 30% hypotensive haemorrhage. B: illustrates the increased vlPAG Fos-IR specific to hypotensive haemorrhage (30% tbv removal) is a consequence of both *hypovolaemia* and *hypotension*. C: illustrates that the vast majority of vlPAG neurons activated by severe *hypovolaemia*, but not by *hypotension*, project to the caudal midline medulla.

decompensatory response evoked by 30% haemorrhage; whereas after pre-collicular decerebration (removal of forebrain only) normal hypovolemic hypotension and bradycardia was observed. These results indicate a *critical role for the midbrain and its descending connections* in mediating hypovolaemic shock.

Earlier findings that: (i) hypotension and bradycardia were evoked by microinjection of excitatory amino acids into the vlPAG of intact or pre-collicular decebrate animals (Carrive and Bandler, 1991, Lovick, 1992a, Depaulis et al., 1994, Keay et al., 1997a); and (ii) hypotensive haemorrhage evoked Fos-expression selectively in the vlPAG (Keay et al., 1997b, Keay et al., 2002), raised the possibility that the critical midbrain region mediating decompensation was the vlPAG. This hypothesis was confirmed by later studies which reported a significant attenuation of haemorrhage-evoked decompensation after bilateral microinjections into the vlPAG of either local anaesthetic (lignocaine) or a synaptic blocker (cobalt chloride) (Cavun and Millington, 2001, Cavun et al., 2001, Dean, 2004).

3.4.2 Ventrolateral PAG Projections to Medullary Cardiovascular Regions:

Previous anatomical tract-tracing studies revealed substantial projections from the vlPAG to multiple medullary cardiovascular regions including: rostral ('vasopressor') (Lovick, 1985, Carrive et al., 1988, Van Bockstaele et al., 1991, Verberne and Boudier, 1991, Lovick, 1992b, Cameron et al., 1995, Henderson et al., 1998b) and caudal ('vasodepressor') parts of the VLM (Van Bockstaele et al., 1991, Cameron et al., 1995, Henderson et al., 1998b), and the vasodepressor part of the CMM (Henderson et al., 1998b). Somewhat surprisingly, given the extensive medullary outputs of the vlPAG, the results reported here indicate that haemorrhage-evoked haemodynamic changes are mediated by only a small subset of these projections. Specifically: (i) almost no vlPAG neurons selectively activated by severe hypovolemia projected to the rostral VLM; and

(ii) only a small number of vlPAG neurons selectively activated by severe hypovolemia projected to the caudal VLM; whereas (iii) nearly all vlPAG neurones selectively activated by severe hypovolemia (loss of 30% tbv) project to the CMM. *In other words, the sympathoinhibition and bradycardia triggered by severe blood loss depends critically on activation of CMM-projecting vlPAG neurons.*

Consistent with this conclusion are earlier findings that microinjection into the CMM of either local anaesthetic (lignocaine) or a synaptic blocker (cobalt chloride) respectively either blocked, or delayed and attenuated, haemorrhage-evoked decompensation (Henderson et al., 1998a, Henderson et al., 2000, Henderson et al., 2002, Heslop et al., 2002). Strikingly, such blockade of the CMM altered neither resting AP or HR, nor did it affect cardiovascular reflexes triggered by either baroreceptor-loading (i.v. phenylephrine) or activation of 5-HT3- sensitive cardiopulmonary afferents (i.v phenylbiguanide or serotonin) (Henderson et al., 2000). In this context the dramatic effects on haemorrhage-evoked decompensation suggest that CMM neurons are recruited only under special circumstances (i.e. injury-related/life-threatening challenges), the adaptive responses to which require more than basic homeostatic cardiovascular adjustments (see also Johansson, 1962). Injury-related signals from nociceptors in deep somatic and visceral structures are known to trigger sudden falls in both AP and HR (i.e., the so called *vaso-vagal* reactions). Such signals are likely to be relayed to the CMM, as its major afferents include inputs from: (i) spinal cord (laminae IV, V and X); (ii) spinal trigeminal nucleus, specifically the transition area between n. interpolaris and n. caudalis; and (iii) solitary tract nucleus, particularly ventrolateral and parasolitary subnuclei (Potas et al., 2003).

The efferent projections of the CMM have been studied recently using a combination of retrograde and anterograde tract tracing techniques (Heslop et al., 2004). The outputs via

which the CMM could mediate haemorrhage-evoked hypotension and bradycardia include projections to: (i) the VLM region which contains vagal (preganglionic) cardiac motor neurons; (ii) the caudal VLM region from which vasodepression can be evoked; (iii) regions containing sympathetic preganglionic neurons (i.e., the IML and to a lesser extent the IMM) in the upper thoracic (T1-T4) and thoraco-lumbar (T9-L2) spinal cord; and (iv) the rostral VLM region from which vasopressor responses can be evoked. The importance of the contributions of each of these pathways has yet to be established (although see Dean and Bago, 2002).

-Chapter 4-

Ascending medullary noradrenergic input to the ventrolateral PAG is critical for the expression of decompensation

4.1 Introduction

Previous studies suggest strongly that the sympathoinhibition, hypotension and bradycardia evoked by hypotensive haemorrhage in the conscious rat is likely mediated via a projecton from the vlPAG to the caudal midline medulla. Microinjection of excitatory amino acids made into the CMM produce both sympathoinhibitory and vasodepressor responses (Henderson et al., 1998, 2000, Heslop et al., 2002, Coleman and Dampney 1995, 1998). As well, inactivation of the CMM with both lignocaine and cobalt chloride has been shown to abolish the hypotension and bradycardia evoked by severe haemorrhage (Henderson et al., 2000, 2002, Heslop et al., 2002). The anatomical studies carried out in the preceding chapter fit well with these reports by showing that CMM projecting vlPAG neurons are activated exclusively by severe hypovolaemia. Still unknown, however, are the afferent pathway(s) which are responsible for depolarising the population of CMM-projecting, vlPAG neurons which trigger decompensation.

As discussed in chapter 1 (section 1.11), early studies in the cat showing that haemorrhage-evoked hypotension was preceded by increased activity of left ventricular cardiac mechano-sensitive vagal afferents led to the hypothesis that decompensation is triggered by a combination of poor diastolic atrial filling, and subsequent contraction of

the myocardium around poorly filled ventricles (Pearce and Henry 1955, Oberg and Thoren 1970, 1972, 1973). This hypothesis (that signals arising from cardiac vagal afferents were responsible for triggering decompensation) gained further support when it was shown that bilateral cervical vagotomy delays the onset of decompensation in the unanaesthetised rabbit (Evans et al., 1994), and abolishes haemorrhage-evoked sympathoinhibition in the unanaesthetised rat (Skoog et al., 1985, Thoren et al., 1988, Togashi et al., 1990). However, recent work showing that: (i) blockade of cardiac spinal afferents with pericardial procaine infusion abolishes decompensation; and (ii) selective cardiac spinal deafferentation (achieved by bilateral stellate ganglionectomy) *but not* selective cardiac vagal deafferentation (achieved by bilateral vagal sensory rhizotomy) significantly delays the onset of decompensation (Troy et al., in press) has raised the possibility that haemorrhage-evoked hypotension may be triggered by signals arising from the heart which are carried by spinal rather than vagal afferents.

Despite these new insights into the peripheral triggers responsible for triggering decompensation, the neuroanatomical pathway through which cardiac afferents (spinal and/or vagal) convey signals from the heart to the ventrolateral PAG remains unknown. Cardiac vagal afferents from the heart terminate within the nucleus of the solitary tract; a central sensory relay nucleus critical for integrating multiple afferent inputs relating to autonomic function (Spyer 1994). Increased numbers of Fos-like immunoreactive neurons have been observed in the NTS following hypotensive haemorrhage (Dun et al., 1993, Buller et al., 1999, Chan and Sawchenko 1994, Chan and Sawchenko 1998). As well, a significant number of catecholaminergic NTS neurons (i.e., those belonging to

either the A2 and/or C2 cell groups) have been found to express Fos protein following hypotensive haemorrhage (Buller et al., 1999, Chan and Sawchenko 1994) suggesting that catecholaminergic neurons within the NTS may play a critical role in triggering decompensation.

Cardiac afferent projections to the spinal cord terminate in the superficial dorsal horn within thoracic spinal segments T2-T6 (White 1933, Meller and Gebhart 1992). Significant brainstem projections arising from superficial spinal cord laminae (lamina 1) have been widely reported. Of particular interest, double-label studies performed in the primate have revealed that ascending neurons within the superficial dorsal horn form direct mono-synaptic connections with A1 noradrenergic neurons (Westlund and Craig 1996); a brainstem cell group known to be critical for eliciting appropriate neuro-endocrine responses to stressful stimulation (Blessing et al., 1980, Day and Sibbald 1990, Sawchenko et al., 1996).

Ventrolateral medullary A1 neurons are 'activated' (i.e., express Fos-IR) following severe hypotension (evoked by haemorrhage and/or graded vena caval occlusion) in both conscious and anaesthetised rats (Buller et al., 1999, Chan and Sawchenko 1994, Chan and Sawchenko 1998). As well, much evidence has been gathered to suggest that A1 catecholaminergic neurons play an important role in mediating the neuro-endocrine response to severe hypovolaemia (Buller et al., 1999, Gieroba et al., 1994, Head et al., 1997). Haemorrhage in the conscious, unrestrained rat and rabbit has been shown to evoke Fos-expression in PVN-projecting medullary catecholaminergic cells, suggesting

that A1 neurons are critical for the regulation of post-haemorrhagic vasopressin release (Gieroba et al., 1992, Day 1989, Lightman et al., 1994).

In addition to providing direct input to hypothalamic nuclei involved in regulating vasopressin release, previous anatomical reports suggest that catecholaminergic neurons located in the lower brainstem project also to the periaqueductal gray (Herbert and Saper 1992). Following large injections of retrograde tracer in the midbrain PAG, significant numbers of double-labelled (PAG-projecting and catecholaminergic) neurons are observed in the region(s) of A1, A2, C1 and C3 cell groups. Further experiments utilising immunohistochemistry directed against phenylethanolamine-N-methyltransferase (PNMT) enabled the authors to conclude that the PAG receives significant input from noradrenergic neurons in both the ventrolateral medulla (A1) and nucleus of the solitary tract (A2), as well as from adrenergic neurons arising from the C1 and C3 cell groups.

Unfortunately, the midbrain PAG injections of retrograde tracer made in the above study were not confined to any one PAG column. As discussed in chapter one, the PAG appreciates a high degree of anatomical specialisation. Neurons located lateral to the aqueduct produce behavioural and cardiovascular excitation when injected with an excitatory amino acid (DLH; hyper-reactivity, hypertension, tachycardia). Conversely, neurons located ventrolateral to the aqueduct produce behavioural and cardiovascular depression (hyporeactivity, quiescence, hypotension, bradycardia). Earlier findings that: (i) hypotension and bradycardia are evoked following microinjection of excitatory amino acids into the vlPAG; (ii) hypotensive haemorrhage selectively evokes Fos-expression in

the ventrolateral PAG; and (iii) haemorrhage-evoked decompensation is significantly attenuated following bilateral microinjection of the local anaesthetic lignocaine or cobalt chloride (an inhibitor of synaptic transmission), strongly suggests that the ventrolateral PAG mediates the decompensatory phase of haemorrhage. If A1 and/or A2 noradrenergic neurons do form part of the afferent pathway responsible for triggering decompensation, naturally one would expect there to be significant and specific projections from these regions onto the vlPAG.

Therefore, the following experiments were performed in order to define possible central afferent pathway(s) responsible for triggering decompensation. An initial series of experiments was designed to quantify the relative pattern of 'activation' (i.e., Fos-IR) of medullary catecholaminergic cell groups following: (i) normotensive (10%) haemorrhage; (ii) hypotensive (30%) haemorrhage; and (iii) euvolaemic hypotension (peripherally-mediated hypotension evoked by sodium nitroprusside infusion). The outcome of these data will provide a valuable first step in evaluating whether decompensation might be triggered by afferent signals arising from medullary catecholaminergic neurons, or whether the activation of such cells, as previously reported by other authors, can be attributed to either: (i) the initial compensatory period of haemorrhage; or (ii) occurring secondary to the fall in AP evoked by severe blood loss.

In a second series of experiments, a combination of retrograde tracer microinjections, *restricted* to the ventrolateral PAG, and immunohistochemical techniques for tyrosine hydroxylase (TH) and phenylethanolamine-*N*-methyltransferase (PNMT) was used to

determine the distribution of medullary catecholaminergic projections to the ventrolateral PAG.

4.2 Materials and Methods – Experimental Series I

4.2.1 Animals and Surgery: Data were obtained from 14 male Sprague-Dawley rats (250-350 grams) in accordance with animal care and ethics protocols (see chapter 2). Prior to surgery all animals were housed in groups of six, kept on a 12 hour light/dark cycle, and had access to food and water *ad libitum.*

4.2.2 Cannulation Procedures: Each of the 14 rats were cannulated for subsequent removal of blood. Each rat was anaesthetised with halothane (2%) and a cannula placed into the right external jugular vein. The cannula (PE tubing, OD= 0.96mm, with a 32mm silastic tip OD= 1.19mm) was passed subcutaneously and exteriorised in the interscapular region. Following cannulation, anaesthesia was discontinued and each animal was given antibiotics (Norocillin, 150mg/kg, i.m.) and fluids (2ml, 0.9% saline i.p.) and returned to its home cage.

4.2.3 Haemorrhage Protocol: Twenty four hours following venous cannulation each rat underwent one of three procedures:

(i) *Normotensive haemorrhage*: withdrawal of 10% total blood volume (t.b.v.) over 10 min. Ten percent (10%) total blood volume is equivalent to withdrawal of 8ml/kg.

(ii) *Hypotensive haemorrhage*: withdrawal of 30% t.b.v. over 20 min (10% over 10 minutes, followed by the removal of an additional 20% over the

subsequent 10min). Thirty percent (30%) total blood volume is equivalent to 24ml/kg.

(iii) *Euvolaemic hypotension*: infusion of sodium nitroprusside, a peripheral vasodilator (1mg/ml solution: 30μl/min over 20 min). As described in the previous chapter this rate of infusion evokes a hypotension identical in size and duration to that evoked by 30% haemorrhage.

Two hours later each animal was deeply anaesthetised (sodium pentobarbital, 90mg/kg i.v.) and rapidly perfused (transcardially) with 500ml of 0.9% saline followed by 500ml of ice cold fixative (4% paraformaldehyde in borate-acetate buffer, pH 9.6). The brains were removed, post-fixed for 4 hours in the same fixative, then cryoprotected for at least 3 days in 10% sucrose in 0.1M phosphate buffer.

4.2.4 Immunohistochemistry: Serial coronal sections of the medulla were cut on a freezing microtome (50μm, one in five series), from the level of the spino-medullary junction to the caudal border of the pons. Free floating sections were initially permeabilised for thirty minutes in 50% alcohol before being washed in 3% H_2O_2 in 50% ethanol. The sections were then rinsed for fifteen minutes in phosphate buffered saline (PBS, pH 7.4) and blocked for ten minutes in 1% phosphate buffered saline horse serum (PBH) before being incubated in rabbit polyclonal antibody to Fos protein (1:2000 dilution in 1% PBH), for 24 hours at 4°C. Following the primary incubation period, the sections were washed in 0.1M PBS for thirty minutes before being incubated for 2 hours at room temperature in biotinylated horse anti-rabbit IgG in a 1:500 dilution with PBH.

After this incubation, the sections were again washed for thirty minutes in 0.1M PBS before being incubated in a 1:1000 dilution of Extravidin peroxidase (in PBS) for 2 hours at room temperature. A final fifteen minute wash in PBS followed this incubation before the sections were placed in 15ml of DAB mix, containing 10mg diaminobenzidine, 0.2ml of 0.4% ammonium chloride in 0.1M phosphate buffer (pH 7.4), 0.2ml of 20% D-glucose in 0.1M phosphate buffer (pH 7.4), and 100µl of NiCl, on ice for 10 minutes. Fifteen microliters (15µl) of glucose oxidase was added to the DAB mix to initiate the chromogenic reaction, which was terminated with three rinses in 0.1M PBS when either Fos-immunoreactive cells were observed under a light microscope, or the background staining became prominent.

Following the initial chromogenic reaction to reveal Fos positive medullary nuclei, the sections were re-incubated in either mouse anti-tyrosine-hydroxylase (Santa Cruz CA; 1:5000 dilution in 1% PBH), or rabbit anti-phenyl-*N*-methyl-transferase (Santa Cruz; PNMT, 1:1000 dilution in 1% PBH) at 4°C for three days.

Following re-incubation in primary antibody, the sections were washed in 0.1M PBS for thirty minutes before being incubated for 2 hours at room temperature in either biotinylated anti-mouse IgG; or biotinylated anti-rabbit IgG, in a 1:500 dilution with PBH. After this incubation, the sections were again washed for thirty minutes in 0.1M PBS before being incubated in a 1:1000 dilution of Extravidin peroxidase (in PBS) for 2 hours at room temperature. A final fifteen minute wash in PBS followed before the sections were placed in 15ml of solution containing 3-amino, 9-ethylcarbazole (AEC; in

5% dimethylformamide and 95% 50mM acetate buffer). The reaction was initiated with H_2O_2 and terminated when neurons reactive for either TH or PNMT were visualised under the light microscope.

Reacted sections were immediately mounted onto twice dipped gelatinised slides, air dried, briefly immersed in glycerol (50% in PBS), and coverslipped with glycerol gelatin.

4.2.5 Materials and Methods – Experimental Series II

All experiments were carried out following the guidelines of the NHMRC/CSIRO/AAA "Code of Practice for the Care and Use of Animals in Research in Australia" and with the approval of the University of Sydney Animal Ethics Committee. Prior to surgery animals were housed in groups of six, kept on a 12 hour light/dark cycle, and had access to food and water *ad libitum*.

4.2.6 Animals and Surgery: Data were obtained from 6 male Sprague-Dawley rats (250-350 grams). Rats were sedated by brief exposure to CO_2 then anaesthetised with an intramuscular injection of ketamine/xylazine (ketamine hydrochloride 75mg/kg:Rompun 4ml/kg) before being fixed in a stereotaxic frame in the "flat-skull" position. Body temperature was maintained at 37°C with a thermoregulatory heating blanket.

4.2.7 vlPAG Retrograde Tracer Microinjections: Retrograde tracer (cholera toxin subunit B (CTb) 1%) was pressure injected into the ventrolateral PAG (for review see Bandler and Keay 2004). Injections were made via an automated air pressure system that applied brief air pulses (10ms) to the pipette barrel. To control the volume of injectate the level of the meniscus in the micropipette was monitored with a calibrated graticule in a dissecting microscope. Coordinates with respect to Bregma were *antero-posterior*; 12 mm caudal, *mediolateral*; 0.6-0.8mm and *dorsoventral*; 5.5mm. All injections were made at a caudal to rostral angle of 30° to prevent leakage of tracer into the dorsally adjacent lateral and dorsolateral PAG columns. Each injection was made slowly over a period of 30 minutes after which time the pipette remained *in situ* for a further 10 minutes. Each animal was subsequently removed from the stereotaxic frame, sutured and treated with antibiotics (Norocillin, 300mg/kg i.m.). The activity, eating, drinking and grooming behaviour of each rat was closely monitored for the duration of the recovery period, which lasted 7 days.

4.2.8 Perfusion and Tissue Processing: Seven days following vlPAG injection of retrograde tracer each animal was sedated with a brief exposure to CO_2 before being deeply anaesthetised with a 1.0ml intraperitoneal injection of Nembutal (60mg/kg). Each animal was subsequently perfused with 500ml 0.9% saline followed by 500ml of ice cold fixative (4% paraformaldehyde in phosphate buffer pH 7.4). The brain of each animal was removed and postfixed overnight in fixative before being transferred to a 30% sucrose solution and cryoprotected for 3-4 days. Serial 50μm thick coronal sections of the

midbrain were cut on a freezing microtome to identify the location and extent of each vlPAG CTB retrograde tracer injection site.

4.2.9 Fluorescent Immunohistochemistry: Serial coronal sections of the medulla were cut on a freezing microtome (50μm, one in five series) from the level of the spino-medullary junction to the caudal border of the pons. Free floating sections were initially washed in phosphate buffered saline (0.1M, pH 7.4) for thirty minutes before being permeabilised with a 30min wash in 50% ethanol. The sections were then rinsed for fifteen minutes in fresh PBS and blocked for ten minutes in phosphate buffered saline horse serum (PBH, 1% with 0.1% Triton-X 100) before being incubated for 72hr at 4°C in a cocktail of goat anti-choleragenoid (1:2000 dilution) and either mouse anti-tyrosine hydroxylase (1:500 dilution) or rabbit anti-phenylethanolamine-N-methyltransferase (PNMT; 1:500 dilution) made up in PBH.

Seventy two hours later the sections were washed for thirty minutes in PBS before being incubated in a cocktail of donkey anti-goat IgG conjugated to Cy-3 (1:200 dilution), and either biotinylated horse anti-mouse IgG (1:500 dilution) or biotinylated horse anti-rabbit IgG (1:500 dilution) made up in PBH for 2hrs at room temperature. The sections were then washed for thirty minutes in PBS before being incubated a final time in Cy-5 conjugated streptavidin (1:500 dilution made up in PBH) for 2hrs at room temperature. Once completed the sections were rinsed for fifteen minutes in PBS, mounted onto twice dipped gelatinised slides and coverslipped with a 50:50 mix of PBS and glycerol.

4.2.10 Analysis – Experimental Series I: For each rat, both the number of single labelled (Fos-IR, TH-IR, and PNMT-IR) and double labelled (Fos/TH and Fos/PNMT) neurons were counted in the nucleus of the solitary tract (NTS) and the ventrolateral medulla (VLM) of individual 50μm coronal sections at seven equidistant medullary levels (-1.0mm, -0.5mm, 0mm, 0.5mm, 1.0mm, 1.5mm, and 2.0mm relative to Obex). The rostral and caudal limits of medullary catecholaminergic cell groups were chosen based on values given in the chemoarchitectonic atlas of the rat brainstem (Paxinos et al., 1999), and on previous studies (Buller et al., 1999, Chan and Sawchenko 1994, Chan and Sawchenko 1998, Chan and Sawchenko 2000, Dayas et al., 2001a, Dayas et al., 2001b). All data are expressed as mean ± SEM for each region based on the combined data from each group of animals.

The ventrolateral medulla and nucleus of the solitary tract are known to contain a mixed, intermingling population of adrenergic and noradrenergic neurons. PNMT is known only to occur in adrenergic cells whereas TH is an immunohistochemical marker for both adrenergic and noradrenergic cells. Thus, the number of noradrenergic neurons was approximated by subtracting the number of PNMT-positive neurons in one section from the number of TH-positive neurons in an immediately adjacent section. The validity of this method is supported by findings that in regions of the brain known to contain adrenergic neurons only (i.e., those cells immunoreactive for PNMT), the number of TH-positive neurons is almost identical (for details see Buller et al., 1999).

For each group, the total number of neurons between experimental groups were compared using non-parametric statistics (Mann-Whitney U-test); $P < 0.05$ was considered significant. Between-group comparisons were made relative to animals subject to normotensive (10%) haemorrhage. The validity of these comparisons is supported by data presented in Chapter 3 which shows that there is no significant difference in the number of Fos-like IR neurons observed in: (i) naïve controls; (ii) animals subject to venous cannulation only; and (iii) animals subject to normotensive (10%) haemorrhage. That is, venous cannulated controls were not used in this instance since the levels of Fos expression in naïve controls, and the venous cannulated group, and the normotensive (10%) haemorrhage group are indistinguishable.

Representative sections were plotted under a light microscope with camera lucida attachment before being reconstructed onto standard atlas sections. Representative photomicrographs were taken with an Olympus microscope (BX 51) and compiled using Adobe Photoshop software.

4.2.11 Analysis – Experimental Series II: The numbers of single-labelled (TH-immunoreactive, PNMT-immunoreactive and CTb-immunoreactive) and double-labelled (TH-IR/Ctb-IR and PNMT-IR/Ctb-IR) neurons were counted (bilaterally) in seven equi-distant coronal sections (–1.0, -0.5, 0, +0.5, +1.0, +1.5, +2.0mm relative to Obex) in both the ventrolateral medulla and nucleus of the solitary tract. Both the ventrolateral medulla and NTS are known to contain a mixed population of adrenergic and noradrenergic neurons. PNMT is known only to occur in adrenergic cells whereas TH is an

immunohistochemical marker for both noradrenergic and adrenergic cells. Thus the number of noradrenergic neurons was approximated by subtracting the number of PNMT-positive neurons in one section from the number of TH-positive neurons in an immediately adjacent section. This method is supported by the report that in regions of the brain known to contain adrenergic neurons only, the number of TH-positive neurons is almost identical (for details see Buller et al., 1999). The presence of fluorescent label (Cy-3 and Cy-5) in neurons was determined under fluorescent illumination at 20x magnification. Double-labelled neurons were identified by switching between filters appropriate for excitation of Cy-3 and Cy-5 fluorophores.

4.3 Results – Experimental series I

Ventrolateral Medulla:

4.3.1 Fos-expression following normotensive (10%) haemorrhage, hypotensive (30%) haemorrhage, and euvolaemic hypotension (SNP infusion):

Representative photomicrographs showing examples of Fos-like immunoreactivity (Fos-IR) following normotensive (10%) haemorrhage, hypotensive (30%) haemorrhage, and euvolaemic hypotension at caudal and rostral levels of the VLM are shown in Figure 4.1. Figures 4.2a-4.2c show camera lucida reconstructions of the location of Fos-IR neurons in seven equidistant medullary coronal sections (-1.0mm, -0.5mm, 0mm, +0.5mm, +1.0mm, +1.5mm, +2.0mm relative to Obex) evoked by: **A** normotensive (10%) haemorrhage; **B** hypotensive (30%) haemorrhage; and **C** euvolaemic hypotension (i.v. infusion of sodium nitroprusside; SNP). The histogram in Figure 4.3 summarises the mean number (±SEM) of Fos-IR neurons observed in the ventrolateral medulla (VLM) evoked by each manipulation. As seen in Figure 4.3 similar numbers of Fos-IR neurons were evoked in the VLM by both normotensive (10%) haemorrhage and euvolaemic hypotension (SNP infusion) (114.0±17.4 and 130.1±22.3 respectively). In contrast, hypotensive (30%) haemorrhage evoked significantly more Fos-IR neurons in the VLM (248.1±23.5; $P<0.05$ Mann-Whitney U-test) compared to both normotensive (10%) haemorrhage and SNP infusion. Inspection of Figure 4.2 reveals that the increase in Fos-IR seen following hypotensive (30%) haemorrhage relative to both (10%) haemorrhage and euvolaemic hypotension was most pronounced at levels caudal to the Obex (i.e., in the region of the A1 cell group).

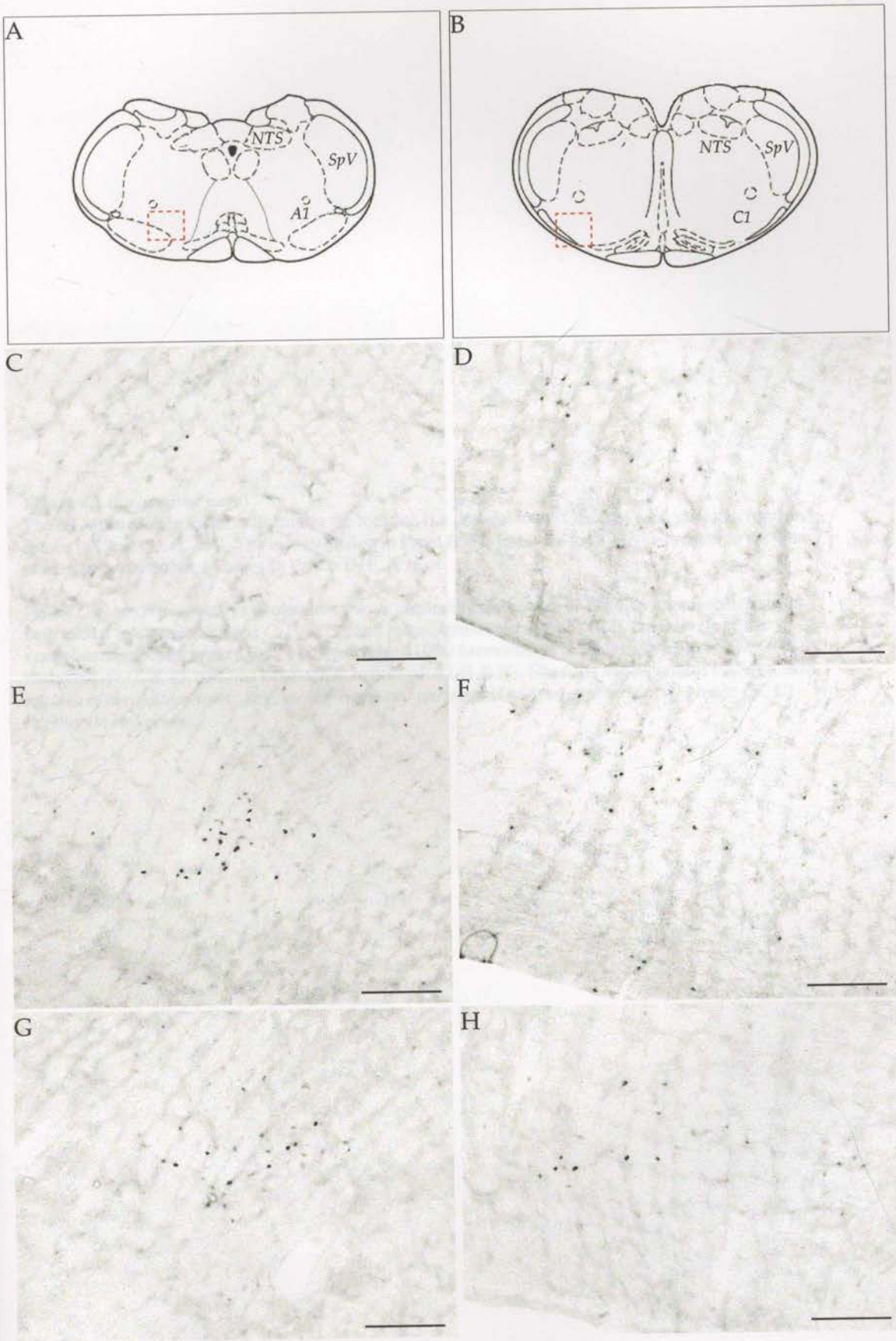
A
NTS
SpV
A1
B
NTS
SpV
C1
C
D
E
F
G
H

Figure 4.1 (*on opposite page*)
The reconstruction in Panel A illustrates the location (i.e., caudal to the Obex) of each photomicrograph shown in Panels C, E, & G. The reconstruction in Panel B illustrates the location (i.e., rostral to the Obex) of each photomicrograph shown in Panels D, F, & H.

Panels C-H are representative photomicrographs illustrating the pattern of Fos-like immunoreactivity at both caudal (photomicrographs C, E, & G), and rostral (photomicrographs D, F, & H) levels of the ventrolateral medulla evoked by: (i) normotensive (10%) haemorrhage (C & D); (ii) hypotensive (30%) haemorrhage (E & F); and (iii) euvolaemic hypotension (G & H). The scale bar represents 0.25mm. *NTS, nucleus of the solitary tract; SpV, spinal trigeminal nucleus; A1, A1 noradrenergic cell group; C1, C1 adrenergic cell group.*

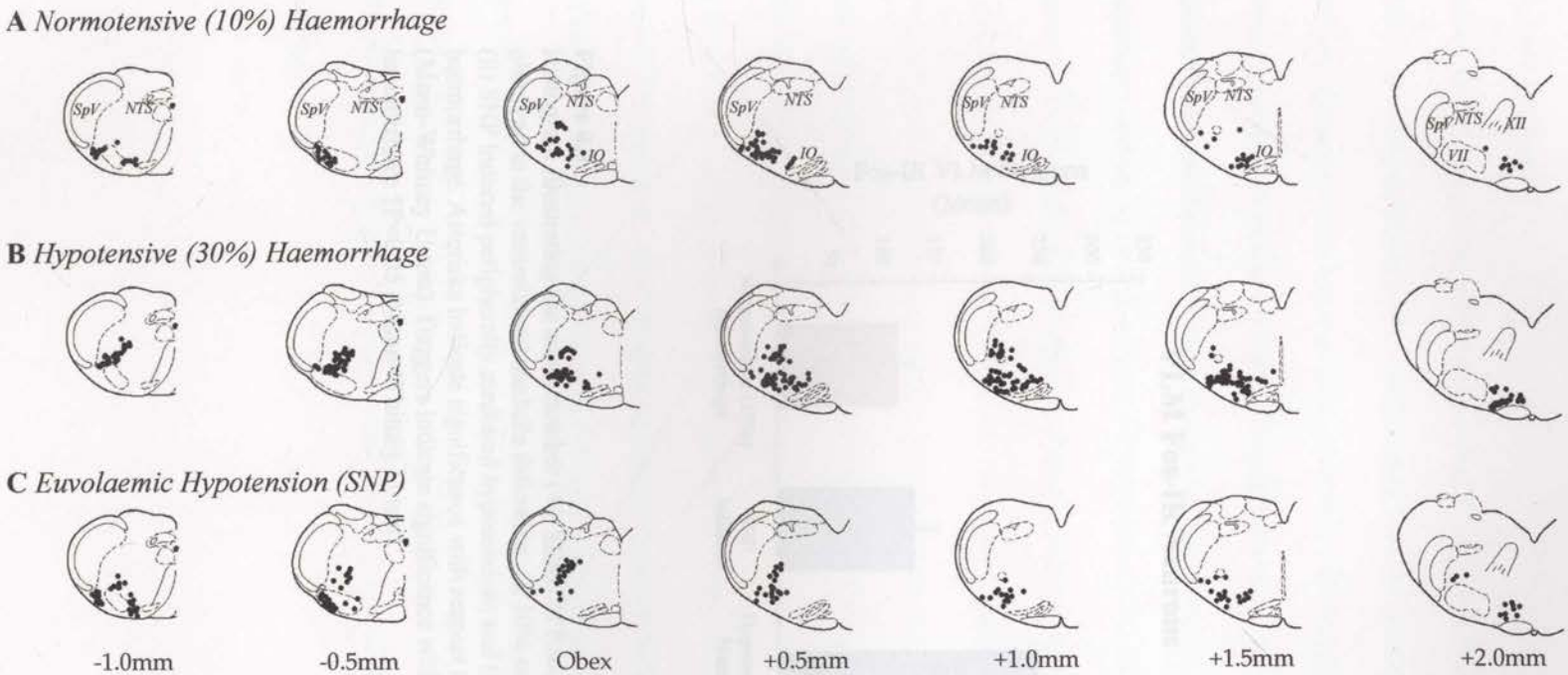

Figure 4.2
Representative camera lucida reconstructions of seven equidistant coronal sections through the ventrolateral medulla showing the location of Fos immunoreactive neurons evoked by **A** normotensive (10%) haemorrhage, **B** hypotensive (30%) haemorrhage, and **C** infusion of the peripheral vasodilator sodium nitroprusside (SNP). The rostro-caudal level of each section is indicated relative to Obex (calamus scriptorius). *SpV, spinal trigeminal nucleus; IO, inferior olivary nucleus; NTS, nucleus of the solitary tract; XII, hypoglossal nerve; VII, facial nucleus.*

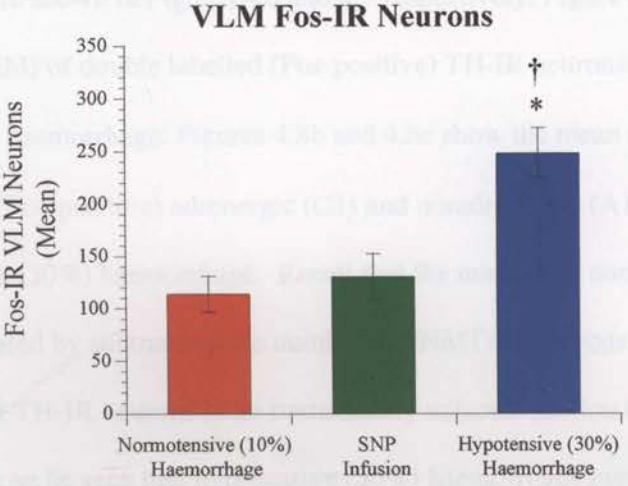

Figure 4.3
Histogram illustrating the mean number (+/- SEM) of Fos-immunoreactive nuclei observed in the ventrolateral medulla following: (i) 10% normotensive haemorrhage; (ii) SNP induced peripherally mediated hypotension; and (iii) 30% hypotensive haemorrhage. Asterisks indicate significance with respect to SNP infusion *P<0.05 (Mann-Whitney U-test). Daggers indicate significance with respect to 10% haemorrhage †P<0.05 (Mann-Whitney U-test).

4.3.2 VLM catecholaminergic neurons which express Fos-IR following hypotensive (30%) haemorrhage:

Representative photomicrographs showing double labelled TH-immunoreactive (TH-IR) and PNMT-immunoreactive (PNMT-IR) neurons are shown in Figures 4.4 and 4.5 respectively. Camera lucida reconstructions showing the location of double labelled TH-IR neurons, and double labelled PNMT-IR neurons at each rostrocaudal level of the medulla analysed are shown in Figures 4.6 and 4.7 respectively. Figure 4.8a shows the mean number (±SEM) of double labelled (Fos-positive) TH-IR neurons evoked by hypotensive (30%) haemorrhage. Figures 4.8b and 4.8c show the mean number (±SEM) of double labelled (Fos-positive) adrenergic (C1) and noradrenergic (A1) neurons evoked also by hypotensive (30%) haemorrhage. Recall that the number of noradrenergic (A1) neurons was estimated by subtracting the number of PNMT-IR neurons in one section from the number of TH-IR neurons in an immediately adjacent section (for details see Methods 4.2.5). It can be seen that hypotensive (30%) haemorrhage evoked substantial numbers of Fos-positive, catecholaminergic cells in the ventrolateral medulla (Figure 4.8a; 174 ± 18.0). Only a small number of these double-labelled catecholaminergic neurons were found to belong to the C1 (adrenergic) cell group (35.4 ± 8.3; Figure 4.8b). In striking contrast, the vast majority of calculated A1 noradrenergic neurons (86%) were found to express Fos-IR following hypotensive (30%) haemorrhage (150 ± 7.9 cells; Figure 4.8c).

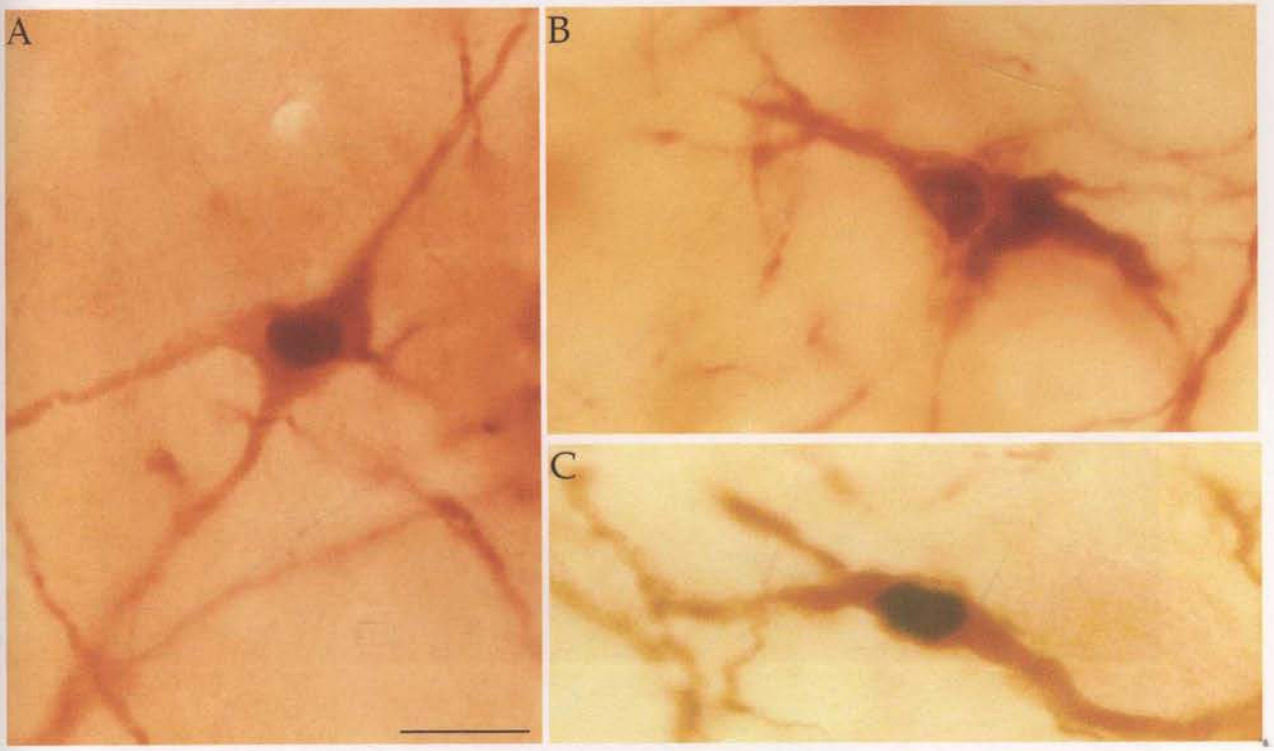

Figure 4.4
High power photomicrographs illustrating three different tyrosine hydroxylase immunoreactive neurons located in the ventrolateral medulla which express Fos protein following hypotensive (30%) haemorrhage. These neurons were located between 1.0mm and 1.5mm caudal to the Obex (Calamus Scriptorius) and are therefore presumed to belong to the A1 noradrenergic cell group. The scale bar represents 20μm.

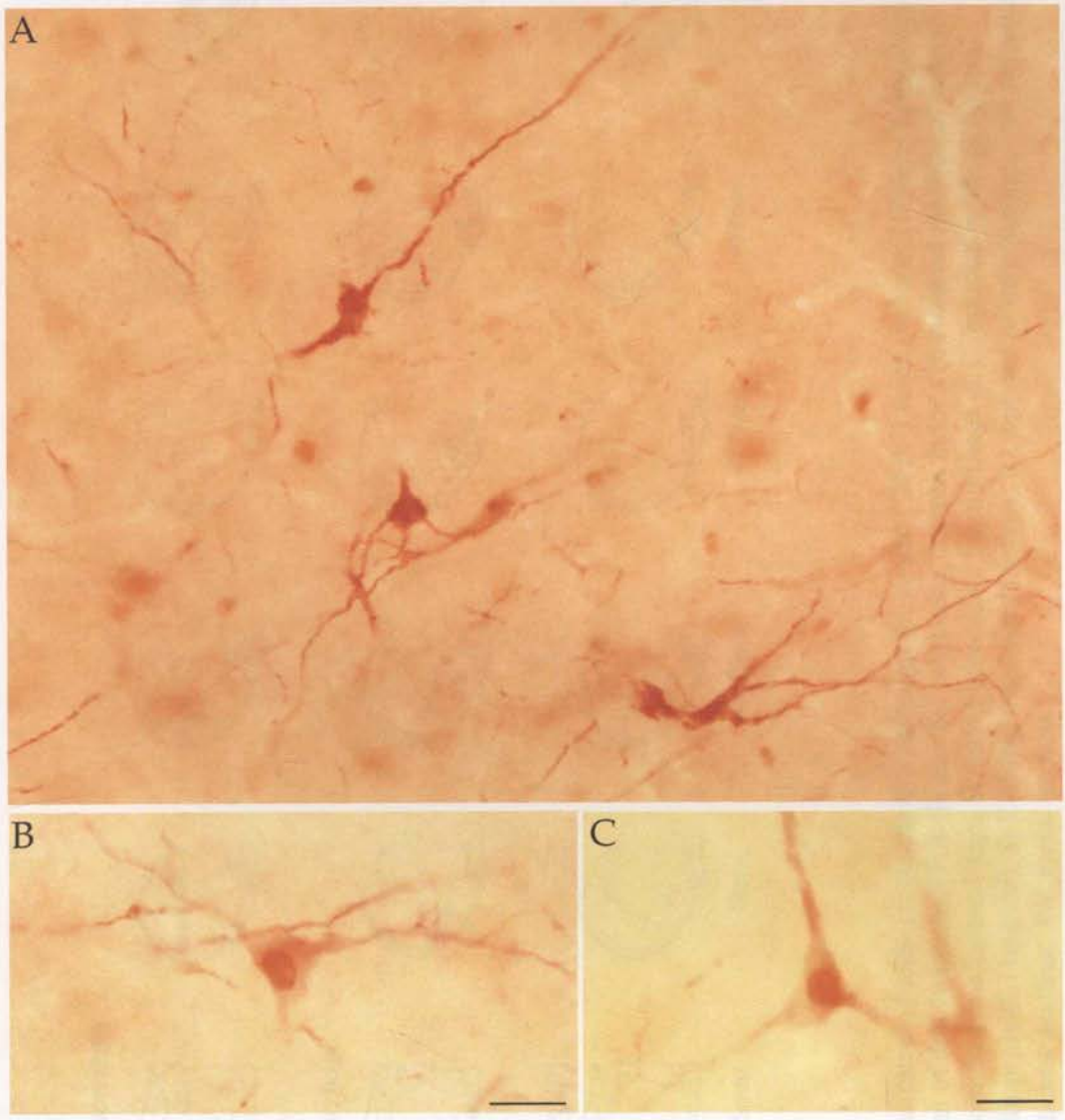

Figure 4.5
Photomicrographs taken of the rostral ventrolateral medulla showing: **A**. three C1 adrenergic (i.e., phenylethanolamine-N-methyltransferase immunoreactive) neurons which *do not* express Fos-like IR following hypotensive (30%) haemorrhage; **B & C**. high power photomicrographs of double labelled (i.e., Fos-positive and phenylethanolamine-N-methyltransferase immunoreactive) C1 adrenergic neurons evoked by hypotensive (30%) haemorrhage. The scale bar represents 20μm.

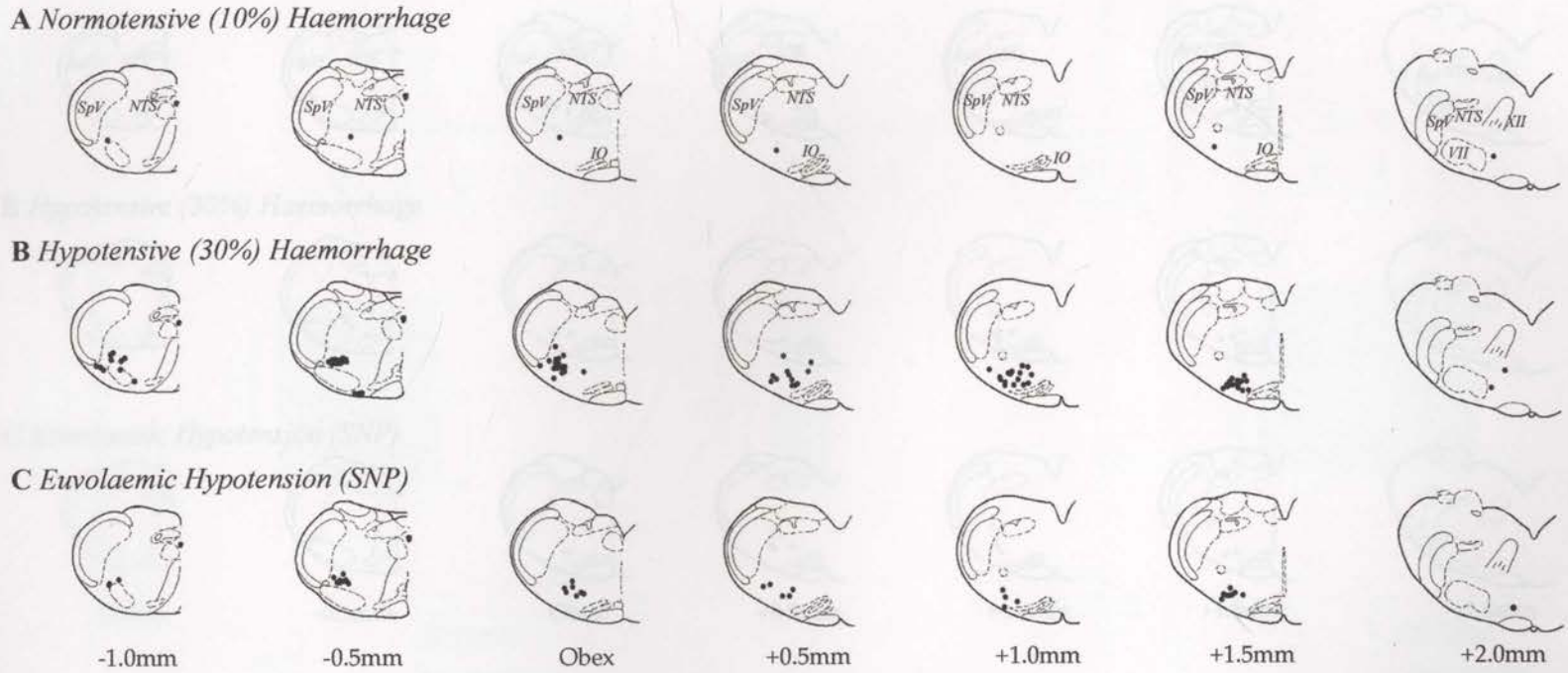

Figure 4.6
Representative coronal camera lucida reconstructions through the caudal (Obex-1.0mm) to rostral (Obex+2.0mm) medulla illustrating the location of double labelled Fos-IR and TH containing neurons in the ventrolateral medulla of animals subjected to A.10% normotensive haemorrhage, B. 30% hypotensive haemorrhage or C. infusion of the peripheral vasodilator sodium nitroprusside (1mg/ml). *SpV, Spinal trigeminal nucleus; IO, inferior olivary nucleus; Pyr, pyramidal tract; LRN, lateral reticular nucleus; VII, facial nucleus.*

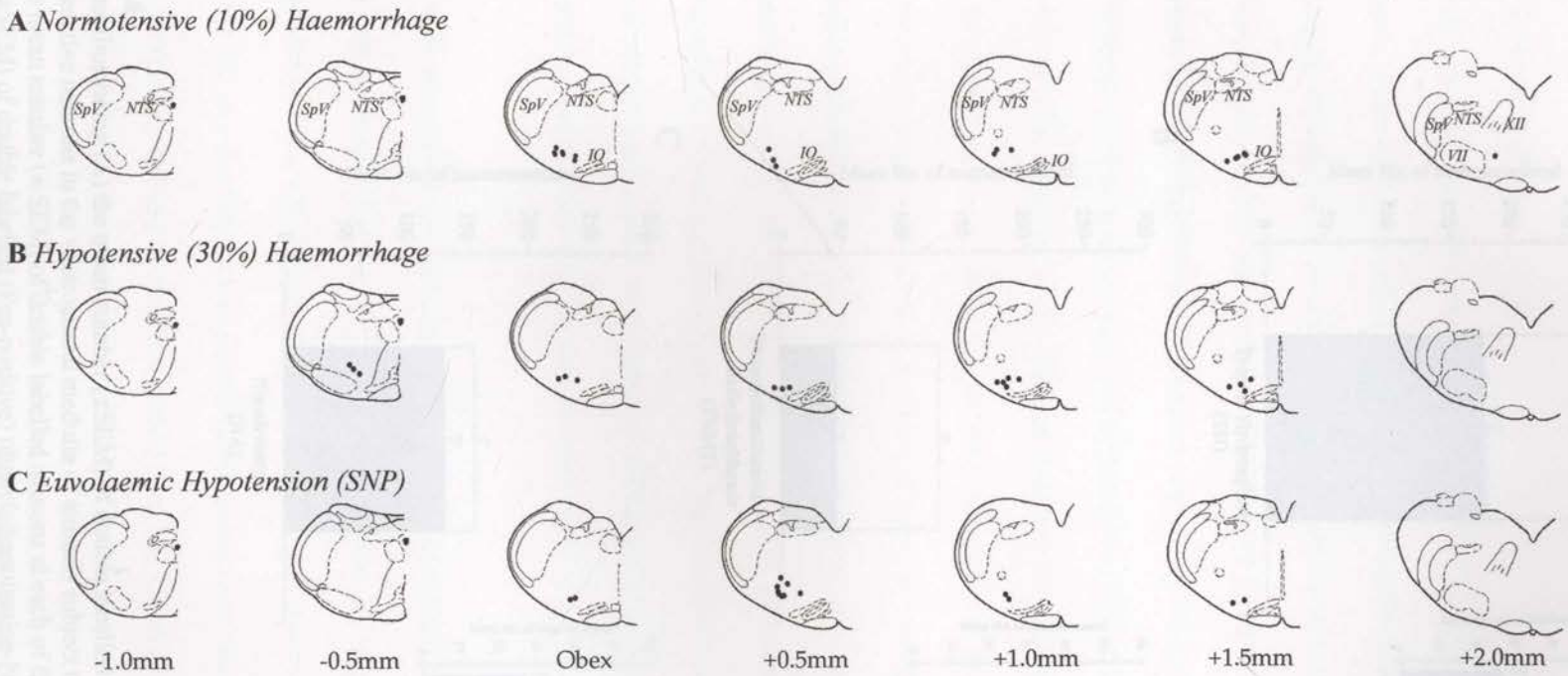

Figure 4.7

Representative coronal camera lucida reconstructions through the caudal (Obex-1.0mm) to rostral (Obex+2.0mm) medulla illustrating the location of double labelled Fos-IR and PNMT containing neurons in the ventrolateral medulla of animals subjected to A. 10% normotensive haemorrhage, B. 30% hypotensive haemorrhage or C. infusion of the peripheral vasodilator sodium nitroprusside (1mg/ml). *SpV, Spinal trigeminal nucleus; IO, inferior olivary nucleus; Pyr, pyramidal tract; LRN, lateral reticular nucleus; VII, facial nucleus.*

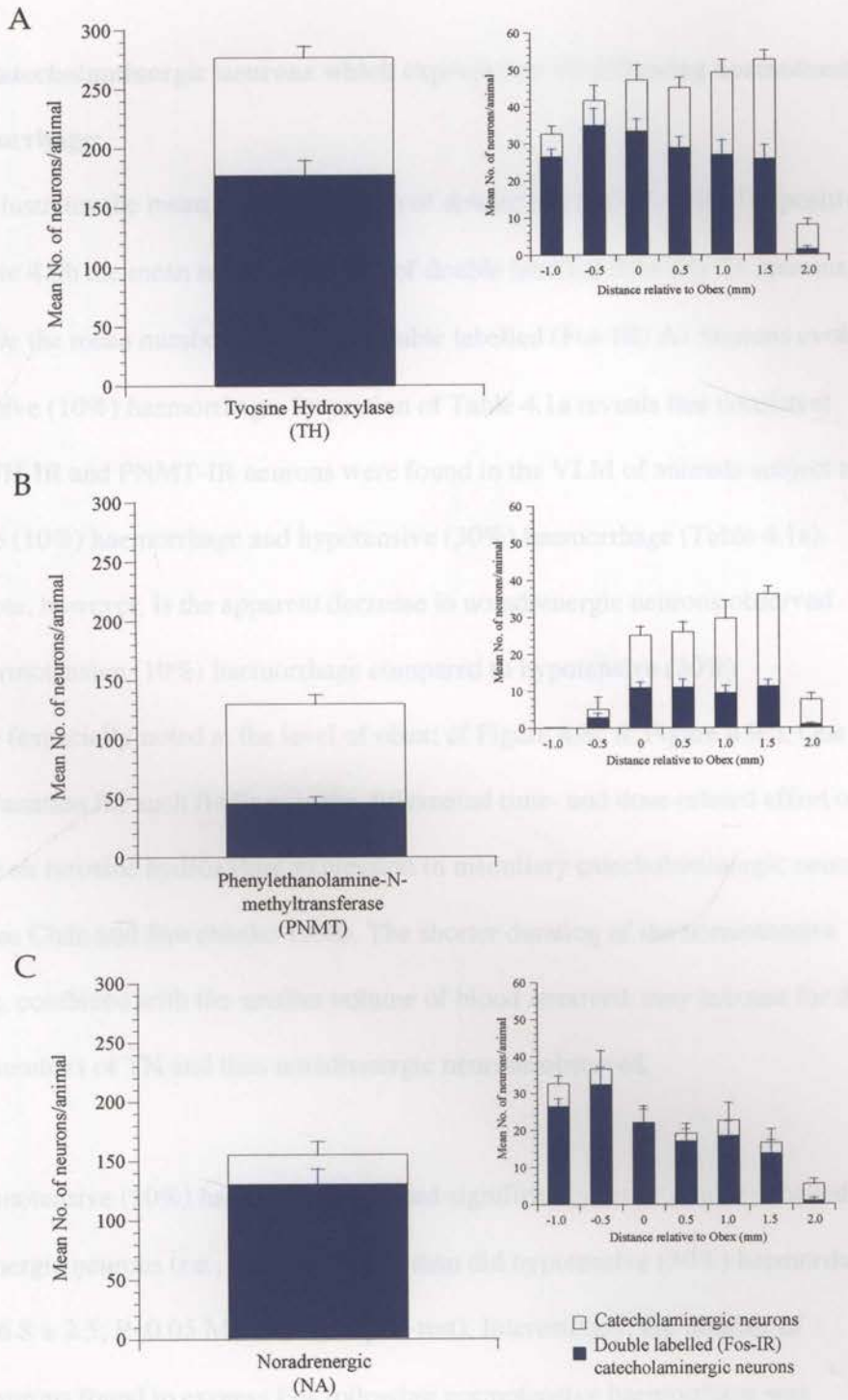

Figure 4.8

Histograms illustrating **(A)** the mean number (±SEM) of double labelled (ie., Fos-positive) tyrosine hydroxylase immunoreactive neurons in the ventrolateral medulla of animals subject to hypotensive (30%) haemorrhage. The insert shows the mean number (± SEM) of double labelled neurons at each of the seven levels analysed; **(B)** the mean number (±SEM) of double labelled (Fos-positive) phenylethanolamine-N-methyltransferase immunoreactive neurons in the ventrolateral medulla of animals subject to hypotensive (30%) haemorrhage. The insert shows the mean number (± SEM) of double labelled neurons at each of the seven levels analysed; **(C)** the mean number (±SEM) of double labelled (Fos-positive) noradrenergic neurons in the ventrolateral medulla of animals subject to hypotensive (30%) haemorrhage. The insert shows the mean number (± SEM) of double labelled neurons at each of the seven levels analysed.

4.3.3 VLM catecholaminergic neurons which express Fos-IR following normotensive (10%) haemorrhage:

Figure 4.9a illustrates the mean number (±SEM) of double labelled (Fos-IR) TH-positive neurons, figure 4.9b the mean number (±SEM) of double labelled (Fos-IR) C1 neurons, and figure 4.9c the mean number (±SEM) of double labelled (Fos-IR) A1 neurons evoked by normotensive (10%) haemorrhage. Inspection of Table 4.1a reveals that consistent numbers of TH-IR and PNMT-IR neurons were found in the VLM of animals subject to normotensive (10%) haemorrhage and hypotensive (30%) haemorrhage (Table 4.1a). Worthy of note, however, is the apparent decrease in noradrenergic neurons observed following normotensive (10%) haemorrhage compared to hypotensive (30%) haemorrhage (especially noted at the level of obex; cf Figure 4.8c & Figure 4.9c). One possible explanation for such findings is the differential time- and dose-related effect of haemorrhage on tyrosine hydroxylase expression in medullary catecholaminergic neurons (for details see Chan and Sawchenko 1998). The shorter duration of the normotensive haemorrhage, combined with the smaller volume of blood removed, may account for the diminished numbers of TH and thus noradrenergic neurons observed.

As well, normotensive (10%) haemorrhage evoked significantly fewer double-labelled catecholaminergic neurons (i.e., Fos-IR/TH-IR) than did hypotensive (30%) haemorrhage (Figure 4.9; 6.8 ± 2.5; $P<0.05$ Mann-Whitney U-test). Interestingly, the number of PNMT-IR neurons found to express Fos following normotensive haemorrhage was identical to the number of double labelled (Fos-IR) TH-positive neurons evoked by

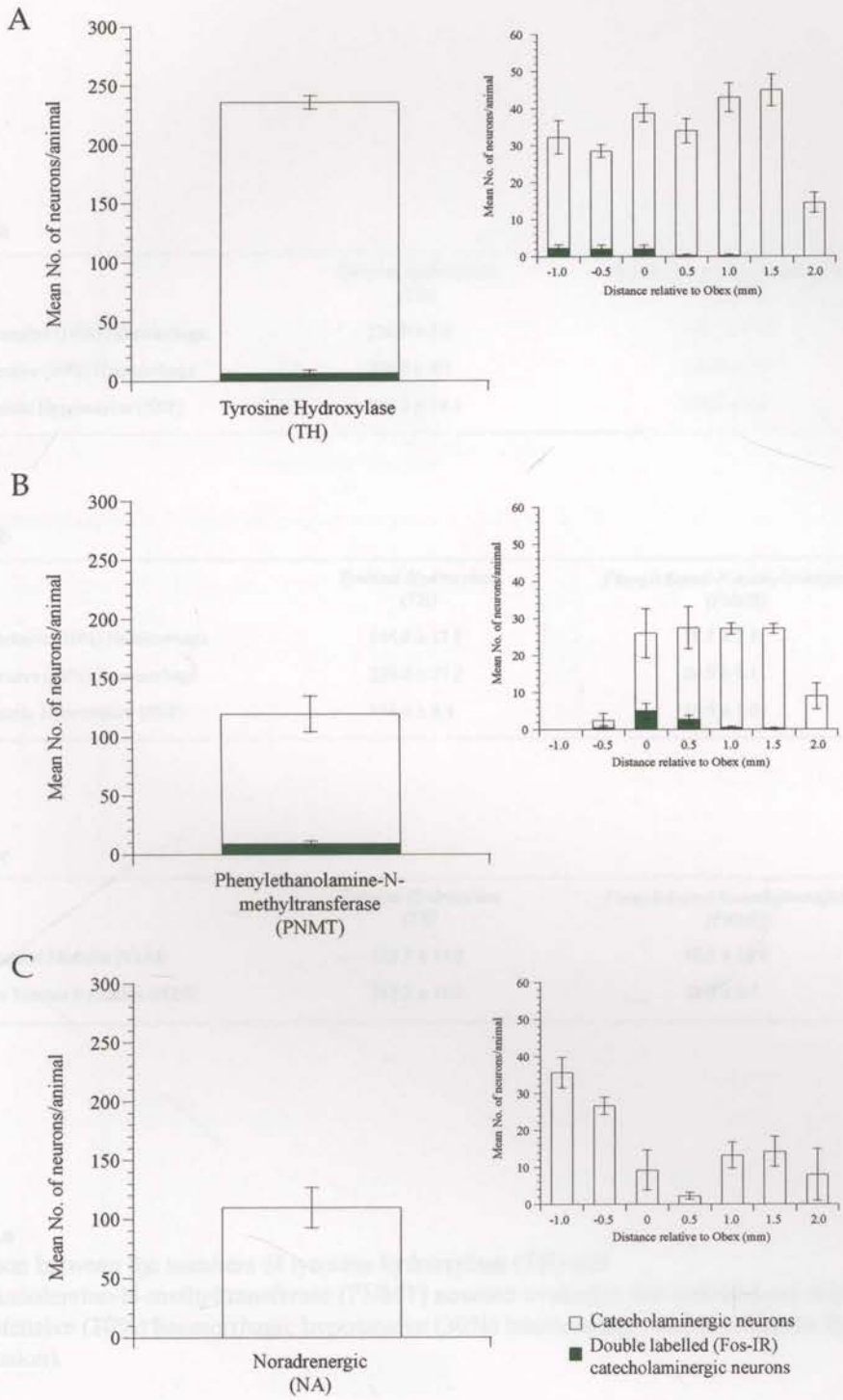

Figure 4.9
Histograms illustrating **(A)** the mean number (±SEM) of double labelled (ie., Fos-positive) tyrosine hydroxylase immunoreactive neurons in the ventrolateral medulla of animals subject to normotensive (10%) haemorrhage. The insert shows the mean number (± SEM) of double labelled neurons at each of the seven levels analysed; **(B)** the mean number (±SEM) of double labelled (Fos-positive) phenylethanolamine-N-methyltransferase immunoreactive neurons in the ventrolateral medulla of animals subject to normotensive (10%) haemorrhage. The insert shows the mean number (± SEM) of double labelled neurons at each of the seven levels analysed; **(C)** the mean number (±SEM) of double labelled (Fos-positive) noradrenergic neurons in the ventrolateral medulla of animals subject to normotensive (10%) haemorrhage. The insert shows the mean number (± SEM) of double labelled neurons at each of the seven levels analysed.The number of noradrenergic neurons shown in (C) was estimated by subtracting the number of PNMT-IR neurons in (B) from the number of TH-IR neurons in (A).

Table 4.1a

	Tyrosine Hydroxylase (TH)	*Phenylethanol-N-methyltransferase (PNMT)*
Normotensive (10%) Haemorrhage	236.0 ± 5.5	128.0 ± 17.8
Hypotensive (30%) Haemorrhage	276.9 ± 9.1	129.7 ± 7.6
Euvolaemic Hypotension (SNP)	249.3 ± 14.1	104.6 ± 9.6

Table 4.1b

	Tyrosine Hydroxylase (TH)	*Phenylethanol-N-methyltransferase (PNMT)*
Normotensive (10%) Haemorrhage	146.0 ± 17.8	18.7 ± 5.3
Hypotensive (30%) Haemorrhage	234.0 ± 27.2	30.9 ± 6.1
Euvolaemic Hypotension (SNP)	174.6 ± 8.4	16.6 ± 1.0

Table 4.1c

	Tyrosine Hydroxylase (TH)	*Phenylethanol-N-methyltransferase (PNMT)*
Ventrolateral Medulla (VLM)	218.7 ± 14.9	88.5 ± 13.6
Nucleus Tractus Solitarius (NTS)	217.3 ± 11.0	51.2 ± 2.7

Table 4.1a
Comparison between the numbers of tyrosine hydroxylase (TH) and phenylethanolamine-N-methyltransferase (PNMT) neurons evoked in the ventrolateral medulla (VLM) by normotensive (10%) haemorrhage; hypotensive (30%) haemorrhage; and euvolaemic hypotension (SNP infusion).

Table 4.1b
Comparison between the numbers of tyrosine hydroxylase (TH) and phenylethanolamine-N-methyltransferase (PNMT) neurons evoked in the nucleus of the solitary tract (NTS) by normotensive (10%) haemorrhage; hypotensive (30%) haemorrhage; and euvolaemic hypotension (SNP infusion).

Table 4.1c
The absolute number of tyrosine hydroxylase (TH) and phenylethanolamine-N-methyltransferase (PNMT) neurons observed in both the ventrolateral medulla (VLM) and nucleus of the solitary tract (NTS) following standard fluorescent immunohistochemical procedures as described in Chapter 4 part II. It can be seen that these numbers of neurons are comparable to those shown in tables 4.1a and table 4.1b.

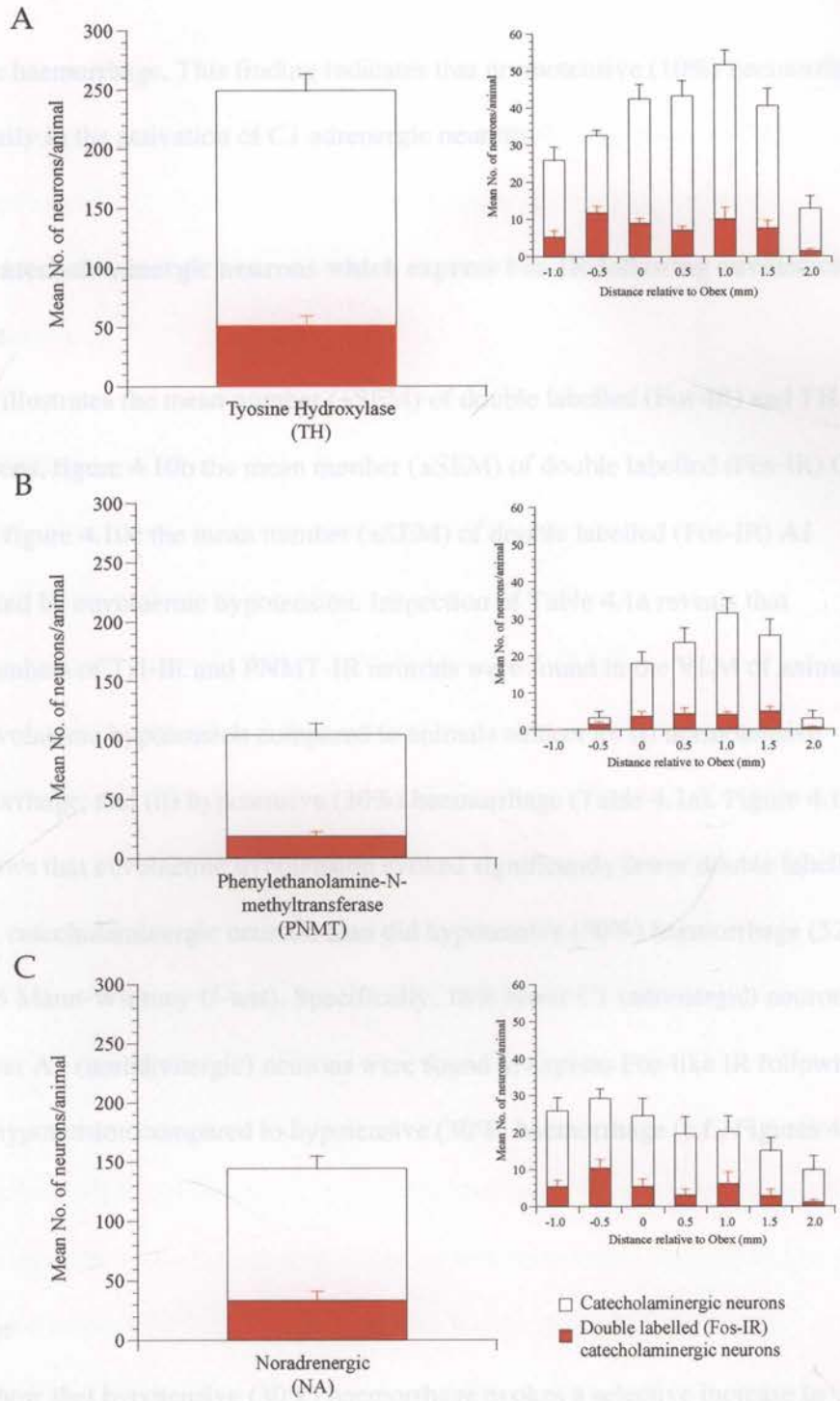

Figure 4.10

Histograms illustrating **(A)** the mean number (±SEM) of double labelled (ie., Fos-positive) tyrosine hydroxylase immunoreactive neurons in the ventrolateral medulla of animals subject to euvolaemic hypotension. The insert shows the mean number (± SEM) of double labelled neurons at each of the seven levels analysed; **(B)** the mean number (±SEM) of double labelled (Fos-positive) phenylethanolamine-N-methyltransferase immunoreactive neurons in the ventrolateral medulla of animals subject to euvolaemic hypotension. The insert shows the mean number (± SEM) of double labelled neurons at each of the seven levels analysed; **(C)** the mean number (±SEM) of double labelled (Fos-positive) noradrenergic neurons in the ventrolateral medulla of animals subject to euvolaemic hypotension. The insert shows the mean number (± SEM) of double labelled neurons at each of the seven levels analysed.

normotensive haemorrhage. This finding indicates that normotensive (10%) haemorrhage results primarily in the activation of C1 adrenergic neurons.

4.3.4 VLM catecholaminergic neurons which express Fos-IR following euvolaemic hypotension:

Figure 4.10a illustrates the mean number (±SEM) of double labelled (Fos-IR) and TH-positive neurons, figure 4.10b the mean number (±SEM) of double labelled (Fos-IR) C1 neurons, and figure 4.10c the mean number (±SEM) of double labelled (Fos-IR) A1 neurons evoked by euvolaemic hypotension. Inspection of Table 4.1a reveals that consistent numbers of TH-IR and PNMT-IR neurons were found in the VLM of animals subject to euvolaemic hypotension compared to animals subject to: (i) normotensive (10%) haemorrhage; and (ii) hypotensive (30%) haemorrhage (Table 4.1a). Figure 4.10, however, shows that euvolaemic hypotension evoked significantly fewer double labelled Fos-positive, catecholaminergic neurons than did hypotensive (30%) haemorrhage (52.0 ± 7.8; $P<0.05$ Mann-Whitney U-test). Specifically, 18% fewer C1 (adrenergic) neurons and 65% fewer A1 (noradrenergic) neurons were found to express Fos-like IR following euvolaemic hypotension compared to hypotensive (30%) haemorrhage (c.f., Figures 4.8 and 4.10).

In summary:

These data show that hypotensive (30%) haemorrhage evokes a selective increase in ventrolateral medullary Fos expression compared to both normotensive (10%) haemorrhage and euvolaemic hypotension. Furthermore, hypotensive (30%) haemorrhage

evokes Fos-expression (i.e., neural activity) in the vast majority (86%) of A1 noradrenergic neurons *but not* C1 adrenergic neurons. Significantly fewer double-labelled A1 (65% fewer) and C1 (18% fewer) neurons were found evoked by euvolaemic hypotension. Normotensive (10%) haemorrhage evoked neural activity only in C1 adrenergic neurons.

Nucleus of the Solitary Tract:

4.3.5 Fos-expression following normotensive (10%) haemorrhage, hypotensive (30%) haemorrhage, and euvolaemic hypotension (SNP infusion):

Representative photomicrographs showing examples of Fos-IR following normotensive (10%) haemorrhage, hypotensive (30%) haemorrhage, and euvolaemic hypotension at caudal and rostral levels of the NTS are shown in Figure 4.11. Figures 4.12a-4.12c show camera lucida reconstructions of the location of Fos-like immunoreactive (Fos-IR) neurons in seven equidistant medullary coronal sections (-1.0mm, -0.5mm, 0mm, +0.5mm, +1.0mm, +1.5mm, +2.0mm relative to Obex) evoked by: **A** normotensive (10%) haemorrhage; **B** hypotensive (30%) haemorrhage; and **C** euvolaemic hypotension (i.v. infusion of sodium nitroprusside; SNP). The histogram in Figure 4.13 summarises the mean number (±SEM) of Fos-positive neurons observed in the nucleus of the solitary tract (NTS) evoked by each manipulation. It can be seen that similar numbers of Fos-IR cells were found in the NTS following hypotensive haemorrhage and euvolaemic hypotension (464 ± 73.0 *vs* 485 ± 39.4; NS, Mann-Whitney U-test). Significantly fewer Fos-IR neurons were evoked by normotensive (10%) haemorrhage (104.3 ± 16.8).

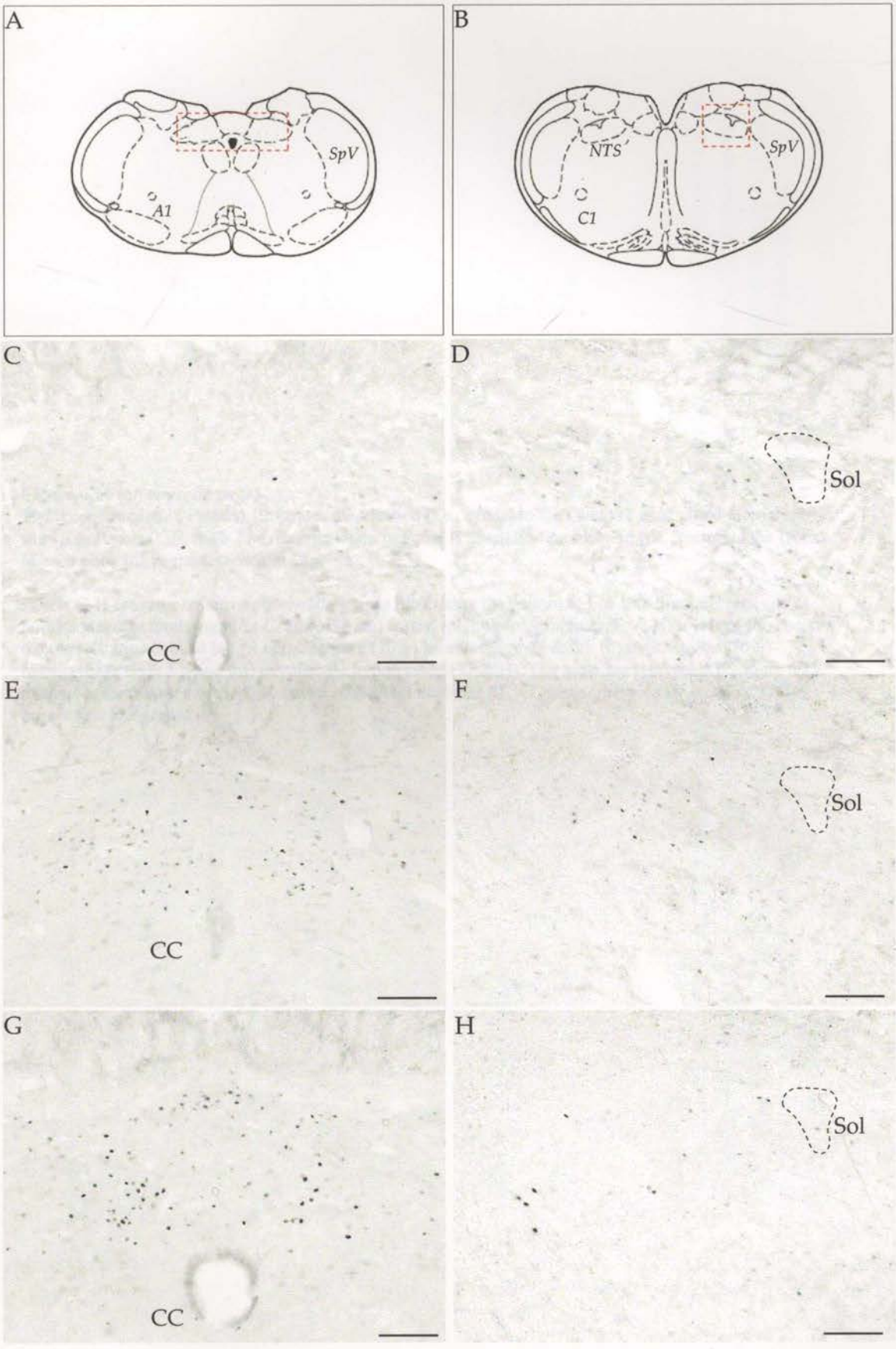
A
SpV
A1
B
NTS
SpV
C1
C
CC
D
Sol
E
CC
F
Sol
G
CC
H
Sol

Figure 4.11 (*on opposite page*)
The reconstruction in Panel A illustrates the location (i.e., caudal to the Obex) of each photomicrograph shown in Panels C, E, & G. The reconstruction in Panel B illustrates the location (i.e., rostral to the Obex) of each photomicrograph shown in Panels D, F, & H.

Panels C-H are representative photomicrographs illustrating the pattern of Fos-like immunoreactivity at both caudal (photomicrographs C, E, & G), and rostral (photomicrographs D, F, & H) levels of the nucleus tractus solitarius evoked by: (i) normotensive (10%) haemorrhage (C & D); (ii) hypotensive (30%) haemorrhage (E & F); and (iii) euvolaemic hypotension (G & H). The scale bar represents 0.25mm. *NTS, nucleus of the solitary tract; SpV, spinal trigeminal nucleus; A1, A1 noradrenergic cell group; C1, C1 adrenergic cell group.*

A *Normotensive (10%) Haemorrhage*

B *Hypotensive (30%) Haemorrhage*

C *Euvolaemic Hypotension (SNP)*

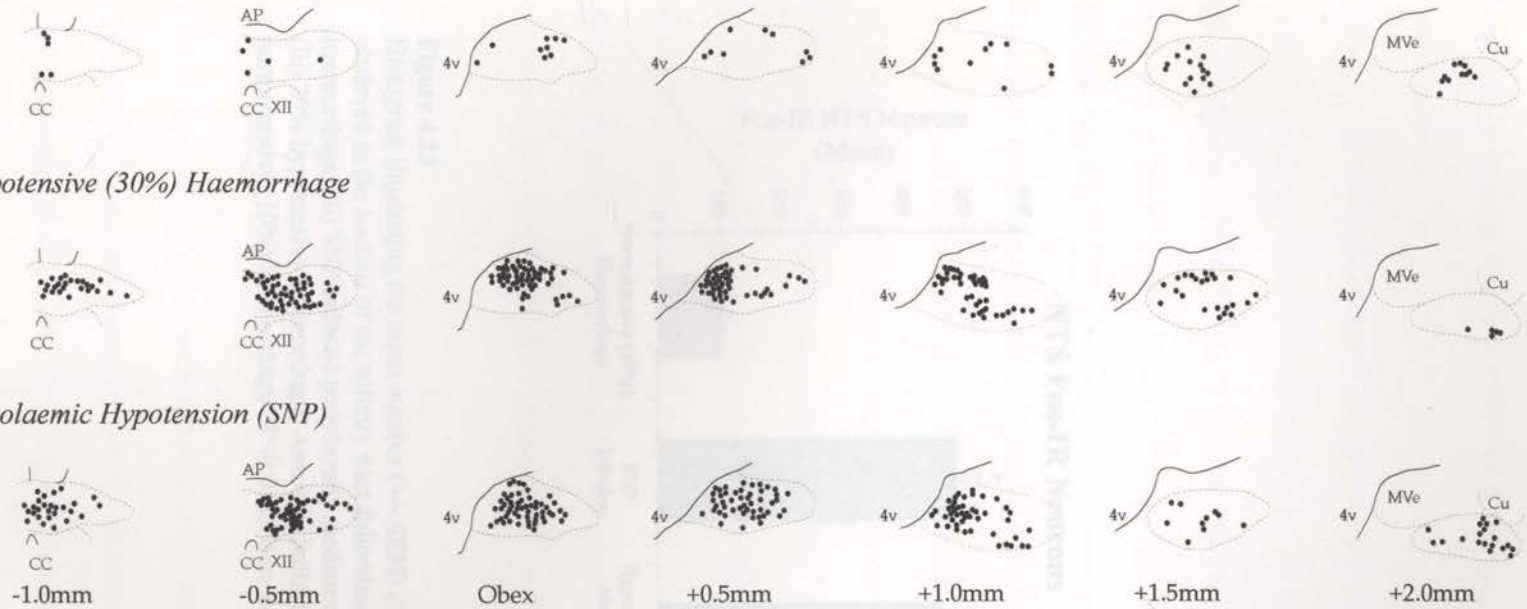

Figure 4.12
Representative coronal camera lucida reconstructions through the caudal (Obex-1.0mm) to rostral (Obex+2.0mm) medulla illustrating the location of Fos-IR neurons in the nucleus tractus solitarius of animals subjected to **A** 10% normotensive haemorrhage, **B** 30% hypotensive haemorrhage or **C** infusion of the peripheral vasodilator sodium nitroprusside (1mg/ml). *CC, central canal; AP, area postrema; 4v, fourth ventricle; MVe, medial vestibular nucleus; Cu, cuneate nucleus; XII, hypoglossal nucleus.*

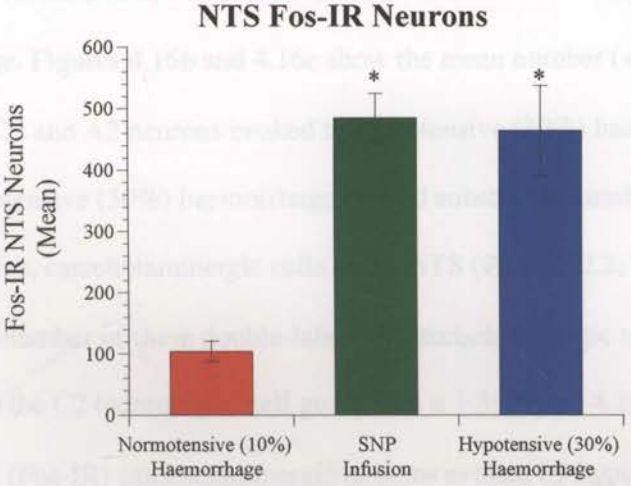

Figure 4.13
Histogram illustrating the mean number (+/- SEM) of Fos-immunoreactive nuclei observed in the nucleus of the solitary tract following: (i) 10% normotensive haemorrhage; (ii) SNP induced peripherally mediated euvolaemic hypotension; and (iii) 30% hypotensive haemorrhage. Asterisks indicate significance with respect to normotensive (10%) haemorrhage *P<0.05 (Mann-Whitney U-test).

4.3.6 NTS catecholaminergic neurons which express Fos-IR following hypotensive (30%) haemorrhage:

Representative camera lucida reconstructions showing the location of double-labelled Fos-TH and Fos-PNMT containing neurons evoked by: (i) normotensive (10%) haemorrhage; (ii) hypotensive (30%) haemorrhage; and (iii) euvolaemic hypotension are shown in Figures 4.14 and 4.15 respectively. Figure 4.16a shows the mean number (±SEM) of double labelled (i.e., Fos-positive) TH-IR neurons evoked by hypotensive (30%) haemorrhage. Figures 4.16b and 4.16c show the mean number (±SEM) of double-labelled (Fos-IR) C2 and A2 neurons evoked by hypotensive (30%) haemorrhage respectively. Hypotensive (30%) haemorrhage evoked substantial numbers of double-labelled Fos-positive, catecholaminergic cells in the NTS (99.7 ± 12.2; Figure 4.16a). Only a very small number of these double-labelled catecholaminergic neurons were found to belong to the C2 (adrenergic) cell group (6.6 ± 1.3; Figure 4.16b). The majority of double-labelled (Fos-IR) catecholaminergic neurons evoked by hypotensive (30%) haemorrhage therefore belong to the A2 cell group (89.7 ± 11.4; Figure 4.16c).

4.3.7 NTS catecholaminergic neurons which express Fos-IR following normotensive (10%) haemorrhage:

Figure 4.17a illustrates the mean number (±SEM) of double labelled (Fos-IR) and TH-positive neurons, figure 4.17b the mean number (±SEM) of double labelled (Fos-IR) C2 neurons, and figure 4.17c the mean number (±SEM) of double labelled (Fos-IR) A2 neurons evoked by normotensive (10%) haemorrhage. Inspection of Table 4.1b reveals that consistent numbers of TH-IR and PNMT-IR neurons were found in the NTS of

A *Normotensive (10%) Haemorrhage*

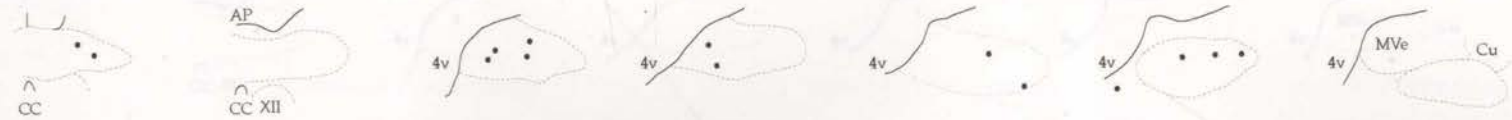

B *Hypotensive (30%) Haemorrhage*

C *Euvolaemic Hypotension (SNP)*

-1.0mm -0.5mm Obex +0.5mm +1.0mm +1.5mm +2.0mm

Figure 4.14
Representative coronal camera lucida reconstructions through the caudal (Obex-1.0mm) to rostral (Obex+2.0mm) medulla illustrating the location of double labelled Fos-IR and tyrosine hydroxylase (TH-IR) containing neurons in the nucleus tractus solitarius of animals subjected to **A** 10% normotensive haemorrhage, **B** 30% hypotensive haemorrhage or **C** infusion of the peripheral vasodilator sodium nitroprusside (1mg/ml). *CC, central canal; AP, area postrema; 4v, fourth ventricle; MVe, medial vestibular nucleus; Cu, cuneate nucleus; XII, hypoglossal nucleus.*

A *Normotensive (10%) Haemorrhage*

B *Hypotensive (30%) Haemorrhage*

C *Euvolaemic Hypotension (SNP)*

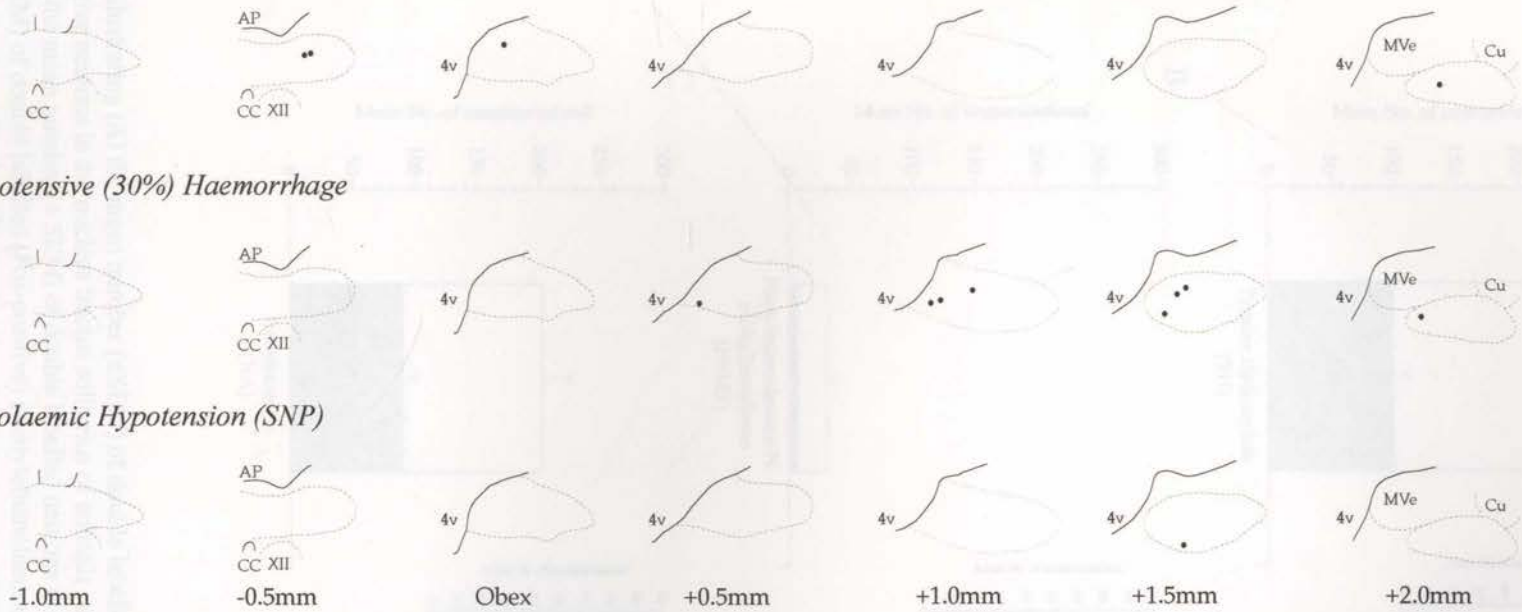

Figure 4.15
Representative coronal camera lucida reconstructions through the caudal (Obex-1.0mm) to rostral (Obex+2.0mm) medulla illustrating the location of double labelled Fos-IR and phenylethanol-N-methyltransferase (PNMT-IR) containing neurons in the nucleus tractus solitarius of animals subjected to **A** 10% normotensive haemorrhage, **B** 30% hypotensive haemorrhage or **C** infusion of the peripheral vasodilator sodium nitroprusside (1mg/ml). *CC, central canal; AP, area postrema; 4v, fourth ventricle; MVe, medial vestibular nucleus; Cu, cuneate nucleus; XII, hypoglossal nucleus.*

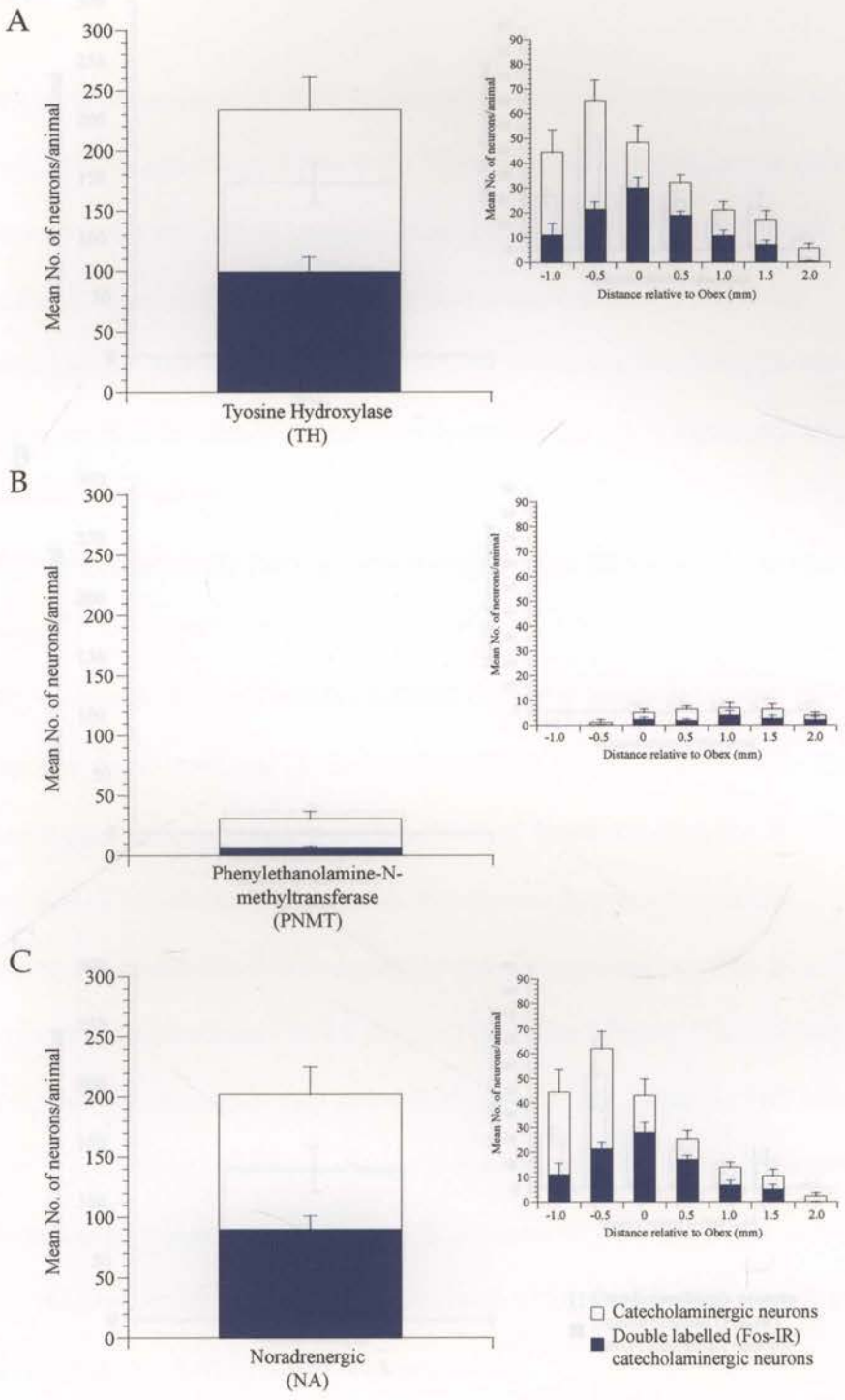

Figure 4.16
Histograms illustrating **(A)** the mean number (±SEM) of double labelled (ie., Fos-positive) tyrosine hydroxylase immunoreactive neurons in the nucleus tractus solitarius of animals subject to hypotensive (30%) haemorrhage. The insert shows the mean number (± SEM) of double labelled neurons at each of the seven levels analysed; **(B)** the mean number (±SEM) of double labelled (Fos-positive) phenylethanolamine-N-methyltransferase immunoreactive neurons in the nucleus tractus solitarius of animals subject to hypotensive (30%) haemorrhage. The insert shows the mean number (± SEM) of double labelled neurons at each of the seven levels analysed; **(C)** the mean number (±SEM) of double labelled (Fos-positive) noradrenergic neurons in the nucleus tractus solitarius of animals subject to hypotensive (30%) haemorrhage. The insert shows the mean number (± SEM) of double labelled neurons at each of the seven levels analysed.

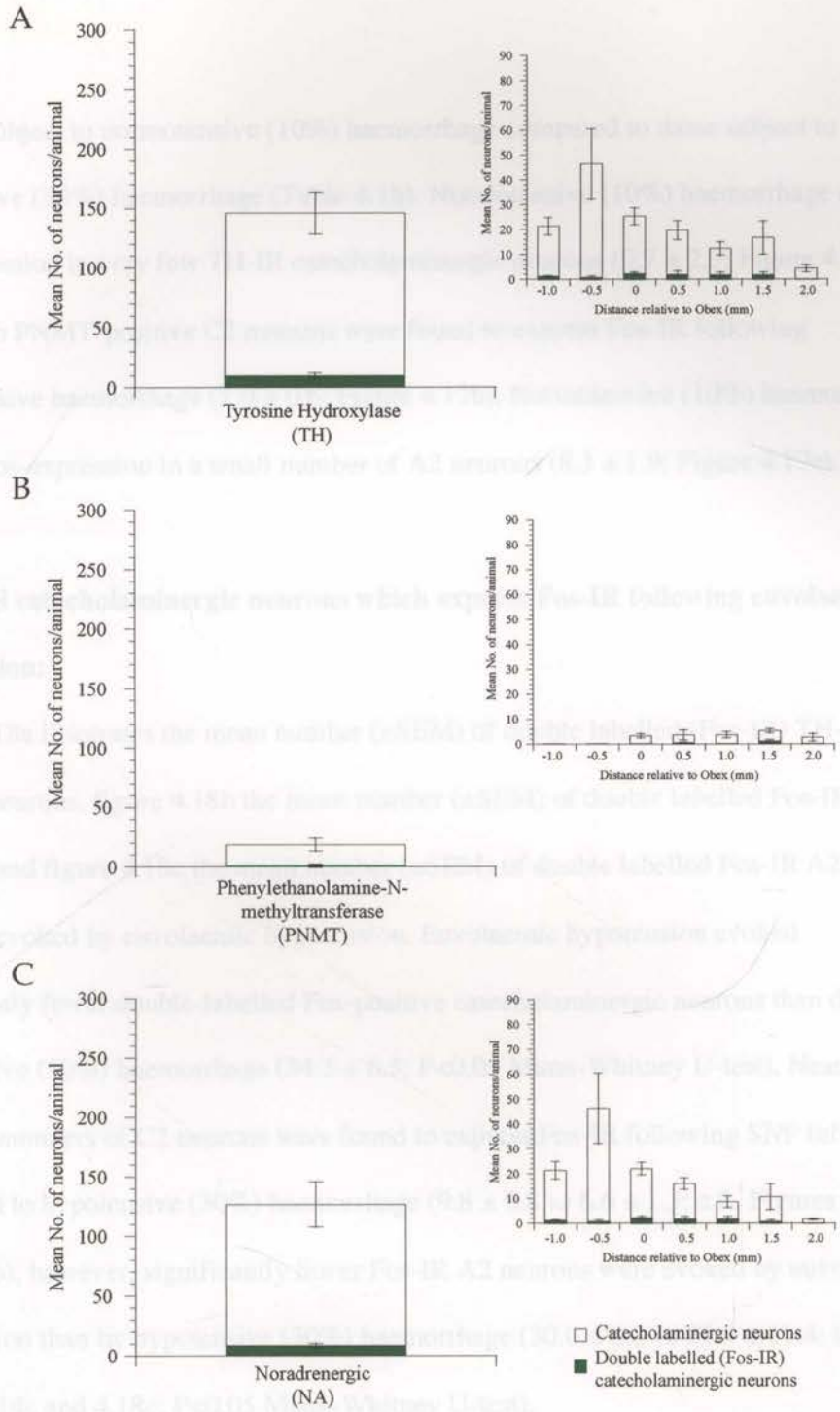

Figure 4.17

Histograms illustrating **(A)** the mean number (±SEM) of double labelled (ie., Fos-positive) tyrosine hydroxylase immunoreactive neurons in the nucleus tractus solitarius of animals subject to normotensive (10%) haemorrhage. The insert shows the mean number (± SEM) of double labelled neurons at each of the seven levels analysed; **(B)** the mean number (±SEM) of double labelled (Fos-positive) phenylethanolamine-N-methyltransferase immunoreactive neurons in the nucleus tractus solitarius of animals subject to normotensive (10%) haemorrhage. The insert shows the mean number (± SEM) of double labelled neurons at each of the seven levels analysed; **(C)** the mean number (±SEM) of double labelled (Fos-positive) noradrenergic neurons in the nucleus tractus solitarius of animals subject to normotensive (10%) haemorrhage. The insert shows the mean number (± SEM) of double labelled neurons at each of the seven levels analysed.The number of noradrenergic neurons shown in (C) was estimated by subtracting the number of PNMT-IR neurons in (B) from the number of TH-IR neurons in (A).

animals subject to normotensive (10%) haemorrhage compared to those subject to hypotensive (30%) haemorrhage (Table 4.1b). Normotensive (10%) haemorrhage evoked Fos-expression in very few TH-IR catecholaminergic neurons (9.7 ± 2.3; Figure 4.17a). Almost no PNMT-positive C2 neurons were found to express Fos-IR following normotensive haemorrhage (1.0 ± 0.6; Figure 4.17b). Normotensive (10%) haemorrhage evoked Fos-expression in a small number of A2 neurons (8.3 ± 1.9; Figure 4.17c).

4.3.8 NTS catecholaminergic neurons which express Fos-IR following euvolaemic hypotension:

Figure 4.18a illustrates the mean number (±SEM) of double labelled (Fos-IR) TH-positive neurons, figure 4.18b the mean number (±SEM) of double labelled Fos-IR C2 neurons, and figure 4.18c the mean number (±SEM) of double labelled Fos-IR A2 neurons, evoked by euvolaemic hypotension. Euvolaemic hypotension evoked significantly fewer double-labelled Fos-positive catecholaminergic neurons than did hypotensive (30%) haemorrhage (34.3 ± 6.5; $P<0.05$ Mann-Whitney U-test). Near identical numbers of C2 neurons were found to express Fos-IR following SNP infusion compared to hypotensive (30%) haemorrhage (9.8 ± 0.8 *vs* 6.6 ± 1.3; c.f., Figures 4.14b and 4.18b), however, significantly fewer Fos-IR A2 neurons were evoked by euvolaemic hypotension than by hypotensive (30%) haemorrhage (30.0 ± 6.0 *vs* 89.7 ± 11.4; c.f., Figure 4.14c and 4.18c; $P<0.05$ Mann-Whitney U-test).

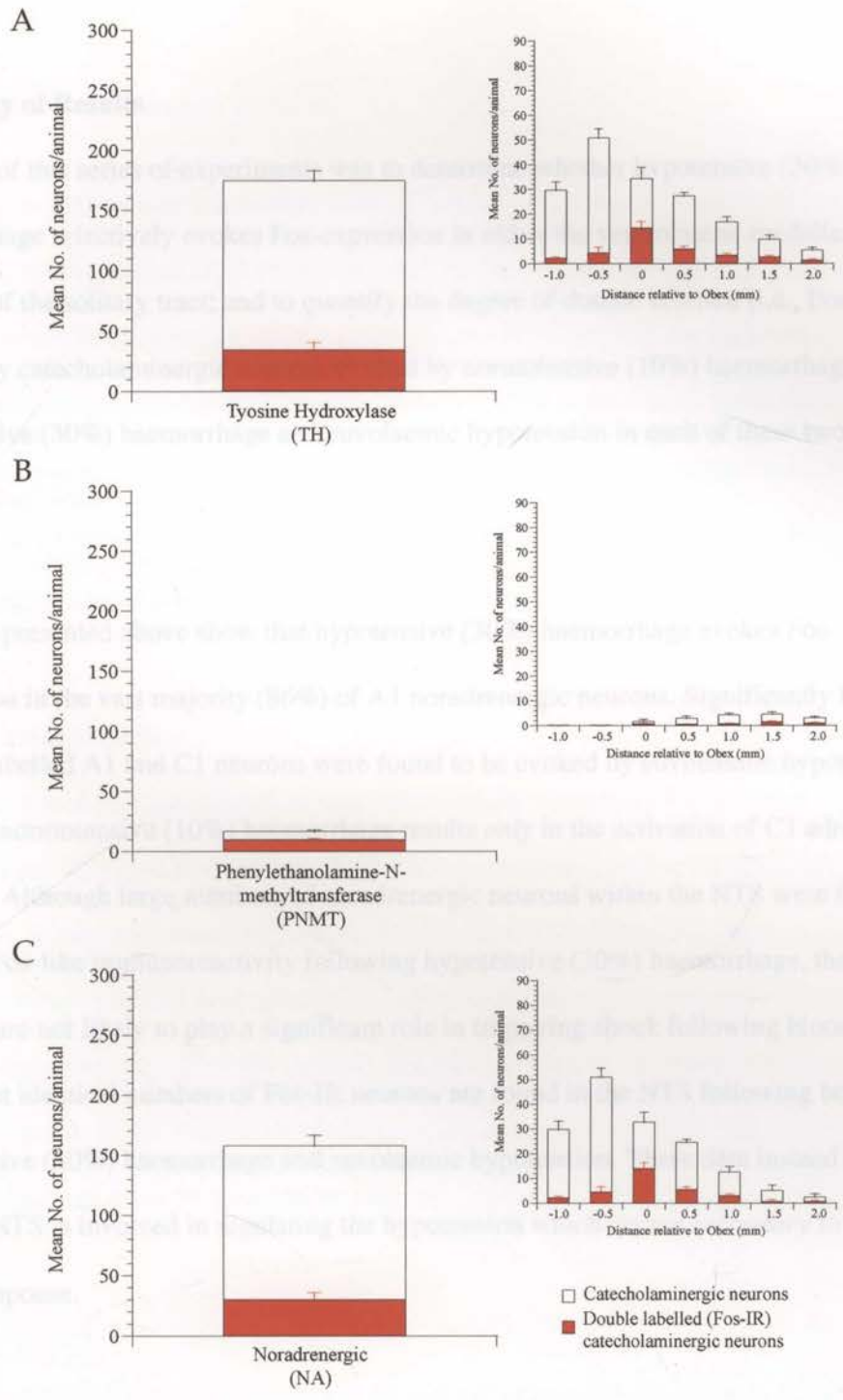

Figure 4.18
Histograms illustrating **(A)** the mean number (±SEM) of double labelled (ie., Fos-positive) tyrosine hydroxylase immunoreactive neurons in the nucleus tractus solitarius of animals subject to euvolaemic hypotension (SNP infusion). The insert shows the mean number (± SEM) of double labelled neurons at each of the seven levels analysed; **(B)** the mean number (±SEM) of double labelled (Fos-positive) phenylethanolamine-N-methyltransferase immunoreactive neurons in the nucleus tractus solitarius of animals subject to euvolaemic hypotension. The insert shows the mean number (± SEM) of double labelled neurons at each of the seven levels analysed; **(C)** the mean number (±SEM) of double labelled (Fos-positive) noradrenergic neurons in the nucleus tractus solitarius of animals subject to euvolaemic hypotension. The insert shows the mean number (± SEM) of double labelled neurons at each of the seven levels analysed.

Summary of Results

The aim of this series of experiments was to determine whether hypotensive (30%) haemorrhage selectively evokes Fos-expression in either the ventrolateral medulla or the nucleus of the solitary tract; and to quantify the degree of double labelled (i.e., Fos-IR) medullary catecholaminergic neurons evoked by normotensive (10%) haemorrhage, hypotensive (30%) haemorrhage and euvolaemic hypotension in each of these two regions.

The data presented above show that hypotensive (30%) haemorrhage evokes Fos-expression in the vast majority (86%) of A1 noradrenergic neurons. Significantly fewer double-labelled A1 and C1 neurons were found to be evoked by euvolaemic hypotension. As well, normotensive (10%) haemorrhage results *only* in the activation of C1 adrenergic neurons. Although large numbers of noradrenergic neurons within the NTS were found to express Fos-like immunoreactivity following hypotensive (30%) haemorrhage, these neurons are not likely to play a significant role in triggering shock following blood loss given that identical numbers of Fos-IR neurons are found in the NTS following both hypotensive (30%) haemorrhage and euvolaemic hypotension. These data instead suggest that the NTS is involved in regulating the hypotension which occurs *secondary* to the shock response.

4.4 Results – Experimental series II

4.4.1 vlPAG retrograde tracer injections: Figure 4.19 shows the location of retrograde tracer injections (cholera toxin subunit B) made in the ventrolateral periaqueductal gray (vlPAG) of each experimental animal (N=6). Figure 4.20 summarises the mean number (±SEM) of retrogradely labelled neurons found in: **A** the ventrolateral medulla (VLM); and **B** the nucleus of the solitary tract (NTS) at each level analysed. Microinjection of CTB into the vlPAG resulted in large numbers of retrogradely labelled neurons at all rostrocaudal levels of both the VLM (329 ± 25) and NTS (502.8 ± 51.8).

Ventrolateral Medulla:

4.4.2 Combined retrograde tracer and immunohistochemistry for tyrosine hydroxylase: Tyrosine hydroxylase (TH) is the enzyme responsible for the synthesis of dopamine, noradrenaline and adrenaline. TH-positive immunoreactive neurons and the extent of double labelled neurons (i.e., TH-positive and retrograde tracer) were examined at seven equidistant levels of the medulla extending from 1.0mm caudal to Obex to 2.0mm rostral to Obex. Only CTB-IR neurons located in the region of TH-immunoreactivity were included in the analysis.

Figure 4.21a illustrates both the mean number (±SEM) of TH-IR neurons and the mean number (±SEM) of double labelled (TH-IR and vlPAG-projecting) neurons at each level of the ventrolateral medulla. Overall approximately 50% of all TH-IR neurons in the ventrolateral medulla were found to project onto the vlPAG. Specifically, it can be seen that: (i) over half of the TH-IR neurons located caudal to the Obex project also to the

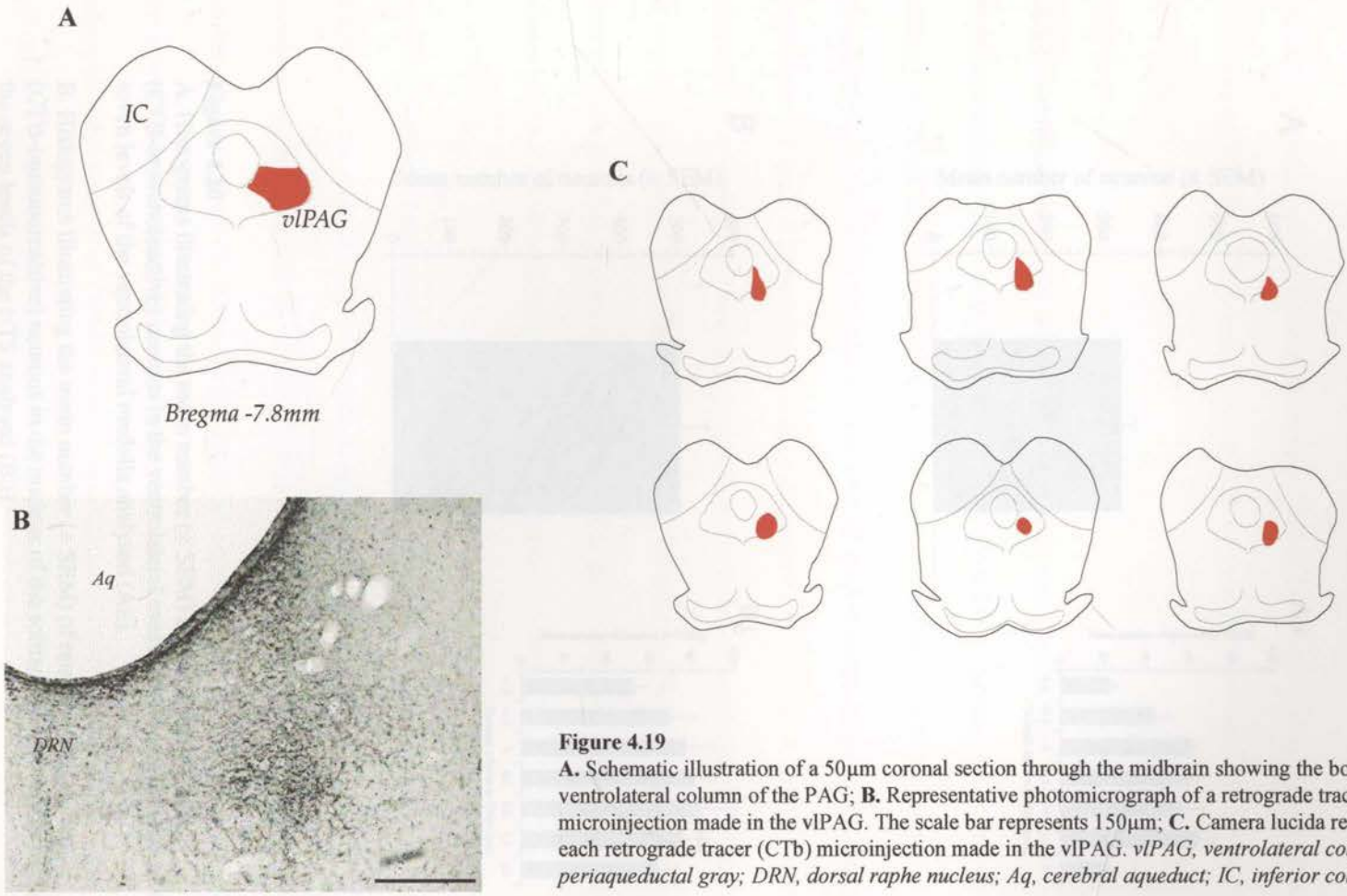

Figure 4.19
A. Schematic illustration of a 50µm coronal section through the midbrain showing the boundaries of the ventrolateral column of the PAG; **B.** Representative photomicrograph of a retrograde tracer (CTb) microinjection made in the vlPAG. The scale bar represents 150µm; **C.** Camera lucida reconstructions of each retrograde tracer (CTb) microinjection made in the vlPAG. *vlPAG, ventrolateral column of the periaqueductal gray; DRN, dorsal raphe nucleus; Aq, cerebral aqueduct; IC, inferior colliculus.*

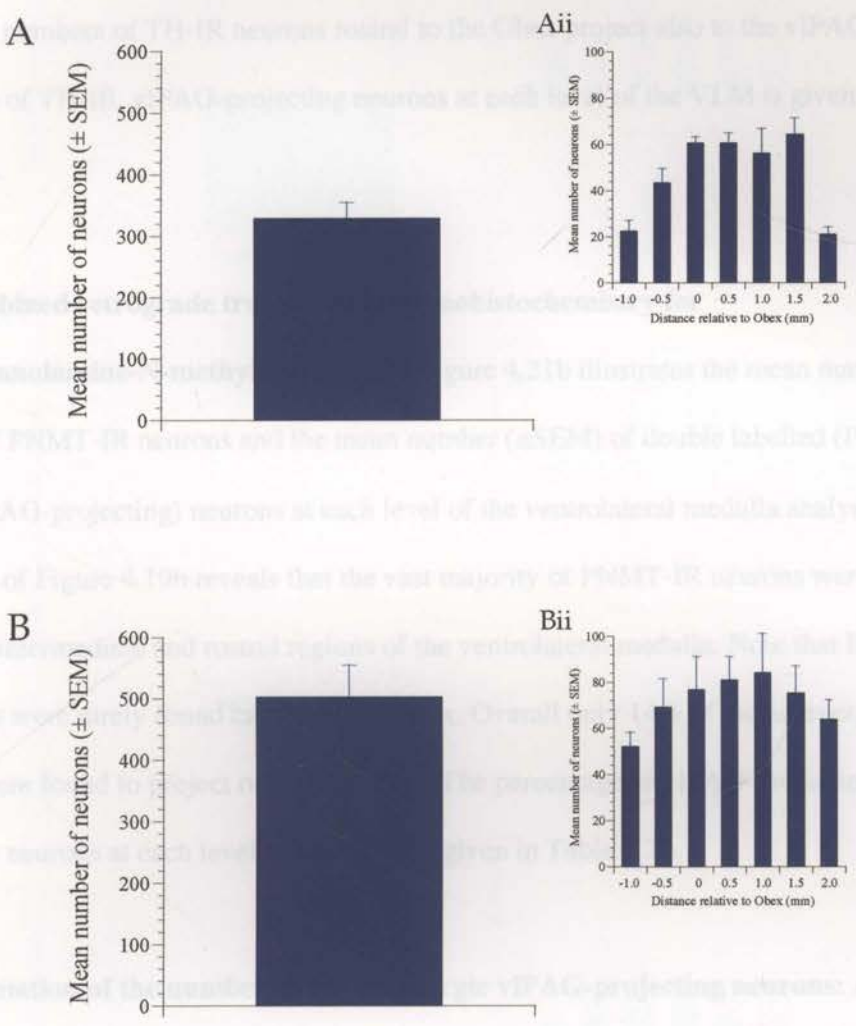

Figure 4.20

A. Histograms illustrating the mean number (± SEM) of retrogradely labelled (CTB-immunoreactive) neurons in the ventrolateral medulla as well as at each of the seven levels of the ventrolateral medulla analysed (Aii).

B. Histograms illustrating the mean number (± SEM) of retrogradely labelled (CTB-immunoreactive) neurons in the nucleus of the solitary tract as well as at each of the seven levels of the NTS analysed (Bii).

vlPAG; (ii) approximately two thirds of the TH-IR neurons located at the level of the Obex and 0.5mm rostral to the Obex project also to the vlPAG; and (iii) fewer but still significant numbers of TH-IR neurons rostral to the Obex project also to the vlPAG. The percentage of TH-IR, vlPAG-projecting neurons at each level of the VLM is given in Table 4.2a.

4.4.3 Combined retrograde tracer and immunohistochemistry for phenylethanolamine-N-methyltransferase: Figure 4.21b illustrates the mean number (±SEM) of PNMT-IR neurons and the mean number (±SEM) of double labelled (PNMT-IR and vlPAG-projecting) neurons at each level of the ventrolateral medulla analysed. Inspection of Figure 4.19b reveals that the vast majority of PNMT-IR neurons were located in intermediate and rostral regions of the ventrolateral medulla. Note that PNMT-IR neurons were rarely found caudal to the Obex. Overall only 14% of the adrenergic neurons were found to project onto the vlPAG. The percentage of vlPAG-projecting adrenergic neurons at each level of the VLM is given in Table 4.2b.

4.4.4 Estimation of the number of noradrenergic vlPAG-projecting neurons: As described in the methods, the ventrolateral medulla contains a mixed population of A1 noradrenergic neurons and C1 adrenergic neurons. PNMT is known only to occur in adrenergic cells, however, TH is an immunohistochemical marker for both noradrenergic and adrenergic cells. Thus the number of noradrenergic neurons was approximated by subtracting the number of PNMT-positive neurons in one section from the number of TH-positive neurons in the immediately adjacent section.

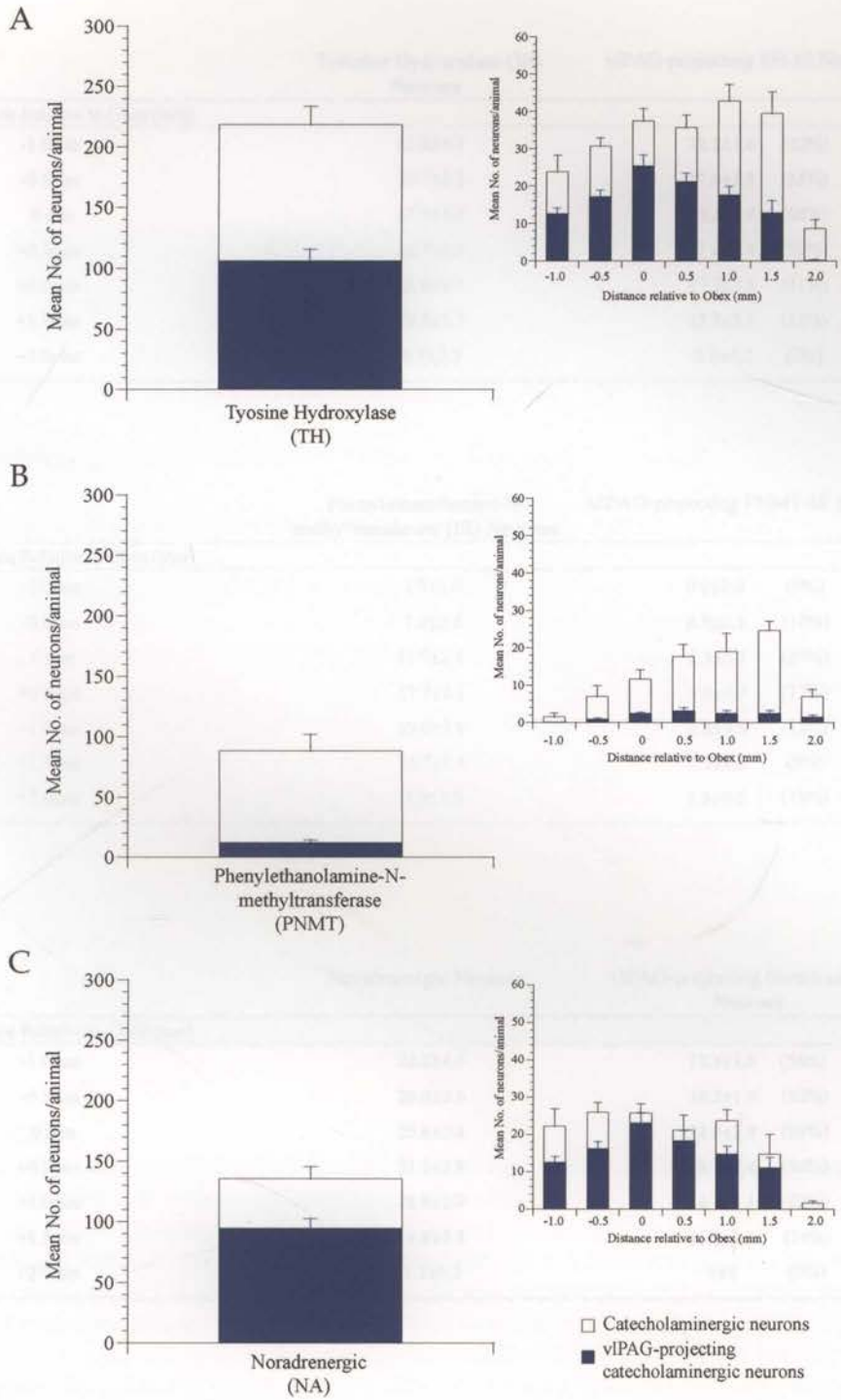

Figure 4.21

Histograms illustrating **(A)** the mean number (±SEM) of vlPAG-projecting, tyrosine hydroxylase immunoreactive neurons in the ventrolateral medulla of animals subject to hypotensive (30%) haemorrhage. The insert shows the mean number (± SEM) of such neurons at each of the seven levels analysed; **(B)** the mean number (±SEM) of vlPAG-projecting, phenylethanolamine-N-methyltransferase immunoreactive (i.e., *adrenergic*) neurons in the ventrolateral medulla of animals subject to hypotensive (30%) haemorrhage. The insert shows the mean number (± SEM) of such neurons at each of the seven levels analysed; **(C)** the mean number (±SEM) of vlPAG-projecting, *noradrenergic* neurons in the ventrolateral medulla of animals subject to hypotensive (30%) haemorrhage. The insert shows the mean number (± SEM) of such neurons at each of the seven levels analysed.

A	Tyrosine Hydroxylase (IR) Neurons	vlPAG-projecting TH-IR Neurons	
Distance Relative to Obex (mm)			
-1.0mm	23.8±4.5	12.5±1.6	(52%)
-0.5mm	30.7±2.2	17.0±1.8	(55%)
0 mm	37.5±3.3	25.3±3.0	(68%)
+0.5mm	35.7±3.4	21.0±2.4	(59%)
+1.0mm	42.8±4.5	17.5±2.3	(41%)
+1.5mm	39.5±5.7	12.7±3.4	(32%)
+2.0mm	8.7±2.3	0.2±0.2	(2%)

B	Phenylethanolamine-N-methyltransferase (IR) Neurons	vlPAG-projecting PNMT-IR Neurons	
Distance Relative to Obex (mm)			
-1.0mm	1.5±1.0	0.0±0.0	(0%)
-0.5mm	7.0±2.8	0.8±0.3	(12%)
0 mm	11.7±2.4	2.3±0.3	(20%)
+0.5mm	17.7±3.1	3.0±0.9	(17%)
+1.0mm	19.0±4.9	2.3±0.8	(12%)
+1.5mm	24.7±2.4	2.3±0.8	(9%)
+2.0mm	7.0±1.9	1.3±0.6	(19%)

C	Noradrenergic Neurons	vlPAG-projecting Noradrenergic Neurons	
Distance Relative to Obex (mm)			
-1.0mm	22.3±4.6	12.5±1.6	(56%)
-0.5mm	26.0±2.6	16.2±1.9	(62%)
0 mm	25.8±2.4	23.0±2.9	(89%)
+0.5mm	21.3±3.9	18.3±2.8	(86%)
+1.0mm	23.8±2.9	14.7±2.1	(62%)
+1.5mm	14.8±5.3	11.0±2.8	(74%)
+2.0mm	1.7±0.5	0±0	(0%)

Table 4.2

A. Table showing the mean number (±SEM) of ventrolateral medullary neurons immunoreactive for tyrosine hydroxylase (TH-IR) and the mean number (±SEM) of ventrolateral medullary tyrosine hydroxylase-IR neurons which project also to the ventrolateral PAG. The number in brackets is the percentage of double labelled (vlPAG-projecting, TH-IR) neurons. **B.** Table showing the mean number (±SEM) of ventrolateral medullary neurons immunoreactive for phenylethanolamine-N-methyltransferase (PNMT-IR) and the mean number (±SEM) of ventrolateral medullary phenylethanolamine-N-methyltransferase-IR neurons which project also to the vlPAG. The number in brackets is the percentage of double labelled (vlPAG-projecting PNMT-IR) neurons. **C.** Table showing the mean number (±SEM) of noradrenergic ventrolateral medullary neurons and the mean number (±SEM) of ventrolateral medullary nordrenergic neurons which project also to the vlPAG. The number in brackets is the percentage of double labelled (vlPAG-projecting noradrenergic neurons). In each table the data are presented for each of the seven levels analysed throughout the rostrocaudal extent of the ventrolateral

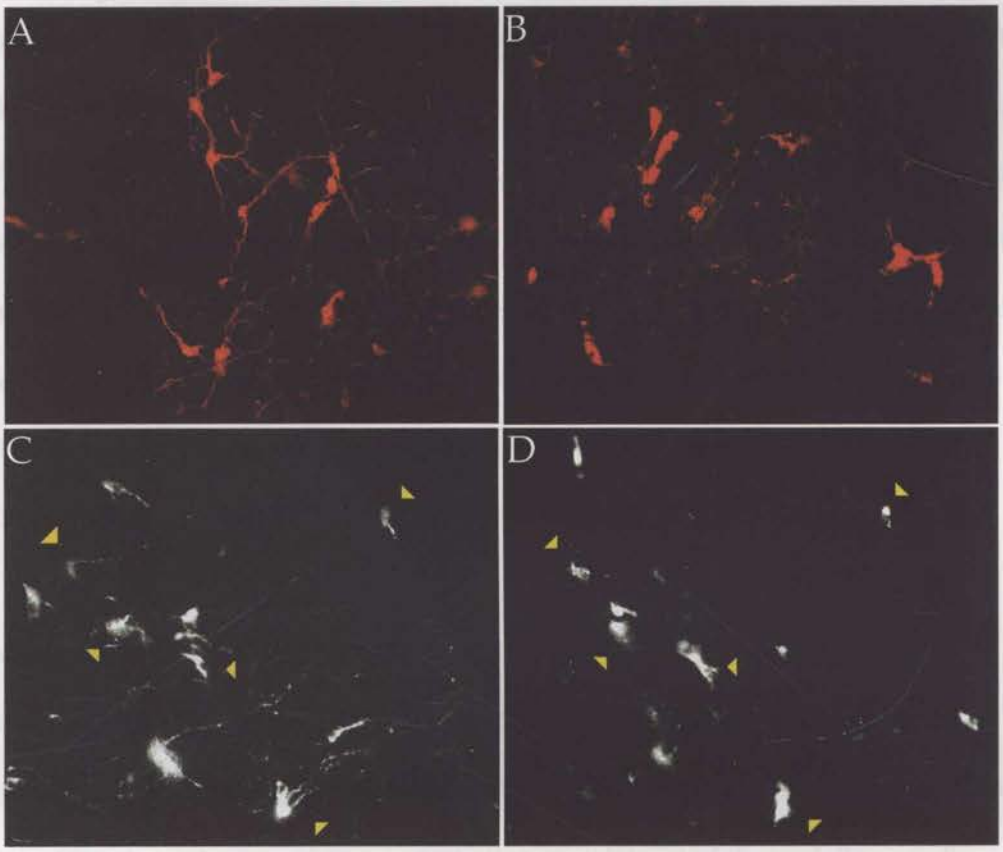

Figure 4.22
Fluorescent photomicrographs of coronal sections through catecholaminergic cell groups in the medulla illustrating **A.** tyrosine hydroxylase immunoreactivity at 0.5mm caudal to the Obex. These neurons are presumed to belong to the A1 noradrenergic cell group; **B.** phenylethanolamine-N-metyltransferase immunoreactivity at 1.5mm rostral to the Obex. These neurons belong to the C1 adrenergic cell group. Photomicrographs C and D illustrate neurons present in the same coronal section which are immunoreactive to antisera directed against tyrosine hydroxylase **(C)** and neurons retrogradely labelled after CTB injection into the ventrolateral PAG **(D)**. The double labelled cells are indicated by arrowheads. The scale bar represents 1mm.

Figure 4.21c shows both the mean number (±SEM) of noradrenergic neurons and the mean number (±SEM) of double labelled (vlPAG-projecting noradrenergic) neurons. Overall, 70% of noradrenergic VLM neurons were found to project onto the vlPAG. Specifically: (i) approximately 50% of the noradrenergic neurons located caudal to the Obex project to the vlPAG (i.e., neurons located in the region 1.0mm caudal to Obex); (ii) *almost all* noradrenergic neurons located at the level of the Obex (89%) and 0.5mm rostral to the Obex (86%) project also to the vlPAG; and (iii) approximately two thirds of noradrenergic neurons located at the rostral pole of the ventrolateral medulla project to the vlPAG (i.e., neurons located in the region 1.5mm rostral to Obex). The percentage of vlPAG-projecting noradrenergic neurons for each level of the VLM is given in Table 4.2c. Representative photomicrographs are shown in Figure 4.22.

4.4.5 Nucleus of the Solitary Tract:

Figure 4.23a illustrates the mean number (±SEM) of TH-IR neurons and the mean number (±SEM) of double labelled (TH-IR and vlPAG-projecting) neurons at each level of the NTS. It can be seen in Figure 4.23a that at each level of the medulla a small number (17%) of TH-IR, NTS neurons project onto the vlPAG. Similarly, a small number of PNMT-IR neurons (22%) project also to the vlPAG (Figure 4.23b). After subtracting the number of PNMT-IR neurons from the number of TH-IR neurons in order to estimate the proportion of double-labelled (i.e., vlPAG-projecting) noradrenergic neurons, it is revealed that approximately 18% of noradrenergic neurons project also the vlPAG (Figure 4.23c). The percentages of TH-IR, PNMT-IR and noradrenergic vlPAG-

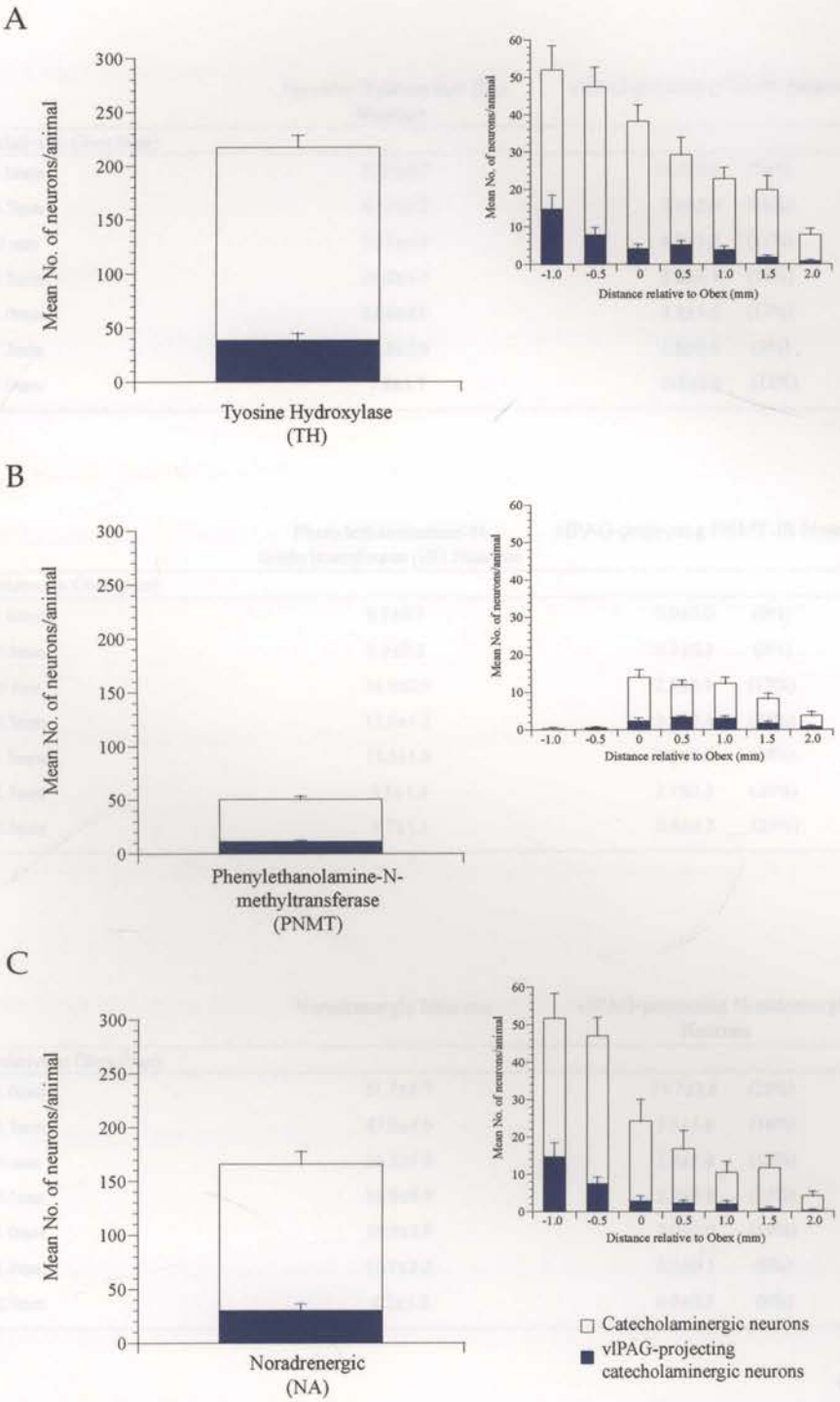

Figure 4.23
Histograms illustrating **(A)** the mean number (±SEM) of vlPAG-projecting, tyrosine hydroxylase immunoreactive neurons in the nucleus of the solitary tract of animals subject to hypotensive (30%) haemorrhage. The insert shows the mean number (± SEM) of such neurons at each of the seven levels analysed; **(B)** the mean number (±SEM) of vlPAG-projecting, phenylethanolamine-N-methyltransferase immunoreactive (i.e., *adrenergic*) neurons in the nucleus of the solitary tract of animals subject to hypotensive (30%) haemorrhage. The insert shows the mean number (± SEM) of such neurons at each of the seven levels analysed; **(C)** the mean number (±SEM) of vlPAG-projecting, *noradrenergic* neurons in the nucleus of the solitary tract of animals subject to hypotensive (30%) haemorrhage. The insert shows the mean number (± SEM) of such neurons at each of the seven levels analysed.

A	Tyrosine Hydroxylase (IR) Neurons	vlPAG-projecting TH-IR Neurons	
Distance Relative to Obex (mm)			
-1.0mm	52.0±6.5	14.7±3.8	(28%)
-0.5mm	47.5±5.2	7.8±2.0	(16%)
0 mm	38.2±4.4	4.2±1.2	(11%)
+0.5mm	29.2±4.7	5.2±1.1	(18%)
+1.0mm	22.8±3.0	3.8±1.0	(17%)
+1.5mm	19.8±3.8	1.8±0.6	(9%)
+2.0mm	7.8±1.7	0.8±0.4	(11%)

B	Phenylethanolamine-N-methyltransferase (IR) Neurons	vlPAG-projecting PNMT-IR Neurons	
Distance Relative to Obex (mm)			
-1.0mm	0.3±0.3	0.0±0.0	(0%)
-0.5mm	0.5±0.3	0.3±0.3	(0%)
0 mm	14.0±2.0	2.3±0.9	(17%)
+0.5mm	12.0±1.2	3.3±0.4	(28%)
+1.0mm	12.3±1.6	3.0±0.6	(24%)
+1.5mm	8.3±1.3	1.7±0.5	(20%)
+2.0mm	3.7±1.1	0.8±0.3	(23%)

C	Noradrenergic Neurons	vlPAG-projecting Noradrenergic Neurons	
Distance Relative to Obex (mm)			
-1.0mm	51.7±6.7	14.7±3.8	(28%)
-0.5mm	47.0±4.9	7.5±1.8	(16%)
0 mm	24.2±5.8	2.8±1.4	(12%)
+0.5mm	16.8±4.9	2.2±0.9	(13%)
+1.0mm	10.5±2.9	2.0±0.9	(19%)
+1.5mm	11.7±3.2	0.7±0.5	(6%)
+2.0mm	4.2±1.2	0.3±0.3	(8%)

Table 4.3
A. Table showing the mean number (±SEM) of NTS neurons immunoreactive for tyrosine hydroxylase (TH-IR) and the mean number (±SEM) of tyrosine hydroxylase-IR NTS neurons which project also to the ventrolateral PAG. The number in brackets is the percentage of double labelled (vlPAG-projecting, TH-IR) neurons. **B.** Table showing the mean number (±SEM) of NTS neurons immunoreactive for phenylethanolamine-N-methyltransferase (PNMT-IR) and the mean number (±SEM) of phenylethanolamine-N-methyltransferase-IR NTS neurons which project also to the vlPAG. The number in brackets is the percentage of double labelled (vlPAG-projecting PNMT-IR) neurons. **C.** Table showing the mean number (±SEM) of noradrenergic NTS neurons and the mean number (±SEM) of nordrenergic NTS neurons which project also to the vlPAG. The number in brackets is the percentage of double labelled (vlPAG-projecting noradrenergic neurons). In each table the data are presented for each of the seven levels analysed throughout the rostrocaudal extent of the NTS.

projecting neurons for each level of the NTS are given in Tables 4.3a, 4.3b, and 4.3c respectively.

Summary of Results

The aim of this series of experiments was to evaluate the extent of medullary adrenergic and noradrenergic projections to the vlPAG.

These data indicate that:

(i) Large numbers of ventrolateral medullary noradrenergic neurons project to the vlPAG.

(i) A much smaller number of ventrolateral medullary adrenergic neurons project to the vlPAG.

(i) The NTS provides a small amount of catecholaminergic input to the vlPAG.

When the results of experimental series I and II are considered together, it appears likely that an ascending *noradrenergic* pathway arising from the ventrolateral medulla may play a key role in triggering decompensation.

The action of noradrenaline on midbrain ventrolateral PAG neurons has previously only been investigated using *in vitro* slice electrophysiology. In this study it was shown that superperfusion of midbrain slices with noradrenaline results in the depolarisation of most vlPAG neurons (Vaughan et al., 1994).

With these findings in mind, one final series of experiments (Experimental series III) used physiological techniques to determine whether the release and subsequent binding of noradrenaline to alpha adrenoreceptors within the vlPAG plays a role in triggering decompensation.

Aims

The aim of this series of experiments was to determine whether noradrenergic neurotransmission within the vlPAG plays a role in the expression of decompensation.

Specifically:

(i) Small microinjections of the excitatory amino acid DLH were made in order to verify that chronically implanted guide cannulae were positioned within the ventrolateral PAG. The guide cannulae were deemed to lie in the vlPAG if the DLH microinjection resulted in a ≥10mmHg fall in arterial pressure.

(ii) Microinjections of the broad-spectrum alpha adrenoreceptor antagonist phentolamine were subsequently made into the ventrolateral PAG in order to evaluate the effect of alpha adrenoreceptor blockade on haemorrhage-evoked hypotension and bradycardia.

4.5 Materials and Methods – Experimental series III

4.5.1 Animals and Surgery: Data were obtained from 25 male Sprague-Dawley rats (250-350 grams). Rats were sedated by brief exposure to CO_2 then anaesthetised with an intramuscular injection of ketamine/xylazine (ketamine hydrochloride 75mg/kg:Rompun 4ml/kg) before being fixed in a stereotaxic frame in the "flat-skull" position. Body temperature was maintained at 37°C with a thermoregulatory heating blanket.

4.5.2 Implantation of intra-cranial guide cannulae: Following induction of anaesthesia a dorsal craniotomy was performed and an area of bone approximately $25mm^2$ removed to facilitate implantation of bilateral stainless steel guide cannulae (ID: 0.18mm; ED: 0.36mm; 1.5mm centre-centre distance apart; Plastics One USA). The guide cannulae were positioned at a 16° rostro-caudal angle, 5mm caudal to the skull marking Bregma and 3mm below the cortical surface according to the atlas of Paxinos and Watson (2000). The guide cannulae were secured to three intra-cranial screws with dental cement. A stainless steel stylet occluded the guide cannula when not in use. At the completion of surgery the rat was removed from the stereotaxic frame and the scalp incision closed. Subsequently each animal was given fluids (2.0ml, 0.9% saline i.p.) and antibiotics (Norocillin 3mg/kg i.m) before being returned to its home cage. The mobility, activity level, eating, drinking and grooming of each rat was closely observed each post-operative day.

4.5.3 Habituation Procedures: Each day subsequent to guide cannulae implantation each rat was taken to the experimental area and handled for approximately ten minutes. During this time the animals head was stroked, particularly around the site of the guide cannulae. As well, each stylet was removed and replaced once during each daily habituation session.

4.5.4 Cannulation Procedures: Seven days following implantation of the guide cannula each rat was anaesthetised with halothane (2% halothane in 100% O_2). Arterial and venous cannulae were placed into the left carotid artery (PE tubing, OD=0.96mm) and right jugular vein (PE tubing, OD=0.96mm; with a 32mm Silastic tip OD=1.19mm) respectively. The cannulae were passed subcutaneously and exteriorised in the interscapular region.

In order to verify that the guide cannulae were correctly positioned within the vlPAG, the guide cannula stylet was removed and replaced with an injection cannula that extended 3.5mm below the tip of the guide. The arterial cannula was connected to a pressure transducer, the signal amplified, filtered (MacLab 8) and displayed "on – line" before a single 50nl microinjection of the excitatory amino acid D-L-homocysteic acid (DLH) was made via Hamilton syringe. The cannula was deemed to be positioned within the vlPAG if the DLH injection evoked a hypotension greater than or equal to 10mmHg. At the conclusion of the experiment the cannula was removed, the stylet replaced and anaesthesia discontinued. Each animal was given fluids (2ml, 0.9% saline i.p.) and returned to its home cage.

4.5.5 Haemorrhage Procedures: Twenty four hours following arterial and venous cannulation, the arterial cannula was connected to a pressure transducer, and the signal amplified, filtered (MacLab 8), displayed "on – line" and recorded on an Apple Macintosh running Chart Software for later "off-line" analysis. The intra-cranial stylet was removed and replaced with injection cannulae containing the non-specific alpha adrenoreceptor antagonist phentolamine (20μg/μl). Baseline arterial pressure was recorded for twenty minutes before 200nl of phentolamine was injected over approximately one minute. Ten minutes following injection of phentolamine each animal was subject to a hypovolaemic (30%) haemorrhage (removal of 30% total blood volume over 20 minutes). The haemorrhage was performed at two rates; removal of 10% total blood volume over 10min followed by removal of 20% total blood volume over the next 10min. At the completion of the haemorrhage period, AP was recorded for the following 40 minutes (post-haemorrhage recovery period). After this time, each animal was deeply anaesthetised with sodium pentobarbitone (1.0ml i.v. Nembutal) and perfused with 500ml 0.9% saline and 500ml ice cold 4% paraformaldahyde.

4.5.6 Histological verification of injection sites: Immediately following transcardial perfusion, each brain was removed and post-fixed for 24hrs in 4% paraformaldehyde solution. Each brain was subsequently cryoprotected in 10% sucrose (made up in 0.1M PBS) for 3-4 days. Serial coronal sections through the midbrain periaqueductal gray were cut, counterstained with Nissl dye and analysed under the light microscope. The rostro-caudal extent of each injection site was plotted using a camera lucida attachment before

being reconstructed onto standard atlas sections taken from the atlas of Paxinos and Watson 2000.

4.5.7 Analysis and Statistics: Mean arterial pressure (AP) was recorded continuously. Heart rate was derived from the raw arterial pressure trace. Baseline measures of both AP and HR were calculated from the average of three ten second (10s) samples taken at 10min, 5min and 20s before commencement of blood withdrawal. Twenty second samples of AP and HR were taken at 2min intervals during the haemorrhage period (0-20min) and at 5min intervals during the 40min post-haemorrhage recovery period. Statistical comparisons between groups (i.e., between un-injected control and phentolamine-injected animals) used a repeated measures two-way ANOVA, followed by Bonferroni-Dunn post-hoc analysis (For details see Ludbrook 1994).

4.6 Results – Experimental series III

4.6.1 Haemorrhage Only Controls: Prior to experimental manipulations the resting AP and HR for this group of animals (N=6) was 115 ± 3mmHg and 398 ± 13bpm respectively. The AP response to hypovolaemic (30%) haemorrhage was biphasic (i.e., occurred in two distinct phases). During the initial 10 minutes AP did not fall significantly below resting baseline values. However, during the 11th minute of blood loss, AP fell to a level significantly below resting baseline values (t-test; $P < 0.05$). Immediately following withdrawal of 30% total blood volume, mean AP was 53 ± 3mmHg. This represented a fall of 54 ± 2% from resting baseline values. The HR response to hypovolaemic (30%) haemorrhage was also observed to be biphasic. There was no change in HR during the first 10 minutes of blood withdrawal, however, during the 11th minute there was a rapid bradycardia to levels significantly below resting baseline values. Following withdrawal of 30% total blood volume, mean HR was 342 ± 29 bpm. This represented a fall of 15 ± 5% compared to resting baseline values (t-test; $P<0.05$).

Both AP and HR were recorded during the post-haemorrhage recovery period (i.e., for 40 minutes following cessation of blood withdrawal). AP was observed to recover slightly, though still remained significantly below resting baseline levels (15% below baseline values at the end of the recording period; Figure 4.27b). Similarly, HR recovered slightly though still remained significantly below baseline values (10% below at the end of the

recording period; Figure 4.27d). Representative AP and HR traces from one experimental animal are shown in Figure 4.28a.

4.6.2 Effects of bilateral intra-vlPAG phentolamine on the haemodynamic response to hypovolaemic (30%) haemorrhage:

Prior to experimental manipulations the resting AP and HR for this group of animals (N=6) was 112 ± 5mmHg and 376 ± 10bpm respectively.

The tip of each injection cannula used in this study was located in the 'vasodepressor' region of the ventrolateral PAG as defined by a DLH-evoked fall in AP ≥ 10mmHg (Figure 4.24). Camera lucida drawings made from Nissl stained coronal sections were used to map the location of, and the rostrocaudal extent of each phentolamine injection made. Each injection site was then systematically reconstructed onto standard atlas sections taken from the atlas of Paxinos and Watson. These reconstructions are shown in Figure 4.25. A representative coronal photomicrograph of one such injection is shown in Figure 4.26.

Bilateral injection of phentolamine made in the vlPAG of conscious, unrestrained animals had no effect on the baseline level of either AP (113.8 ± 5.6mmHg prior to injection *vs* 115.0 ± 4.2mmHg post injection) or HR (396.5 ± 8.7 bpm prior to injection *vs* 411.5 ± 17.4 bpm post injection). However, phentolamine administration made 10min prior to hypovolaemic haemorrhage resulted in a significant delay and attenuation of haemorrhage-evoked hypotension. That is, AP did not fall significantly below baseline

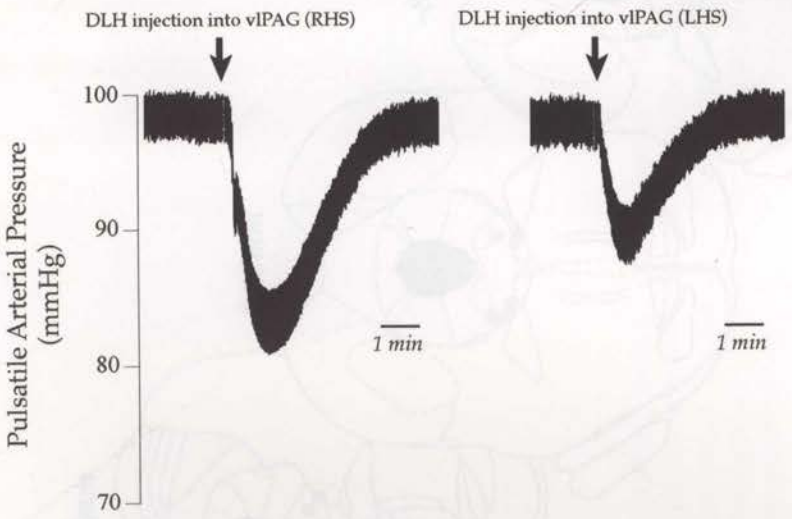

Figure 4.24
Pulsatile arterial pressure traces illustrating the fall in AP evoked by a single 50nl injection of the excitatory amino acid D-L-homocysteic acid (DLH) into each side of the vlPAG. Each injection was made at the point indicated by the arrow above the trace. The injection cannula was deemed to be correctly positioned in the vlPAG if AP fell 10mmHg or more. The scale bar represents 1 minute.

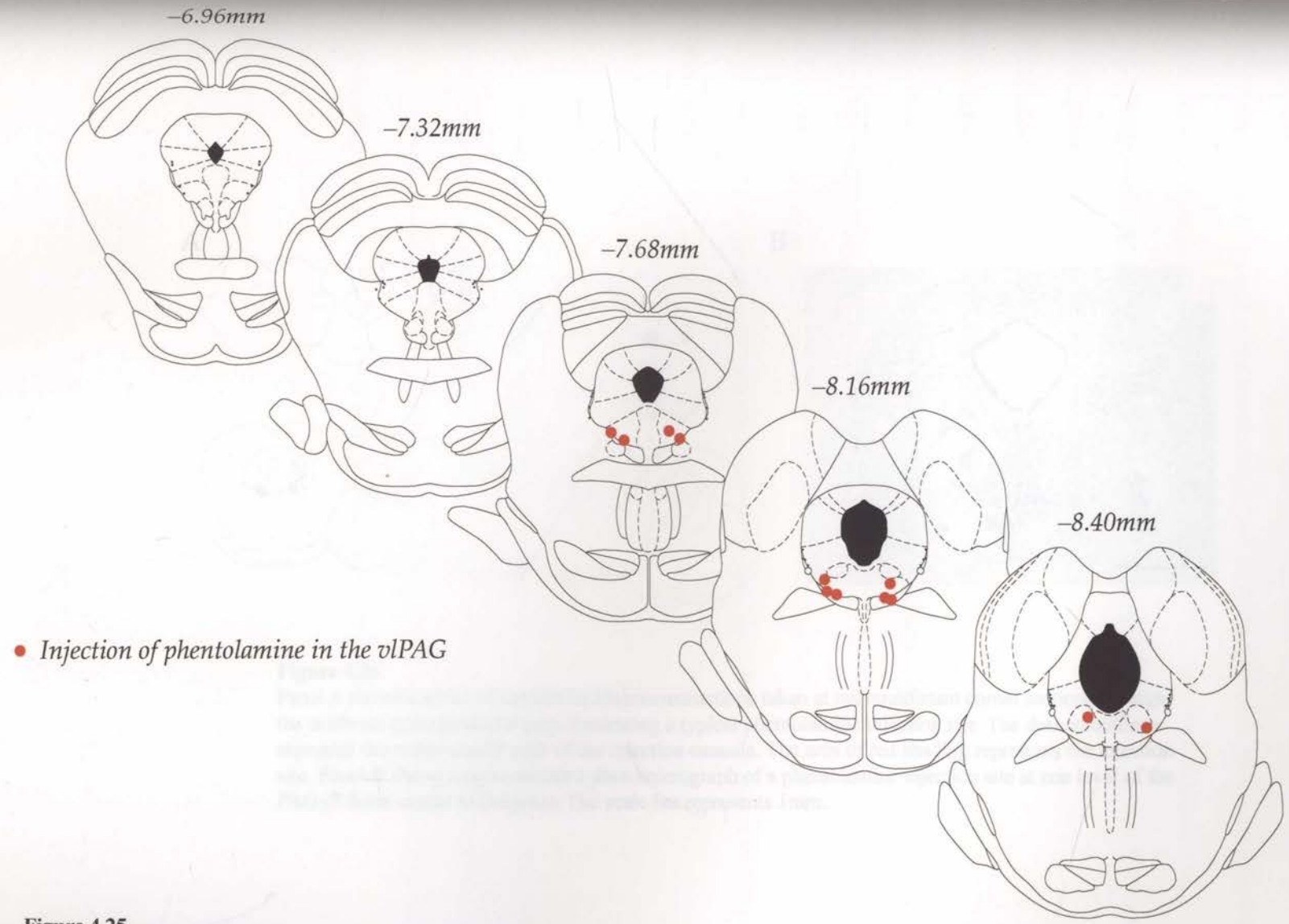

Figure 4.25
Schematic representation of serial equidistant cornal sections throughout the periaqueductal gray showing the location of each bilateral injection of phentolamine methanesulphonate. Each site represents the tip of the injection cannulae. Sections were adapted from the atlas of Paxinos and watson 2005.

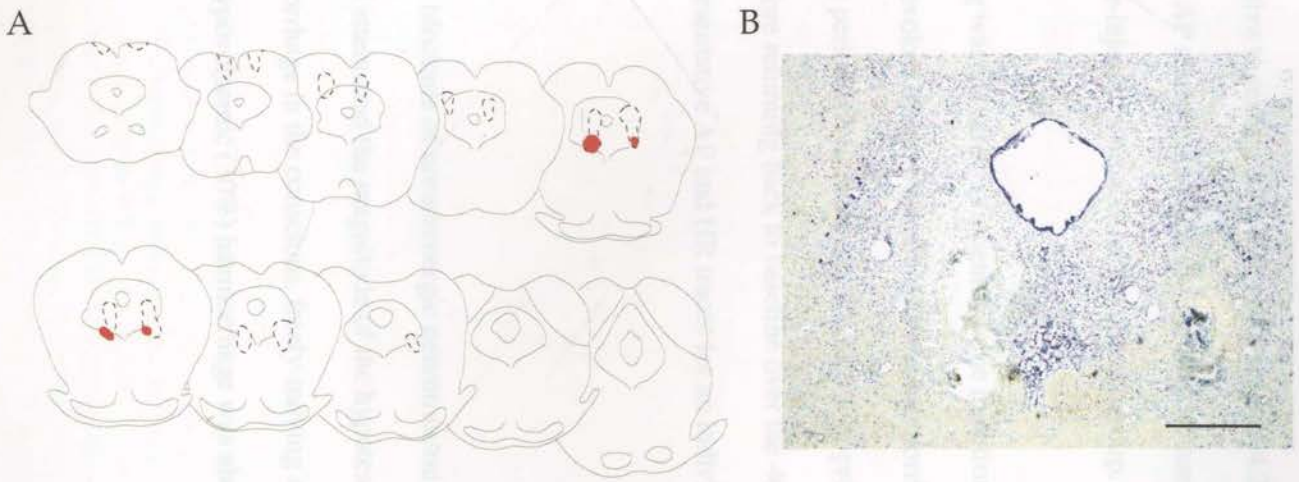

Figure 4.26
Panel A shows a series of camera lucida reconstructions taken at ten equidistant cornal sections through the midbrain periaqueductal gray illustrating a typical phentolamine injection site. The dashed outlines represent the rostro-caudal path of the injection cannula. The area of red shading represents the injection site. Panel B shows a representative photomicrograph of a phentolamine injection site at one level of the PAG (7.8mm caudal to Bregma). The scale bar represents 1mm.

values until the 16th minute of the haemorrhage period (compared to the 10th minute in control animals). This occurred after approximately 22% of total blood volume had been withdrawn. At the end of the haemorrhage period, AP had fallen to 65 ± 7mmHg, a fall of 43 ± 5% relative to resting baseline values (Figure 4.27). There was no significant difference in AP at any time point during the post-haemorrhage recovery period between phentolamine-injected animals and the control group.

More striking was the effect of phentolamine injections into the vlPAG on the bradycardia evoked by hypovolaemic (30%) haemorrhage. Throughout the 20min haemorrhage period HR increased to 20 ± 3.5% of pre-haemorrhage resting values (at the 17th min) before returning back to baseline over the 40min post-haemorrhage recovery period. Representative AP and HR traces for an individual animal are shown in Figure 4.28b.

Summary:

In summary, blockade of noradrenergic neurotransmission within the vlPAG delayed the onset of, and attenuated the magnitude of the hypotension evoked by hypovolaemic (30%) haemorrhage in the conscious, freely-moving rat. In addition, the bradycardia evoked by hypovolaemic (30%) haemorrhage was abolished.

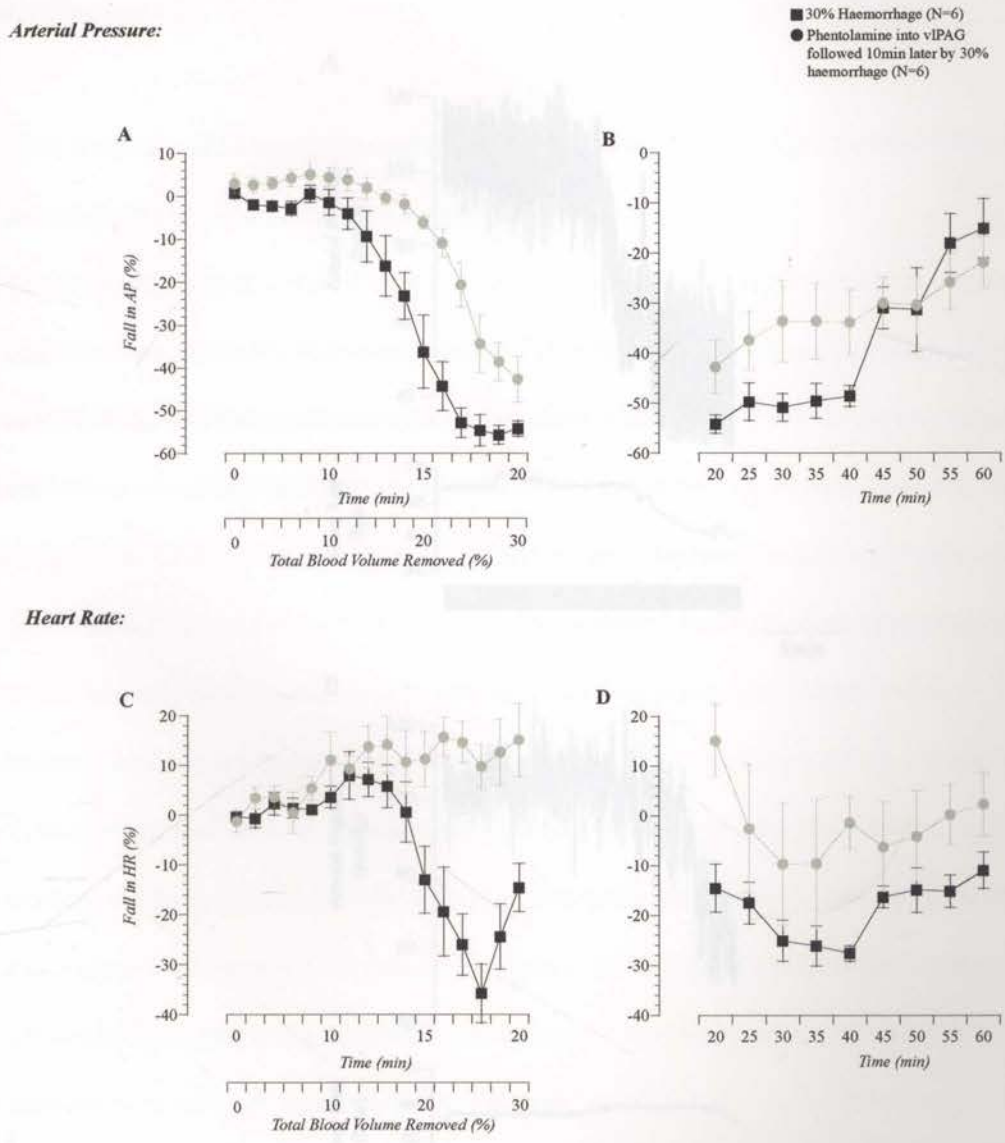

Figure 4.27

Mean changes (+/-SEM) in arterial pressure (AP) expressed as a percentage change from pre-stimulus baseline values following: (i) 30% haemorrhage alone; and (ii) bilateral microinjection of phentolamine made in the vlPAG followed 10min later by a 30% haemorrhage. Panel **A** shows the initial twenty minute haemorrhage period, and panel **B** shows the period of recompensation (20min-60min post-haemorrhage). Significant differences in mean AP between control haemorrhage and haemorrhage following phentolamine administration are shown by asterisks (repeated measures two-way ANOVA with Bonferroni-Dunn post-hoc analysis; * indicates $P<0.05$.

Mean changes (+/-SEM) in heart rate (HR) expressed as a percentage change from pre-stimulus baseline values of animals following either: (i) 30% haemorrhage alone; or (ii) bilateral microinjection of phentolamine made in the vlPAG followed 10min later by a 30% haemorrhage. Panel **C** shows the initial twenty minute haemorrhage period, and panel **D** shows the period of recompensation (20min-60min post-haemorrhage). Statistical analysis used a repeated measures two-way ANOVA followed by Bonferroni-Dunn post-hoc correction.

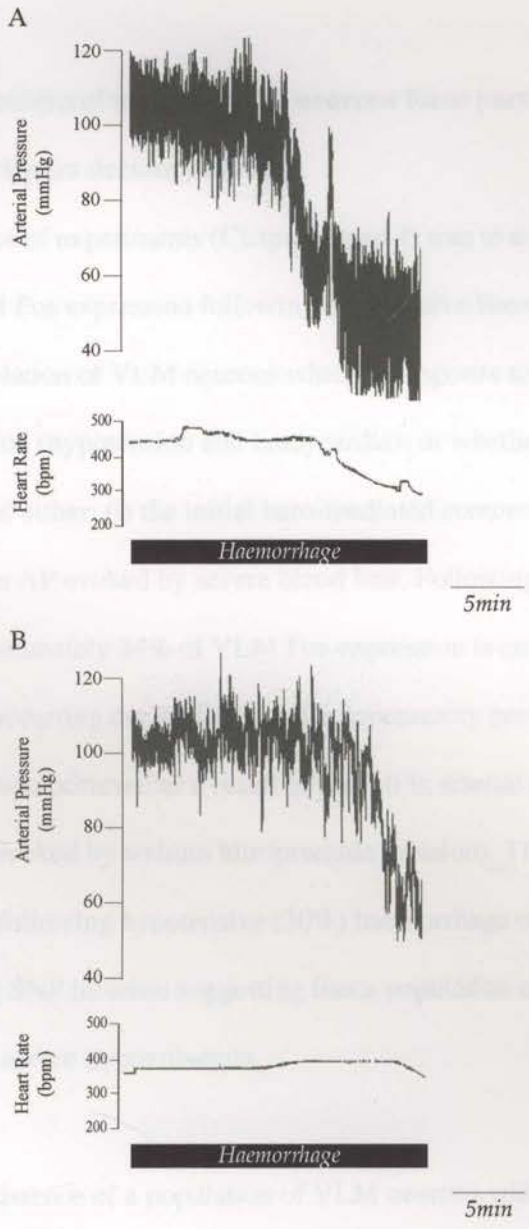

Figure 4.28
Pulsatile arterial pressure and heart rate traces following **A** hypovolaemic (30%) haemorrhage; and **B** hypovolaemic (30%) haemorrhage following bilateral injection of phentolamine (200nl) into the ventrolateral periaqueductal gray. Note that injection of phentolamine into the vlPAG delayed and attenuated the fall in AP, and abolished the bradycardia evoked by hypovolaemic haemorrhage. The scale bar represents 5min.

4.7 Discussion:

4.7.1 Evidence that ventrolateral medullary A1 neurons form part of the central neural pathway which triggers decompensation:

The aim of the initial series of experiments (Chapter 4 part I) was to evaluate whether the observed increase in VLM Fos expression following hypotensive haemorrhage was due to the activation of a population of VLM neurons which in response to severe blood loss may trigger decompensation (hypotension and bradycardia); or whether their activation occurs as a consequence of either: (i) the initial baro-mediated *compensatory* period; or (ii) *secondary* to the fall in AP evoked by severe blood loss. Following hypotensive (30%) haemorrhage approximately 34% of VLM Fos-expression is attributable to baroreceptor unloading (occurring during the initial compensatory period). An additional 13% of VLM Fos expression occurred as a result of the fall in arterial pressure (i.e., euvolaemic hypotension evoked by sodium nitroprusside infusion). Thus, 53% of the Fos-expression observed following hypotensive (30%) haemorrhage occurs over and above that seen following SNP infusion suggesting that a population of VLM neurons are selectively 'activated' by severe hypovolaemia.

Having established the existence of a population of VLM neurons which are activated specifically by decompensation, double labelling experiments were carried out in order to classify the phenotype of these neurons (Chapter 4 part I). Experiments combining Fos-expression with immunohistochemistry for both tyrosine hydroxylase and phenylethanolamine-n-methyltransferase revealed that hypotensive (30%) haemorrhage

activated almost 90% of VLM *noradrenergic* neurons. Significantly fewer noradrenergic neurons were found to be activated following euvolaemic hypotension (23%). Normotensive (10%) haemorrhage resulted only in the 'activation' of adrenergic ventrolateral medullary neurons (i.e., C1 neurons).

The finding that hypotensive (30%) haemorrhage evokes Fos-expression in almost all A1 noradrenergic neurons suggested that these neurons might play a role in triggering decompensation. Therefore, the next series of experiments (Chapter 4 part II) were designed to evaluate the extent to which medullary noradrenergic neurons project specifically to the vlPAG. It was found that the vlPAG receives direct noradrenergic input from the ventrolateral medulla.

The final series of physiological experiments (Chapter 4 part III) utilised bilateral intra-vlPAG injections of the broad-spectrum alpha adrenoreceptor antagonist phentolamine to demonstrate that blockade of noradrenergic neurotransmission results in a delay and attenuation of the hypotension evoked by severe hypovolaemic haemorrhage. Taken together, these data suggest that vlPAG-projecting, noradrenergic VLM neurons (i.e., A1 cell group) may play a key role in triggering decompensation.

4.7.2 The ventrolateral medulla mediates the central response to cardiovascular challenges:

It is well documented that neurons within the ventrolateral medulla are involved in the reflex regulation and maintenance of arterial pressure (Dampney 1994, Guyenet et al.,

1987, Aicher et al., 1995, Jeske et al., 1995). Activation of neurons caudal to the Obex (CVLM; including the A1 *noradrenergic* cell group) has been shown to evoke vasodepression (moderate hypotension and bradycardia) in addition to decreases in sympathetic nerve activity (Henderson et al., 2000, Dampney 1994). Furthermore, caudal VLM neurons have been shown to relay cardiovascular afferent information to other brainstem and hypothalamic structures involved in the reflex regulation of arterial pressure as well as both intra- and extracellular fluid regulation (Haselton and Guyenet 1990, Barman and Gebber 1987, Sawchenko et al., 1985, Simerly and Swanson 1986)

In contrast, activation of neurons rostral to the Obex (RVLM; including the C1 *adrenergic* cell group) has been shown to elicit vasopressor responses, that is, increases in arterial pressure, heart rate and sympathetic nerve activity (Aicher et al., 1995, Dampney 1994, Dampney et al., 1988, Madden and Sved 2003). The vast majority of RVLM neurons have been shown to project to the intermediolateral cell column of the thoracolumbar spinal cord where they innervate sympathetic preganglionic neurons (Jeske et al., 1995). In addition, neurons within the rostral VLM have also been shown to project to forebrain structures involved in cardiovascular and fluid homeostasis (Herbert and Saper 1992, Shioda et al., 1992, Cunningham et al., 1990).

Many experimental reports have focussed on the role of the VLM in the short-term regulation of arterial pressure. It is widely accepted that both the CVLM and RVLM are critical brainstem structures subserving the baroreflex (see Aicher et al., 1995 or Dampney 1994 for review). Reports that selective destruction of C1 neurons following

anti-dopamine β-hydroxylase injection into the RVLM significantly decreases resting AP and attenuates the baroreflex in the conscious rat, suggests that the baroreflex is mediated chiefly by adrenergic pre-sympathetic neurons within the ventrolateral medulla. (Madden and Sved 2003). The finding in the present study that normotensive (10%) haemorrhage evokes Fos-expression in adrenergic VLM neurons only fits well with these reports in light of the fact that the initial compensatory phase of haemorrhage is mediated by the arterial baroreflex (for review see Dampney 1994, Schadt and Ludbrook 1991, Evans et al., 2001).

4.7.3 Noradrenergic A1 projections to vlPAG as a possible trigger for decompensation:

Previous studies have observed substantial activation of brainstem catecholaminergic (noradrenergic and adrenergic) neurons following both moderate and severe blood loss (Chan and Sawchenko 1994, Chan and Sawchenko 1998, Dayas et al., 2001a, Dun et al., 1993). The series of experiments performed in Chapter 4 revealed that: (i) nearly all noradrenergic ventrolateral medullary neurons are activated by hypotensive (30%) haemorrhage; (ii) the vlPAG receives dense input from noradrenergic ventrolateral medullary neurons; and (iii) that blockade of alpha adrenoreceptors in the vlPAG significantly delays and attenuates decompensation. Taken together, these data suggest that vlPAG-projecting A1 neurons may be responsible for providing afferent drive onto the vlPAG thus resulting in the expression of decompensation.

Previous studies from this laboratory have reported that bilateral blockade of a restricted portion of the ventrolateral medulla (vasodepressor region encompassing the CVLM and A1 noradrenergic cell group) with cobalt chloride results in an attenuation of haemorrhage-evoked hypotension, and strikingly, abolishes haemorrhage-evoked bradycardia (Henderson et al., 2000). These findings fit well with the hypothesis that a population of neurons in the caudal ventrolateral medulla relay signals received from the periphery (possibly via spinal projections) to the ventrolateral PAG in order to trigger decompensation.

Interestingly, Henderson et al., (2000) failed to abolish the haemorrhage-evoked hypotension with bilateral injections of cobalt chloride into the CVLM. As reported in this study, activation of noradrenergic VLM neurons occurs at all rostrocaudal levels of the VLM (from –1.0mm caudal to Obex to +1.5mm rostral to Obex; see Chapter 4 Figures 4.6 and 4.8). In addition, the greatest number of both vlPAG-projecting A1 neurons, and double labelled (haemorrhage-evoked Fos-IR) A1 neurons are located at the level of Obex and half a millimetre beyond (Obex+0.5mm); slightly more rostral than the region targeted in the study of Henderson et al., 2000.

It is therefore not surprising that only a moderate attenuation of the fall in AP was observed in Henderson et al., 2000 given that the restricted location of cobalt chloride injections would, in all probability, have been insufficient to abolish the function of *all* vlPAG-projecting, ventrolateral medullary noradrenergic neurons.

4.7.4 Actions of noradrenaline on vlPAG neurons – activation of descending medullary projections to the caudal midline medulla which mediate decompensation:

The anatomical data presented in Chapter three suggests that decompensation is likely to be mediated by descending ventrolateral PAG projections to a restricted caudal midline medullary 'vasodepressor' region (CMM). If noradrenergic neurotransmission in the vlPAG were indeed critical for the expression of decompensation then one would expect midline medullary neurons to respond to noradrenaline-induced depolarisation of PAG neurons.

Past reports by Behbehani and colleagues have shown that iontophoretic deposition of noradrenaline in the PAG results in excitation of neurons located in midline medullary nuclei (Behbehani et al., 1981). Unfortunately, in the above study, no histological reconstructions of midline medullary recording sites were shown making it difficult to determine the exact location of the nuclei from which recordings were made. However, the approach described and the co-ordinates given in their publication strongly suggests that recordings were made from neurons located in the region of the CMM. These data suggest, therefore, that vlPAG noradrenergic neurotransmission is capable of exciting neurons in a region known to be critical for the expression of decompensation (i.e., the CMM).

4.7.5 Alternate medullary pathways involved in stimulating the release of vasopressin from the hypothalamus:

It is interesting to note that the main function usually ascribed to ventrolateral medullary A1 noradrenergic neurons following a severe cardiovascular challenge (i.e., haemorrhage) has been to stimulate the release of vasopressin from the hypothalamus (Buller et al., 1999, Renaud 1996, Larsen and Vrang 1995, Head et al., 1987, Gieroba et al., 1994, Lipinska et al., 2004). Plasma vasopressin levels are known to increase only during the decompensatory phase of blood loss (Ludbrook et al., 1988, Oliver et al., 1990, Quail et al., 1987, Schadt and Hasser 1991), a finding which suggests that vasopressin plays *no role* in maintaining blood pressure following acute reductions in central blood volume. Direct support for such a notion arises from data showing that administration of V_1 receptor antagonists prior to severe haemorrhage does not alter the haemodynamic response to blood loss in either conscious rabbits or rats (Korner et al., 1990, Schadt and Hasser 1991, Fejes-Toth et al., 1988). Vasopressin, therefore, is suggested to play only a role in the recovery from acute hypotension.

Early studies performed in the rat and rabbit suggested that the post-haemorrhagic release of vasopressin was likely mediated by a projection to the supraoptic (SON) and paraventricular (PVN) nuclei of the hypothalamus from the A1 noradrenergic cell group. More recent data, however, suggests that the release of vasopressin subsequent to severe blood loss involves activation of an additional vasopressin-stimulatory pathway.

Experiments performed in cavally occluded animals have shown that following a *moderate* reduction in central blood volume, the integrity of hypothalamic-projecting A1

neurons is critical for the post-haemorrhage release of vasopressin (Renaud 1996, Larsen and Vrang 1995, Head et al., 1987, Gieroba et al., 1994, Lipinska et al., 2004, Head et al., 1987, Smith et al., 1995). In contrast, following a *severe* reduction in central blood volume, vasopressin release switches to being *independent* of A1 neurons (Smith et al., 1995), that is, the firing rate of functionally-identified vasopressin-secreting neurons is not reduced following interruption of A1 neuronal function. Further support for the hypothesis that vasopressin release occurs independent of A1 neuronal function arises from experiments performed in decerebrate animals showing that when the hypothalamus is disconnected from the mesencephalon, the decompensatory phase of haemorrhage, and the post-haemorrhagic recovery of arterial pressure is preserved (Troy et al., 2002).

At present, alternate neural pathways responsible for triggering the release of vasopressin following severe hypovolaemia have not been fully elucidated. However, it has been suggested that the most likely source of afferent input to the hypothalamus arises from a central pathway sensitive to cerebral ischaemia. This hypothesis arose from observations that the release of vasopressin from the hypothalamus under such conditions occurs independent of peripheral cardiovascular receptors (Shen et al., 1991, Khanna et al., 1994, Wang et al., 1988).

Hypotensive haemorrhage sufficient to lower AP to 44-50 mmHg surpasses the autoregulatory level required to maintain cerebral blood flow. This under-perfusion results in cerebral ischaemia (Skarphedinsson et al., 1986). In both rat and rabbit, cerebral ischemia evoked by occlusion of the vertebral arteries evokes a characteristic pattern of

cardiovascular and respiratory changes (i.e., sympathoexcitation) (Guyenet and Brown 1986). The rostral ventrolateral medulla has been shown to be responsible for integrating the sympathomotor and respiratory responses to cerebral ischaemia (Guyenet et al., 1990, Haselton and Guyenet 1989). Neurons located in this region increase their discharge rate during cerebral ischaemia (Heary et al., 1993, Guyenet and Brown 1986), and furthermore, the response to cerebral ischaemia can be abolished altogether following electrolytic lesions of the rostral VLM (Guyenet and Brown 1986, Haselton and Guyenet 1989, Dampney and Moon 1980).

Thus, it has been hypothesised that following severe hypotensive haemorrhage, neurons in the rostral VLM, which are sensitive to cerebral ischaemia, provide input to the hypothalamus to stimulate the release of vasopressin. Supporting this hypothesis is recent evidence showing that selective destruction of C1 (i.e., adrenergic) neurons results in decreased plasma vasopressin levels following a hypotensive challenge (Madden et al., 2006).

Several past studies give anatomical plausibility to this hypothesis. First, a substantial number of adrenergic rostral VLM neurons have been shown to project to the hypothalamus (Haselton and Guyenet 1990, Barman and Gebber 1987, Sawchenko et al., 1985, Simerly and Swanson 1986). Second, excitation of the rostral VLM in the rat elicits the release of vasopressin from the pituitary (Ross et al., 1984). Finally, Fos-like immunoreactivity is observed in large numbers of magnocellular neurons within the

supra-optic nucleus following electrical stimulation of the ventrolateral medulla (Shioda et al., 1998).

Adrenergic C1 neurons within the rostral VLM project to both the parvicellular (pPVN) division and the magnocellular division (mPVN) of the paraventricular nucleus of the hypothalamus (PVN; Shioda et al., 1992, Cunningham et al., 1990, Sawchenko and Swanson 1982). The C1-mPVN projection may therefore provide an anatomical substrate which triggers the release of vasopressin from the posterior pituitary. Furthermore, the projection from the C1 cell group to the pPVN raises the possibility that it is via this projection that neurons in the external median eminence regulate the release of corticotropin from the anterior pituitary subsequent to the fall in AP evoked by a reduction in central blood volume (Darlington et al., 1992, Darlington et al., 1986).

4.7.6 No evidence of a role for the NTS in triggering decompensation:

As described in Chapter 4 (part I) there was no difference in the number of Fos-like IR cells evoked in the NTS by either hypotensive haemorrhage or SNP infusion. This result suggests that the observed neural activation within the NTS occurs secondary to the fall in AP, that is, as a consequence of decompensation. The NTS receives dense vagal afferent input and has been identified as a critical component of the baroreflex arc (for review see chapter one introduction, Dampney 1994, Guyenet 2006). Although early work in the rabbit suggested strongly that decompensation was triggered by cardiopulmonary vagal afferents, recent experiments performed by Troy et al., have demonstrated that vagal afferents play *no role* in triggering decompensation (Troy et al.,

in press). These findings fit well with the present report that no additional increase in neural activity within the NTS occurs during hypotensive haemorrhage over and above that seen during SNP infusion. This finding, coupled with the comparatively small number of catecholaminergic projections to the vlPAG make it *unlikely* that the NTS, and therefore signals arising from cardiac vagal afferents, play a critical role in triggering decompensation.

-Chapter 5-

The role of noradrenergic neurotransmission within the ventrolateral PAG under conditions of halothane anaesthesia

5.1 Introduction

The haemodynamic response to blood loss is profoundly altered by anaesthesia. At present the most commonly used inhalation anaesthetics in the clinical setting are halogenated anaesthetics such as sevoflurane, desflurane and isoflurane. Induction of anaesthesia with halogenated anaesthetics has been shown to evoke a significant hypotension (Vidal et al., 2006, O'Conner et al., 2006, Borer et al., 2006, Bostrom et al., 2006). Furthermore, under conditions of halogenated anaesthesia even *moderate* hypovolaemia can lead to shock and ultimately death (Caplan et al., 1988, Vatner 1978). Understanding the complex interaction(s) between halogenated anaesthetics and the central mechanism underlying hypovolaemia therefore represents an important clinical issue.

Following induction of general anaesthesia with halothane dramatic changes in catecholamine concentrations are observed at three central sites: (i) the nucleus accumbens; (ii) the locus coeruleus; and (iii) the ventrolateral periaqueductal gray (vlPAG) (Roizen et al., 1976). These changes in catecholamine concentration are reported to underlie the action of halothane as an effective inhalational anaesthetic (Ngai et al., 1969). Interestingly of these three regions it is the vlPAG which shows the most

striking and significant elevation in noradrenaline (NA) concentration (Roizen et al., 1976).

In an effort to delineate the central afferent pathway responsible for triggering hypovolaemic shock, the experiments performed in the previous three chapters revealed that the vlPAG receives dense ascending input from noradrenergic neurons in the ventrolateral medulla (the A1 cell group). Strikingly, the vast majority of these neurons are 'activated' following hypotensive haemorrhage suggesting that a noradrenergic mechanism within the vlPAG may trigger the hypotension evoked by severe blood loss. Further experiments showing that bilateral microinjections of phentolamine, a broad spectrum alpha receptor antagonist, made in the vlPAG significantly delayed and attenuated the magnitude of haemorrhage-evoked hypotension lend further support to the hypothesis that vlPAG noradrenergic neurotransmission is critical for the expression of decompensation.

Interestingly a past study from this laboratory revealed that halothane anaesthesia alone evoked Fos-expression in vlPAG-projecting, A1 noradrenergic neurons (Clement et al., 1998). The authors concluded that perhaps activation of this pathway by halogenated anaesthetics explains why decompensation is dramatically potentiated in anaesthetised animals (Ong et al., 1984, Ingwersen et al., 1987, Seyde and Longnecker 1984, Van Leeuwen et al., 1990), and why in humans, induction of general anaesthesia is usually associated with a significant hypotension (McKinney and Fee 1998, Kadam et al., 1993, Ebert et al., 1985).

To further investigate this possibility this series of experiments aimed to determine whether unilateral blockade of noradrenergic neurotransmission within the vlPAG has any effect of the haemodynamic response to severe blood loss under conditions of halogenated anaesthesia.

5.2 Materials and Methods

5.2.1 Animals and Surgery: Data were obtained from 30 male Sprague-Dawley rats (250 – 350 grams). Rats were initially anaesthetised in an air-tight box with halothane (5% in 100% O_2) and then via custom built face mask (2% halothane in 100% O_2). Anaesthesia was maintained at this level for all surgical and experimental procedures. Body temperature was maintained at 37°C with a thermoregulatory heating blanket.

The left carotid artery was dissected free from all surrounding connective tissue and cannulated for the measurement of arterial pressure. The arterial cannula was connected to a pressure transducer and the signal amplified, filtered (MacLab 8), displayed "on – line" and recorded on an Apple Macintosh running Chart Software for later "off-line" analysis. Heart rate was derived from the raw arterial pressure trace. Once instrumented, each rat was then transferred to a stereotaxic frame and placed in the "flat skull" position. Anaesthesia was maintained at 2% in 100% O_2 by way of custom built face mask on the stereotaxic frame.

5.2.2 Haemorrhage following microinjection of phentolamine: Fifteen (15) animals were instrumented with both arterial and venous cannulae (for measurement of arterial pressure and removal of blood respectively) before being placed in a stereotaxic frame. A single barrel micropipette (tip diameter 10 - 30μm) was used to make a unilateral injection of phentolamine methanesulphate (200nl; 10μg in 0.5μl 0.9% saline) in a manner identical to that which has been described previously (see Chapter 2). All injections contained Fluorogold (0.05%) for histological verification of the injection site.

Unilateral microinjections were made given that the aim of these experiments was only to evaluate the relative contribution that noradrenergic neurotransmission within the vlPAG (triggered by vlPAG-projecting A1 neurons) has on prematurely triggering decompensation in the anaesthetised animal.

Ten (10) minutes (N=6) following phentolamine administration, each animal underwent an 18% haemorrhage over 20 minutes. As discussed in chapter one (section 1.3), haemorrhage performed under general anaesthesia results in a premature sympathoinhibition and greatly potentiated hypotension. Therefore, in the present series of investigations, a small percentage of total blood volume was removed to prevent premature death. The haemorrhage, however, was still performed at two rates: removal of 6% total blood volume over 10 minutes followed by removal of 12% total blood volume over 10 minutes. This protocol ensured approximately equal periods of compensation and decompensation. Forty minutes after the end of the haemorrhage period, the level of anaesthesia was deepened (5% in 2 litres O_2) and the animal perfused with 500ml 0.9% saline followed by 500ml of 4% paraformaldehyde (pH 9.6 at 4°C).

The brains were removed, postfixed for 24hr in 4% paraformaldehyde at 4°C, and cryoprotected in 30% sucrose for 2-3 days. Serial coronal sections (50μm) of the midbrain were cut on a freezing microtome, collected in phosphate buffered saline (pH 7.4), mounted onto twice dipped gelatinised slides and coverslipped with Fluromount mounting media. Sections were analysed under UV-illumination. The small deposit of

Fluorogold was used to define injection sites, which were reconstructed using a camera lucida attachment.

5.2.3 Haemorrhage following microinjection of Prazosin or Yohimbine: Fourteen (14) animals were instrumented with both arterial and venous cannulae (for measurement of arterial pressure and removal of blood respectively). Animals were subsequently placed in a stereotaxic apparatus and 200nl of either: (i) the specific alpha 1 receptor antagonist prazosin hydrochloride (10μg in 0.9% physiological saline; pH 7.4); or (ii) the specific alpha 2 receptor antagonist yohombine hydrochloride (10μg in 0.9% physiological saline; pH 7.4) was injected into the vlPAG in a manner identical to that described previously. Each drug solution contained traces of Fluorogold for post mortem histological verification of injection sites. Ten (10) minutes following drug administration, each animal underwent an 18% haemorrhage over 20 minutes. The haemorrhage was performed at two rates: removal of 6% total blood volume over 10 minutes followed by removal of 12% total blood volume over 10 minutes. This protocol ensured approximately equal periods of compensation and decompensation. Forty minutes after the end of the haemorrhage period, the level of anaesthesia was deepened (5% in 2 litres O_2) and the animal subsequently perfused with 500ml 0.9% saline followed by 500ml of 4% paraformaldehyde (pH 9.6 at 4°C).

The brains were removed, postfixed for 24hr in 4% paraformaldehyde at 4°C, and cryoprotected in 30% sucrose for 2-3 days. Serial coronal sections (50μm) of the midbrain were cut on a freezing microtome, collected in phosphate buffered saline (pH

7.4), mounted onto twice dipped gelatinised slides and coverslipped with Fluoromount mounting media. Sections were analysed under UV-illumination. The small deposit of Fluorogold was used to define injection sites which were reconstructed using a camera lucida attachment.

5.2.4 Microinjection of noradrenaline hydrochloride: Four animals were instrumented with arterial cannulae and placed in a stereotaxic frame. A single barrel micropipette was used to make a small unilateral injection of noradrenaline hydrochloride (200nl; 15μg in 0.5μl 0.9% saline) into the vlPAG. Each injection contained a small amount of Fluorogold (0.05%) for later histological verification of the injection site. One hour following injection of noradrenaline, the level of anaesthesia was deepened and the animal perfused with 500ml 0.9% saline followed by 500ml of 4% paraformaldehyde (pH 9.6 at 4°C). The brains were subsequently removed, postfixed for 24hr in 4% paraformaldehyde at 4°C, and cryoprotected in 30% sucrose for 2-3 days.

Serial coronal sections (50μm) of the midbrain were cut on a freezing microtome, collected in phosphate buffered saline (pH 7.4), mounted onto twice dipped gelatinised slides and coverslipped with Fluromount mounting media. Sections were analysed using fluorescent optics. The small deposit of Fluorogold was used to define injection sites which were reconstructed using a camera lucida attachment.

5.2.5 Analysis and Statistics: Mean arterial pressure (AP) was recorded continuously. Heart rate was derived from the raw arterial pressure trace. Baseline measures of both AP and HR were calculated from the average of three ten second (10s) samples taken at 10min, 5min and 20s before commencement of blood withdrawal. Twenty second samples of AP and HR were taken at 2min intervals during the haemorrhage period (0-20min) and at 5min intervals during the 40min post-haemorrhage recovery period. Statistical comparisons between groups (i.e., between un-injected and injected animals) used a repeated measures two-way ANOVA, followed by Bonferroni-Dunn post-hoc analysis (For details see Ludbrook 1994). A non-parametric Mann-Whitney U-test was used to determine the statistical validity of the percent fall in both arterial pressure and heart rate, relative to resting baseline values, in un-injected control animals subject to 18% haemorrhage alone.

5.3 Results

5.3.1 Haemorrhage Only: Removal of 18% total blood volume (6% over 10min followed by 12% over 10min; N=6), over a 20-min period, produced a biphasic haemodynamic response. During the first 13 minutes of blood loss, AP was maintained within 10% of baseline values (*Compensation*). From this point onward (removal of approximately 12% total blood volume) (*Decompensation*) AP fell rapidly and by the end of the haemorrhage had reached a level 51% below pre-haemorrhage baseline values (mean fall from 91±5 mmHg to 44.9±3 mmHg; Figure 5.2a&b). Similarly, HR was maintained within 5% of baseline values until approximately the 12th minute of the haemorrhage period. At the end of the haemorrhage period HR had fallen 21.7±1.8% relative to pre-haemorrhage baseline values (mean fall from 340±18 bpm to 274±11 bpm; Figure 5.2c&d).

5.3.2 Haemorrhage (18%) following vlPAG phentolamine: In 6 rats, unilateral injections of phentolamine were made into the vlPAG 10min prior to an 18% haemorrhage. Microinjection of phentolamine did not significantly alter resting AP or HR (Figure 5.1a). Inspection of Figure 5.2a shows that following 18% haemorrhage there was a striking delay and attenuation of the magnitude of the fall in AP. That is, AP did not reach a level 10% below baseline until the 17th minute of the haemorrhage. At the completion of the haemorrhage, AP had only fallen approximately 20% relative to pre-haemorrhage baseline values. Although the magnitude of haemorrhage-evoked bradycardia was smaller following phentolamine administration, this effect did not reach statistical significance (repeated measures two-way ANOVA; Figure 5.2c).

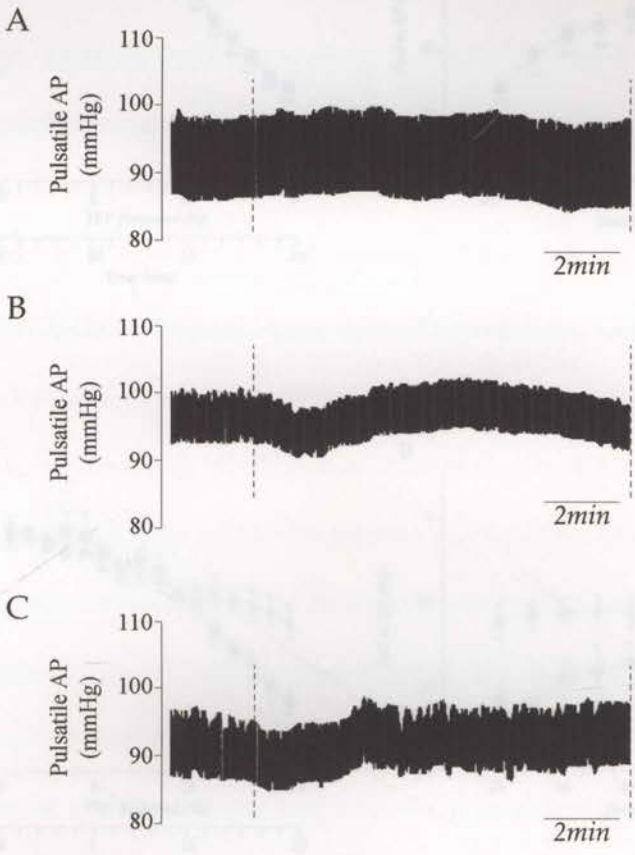

Figure 5.1
Effect of unilateral microinjection of **A** phentolamine methanesulphonate; **B** prazosin hydrochloride; and **C** yohimbine hydrochloride on pulsatile arterial pressure. Each microinjection was made in the ventrolateral periaqueductal gray (vlPAG) of halothane anaesthetised rats over a 15 second period. The duration of each recording as shown is ten (10) minutes. The scale bar represents 2 minutes.

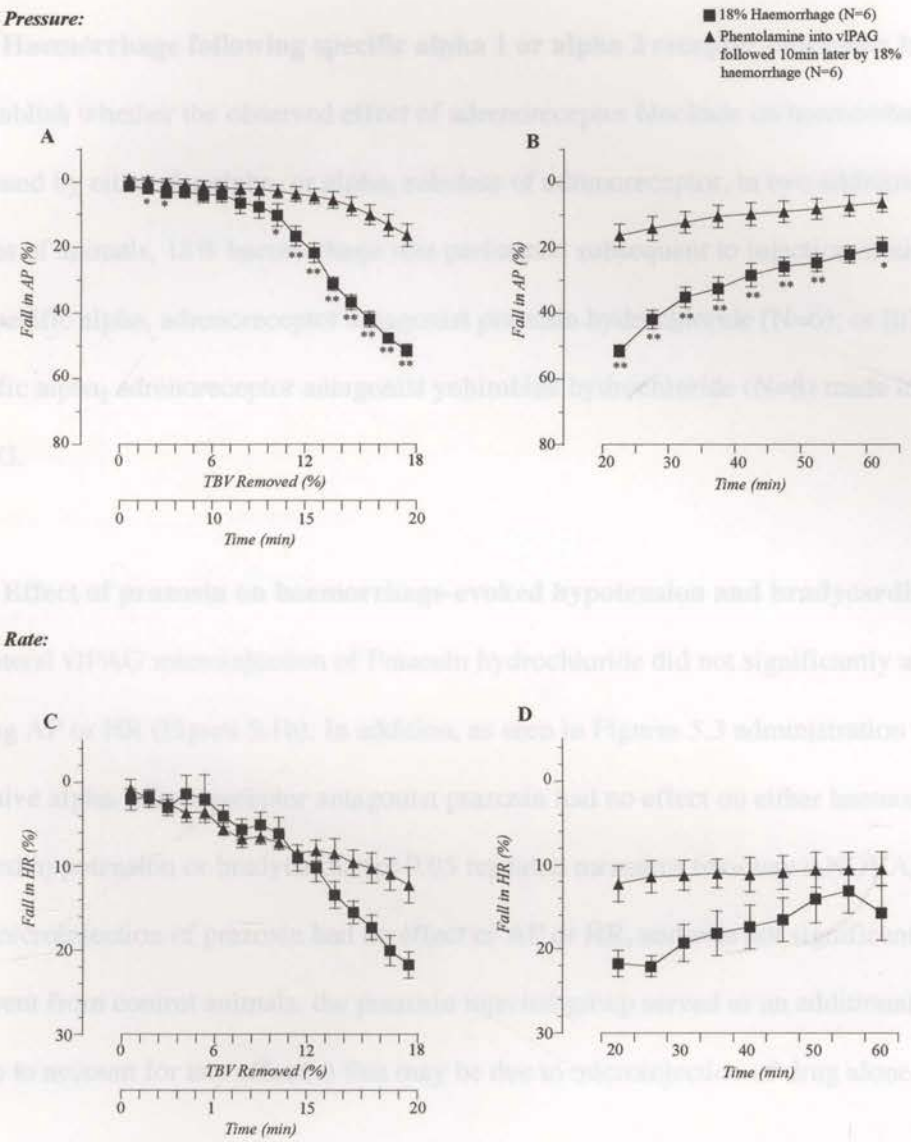

Figure 5.2

Mean changes (+/-SEM) in arterial pressure (AP) expressed as a percentage change from pre-stimulus baseline values of (i) 18% haemorrhage; and (ii) unilateral microinjection of phentolamine into the vlPAG followed 10min later by an 18% haemorrhage. Panel **A** shows the initial twenty minute haemorrhage period, and panel **B** shows the period of recompensation (20min-60min post-haemorrhage). Significant differences in mean AP between control haemorrhage and haemorrhage following phentolamine administration are shown by asterisks (repeated measures two-way ANOVA with Bonferroni-Dunn post-hoc analysis; * indicates $P<0.05$; ** indicates $P<0.005$).

Mean changes (+/-SEM) in heart rate (HR) expressed as a percentage change from pre-stimulus baseline values of animals subjected to either: (i) 18% haemorrhage; or (ii) unilateral microinjection of phentolamine into the vlPAG followed 10min later by an 18% haemorrhage. Panel **C** shows the initial twenty minute haemorrhage period, and panel *D* shows the period of recompensation (20min-60min post-haemorrhage). Statistical analysis using a repeated measures two-way ANOVA revealed no significant difference between

5.3.3 Haemorrhage following specific alpha 1 or alpha 2 receptor blockade: In order to establish whether the observed effect of adrenoreceptor blockade on haemorrhage was mediated by either the $alpha_1$ or $alpha_2$ subclass of adrenoreceptor, in two additional groups of animals, 18% haemorrhage was performed subsequent to injection of either: (i) the specific $alpha_1$ adrenoreceptor antagonist prazosin hydrochloride (N=6); or (ii) the specific $alpha_2$ adrenoreceptor antagonist yohimbine hydrochloride (N=8) made into the vlPAG.

5.3.4 Effect of prazosin on haemorrhage-evoked hypotension and bradycardia: Unilateral vlPAG microinjection of Prazosin hydrochloride did not significantly alter resting AP or HR (Figure 5.1b). In addition, as seen in Figures 5.3 administration of the selective $alpha_1$ adrenoreceptor antagonist prazosin had no effect on either haemorrhage-evoked hypotension or bradycardia ($p>0.05$ repeated measures two-way ANOVA). Given that microinjection of prazosin had no effect of AP or HR, and was not significantly different from control animals, the prazosin injected group served as an additional control group to account for any effect(s) that may be due to microinjection of drug alone.

5.3.5 Effect of yohimbine on haemorrhage-evoked hypotension and bradycardia: Unilateral microinjection of the specific $alpha_2$ receptor antagonist yohimbine made in the vlPAG did not significantly alter resting AP or HR (Figure 5.1c). However, yohimbine administration made prior to hypovolaemic (18%) haemorrhage resulted in a striking delay and attenuation of the fall in AP evoked by 18% haemorrhage (percentage; Figure 5.4a). That is, AP did not reach a level 10% below baseline until the 15^{th} minute of

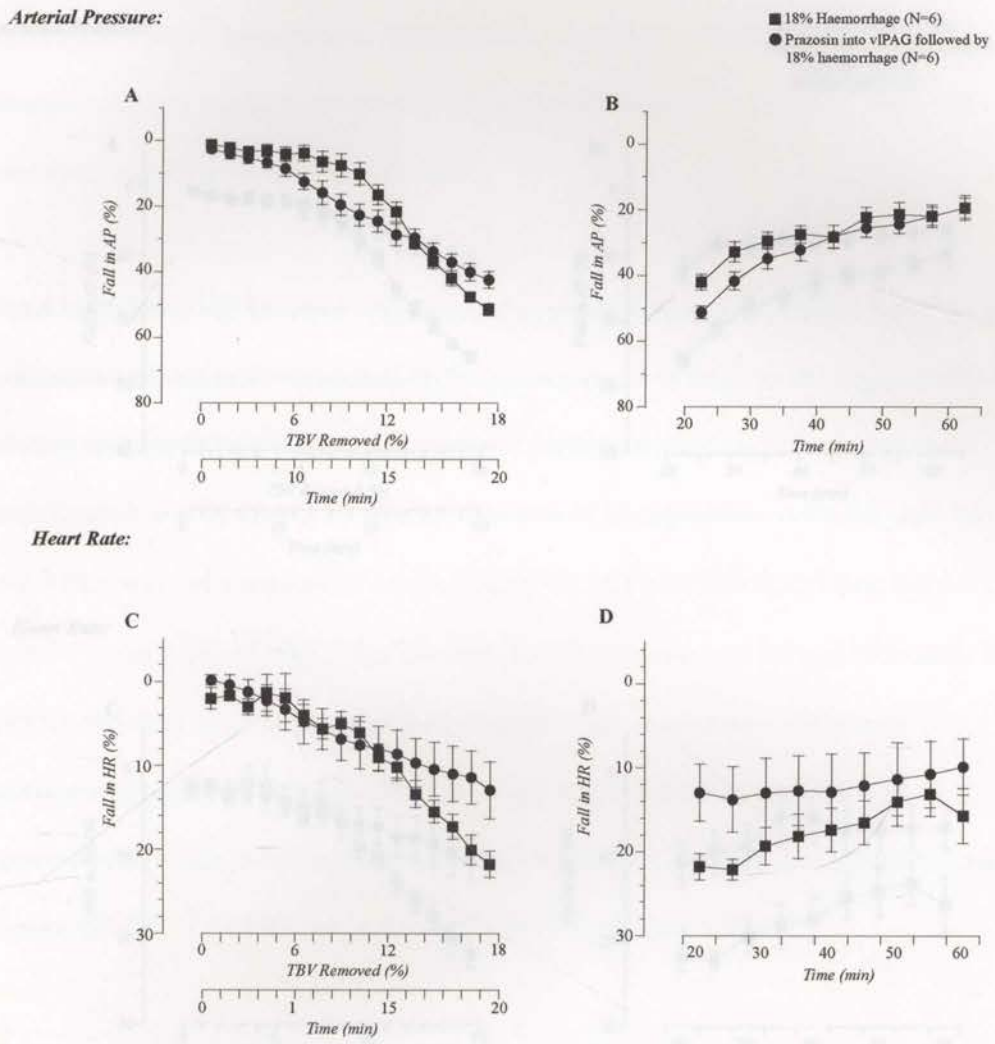

Figure 5.3

Mean changes (+/-SEM) in arterial pressure (AP) expressed as a percentage change from pre-stimulus baseline values in animals subject to: (i) 18% haemorrhage; and (ii) unilateral microinjection of prazosin into the vlPAG followed by an 18% haemorrhage. Panel **A** shows the initial twenty minute haemorrhage period, and panel **B** shows the period of recompensation (20min-60min post-haemorrhage). Statistical analysis using a repeated measures two-way ANOVA revealed no significant difference between the two experimental groups.

Mean changes (+/-SEM) in heart rate (HR) expressed as a percentage change from pre-stimulus baseline values of animals subjected to either: (i) 18% haemorrhage; or (ii) unilateral microinjection of prazosin into the vlPAG followed 10min later by an 18% haemorrhage. Panel **C** shows the initial twenty minute haemorrhage period, and panel **D** shows the period of recompensation (20min-60min post-haemorrhage). Statistical analysis using a repeated measures two-way ANOVA revealed no significant difference between the two experimental groups.

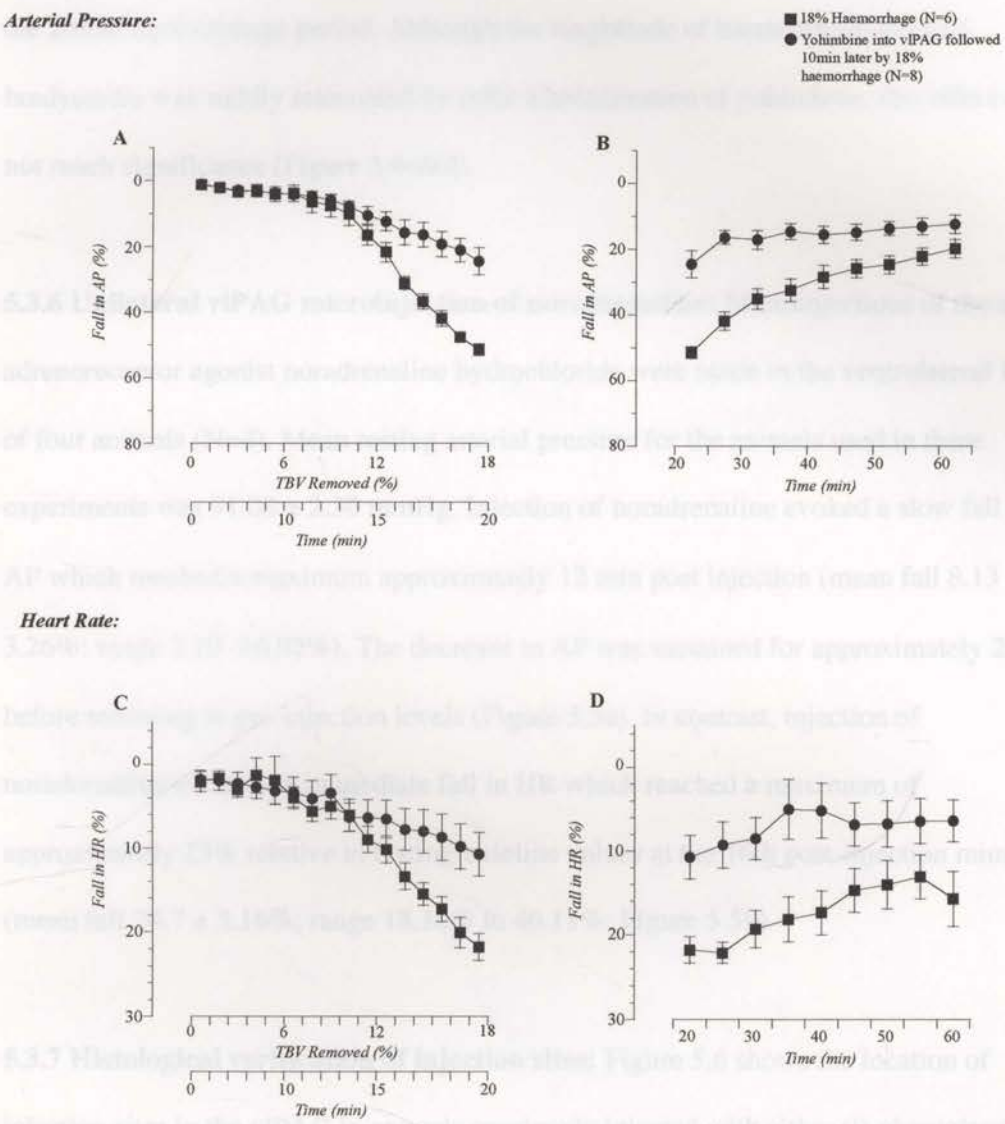

Figure 5.4
Mean changes (+/-SEM) in arterial pressure (AP) expressed as a percentage change from pre-stimulus baseline values of (i) 18% haemorrhage; and (ii) unilateral microinjection of yohimbine into the vlPAG followed 10min later by an 18% haemorrhage. Panel **A** shows the initial twenty minute haemorrhage period, and panel **B** shows the period of recompensation (20min-60min post-haemorrhage). Significant differences in mean AP between control haemorrhage and haemorrhage following phentolamine administration are shown by asterisks (repeated measures two-way ANOVA with Bonferroni-Dunn post-hoc analysis; * indicates $P<0.05$; ** indicates $P<0.005$).

Mean changes (+/-SEM) in heart rate (HR) expressed as a percentage change from pre-stimulus baseline values of animals subjected to either: (i) 18% haemorrhage; or (ii) unilateral microinjection of yohimbine into the vlPAG followed 10min later by an 18% haemorrhage. Panel **C** shows the initial twenty minute haemorrhage period, and panel **D** shows the period of recompensation (20min-60min post-haemorrhage). Statistical analysis used a repeated measures two-way ANOVA followed by Bonferroni-Dunn post-hoc correction.

the haemorrhage, and had fallen only 24.5±4.1% relative to baseline values by the end of the 20min haemorrhage period. Although the magnitude of haemorrhage-evoked bradycardia was mildly attenuated by prior administration of yohimbine, this effect did not reach significance (Figure 5.4c&d).

5.3.6 Unilateral vlPAG microinjection of noradrenaline: Microinjections of the alpha adrenoreceptor agonist noradrenaline hydrochloride were made in the ventrolateral PAG of four animals (N=4). Mean resting arterial pressure for the animals used in these experiments was 91.08 ± 2.30 mmHg. Injection of noradrenaline evoked a slow fall in AP which reached a maximum approximately 12 min post injection (mean fall 8.13 ± 3.26%; range 3.19 -16.92%). The decrease in AP was sustained for approximately 20 min before returning to pre-injection levels (Figure 5.5a). In contrast, injection of noradrenaline evoked an immediate fall in HR which reached a maximum of approximately 25% relative to resting baseline values at the 16th post-injection minute (mean fall 24.7 ± 5.16%; range 18.16% to 46.11%; Figure 5.5b).

5.3.7 Histological verification of injection sites: Figure 5.6 shows the location of injection sites in the vlPAG in animals previously injected with either (i) phentolamine; (ii) prazosin hydrochloride; or (iii) yohimbine hydrochloride. It can be seen that all injections were located in the region previously defined as the vasodepressor region of the vlPAG.

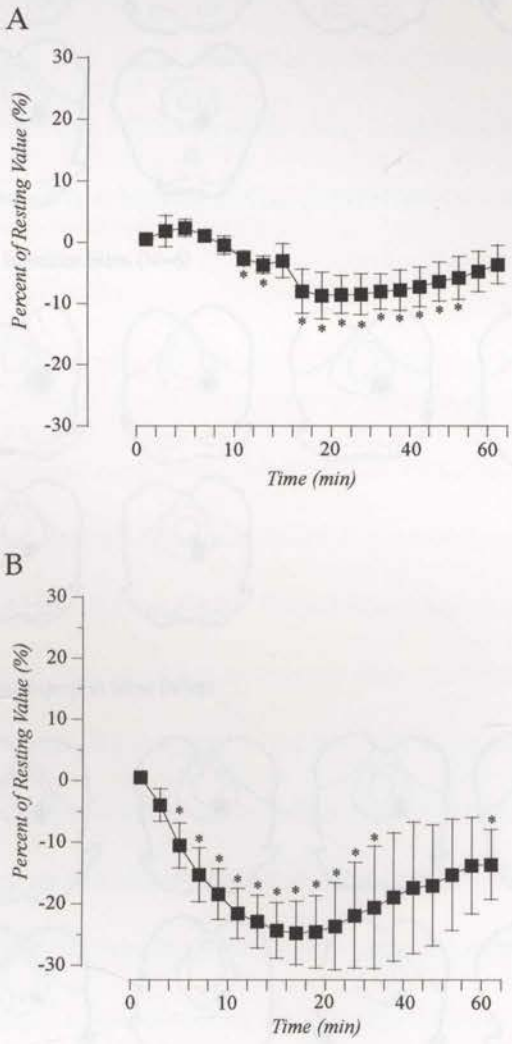

Figure 5.5
Graphs illustrating the effect of unilateral vlPAG microinjection of the alpha receptor agonist noradrenaline hydrochloride on **A** resting arterial pressure; and **B** resting heart rate. Data are expressed as mean percent change (+/- SEM) from pre-injection baseline values. Asterisks indicate significance, * $p<0.05$ (ANOVA).

A Phentolamine Injection Sites (N=6)

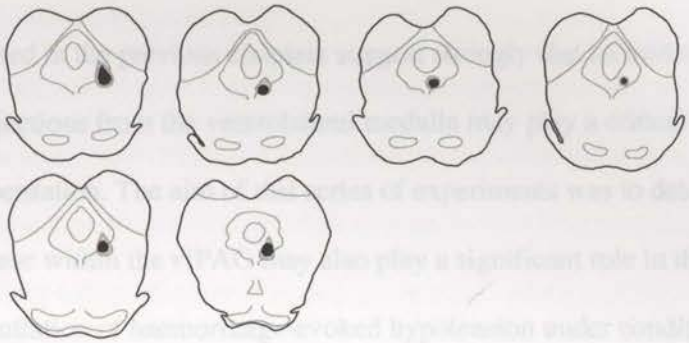

B Prazosin Injection Sites (N=6)

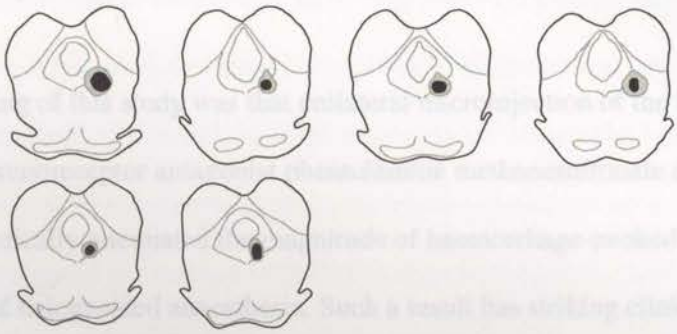

C Yohimbine Injection Sites (N=8)

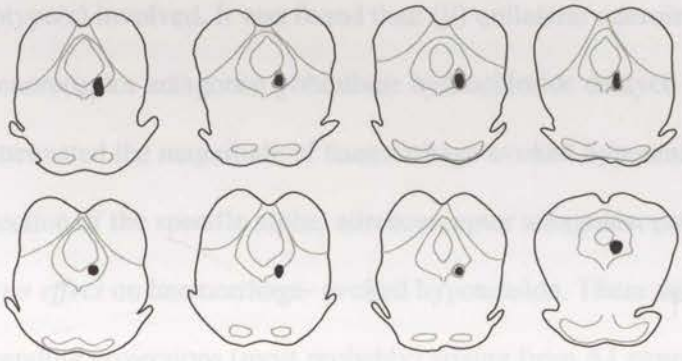

Figure 5.6
Camera lucida reconstructions of coronal sections through the midbrain periaqueductal gray illustrating the location of **A.** phentolamine methanesulphonate injections; **B.** prazosin hydrochloride injections; and **C.** yohimbine hydrochloride injections. The dark black shading represens the core of the injection site, the gray shading represents the halo surrounding the core. Each injection was identified by the presence of small deposits of Fluorogold.

5.4 Discussion

The results presented in the previous chapters suggest strongly that ascending noradrenergic projections from the ventrolateral medulla may play a critical role in triggering decompensation. The aim of this series of experiments was to determine if noradrenaline release within the vlPAG may also play a significant role in the premature initiation and potentiation of haemorrhage-evoked hypotension under conditions of halothane anaesthesia.

The principle finding of this study was that unilateral microinjection of the broad spectrum alpha-adrenoreceptor antagonist phentolamine methanesulfonate delayed the onset of and dramatically attenuated the magnitude of haemorrhage-evoked hypotension under conditions of halogenated anaesthesia. Such a result has striking clinical implications, thus the study was extended in order to characterise the specific alpha-adrenoreceptor subtype(s) involved. It was found that: (ii) unilateral microinjection of the specific alpha$_2$ adrenoreceptor antagonist yohimbine hydrochloride delayed the onset of and dramatically attenuated the magnitude of haemorrhage-evoked hypotension; and (iii) unilateral microinjection of the specific alpha$_1$ adrenoreceptor antagonist prazosin hydrochloride had *no effect* on haemorrhage- evoked hypotension. These data support the hypothesis that ascending projections (most probably) arising from A1 neurons in the ventrolateral medulla release noradrenaline within the vlPAG in order to trigger decompensation and provide evidence which strongly suggests that it is alpha$_2$ adrenoreceptors which play a key role in this circuit.

5.4.1 Specificity of Phentolamine, Prazosin and Yohimbine for the different subtypes of alpha adrenergic receptors:

Phentolamine methanesulfonate is a well characterised, competitive non-selective alpha adrenergic receptor antagonist. Pharmacological studies utilising radioligand binding techniques have shown conclusively that phentolamine prevents noradrenaline binding to both $alpha_1$ and $alpha_2$ adrenoreceptors (Venugopalan et al., 2006, Herold et al., 2005, Trendelenburg et al., 2003, Sagen et al., 1983, Gomes et al., 1980, Jones et al., 1985). The volume and concentration used in this study was chosen because it lies well within the concentrations used in previous studies. Specifically, phentolamine administered at the dose used in this study (0.25nmol. in 0.5µl physiological saline; pH 7.4) has previously been shown to: (i) antagonise the hypotensive response to noradrenaline injected into the nucleus of the solitary tract (NTS) (Zandenberg et al., 1979); (ii) produce hypoalgesia when injected into the nucleus raphe magnus (Sagen et al., 1983, Hammond et al., 1980a, Hammond et al., 1980b, Sagen and Proudfit 1981); and (iii) significantly attenuate morphine-induced analgesia evoked from the ventrolateral PAG (Tive and Barr 1992).

In contrast, prazosin hydrochloride is a selective $alpha_1$ receptor antagonist, and yohimbine hydrochloride a selective $alpha_2$ adrenoreceptor antagonist (Millan et al., 1994, Trendelenberg et al., 1993, Doxey et al., 1984, Redfern and Williams 1995, Starke et al., 1975, Cheung et al., 1986, Lee et al., 2004, Buzsaki et al., 1991, Patel et al., 2001). $Alpha_2$ adrenoreceptors can be further subdivided into A, B, and C receptor subtypes. Both the B and C subtypes of $alpha_2$ receptors have been shown to display high affinity

for the selective alpha$_1$ receptor antagonist prazosin in addition to the selective alpha$_2$ adrenoreceptor antagonists yohimbine, idazoxan (RX 781094), rauwolscine, corynanthine and delequamine (Bylund 1992, Redfern and Williams 1995, Doxey et al., 1984). Thus it can be concluded that yohimbine selectively acts at alpha$_{2A}$ adrenoreceptors.

5.4.2 Methodological Considerations:

This series of experiments utilised intra-vlPAG microinjection of alpha receptor antagonists to investigate the contribution of noradrenaline release (and subsequent binding to different subtypes of adrenergic receptors) in the vlPAG on haemorrhage-evoked hypotension. Each microinjection was made slowly in order to minimise damage to surrounding neural tissue and fibres of passage. Furthermore, injections were made at a 30° caudal to rostral angle in order to minimise the spread of injectate up the pipette track into the dorsally adjacent lateral and dorsolateral PAG columns.

Given that such striking results were obtained in this series of experiments, it is plausible to suggest that the observed effects may be a consequence of complete vlPAG inactivation similar to that which has previously been reported in the conscious rat following bilateral injection of lignocaine, cobalt chloride or muscimol (Cavun and Millington 2001, Dean 2004). However, there is no evidence in the literature to suggest that phentolamine, prazosin or yohimbine are neurotoxic or have the ability to block synaptic transmission (Stone et al., 2004, Angyan and Angyan 1999, Taiwo and Levine 1988, Buzsaki et al., 1991). Moreover, the dose and volume of each antagonist used in this series of experiments mirrors that used in prior experiments in which phentolamine,

prazosin and/or yohimbine were administered to central neural sites (for details see Zandenberg et al., 1979, Perez et al., 1998, Tive and Barr 1992, Sagen et al., 1983).

The addition of a visual marker (Fluorogold) was utilised to provide an indication of the spread of injectate. The volume of each injection was 200nl, considerably smaller than that used in previous vlPAG inactivation studies with lignocaine, cobalt chloride or muscimol (cf. Cavun and Millington 2001, Cavun et al., 2001, Cavun et al., 2004, Dean 2004). Assuming then that each injection is a perfect sphere, the maximum possible diameter of spread is 0.75mm. Post-mortem histology suggested a rostrocaudal spread of approximately 0.5mm, and a mediolateral spread of approximately 0.2mm consistent with what has previously been reported by this laboratory for previous microinjection studies (Henderson et al., 2000, Heslop et al., 2002). Taken together, such limited spread combined with the small injection volume makes it unlikely that the injectate spread into the cerebral aqueduct to act at nuclei other than the vlPAG.

It is important to recall that all microinjections made in this study were unilateral. This was done as a first step in order to evaluate the contribution that noradrenergic neurotransmission, triggered as a result of vlPAG-projecting A1 neurons, has on evoking the premature fall in AP and HR under conditions of halothane anaesthesia. It was, therefore, surprising that such a striking result was obtained. One possible explanation may be that the decompensatory response is significantly delayed such that decompensation will occur if bleeding were to continue over a longer time period.

Inspection of Figure 5.2 and Figure 5.4 suggests this may be likely given the downward trend of the AP trace in both phentolamine- and yohimbine-injected groups.

5.4.3 Patterns of haemorrhage-evoked hypotension is unaltered by halothane anaesthesia:

Unlike the experiments performed in the previous chapters, each experimental haemorrhage in this study was performed under halothane anaesthesia. Anaesthesia is known to evoke a premature and potentiated hypotension in response to a moderate amount of blood loss (Caplan et al., 1988, Vatner 1978). For this reason, less blood volume was removed (removal of 18% total blood volume compared to 30% total blood volume in the freely moving animal), however, the two-rate protocol was preserved (removal of 6% total blood volume over 10min followed by 12% over the second ten minutes) to ensure equal periods of compensation and decompensation.

As seen in the results, removal of 18% total blood volume under halothane anaesthesia evokes a biphasic AP response. Initially, as blood was removed AP was maintained at normal levels. Following the withdrawal of approximately 10% total blood volume, a profound fall in AP was observed (up to a maximum of 51% below pre-haemorrhage baseline values). Although the amount of blood loss necessary to trigger decompensation depends on species and conditions (i.e., anaesthesia), the biphasic response to haemorrhage observed in this study is identical to that observed in previous chapters, as well as that seen in humans, rabbits, dogs and rats (Shen et al., 1989, Chalmers et al., 1967, Troy et al., 2003, Yamashita et al., 1996).

5.4.4 Decompensation depends on the ventrolateral PAG:

The striking response observed following phentolamine and yohimbine administration into the ventrolateral PAG provides further evidence that the integrity of the vlPAG is critical for the timing and magnitude of haemorrhage-evoked hypotension. Early reports that removal of the forebrain and midbrain blocked the decompensatory response; whereas removal of the forebrain only preserved decompensation, indicated that the midbrain was critical for the expression of haemorrhage-evoked hypotension (Evans et al., 1991, Troy et al., 2003). Further reports that microinjection of excitatory amino acids into the ventrolateral column of the midbrain PAG produced profound hypotension and bradycardia; and that hypotensive haemorrhage evoked Fos expression selectively within the vlPAG provided strong evidence suggesting that the ventrolateral PAG was the likely midbrain site responsible for mediating decompensation (Carrive et al., 1991, Keay et al., 2002, Bandler and Shipley 1994, Keay et al., 1997).

The notion that the vlPAG is the critical neural site responsible for the expression of decompensation was confirmed when it was shown that intra-vlPAG microinjection of lignocaine, cobalt chloride and muscimol resulted in a significant attenuation of haemorrhage-evoked hypotension and sympathoinhibition in the conscious rat (Cavun and Millington 2001, Dean 2004). The finding reported here that haemorrhage-evoked hypotension is similarly attenuated by phentolamine extends previous work by showing that noradrenergic neurotransmission within the vlPAG is critical for the expression of decompensation. Furthermore, given that prior administration of yohimbine *but not* prazosin resulted also in a dramatic attenuation of haemorrhage-evoked hypotension, it

can be concluded that decompensation is most likely mediated by the action of noradrenaline at alpha$_{2A}$ adrenoreceptors in the vlPAG.

5.4.5 Noradrenergic inputs to the vlPAG:

If, as suggested by these data, noradrenaline release within the vlPAG is critical for the expression of decompensation then it seems logical that two criteria should be met. First, vlPAG alpha$_{2A}$ adrenoreceptor activation with the appropriate adrenoreceptor ligand should result in AP and HR changes characteristic of decompensation. Second, the vlPAG must receive input from noradrenergic neurons.

Intra-vlPAG microinjection of noradrenaline produces hypotension and bradycardia:

Previous single cell electrophysiological experiments have shown that noradrenaline depolarises vlPAG neurons *in vitro* (Vaughan et al., 1994). Functionally, depolarisation of vlPAG neurons results in hypotension and bradycardia (for review see Keay and Bandler 2004). As shown in this chapter, noradrenaline microinjections made in the vlPAG of anaesthetised rats results also in hypotension (8.13 ± 3.26%) and bradycardia (24.7 ± 5.16%). These data suggest therefore, that noradrenaline, the endogenous ligand of alpha$_{2A}$ adrenoreceptors, depolarises vlPAG neurons *in vivo* to produce cardiovascular changes similar to those evoked by severe blood loss.

Noradrenergic inputs to the vlPAG:

Early anatomical studies revealed that the PAG receives dense noradrenergic input from the A1 and A2 cell groups in the ventrolateral medulla and nucleus of the solitary tract

respectively (Herbert and Saper 1992). Extending these findings by limiting retrograde tracer injection sites to the ventrolateral PAG, the results presented in chapter 4 (part II) indicate that the vlPAG receives specific noradrenergic input from the ventrolateral medulla (A1 cell group). As shown in chapter 4 (part I), almost all neurons in the A1 cell group express Fos-like immunoreactivity following severe blood loss. Taken together, these data suggest that activation of the A1-vlPAG pathway by severe blood loss may be a critical source of noradrenergic input to the vlPAG.

5.4.6 Location of alpha$_2$ adrenoreceptors:

Early studies utilising *in situ* hybridisation revealed that the PAG contains high levels of messenger RNA for alpha$_2$ adrenoreceptors (Zeng and Lynch 1991, McCune et al., 1993, Nicholas et al., 1993, Scheinin et al., 1994). Further work employing ligand binding autoradiography and immunohistochemical techniques to map the precise location of alpha$_2$ adrenoreceptor subtypes throughout the central nervous system showed that alpha$_{2A}$ adrenoreceptors are densely clustered in the ventrolateral column of the PAG at both rostral and caudal levels (Boyajian et al., 1987, Talley et al., 1996, Rosin et al., 1993, Aoki et al., 1994). As well, alpha$_{2A}$ receptors have been observed at the caudal pole of both dorsolateral and lateral PAG columns although the intensity and density of receptor staining is significantly less that that seen in the ventrolateral column (Talley et al., 1994).

Since their detection, much debate has arisen as to the location of alpha$_2$ receptors relative to the synapse. Initial studies performed in the periphery concluded that alpha$_{2A}$

adrenoreceptors were pre-synaptic autoreceptors which function to limit the amount of noradrenaline released into the synaptic cleft following depolarisation (Yamaguchi 1982, Langer 1974). However, recent anatomical data strongly suggests that alpha$_{2A}$ receptors are also found on the post-synaptic cell membrane.

When viewed under the light microscope alpha$_{2A}$ receptor staining reveals discrete, uniform patterns of punctate immunoreactivity observed with diffuse neuropil staining (Talley et al., 1996, Rosin et al., 1993, Guyenet et al., 1994). Rosin et al., point out that this pattern of staining closely resembles that of glycine receptors and is attributed to their post-synaptic location (Rosin et al., 1993, Wenthold et al., 1990). Moreover, it is unlikely that the punctate pattern of staining seen for alpha$_2$ receptors is due to their association with pre-synaptic terminals as the puncta are observed in close contiguity with cell bodies (Zeng and Lynch 1991, Rosin et al., 1993, Talley et al., 1996), and there is thus far no evidence that individual puncta are linked by neuronal processes resembling axons or *en passant* varicosities (Rosin et al., 1993).

To summarise, whilst alpha$_2$ adrenoreceptors have traditionally been thought to occur only on pre-synaptic noradrenergic terminals, anatomical evidence suggests that they may also be located on the post-synaptic cell membrane. Moreover, in contrast to what is observed in peripheral tissue, pharmacological and physiological evidence exists which suggests that activation of alpha$_2$ adrenoreceptors results in the depolarisation of the post-synaptic neuron on which they are located (Szafarczyk et al., 1990, Millan et al., 1994). In the context of the present series of experiments, activation of alpha$_2$ receptors results in

the depolarisation of post-synaptic ventrolateral PAG neurons (on which they are located), which in turn triggers the sympathoinhibition and hypotension characteristic of the cardiovascular response to severe blood loss.

5.4.7 Involvement of central alpha$_{2A}$ adrenoreceptors in the regulation of sympathetic outflow, arterial pressure and heart rate:

The decompensatory phase of severe blood loss is characterised by a striking decrease in sympathetic nerve activity, arterial pressure and heart rate. As demonstrated in this study, binding of the appropriate receptor ligand to intrinsic vlPAG alpha$_{2A}$ receptors produces autonomic changes similar to those evoked by severe blood loss. Additionally, vlPAG microinjection of the specific alpha$_{2A}$ receptor antagonist yohimbine delays and attenuates the fall in arterial pressure evoked by severe blood loss. Taken together, these findings suggest that alpha$_{2A}$ adrenoreceptors form a critical part of the central circuit precipitating shock following haemorrhage.

Past studies focussing on alpha$_{2A}$ receptor-mediated sympathetic regulation have shown that activation of brainstem alpha$_{2A}$ receptors with various centrally acting alpha$_2$ agonists evokes a striking decrease in arterial pressure and heart rate (Macmillan et al., 1996, Ruffolo et al., 1993). This cardiovascular 'depressor' response can be abolished following mutation of the alpha$_{2A}$ adrenoreceptor and/or pharmacological blockade of central alpha$_2$ receptors with yohimbine (Macmillan et al., 1996, de Jonge et al., 1982, Borkowski and Finch 1979, Conner et al., 1981, Hamilton et al., 1980, Heise and

Kroneberg 1972, Kubo and Misu 1981, Sinha and Schmidt 1974, Zandenberg et al., 1979, Philippu and Schartner 1976).

Further evidence that alpha$_2$ adrenoreceptors are involved in sympathetic nervous system regulation arises from physiological data showing that microinjection of yohimbine into the thoracic spinal cord of the pigeon attenuates the inhibitory effects produced by alpha$_2$ agonists on post-ganglionic sympathetic nerve discharge (Guyenet and Stornetta 1982). Thus activation of central alpha$_2$ adrenoreceptors modulates sympathetic nerve activity to produce a hypotension and bradycardia similar to that evoked by severe blood loss. These data add strength to the hypothesis that severe blood loss results in activation of vlPAG alpha$_{2A}$ adrenoreceptors to produce a sympathoinhibition and consequent hypotension and bradycardia.

5.4.8 Central alpha$_{2A}$ receptors modulate behavioural states:

As well as resulting in a *centrally-mediated* sympathoinhibition, severe blood loss evokes concomitant alterations in the behavioural state of humans and conscious animals (rat, rabbit) (Morris 1867, Barcroft 1967, Persson and Svensson 1981). Such behavioural changes are characterised by quiescence, hyporeactivity and withdrawal from the surrounding environment. Consistent with the hypothesis that the vlPAG is capable of producing an integrated behavioural and cardiovascular response to severe blood loss, stimulation of the vlPAG with excitatory amino acids results also in quiescence (cessation of ongoing spontaneous motor activity) and hyporeactivity (failure of an age

and weight matched partner animal to evoke orientation, startle reactions or vocalisation) (Depaulis et al., 1994).

Early work using human subjects has shown that intravenous administration of yohimbine evokes striking alterations in behavioural state. Subjects who receive yohimbine (0.5mg/kg) become restless, tremulous, and feelings of impatience and unrest are often experienced (Holmberg and Gershon 1960). Subsequent work using conscious animals (dog, rat) reports similar findings of pronounced behavioural arousal following both intravenous and intraventricular microinjection of yohimbine. Lang et al., (1975) reported that conscious dogs and rats become more alert, show a striking increase in motor activity (e.g., make vigorous attempts to escape from their home cage) and exhibit intense vocalisations. That identical behavioural changes are evoked following both peripheral and central administration suggests that yohimbine produces behavioural alterations by antagonising *central* alpha$_2$ receptors. Moreover, the finding that antagonism of central alpha$_2$ receptors results in *behavioural excitation* suggests that under normal circumstances, an important function of alpha$_2$ receptors may be to bias an animal towards a more passive behavioural state.

In addition to being modulated by alpha$_2$ adrenoreceptor antagonists, the behavioural state of an animal has also been shown to be altered following administration of the alpha$_2$ receptor agonist clonidine. Smith et al., (2003) have recently shown that clonidine reduces awareness in human subjects. As well, central administration of clonidine in both conscious unrestrained, and propofol anaesthetised rats and cats evokes quiescence and a

reduction in the frequency of so-called 'natural behaviours' (Yamazato et al., 2001, Ally 1997). Interestingly, the study by Ally (1997) suggests that clonidine may produce these behavioural changes by acting at the level of the periaqueductal gray (Ally 1997). It is interesting to note that in all cases, clonidine-evoked behavioural depression was accompanied by vasodepressor responses and a reduction in sympathetic nerve activity. This suggests that under certain conditions the action of noradrenaline at alpha$_2$ receptors may produce an integrated cardiovascular and behavioural response. The ability of noradrenaline to produce behavioural changes through actions at vlPAG adrenoreceptors, especially under conditions of severe blood loss, is the subject of future investigations.

5.4.9 Synergistic interaction of alpha$_{2A}$ receptor with opioid receptors:

Alpha$_2$ receptors belong to the super family of G-protein coupled receptors (guanyl nucleotide binding). All alpha$_2$ adrenoreceptor subtypes share a common signal transduction pathway, viz. mediated via pertussis toxin-sensitive inhibitory proteins G_i and G_o. The structure of alpha$_2$ receptors consists of seven putative membrane-spanning domains with a long (approximately 150 amino acids) third intracellular loop (Harrison et al., 1991, Hayar and Guyenet 1999).

Alpha$_2$ adrenoreceptors are phosphorylated in an agonist dependent fashion. Upon activation, the receptor is phosphorylated by the GRK2 protein which interacts with the receptor domain (Pao and Benovic 2005). Phosphorylation occurs at four adjacent serines in the third intracellular loop. Additionally, receptor activation leads to the activation of

the mitogen-activated protein kinase cascade Ras, as well as phospholipase D (Pao and Benovic 2005, Harrison et al., 1991).

The discovery that the long third intracellular loop - characteristic of alpha$_2$ adrenoreceptor structure – interacts with a variety of scaffolding and signalling proteins (eg. spinophilin, arrestin 3, 14-3-3ζ) led to the discovery that alpha$_2$ adrenoreceptors functionally interact with other receptors, in particular, opioid receptors (Wang and Limbird 2002, Rios et al., 2004). Furthermore, the observation that co-administration of opiates and alpha$_2$-adrenoreceptor agonists enhances spinal anti-nociception further led to the suggestion that adrenoreceptors and opioid receptors function synergistically to enhance the effects of one another (Stone et al., 1997).

Anatomical studies have revealed that both opioid (μ and δ subtypes) and alpha$_2$ receptors are extensively co-localised at both the cellular and subcellular level (Milner et al., 2002). Furthermore, both receptors have been described on substance P containing neurons suggesting that these receptors are expressed in the same cell (Robertson et al., 1999, Stone et al., 1998). Delta (δ) opioid and alpha$_2$ adrenoreceptors have recently been characterised as an interacting complex using BRET assay (bioluminescence resonance energy transfer) technology (Rios et al., 2004).

Delta opioid receptor subtypes were first implicated in the expression of decompensation when in 1979 Faden and Holaday reported that intravenous injection of naloxone, a broad spectrum opioid receptor antagonist, significantly attenuated the hypotension evoked by

haemorrhage in the conscious rat (Faden and Holaday 1979). Further work utilising specific opioid receptor antagonists in both anaesthetised and un-anaesthetised rat and rabbit models of haemorrhagic shock have extended these original findings to show that haemorrhage-evoked hypotension depends on central delta (δ) opioid receptors (Sandor et al., 1987, Schadt and Ludbrook 1991, Ludbrook and Ventura 1994, Hasser and Schadt 1992).

The vlPAG receives dense innervation from opioid-ergic neurons (Martin-Schild et al., 1999, Schreff et al., 1998). Microinjection of the specific δ opioid receptor agonist DPDPE into the vlPAG evokes hypotension (17±2.3 mmHg) and bradycardia (31±5.5 bpm) (Keay at al., 1997), as does microinjection of β-endorphin, the endogenous ligand for the δ-opioid receptor (Cavun et al., 2001b). Following blockade of intrinsic vlPAG δ-opioid receptors with naloxone and/or naltrindole, haemorrhage-evoked hypotension is completely abolished (Cavun et al., 2001b). These data suggest that delta opioid receptors located within the vlPAG, are critical for the expression of decompensation. However, whether opioid receptors function independently or in synergy with $alpha_{2A}$ adrenoreceptors as these data would suggest, remains to be determined.

5.4.10 Descending vlPAG projections mediating decompensation:

The data presented in chapter three strongly suggests that decompensation is mediated via descending vlPAG output projections to the caudal midline medulla (CMM). In a series of double label experiments performed to identify possible descending vlPAG projections responsible for mediating decompensation, it was found that vlPAG neurons '*specifically*

activated' by hypotensive haemorrhage project predominantly to the vasodepressor region of the caudal midline medulla (CMM).

Having established in this study that alpha$_2$ adrenoreceptors within the vlPAG are an essential component of the central circuit triggering decompensation, it follows therefore that alpha$_2$ receptors must be present on vlPAG neurons which project to the CMM. A recent study from this laboratory has shown that alpha$_{2A}$ receptors are located post-synaptically on the cell bodies, proximal dendrites and axonal processes of CMM-projecting vlPAG neurons. Many CMM-projecting vlPAG neurons not immunoreactive for alpha$_{2A}$ receptors were observed to be in close proximity to pre-synaptic clusters of alpha$_{2A}$ adrenoreceptors. Moreover, large numbers of astrocytes displayed extensive alpha$_{2A}$ receptor immunoreactivity in addition to showing extended processes either contacting or in close proximity to CMM-projecting neurons, suggesting that they may also play a role in signalling pathways which trigger decompensation. (Alfonso Manuel Arguetta., Honours Thesis 2006). When considered together, these data strongly support the pharmacological data presented in this chapter suggesting that decompensation is triggered as a result of noradrenergic neurotransmission, acting at alpha$_{2A}$ adrenoreceptors, within the vlPAG.

Summary

The aim of this series of experiments was to determine if noradrenaline release within the vlPAG was critical for the expression of decompensation under conditions of halothane anaesthesia. It was found that noradrenaline evokes a small but significant hypotension and bradycardia. As well, prophylactic administration of the broad-spectrum alpha adrenoreceptor antagonist phentolamine results in a striking attenuation of haemorrhage-evoked hypotension. That yohimbine *but not* prazosin results also in a similar attenuation of haemorrhage-evoked hypotension strongly suggests that decompensation may be triggered by the release and subsequent binding of noradrenaline to $alpha_{2A}$ receptors within the vlPAG.

-Chapter 6-

Summary and Conclusions

6.1 Summary of aims and results

The haemodynamic response to severe blood loss is characterised by two successive phases: (i) an initial *compensatory* phase during which arterial pressure (AP) is maintained at normal levels; and (ii) a subsequent *decompensatory* phase characterised by a sudden fall in AP due to a centrally-mediated sympathoinhibition. Previous experimental reports have revealed that the ventrolateral column of the periaqueductal gray (vlPAG) plays a central role in mediating *behaviourally-coupled* cardiovascular responses, and more specifically, mediating the response evoked by severe blood loss. Injection of excitatory amino acid (DLH) evokes a similar reaction to that seen following severe blood loss, namely hypotension, bradycardia, quiescence and hyporeactivity. Furthermore, blockade of neural activity within the vlPAG has been shown to abolish the hypotension and bradycardia evoked by severe blood loss. With these findings in mind, the first set of experiments (described in Chapter 3) aimed to identify a descending output pathway(s) through which vlPAG neurons trigger sympathoinhibition, hypotension and bradycardia in response to severe blood loss.

The experiments described in chapter 4 were designed to identify the central afferent pathway(s) responsible for triggering decompensation. These experiments aimed to

describe a neural pathway which when activated, results in the depolarisation of vlPAG neurons which trigger decompensation.

In the final series of experiments (chapter 5), the haemodynamic response to severe blood loss was investigated under conditions of halothane anaesthesia.

Experimental Series 1- Descending output pathway(s) responsible for mediating decompensation

Immunohistochemical detection of the protein product (Fos) of the immediate early gene *c-fos* was used as a marker of haemorrhage-evoked neural activity within the periaqueductal gray. The first major finding was that hypovolaemic (30%) haemorrhage selectively evoked Fos expression (i.e., neural activity) within the ventrolateral PAG. These findings are consistent with the hypothesised role of the vlPAG as being the central neural site responsible for mediating the cardiovascular reaction to severe blood loss. Furthermore, these data extend previous reports by showing that the increase in Fos expression following hypovolaemic (30%) haemorrhage occurs over and above that seen following both normotensive (10%) haemorrhage and euvolaemic (peripherally-mediated) hypotension. Thus, the increase in Fos expression may be interpreted as being *specific* to the decompensatory phase of blood loss.

In a second set of experiments combining retrograde tracer and Fos immunohistochemistry, it was revealed that ventrolateral PAG neurons selectively activated by severe haemorrhage project overwhelmingly to the vasodepressor region of

the caudal midline medulla (CMM). This finding correlates well with previous experimental reports showing that the integrity of the CMM is critical for mediating severe, behaviourally-coupled, cardiovascular challenges such as haemorrhage (Henderson et al., 2000, 2002) .

Experimental Series 2 – Potential sources of afferent drive onto the ventrolateral PAG

The experiments described in Chapter 3 demonstrated that severe hypovolaemic haemorrhage selectively activated neurons within the ventrolateral PAG. The aim of this series of experiments was to determine: (i) which population(s) of medullary neurons were activated by severe blood loss; (ii) which population(s) of activated medullary neurons projected onto the ventrolateral PAG; and (iii) whether these neurons play a role in triggering decompensation.

In an initial set of experiments (chapter 4 part I) immunohistochemical detection of the protein product (Fos) of the immediate early gene c-fos was used as a marker of haemorrhage-evoked neural activity within the medulla. The first main finding was that hypovolaemic haemorrhage evoked an increase in Fos expression within the ventrolateral medulla, most notably caudal to the level of the Obex. This region has been well described and is known to contain the noradrenergic (A1) neural population. Subsequent double label studies revealed that *almost all* A1 noradrenergic neurons are activated by hypovolaemic haemorrhage but *not* by either normotensive haemorrhage or euvolaemic hypotension. Thus, the increase in Fos expression may be interpreted as being specific to the *decompensatory* phase of blood loss.

Previous studies have established that large numbers of A1 noradrenergic neurons are recruited by various physical stressors; including haemorrhage (Dayas et al., 2001a, 2001b). Additionally, the hypotension evoked by severe blood loss is significantly attenuated following blockade of the caudal ventrolateral medulla – including the A1 cell group. These data raise the possibility that A1 neurons may be responsible for providing afferent drive onto the ventrolateral PAG in order to trigger decompensation.

To determine whether ventrolateral medullary catecholaminergic neurons provide significant afferent input to the vlPAG, injections of retrograde tracer were made into the ventrolateral PAG and combined with immunohistochemistry for both tyrosine hydroxylase and phenylethanolamine-N-methyltransferase. It was revealed that noradrenergic neurons in the ventrolateral medulla provide a major source of input onto the vlPAG.

The final series of experiments (chapter 4 part III) used a physiological approach to investigate whether noradrenaline release within the ventrolateral PAG plays a role in triggering decompensation. Bilateral microinjections of the non-specific alpha adrenoreceptor antagonist phentolamine in the ventrolateral PAG of conscious rats significantly delayed and attenuated the hypotension evoked by severe haemorrhage. This finding confirmed that noradrenergic neurotransmission within the ventrolateral PAG plays a key role in the mechanisms triggering decompensation. When considered with the above anatomical data, it is likely that noradrenaline release arises from activation of the A1-ventrolateral PAG pathway.

Experimental Series 3 – The role of noradrenaline in triggering decompensation under conditions of halogenated anaesthesia.

Halogenated anaesthesia has been shown to lead to a premature and potentiated decompensatory phase of haemorrhage (Caplan et al., 1988, Vatner 1978). Interestingly, halothane anaesthesia has also been shown to evoke activation of ventrolateral PAG-projecting A1 medullary neurons (Clement et al., 1998). In light of this evidence, the discovery that the A1 – ventrolateral PAG pathway likely plays a key role in triggering decompensation suggests that premature activation of this pathway may be responsible for potentiating haemorrhage-evoked hypotension under conditions of halogenated anaesthesia.

To investigate this question, microinjections of: (i) the non-specific alpha adrenoreceptor antagonist phentolamine; (ii) the $alpha_1$ adrenoreceptor antagonist prazosin; or (iii) the selective $alpha_2$ adrenoreceptor antagonist yohimbine were made into the ventrolateral PAG of anaesthetised animals prior to hypovolaemic haemorrhage. It was found that both phentolamine and yohimbine dramatically attenuated the hypotension evoked by hypovolaemic haemorrhage. In contrast prazosin had no effect on haemorrhage-evoked hypotension. These data suggest that $alpha_2$ adrenoreceptors within the ventrolateral PAG play a key role in mediating decompensation under conditions of halogenated anaesthesia.

6.2 Central events precipitating shock after injury

The PAG has recently been recognised as being a neural structure that integrates both the behavioural and cardiovascular components of the response to injury. Past findings have shown that the ventrolateral column of the PAG co-ordinates quiescence, hyporeactivity, hypotension and bradycardia in response to deep pain and haemorrhage, in addition to other inescapable stressors. This response has been classified as a *passive coping* strategy to injury and is an adaptive response essential for the survival of the individual.

A schematic illustration of the proposed central pathway mediating hypovolaemic shock, as suggested by the results of the studies presented in this thesis, is illustrated in Figure 6.1. Severe blood loss results in the selective activation of A1 noradrenergic neurons located within the ventrolateral medulla. Noradrenergic A1 neurons provide significant afferent drive onto the ventrolateral PAG. Activation of ventrolateral PAG-projecting, noradrenergic neurons results in the release of noadrenaline within the vlPAG and depolarisiation of descending vlPAG output neurons which project to the caudal midline medulla (CMM) in order to trigger the sympathoinhibition, hypotension and bradycardia characteristic of hypovolaemic shock.

It is also suggested that premature activation of A1 noradrenergic neurons results in the potentiation of decompensation under conditions of anaesthesia, and that alpha$_2$ adrenoreceptors play a key role in this circuit.

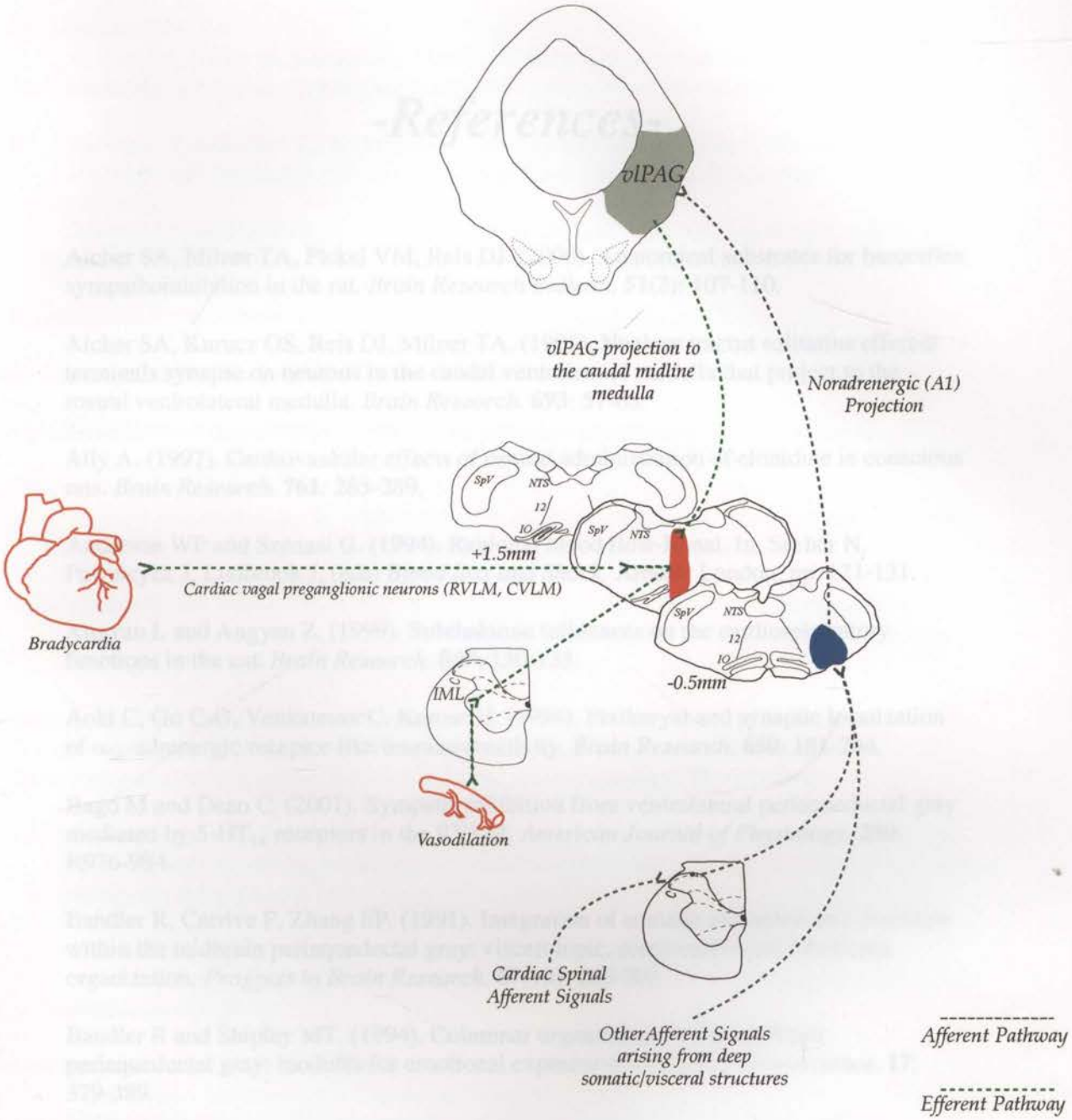

Figure 6.1
Schematic summary diagram illustrating a proposed central pathway responsible for triggering decompensation. Cardiac spinal afferent neurons in addition to other, as yet undefined peripheral triggers result in the activation of noradrenergic A1 neurons which are located in the ventrolateral medulla (predominantly) caudal to the obex. These noradrenergic neurons then project onto the vlPAG resulting in the release of noradrenaline and subsequent depolarisation of vlPAG neurons which triggers decompensation via descending projections to the caudal midline medulla. *vlPAG, ventrolateral periaqueductal gray; SpV, spinal trigeminal nucleus; NTS, nucleus of the solitary tract; IO, inferior olivary nucleus; 12, hypoglossal nerve.*

-References-

Aicher SA, Milner TA, Pickel VM, Reis DJ. (2000). Anatomical substrates for baroreflex sympathoinhibition in the rat. *Brain Research Bulletin.* **51**(2): 107-110.

Aicher SA, Kurucz OS, Reis DJ, Milner TA. (1995). Nucleus tractus solitarius efferent terminals synapse on neurons in the caudal ventrolateral medulla that project to the rostral ventrolateral medulla. *Brain Research.* **693**: 51-63.

Ally A. (1997). Cardiovascular effects of central administration of clonidine in conscious rats. *Brain Research.* **761**: 283-289.

Anderson WP and Szenasi G. (1994). Regional blood flow-Renal. In Secher N, Pawelcyzk J, Ludbrook J, (eds) *Blood loss and Shock.* Arnold, London, pp. 121-131.

Angyan L and Angyan Z. (1999). Subthalamic influences on the cardiorespiratory functions in the cat. *Brain Research.* **847**: 130-133.

Aoki C, Go C-G, Venkatesan C, Kurose H. (1994). Perikaryal and synaptic localization of α_{2A}-adrenergic receptor-like immunoreactivity. *Brain Research.* **650**: 181-204.

Bago M and Dean C. (2001). Sympathoinhibition from ventrolateral periaqueductal gray mediated by 5-HT_{1A} receptors in the RVLM. *American Journal of Physiology.* **280**: R976-984.

Bandler R, Carrive P, Zhang SP. (1991). Integration of somatic and autonomic reactions within the midbrain periaqueductal gray: viscerotopic, somatotopic and functional organization. *Progress in Brain Research.* **87**(13): 269-305.

Bandler R and Shipley MT. (1994). Columnar organization of the midbrain periaqueductal gray: modules for emotional expression? *Trends in Neuroscience.* **17**: 379-389.

Bandler R, Depaulis A, Vergnes M. (1985a). Identification of midbrain neurones mediating defensive behaviour in the rat by microinjections of excitatory amino acids. *Behavioral Brain Research.* **15:** 107-119.

Bandler R, Prineas S, McCulloch T. (1985b). Further localisation of midbrain neurones mediating the defence reaction in the cat by microinjections of excitatory amino acids. *Neuroscience Letters.* **56:** 311-316.

Banner SE, Carter M, Sanger GL. (1995). 5-Hydroxytryptamine 3 receptor antagonism modulates a noxious visceral pseudoaffective reflex. *Neuropharmacology*. **34**: 263-267.

Barcroft H, Edholm OG, McMichael J, Sharpey-Schafer EP. (1944). Posthaemorrhagic fainting study by cardiac output and forearm flow. *The Lancet*. **I:** 489-490

Barman SM and Gebber GL. (1987). Lateral tegmental field neurons of cat medulla: a source of basal activity of ventrolateral medullospinal sympathoexcitatory neurons. *Journal of Neurophysiology*. **57**: 1410-1424.

Behbehani MM, Pomeroy SL, Mack CE. (1981). Interaction between central gray and nucleus raphe magnus: Role of norepinephrine. *Brain Research Bulletin*. **6**: 361-364.

Bennet T and Gardiner SM. (1982). The influence of naloxone on haemorrhagic hypotension in Brattleboro rats. *Journal of Physiology*. **332**: 69-70.

Bernard JF and Bandler R. (1998). Parallel circuits for emotional coping behaviour: new pieces in the puzzle. *Journal of Comparative Neurology*. **401**: 429-36.

Blair RW and Evans AR. (1991). Responses of medullary raphespinal neurons to coronary artery occlusion, epicardial bradykinin, and cardiac mechanical stimuli in cats. *Journal of Neurophysiology*. **66**: 2095-2106.

Blake DW, Van Leeuwen AF, Petring OU, Ludbrook J, Ventura S. (1995). Haemodynamic response to simulated haemorrhage in the rabbit: interaction of i.v. anaesthesia and hypoxia. *British Journal of Anaesthesiology*. **75**: 610-650.

Borer KE and Clarke KW. (2006). The effect of hyoscine on dobutamine requirement in spontaneously breathing horses anaesthetised with halothane. *Veterinary Anaesthesia and Analgesia*. **33**: 149-157.

Bostrom IM, Nyman G, Hoppe A, Lord P. (2006). Effects of meloxicam on renal function in dogs with hypotension during anaesthesia. *Veterinary Anaesthesia and Analgesia*. **33**: 62-69.

Boyajian CL, Loughlin SE, Leslie FM. (1987). Anatomical evidence for alpha-2 adrenoceptor heterogeneity: Differential autoradiographic distributions of [^{3}H]rauwolscine and [^{3}H]idazoxan in rat brain. *Journal of Pharmacology and Experimental Therapeutics*. **241**: 1079-1091.

Boyle WA and Maher GM. (1995). Endothelium-independent vasoconstricting and vasodilating actions of halothane on rat mesenteric resistance blood vessels. *Anesthesiology*. **82**: 221-235.

Brasch H and Zetler G. (1982). Caerulein and morphine in a model of visceral pain. Effects of the hypotensive response to renal pelvis distension in the rat. *Naunyn Schmiedbergs Archive of Pharmacology*. **319**: 161-167.

Brooks DP, Share L, Crofton JT. (1986a). Central adrenergic mechanisms in hemorrhage-induced vasopressin secretion. *American Journal of Physiology*. **251**: H1158-1162.

Brooks DP, Share L, Crofton JT. (1986b). Central adrenergic control of vasopressin release. *Neuroendocrinology*. **42**: 416-420.

Brown DL and Guyenet PG. (1985). Electrophysiological study of cardiovascular neurons in the rostral ventrolateral medulla in rats. *Circulation Research*. **56**: 359-369.

Buller KM, Smith DW, Day TA. (1999). Differential recruitment of hypothalamic neuroendocrine and ventral medulla catecholaminergic cells by non-hypotensive and hypotensive haemorrhages. *Brain Research*. **834**: 42-54.

Burke SL and Dorward PK. (1988). Influence of endogenous opiates and cardiac afferents on renal nerve activity during haemorrhage in conscious rabbits. *Journal of Physiology*. **402**: 9-27.

Buzsaki G, Kennedy B, Solt VB, Ziegler M. (1991). Noradrenergic control of thalamic oscillation: the role of alpha-2 receptors. *European Journal of Neuroscience*. **3**: 222-229.

Cameron AA, Khan IA, Westlund KN, Willis WD. (1995). The efferent projections of the periaqueductal gray in the rat: A *phaseolus vulgaris*-Leucoagglutinin study II. Descending projections. *Journal of Comparative Neurology*. **351**: 585-601.

Cao WH and Morrison SF. (2003). Disinhibition of rostral raphe pallidus neurons increases cardiac sympathetic nerve activity and heart rate. *Brain Research*. **980**: 1-10.

Caplan RA, Ward RJ, Posner K, Cheney FW. (1988). Unexpected cardiac arrest during spinal anaesthesia: a closed claims analysis of predisposing factors. *Anesthesiology*. **68**: 5-11.

Carrive P and Bandler R. (1991). Control of extracranial and hindlimb blood flow by the midbrain periaqueductal gray of the cat. *Experimental Brain Research*. **84**: 599-606.

Carrive P, Dampney RAL, Bandler R. (1987). Excitation of neurons in a restricted portion of the midbrain periaqueductal gray elicits both behavioural and cardiovascular components of the defense reaction in the unanaesthetised decerebrate cat. *Neuroscience Letters*. **81**: 273-278.

Carrive P, Bandler R, Dampney RAL. (1989). Somatic and autonomic integration in the midbrain of the unanaesthetised decerebrate cat: a distinctive pattern evoked by excitation of neurons in the subtentorial portion of the midbrain periaqueductal gray. *Brain Research*. **483**: 251-258.

Cavun S and Millington WR. (2001a). Evidence that hemorrhagic hypotension is mediated by the ventrolateral periaqueductal gray region. *American Journal of Physiology*. **281**: 747-752.

Cavun S, Resch GE, Evec AD, Rapacon-Baker MM, Millington WR. (2001b). Blockade of delta opioid receptors in the ventrolateral periaqueductal gray region inhibits the fall in arterial pressure evoked by haemorrhage. *Journal of Pharmacology and Experimental Therapeutics*. **297**: 612-619.

Cavun S, Goktalay G, Millington WR. (2004). The hypotension evoked by visceral nociception is mediated by delta opioid receptors in the periaqueductal gray. *Brain Research*. **1019**: 237-245.

Cespuglio R, Rousset C, Debilly G, Rochat C, Millan MJ. (2005). Acute administration of the novel serotonin and noradrenaline reuptake inhibitor, S33005, markedly modifies sleep-wake cycle architecture in the rat. *Psychopharmacology (Berlin)*. **181**: 639-652.

Chalmers JP, Korner PI, White SW. (1967a). The effects of haemorrhage in the unanaesthetised rabbit. *Journal of Physiology*. **189**(3): 367-391.

Chalmers JP, Korner PI, White SW. (1967b). Effects of haemorrhage on the distribution of blood flow in the rabbit. *Journal of Physiology London*. **192**: 561-574.

Chan RKW and Sawchenko PE. (1994). Spatially and temporally differentiated patterns of c-fos expression in brainstem catecholaminergic cell groups induced by cardiovascular challenges in the rat. *Journal of Comparative Neurology*. **348**: 433-460.

Chan RKW and Sawchenko PE. (1998). Organisation and transmitter specificity of medullary neurons activated by sustained hypertension: Implications for understanding baroreceptor circuitry. *The Journal of Neuroscience*. **18**(1): 371-387.

Chan RKW and Sawchenko PE. (1998). Differential time- and dose-related effects of haemorrhage on tyrosine hydroxylase and neuropeptide Y mRNA expression in medullary catecholamine neurons. *European Journal of Neuroscience*. **10**: 3747-3758.

Chan RKW, Peto CA, Sawchenko PE. (2000). Fine structure and plasticity of barosensitive neurons in the nucleus of solitary tract. *Journal of Comparative Neurology*. **422**: 338-351.

Chen S and Aston-Jones G. (1995). Anatomical evidence for inputs to ventrolateral medullary catecholaminergic neurons from the midbrain periaqueductal gray of the rat. *Neuroscience Letters*. **195**: 140-144.

Chen S and Aston-Jones G. (1996). Extensive projections from the midbrain periaqueductal gray to the caudal ventrolateral medulla: a retrograde and anterograde tracing study in the rat. *Neuroscience*. **71**: 443-459.

Cho HJ, Yoon KT, Kim HS, Lee SJ, Kim JK, Kim DS, Lee WJ. (1999). Expression of brain-derived neurotrophic factor in catecholaminergic neurons of the rat lower brainstem after colchicine treatment or hemorrhage. *Neuroscience*. **92**: 901-909.

Choi D, Li D, Raisman G. (2002). Fluorescent retrograde neuronal tracers that label the rat facial nucleus: a comparison of Fast Blue, Fluoro-ruby, Fluoro-emerald, Fluoro-gold and DiI. *Journal of Neuroscience Methods*. **117**: 167-172.

Ciriello J. (1983). Brainstem projections of aortic baroreceptor afferent fibres in the rat. *Neuroscience Letters*. **36**: 37-42.

Ciriello J and Calaresu FR. (1983). Central projections of afferent renal fibres in the rat: an anterograde transport study of horseradish peroxidase. *Journal of the Autonomic Nervous System*. **8**: 273-285.

Clement CI, Keay KA, Owler BK, Bandler R. (1996). Common patterns of increased and decreased Fos expression in midbrain and pons evoked by noxious deep somatic and visceral manipulations in the rat. *Journal of Comparative Neurology*. **366**: 495-515.

Clement CI, Keay KA, Bandler R. (1998). Medullary catecholaminergic projections to the ventrolateral periaqueductal gray region activated by halothane anaesthesia. *Neuroscience*. **86**: 1273-1284.

Clement CI, Keay KA, Podzebenko K, Gordon BD, Bandler R. (2000). Spinal sources of noxious visceral and noxious deep somatic afferent drive onto the ventrolateral periaqueductal gray of the rat. *Journal of Comparative Neurology*. **425**: 323-44.

Cobos A, Lima D, Almeida A, Tavares I. (2003). Brain afferents to the lateral caudal ventrolateral medulla: a retrograde and anterograde tracing study in the rat. *Neuroscience*. **120**: 485-498.

Coleman MJ and Dampney RA. Powerful depressor and sympathoinhibitory effects evoked from neurons in the caudal raphe pallidus and obscurus. *American Journal of Physiology*. **268**: R1295-302.

Coleman MJ and Dampney RA. (1998). Sympathoinhibition evoked from caudal midline medulla is mediated by GABA receptors in rostral VLM. *American Journal of Physiology*. **274**: R318-23.

Commons KG, Beck SG, Rudoy C, Van Bockstaele EJ. (2001). Anatomical evidence for presynaptic modulation by the delta opioid receptor in the ventrolateral periaqueductal gray of the rat. *Journal of Comparative Neurology*. **430**: 200-208.

Commons KG. (2003). Translocation of presynaptic delta opioid receptors in the ventrolateral periaqueductal gray after swim stress. *Journal of Comparative Neurology*. **464**: 197-207.

Conzen PF, Vollmar B, Habazettl, Frink EJ, Peter K, Messmer K. (1992). Systemic and regional hemodynamics of isoflurane and sevoflurane in rats. *Anesthesia and Analgesia*. **74**: 79-88.

Cornish KG, Gilmore JP, McCulloch T. (1988). Central blood volume and blood pressure in conscious primates. *American Journal of Physiology*. **254**: H693-701.

Courneya CA. and Korner PI. (1991). Neurohumoral mechanisms and the role of arterial baroreceptors in the reno-vascular response to haemorrhage in rabbits. *Journal of Physiology (London)*. **437**: 393-407.

Courneya CA. (1996). Impaired renin response to haemorrhage in hypertensive rabbits. *American Journal of Physiology*. **271**: H1524-1530.

Craig AD and Kniffki KD. (1985). Spinothalamic lumbosacral lamina I cells responsive to skin and muscle stimulation in the cat. *Journal of Physiology (London)*. **365**: 197-221.

Craig AD. (1995). Distribution of brainstem projections from spinal lamina I neurons in the cat and monkey. *Journal of Comparative Neurology*. **361**: 225-248.

Cravo SL, Morrison SF, Reis DJ. (1991). Differentiation of two cardiovascular regions within the caudal ventrolateral medulla. *American Journal of Physiology*. **261**: R985-994.

Cunningham ET, Bohn MC, Sawchenko PE. (1990). Organisation of adrenergic inputs to the paraventricular and supraoptic nuclei of the hypothalamus in the rat. *Journal of Comparative Neurology*. **292**: 651-667.

D'Amato R and Holaday JW. (1984). Multiple opioid receptors in endotoxic shock: evidence for delta involvement and mu-delta interactions in vivo. *Proceedings of the National Academy of Science USA*. **81**: 2898-2901.

Dampney RA and Horiuchi J. (2003). Functional organization of central cardiovascular pathways: studies using c-fos gene expression. *Progress in Neurobiology*. **71**: 359-384.

Dampney RA, Polson JW, Potts PD, Hirooka Y, Horiuchi J. (2003). Functional organization of brain pathways subserving the baroreceptor reflex: studies in conscious animals using immediate early gene expression. *Cellular and Molecular Neurobiology*. **23**: 597-616

Dampney RA, Coleman MJ, Fontes MA, Hirooka Y, Horiuchi J, Li YW, Polson JW, Potts PD, Tagawa T. (2002). Central mechanisms underlying short- and long-term regulation of the cardiovascular system. *Clinical and Experimental Pharmacology and Physiology*. **29**: 261-268.

Dampney RAL and Moon EA. (1980). Role of ventrolateral medulla in vasomotor response to cerebral ischemia. *American Journal of Physiology*. **239**: H349-358.

Dampney RAL (1994). Functional organization of central pathways regulating the cardiovascular system. *Physiological Reviews*. **74**:323-364.

Dampney RAL, Blessing WW and Tan E. (1988). Origin of tonic GABAergic inputs to vasodepressor neurons in the subretrofacial nucleus of the rabbit. *Journal of the Autonomic Nervous System*. **24**: 277-239.

Darlington DN, Shinsako J, Dallman MF. (1986). Responses of ACTH, epinephrine, norepinephrine, and cardiovascular system to hemorrhage. *American Journal of Physiology*. **251**: H612-618.

Darlington DN, Barraclough CA, Gann DS. (1992). Hypotensive hemorrhage elevates corticotropin-releasing hormone messenger ribonucleic acid (mRNA) but not vasopressin mRNA in the rat hypothalamus. *Endocrinology*. **130**: 1281-1288.

Dawes GS. (1947). Studies on veratrum alkaloids. VII. Receptor areas in the coronary arteries and elsewhere as revealed by the use of veratridine. *Journal of Pharmacology and Experimental Therapeutics*. **89**: 325-342.

Day TA. (1989). Control of neurosecretory vasopressin cells by noradrenergic projections of the caudal ventrolateral medulla. *Progress in Brain Research*. **81**: 303-317.

Dayas CV, Buller KM, Crane JW, Day TA. (2001a). Stressor categorisation: acute physical and psychological stressors elicit distinctive recruitment patterns in the amygdala and in medullary noradrenergic cell groups. *European Journal of Neuroscience*. **14**: 1143-1152.

Dayas CV, Buller KM, Day TA. (2001b). Medullary neurons regulate hypothalamic corticotropin-releasing factor cell responses to an emotional stressor. *Neuroscience*. **105**: 707-719.

Dean C. (2004). Hemorrhagic sympathoinhibition mediated through the periaqueductal gray in the rat. *Neuroscience Letters*. **354**: 79-83.

Dean C and Bago M. (2002). Renal sympathoinhibition mediated by 5-HT(1A) receptors in the rvlm during severe haemorrhage in rats. *American Journal of Physiology*. **282:** R122-130.

De Luca-Vinhas MCZ, Macedo CE, Brandao ML. (2006). Pharmacological assessment of the freezing, antinociception, and exploratory behavior organised in the ventrolateral periaqueductal gray. *Pain.* **121**: 94-104.

Depaulis A, Keay KA, Bandler R. (1992). Longitudinal neuronal organization of defensive reactions in the midbrain periaqueductal gray region of the rat. *Experimental Brain Research.* **90**: 307-318.

Depaulis A, Keay KA, Bandler R. (1994). Quiescence and hyporeactivity evoked by activation of cell bodies in the ventrolateral midbrain periaqueductal gray of the rat. *Experimental Brain Research.* **99**: 75-83.

Ding YF. (2001). Renal ischemia-induced Fos expression in catecholaminergic neurons of rats. *Sheng Li Xue Bao.* **53**: 445-450.

Ditting T, Hilgers KF, Scrogin KE, Stetter A, Linz P, Veelken R. (2005). Mechanosensitive cardiac C-fibre response to changes in left ventricular filling, coronary perfusion pressure, hemorrhage, and volume expansion in rats. *American Journal of Physiology.* **288**: H541-552.

Donovan MK, Wyss JM, Winternitz SR. (1983). Localisation of renal sensory neurons using the fluorescent dye technique. *Brain Research.* **259**: 119-122.

Doxey JC, Lane AC, Roach AG, Virdee NK. (1984). Comparison of the α-adrenoceptor antagonist profiles of idazoxan (RX 781094), yohimbine, rauwolscine and corynanthine. *Naunyn-Schmiedebergs Archives of Pharmacology.* **325**: 136-144.

Dun NJ, Dun SL, Chiaia NL. (1993). Hemorrhage induces Fos immunoreactivity in rat medullary catecholaminergic neurons. *Brain Research.* **608**: 223-232.

Ebert TJ, Kotrly KJ, Vucins EJ, Pattison CZ, Kampine JP. (1985). Halothane anesthesia attenuates cardiopulmonary baroreflex control of peripheral resistance in humans. *Anesthesiology.* **63**: 668-674.

Elam M, Svensson TH, Thoren P. (1985). Differentiated cardiovascular afferent regulation of locus coeruleus neurons and sympathetic nerves. *Brain Research.* **358**: 77-84.

Esclapez M, Tillakaratne NJK, Tobin AJ, Houser CR. (1993). Comparative localisation of mRNAs encoding two forms of glutamic acid decarboxylase with nonradioactive in situ hybridisation methods. *Journal of Comparative Neurology.* **331**: 339-362.

Esclapez M, Tillakaratne NJK, Kaufman DL, Tobin AJ, Houser CR. (1994). Comparative localization of two forms of glutamic acid decarboxylase and their mRNAs in rat brain supports the concept of functional differences between the forms. *The Journal of Neuroscience.* **14**: 1834-1855.

Evans RG, Ludbrook J, Potocnik SJ. (1989). Intracisternal naloxone and cardiac nerve blockade prevent vasodilation during simulated haemorrhage in awake rabbits. *Journal of Physiology*. **409**: 1-14.

Evans RG, Ludbrook J, Van Leeuwen AF. (1989). Role of central opiate receptor subtypes in the circulatory responses of awake rabbits to graded caval occlusion. *Journal of Physiology*. **419**: 15-31.

Evans RG, Ludbrook J, Woods RL, Casley D. (1991). Influence of higher brain centres and vasopressin on the haemodynamic response to acute central hypovolemic in rabbits. *Journal of the Autonomic Nervous System*. **35**: 1-14.

Evans RG, Haynes JM, Ludbrook J. (1993). Effects of 5-HT receptor and alpha 2 adrenoreceptor ligands on the haemodynamic response to acute central hypovolemia in conscious rabbits. *British Journal of Pharmacology*. **109**: 37-47.

Evans RG and Ludbrook J. (1991). Chemosensitive cardiopulmonary afferents and the haemodynamic response to simulated haemorrhage in conscious rabbits. *British Journal of Pharmacology*. **102**: 533-539.

Evans RG, Ludbrook J, Ventura S. (1994). Role of vagal afferents in the haemodynamic response to acute central hypovolemia in unanaesthetised rabbits. *Journal of the Autonomic Nervous System*. **46**: 251-260.

Evans RG, Ventura S, Dampney RAL, Ludbrook J. (2001). Neural mechanisms in the cardiovascular responses to acute central hypovolaemia. *Clinical and Experimental Pharmacology and Physiology*. **28**: 479-487.

Faden AI and Holaday JW. (1979). Opiate antagonists: a role in the treatment of hypovolemic shock. *Science*. **205**: 317-318.

Fan L and McIntosh TK. (1993). Regulation of the gene expression of preproenkephalin in the rat brain: influence of hemorrhage. *Circulatory Shock*. **40**: 24-28.

Farkas E, Jansen AS, Loewy AD. (1998). Periaqueductal gray matter input to cardiac-related sympathetic neurons. *Brain Research*. **792**: 179-92.

Fennessy MR and Rattray JF. (1971). Cardiovascular effects of intravenous morphine in the anaesthetised rat. *European Journal of Pharmacology*. **14**: 1-8.

Fejes-Toth G, Brinck-Johnsen T, Naray-Fejes-Toh A. (1988). Cardiovascular and hormonal response to hemorrhage in conscious rats. *American Journal of Physiology* **254**: H947-953.

Feuerstein G, Chiueh CC, Kopin IJ. (1981). Effect of naloxone on the cardiovascular and sympathetic response to hypovolemic hypotension in the rat. *European Journal of Pharmacology*. **75**: 65-69.

Fitzpatrick AP, Banner N, Cheng A, Yacoub M, Sutton R. (1993). Vasovagal reactions may occur after orthotopic heart transplantation. *Journal of the American College of Cardiology*. **21**: 1132-1137.

Gatti PJ, Homby PJ, Mandal AK, Norman WP, DaSilva AMT, Gillis RA. (1995). Cardiovascular neurons in cat caudal ventrolateral medulla: location and characterisation of GABAergic input. *Brain Research*. **693**: 80-87.

Gebhart GF and Ossipov MH. (1986). Characterisation of inhibition of the spinal nociceptive tail-flick reflex in the rat from the medullary lateral reticular nucleus. *Journal of Neuroscience*. **6**: 701-713.

Gieroba ZJ, Fullerton MJ, Funder JW, Blessing WW. (1992). Medullary pathways for adrenocorticotropic hormone and vasopressin secretion in rabbits. *American Journal of Physiology*. **262**: R1047-1056.

Gieroba ZJ, Shapoval LN, Blessing WW. (1994). Inhibition of the A1 area prevents haemorrhage-induced secretion of vasopressin in rats. *Brain Research*. **657**: 330-332.

Gilbey MP, Coote JH, Macleod VH, Peterson DF. (1981). Inhibition of sympathetic activity by stimulating in the raphe nuclei and the role of 5-hydroxytryptamine in this effect. *Brain Research*. **226**: 131-142.

Golanov EV, Cherkovich GM, Suchkov VV. (1983). Effect of naloxone in hypotension induced by acute blood loss in baboons (papio hamadryas). *Bulletin of Experimental Biology and Medicine*. **96**: 1428-1431.

Gorden FJ (1986). Central opioid receptors and baroreflex control of sympathetic and cardiovascular function. *Journal of Pharmacology and Experimental Therapeutics*. **237**: 428-436.

Guyenet PG and Stornetta RL. (1982). Inhibition of sympathetic preganglionic discharges by epinephrine and alpha-methylepinephrine. *Brain Research*. **235**: 271-283.

Guyenet PG and Brown DL. (1986). Unit activity in nucleus paragigantocellularis lateralis during cerebral ischemia in the rat. *Brain Research*. **364**: 301-314.

Guyenet PG, Filtz TM, Donaldson SR. (1987). Role of excitatory amino acids in rat vagal and sympathetic baroreflexes. *Brain Research*. **407**: 272-84.

Guyenet PG, Darnall RA, Riley TA. (1990). Rostral ventrolateral medulla and sympathorespiratory integration in rats. *American Journal of Physiology*. **259**: R1063-1074.

Guyenet PG, Stornetta RL, Riley T, Norton FR, Rosin DL, Lynch KR. (1994). Alpha2A-adrenergic receptors are present in lower brainstem catecholaminergic and serotonergic neurons innervating spinal cord. *Brain Research*. **638**: 285-294.

Haeusler G. (1974). Clonidine-induced inhibition of sympathetic nerve activity: no indication for a central presynaptic or an indirect sympathomimetic mode of action. *Naunyn-Schmeidebergs Archives of Pharmacology*. **286**: 97-111.

Haggendal J. (1986). On the patterns of blood pressure, heart rate and blood levels of noradrenaline and adrenaline during haemorrhage in the rat. *Acta Physiologica Scandinavica*. **127**: 513-522.

Hainsworth R. (1991). Reflexes from the heart. *Physiological Reviews*. **71**: 617-658.

Hammond DL, Levy RA, Proudfit HK. (1980). Hypoalgesia following microinjection of noradrenergic antagonists in the nucleus raphe magnus. *Pain*. **9**: 85-101.

Hammond DL, Levy RA, Proudfit HK. (1980). Hypoalgesia induced by microinjection of a norepinephrine antagonist in the raphe magnus: reversal by intrathecal administration of a serotonin antagonist. *Brain Research*. **201**: 475-479.

Harrison JK, Pearson WR, Lynch KR. (1991). Molecular characterisation of α_1- and α_2-adrenoceptors. *Trends in Pharmacological Sciences*. **12**: 62-67.

Haselton JR and Guyenet PG. (1989). Central respiratory modulation of medullary sympathoexcitatory neurons in rat. *American Journal of Physiology*. **256**: R739-750.

Haselton JR and Guyenet PG. (1990). Ascending collaterals of medullary barosensitive neurons and C1 cells in rats. *American Journal of Physiology*. **258**: R1051-1063.

Hasser EM and Schadt JC. (1992). Sympathoinhibition and its reversal by naloxone during hemorrhage. *American Journal of Physiology*. **262**: R444-451.

Hayar A and Guyenet PG. (1999). α_2-Adrenoceptor-mediated presynaptic inhibition in bulbospinal neurons of rostral ventrolateral medulla. *American Journal of Physiology*. **277**: H1069-1080.

Head GA, Quail AQ, Woods RL. (1987). Lesions of A1 noradrenergic cells affect AVP release and heart rate during hemorrhage. *American Journal of Physiology*. **253**: H1012-1017.

Heary RF, Maniker AH, Krieger AJ, Sapru HN. (1993). Cardiovascular responses to global ischemia: role of excitatory amino acids in the ventrolateral medullary pressor area. *Journal of Neurosurgery*. **78**: 922-928.

Henderson LA, Keay KA and Bandler R. (1998). The ventrolateral periaqueductal gray projects to caudal brainstem depressor regions: a functional anatomical and physiological study. *Neuroscience*. **82**(1): 201-221.

Henderson LA, Keay KA, Bandler R. (2000). Caudal midline medulla mediates behaviourally-coupled but not baroreceptor-mediated vasodepression. *Neuroscience*. **98**: 779-92.

Henderson LA, Keay KA, Bandler R. (2000). Hypotension following acute hypovolaemia depends on the caudal midline medulla. *Neuroreport*. **9**: 1839-44.

Herman NL and Kostreva DR. (1986). Alterations in cardiac [^{14}C] deoxyglucose uptake induced by two renal afferent stimuli. *American Journal of Physiology*. **251**: R867-877.

Herold S, Hecker C, Deitmer JW, Brockhaus J. (2005). α1-Adrenergic modulation of synaptic input to purkinje neurons in rat cerebellar brain slices. *Journal of Neuroscience Research*. **82**: 571-579.

Heslop DJ, Keay KA, Bandler R. (2002). Haemorrhage-evoked compensation and decompensation are mediated by distinct caudal midline medullary regions in the urethane-anaesthetised rat. *Neuroscience*. **113**: 555-67.

Heslop DJ, Bandler R, Keay KA. (2004). Haemorrhage-evoked decompensation and recompensation mediated by distinct projections from rostral and caudal midline medulla in the rat. *European Journal of Neuroscience*. **20**: 2096-2110.

Hintze TH and Vatner SF. (1982). Cardiac dynamics during hemorrhage: relative unimportance of adrenergic inotropic responses. *Circulation Research*. **50**: 705-713.

Holaday JW and Faden AI. (1978). Naloxone reversal of endotoxin hypotension suggests role of endorphins in shock. *Nature*. **275**: 450-451.

Holaday JW, O'Hara M, Faden AI. (1981). Hypophysectomy alters cardiorespiratory variables: central effects of pituitary endorphins in shock. *American Journal of Physiology*. **241**: H479-485.

Holaday J. (1983). Cardiovascular effects of endogenous opiate systems. *Annual Reviews of Pharmacology and Toxicology*. **23**: 541-594.

Holmberg G and Gershon S. (1960). Autonomic and psychic effects of yohimbine hydrochloride. *Psychopharmacologia*. **2**: 93-106.

Homi HM, Mixco JM, Sheng H, Grocott HP, Pearlstein RD, Warner DS. (2003). Severe hypotension is not essential for isoflurane neuroprotection against forebrain ischemia in mice. *Anesthesiology*. **99**: 1145-1151.

Horiuchi J, Potts PD, Polsen JW, Dampney RAL. (1999). Distribution of neurons projecting to the rostral ventrolateral medullary pressor region that are activated by sustained hypotension. *Neuroscience*. **89**: 1319-29.

Housmans PR and Murat I. (1988). Comparative effects of halothane, enflurane, and isoflurane at equipotent anesthetic concentrations on isolated ventricular myocardium of the ferret. I. contractility. *Anesthesiology*. **69**: 451-463.

Hua F, Ricketts BA, Reifsteck A, Ardell JL, Williams CA. (2003). Myocardial ischemia induces the release of substance P from cardiac afferent neurons in rat thoracic cord. *American Journal of Physiology*. **286**: H1654-1664.

Hua F, Harrison T, Qin C, Reifsteck A, Ricketts B, Carnel C, Williams CA. (2004). c-Fos expression in rat brain stem and spinal cord in response to activation of cardiac ischemia-sensitive afferent neurons and electrostimulatory modulation. *American Journal of Physiology*. **287**: H2728-2738.

Ingwersen W, Allen DG, Dyson DH, Black WD, Goldberg MT, Valliant AE. (1987). Cardiopulmonary effects of a halothane/oxygen combination in hypovolemic cats. *Canadian Journal of Veterinary Research*. **52**: 428-433.

Janss AJ and Gebhart GF. (1988). Quantitative characterisation and spinal pathway mediating inhibition of spinal nociceptive transmission from the lateral reticular nucleus in the rat. *Journal of Neurophysiology*. **59**: 226-247.

Janss AJ and Gebhart GF. (1987). Spinal monoaminergic receptors mediate the antinociception produced by glutamate in the medullary lateral reticular nucleus. *Journal of Neuroscience*. **7**: 2862-73.

Jeske I, Morrison SF, Cravo SL, Reis DJ. (1993). Identification of baroreceptor reflex interneurons in the caudal ventrolateral medulla. *American Journal of Physiology*. **264**: R169-178.

Jeske I, Reis DJ, Milner TA. (1995). Neurons in the barosensitive area of the caudal ventrolateral medulla project monosynaptically onto sympathoexcitatory bulbospinal neurons in the rostral ventrolateral medulla. *Neuroscience*. **65**: 343-353.

Johansson B. (1962). Circulatory responses to stimulation of somatic afferents. *Acta Physiologica Scandinavica*. **57**: 1-91.

Johnson JM. (1994). Skin, muscle and splanchnic circulations. In: N. Scher, J. Pawelcyzk and J. Ludbrook (Eds) *Blood Loss and Shock*. London: Edward Arnold, pp 133-143.

Kadam PP, Saksena SG, Jagtap SR, Pantavaidya SM. (1993). Hypotensive anesthesia for spine surgery – nitroglycerin vs halothane. *Journal of Postgraduate Medicine*. **39**: 26-28.

Keay KA, Clement CI, Owler BK, Depaulis A, Bandler R. (1994). Convergence of deep somatic and visceral nociceptive information onto a discrete ventrolateral midbrain periaqueductal gray region. *Neuroscience*. **61**(4): 727-732.

Keay KA and Bandler R. (1993). Deep and superficial noxious stimulation increases Fos-like immunoreactivity in different regions of the midbrain periaqueductal gray of the rat. *Neuroscience Letters*. **154**: 23-26.

Keay KA, Crowfoot LJ, Floyd NS, Henderson LA, Christie MJ, Bandler R. (1997). Cardiovascular effects of microinjections of opioid agonists into the 'depressor' region of the ventrolateral periaqueductal gray region. *Brain Research*. **762**: 61-71.

Keay KA, Li QF, Bandler R. (2000). Muscle pain activates a direct projection from ventrolateral periaqueductal gray to rostral ventrolateral medulla in rats. *Neuroscience Letters*. **290**: 157-160.

Keay KA, Clement CI, Matar WM, Heslop DJ, Henderson LA, Bandler R. (2002). Noxious activation of spinal or vagal afferents evokes distinct patterns of fos-like immunoreactivity in the ventrolateral periaqueductal gray of unanaesthetised rats. *Brain Research*. **948**: 122-30.

Kerman IA, Akil H, Watson SJ. (2006). Rostral elements of sympatho-motor circuitry: a virally mediated transsynaptic tracing study. *Journal of Neuroscience*. **26**: 3423-3433.

Kalyuzhny AE, Arvidsson U, Wu W, Wessendorf MW. (1996). Mu-opioid and delta opioid receptors are expressed in brainstem antinociceptive circuits: studies using immunocytochemostry and retrograde tract tracing. *Journal of Neuroscience*. **16**: 6490-6503.

Kalyuzhny AE and Wessendorf MW. (1998). Relationship of mu- and delta-opioid receptors to GABAergic neurons in the central nervous system, including antinociceptive brainstem circuits. *Journal of Comparative Neurology*. **392**: 528-547.

Khachaturian H, Lewis ME, Schafer MK, Watson SJ. (1985). Anatomy of the CNS opioid systems. *Trends in Neuroscience*. **8**: 111-119.

Kiem D, Barna I, Keonig J, Makara G. (1995). Adrenocorticotropin, prolactin and beta-endorphin stimulatory actions of alpha-2 adrenoceptor antagonists. *Neuroendocrinology*. **61**: 152-158.

Knuepfer MM, Akeyson EW, Schramm LP. (1988). Spinal projections of renal afferent nerves in the rat. *Brain Research*. **446**: 17-25.

Kobinger W and Pichler L. (1976). Centrally induced reduction in sympathetic tone – a postsynaptic α-adrenoceptor-stimulating action of imadazolines. *European Journal of Pharmacology*. **40**: 311-320.

Korner PI, Oliver JR, Zhu JL, Gipps J, Hanneman F. (1990). Autonomic, hormonal and local circulatory effects of hemorrhage in conscious rabbits. *American Journal of Physiology*. **258**: H229-239.

Koyama S, Sawana F, Matsuda Y, Saeki Y, Shibamoto T, Hayashi T, Matsubayashi Y, Kawamoto M. (1992). Spatial and temporal differing control of sympathetic activities during haemorrhage. *American Journal of Physiology*. **31**: R579-585.

Krieger JE and Graeff FG. (1985). Defensive behavior and hypertension induced by glutamate in the midbrain central gray of the rat. *Brazilian Journal of Medical and Biological Research*. **18:** 61-67.

Kubo T and Kihara M. (1991). Unilateral blockade of excitatory amino acid receptors in the nucleus tractus solitarii produces an inhibition of baroreflexes in rats. *Naunyn Schmiedebergs Archives of Pharmacology*. **343**: 317-22.

Lang WJ, Lambert GA, Rush ML. (1975). The role of the central nervous system in the cardiovascular response to yohimbine. *Archives Internationales de Pharmacodynamie et de Therapie*. **217**: 57-67.

Langer SZ. (1974). Presynaptic regulation of catecholamine release. *Biochemical Pharmacology*. **23**: 1793-1800.

Lappe RW, Webb RL, Brody MJ. (1985). Selective destruction of renal afferent verses efferent nerves in rats. *American Journal of Physiology*. **249**: R634-637.

Lapiz MD and Morilak DA. (2006). Noradrenergic modulation of cognitive function in rat medial prefrontal cortex as measured by attentional set shifting capability. *Neuroscience*. **137**: 1039-1049.

Larsen PJ and Vrang N. (1995). Neurones projecting to the hypothalamus from the brainstem A1 catecholaminergic cell group express glutamate-R2,3 receptor immunoreactivity. *Brain Research*. **705**: 209-215.

Larson PD, Zhong S, Gebber GL, Barman SM. (2000). Differential pattern of spinal sympathetic outflow in response to stimulation of the caudal medullary raphe. *American Journal of Physiology*. **279**: R210-221.

Lena I, Parrot S, Deschaux O, Muffat-Joly S, Sauvinet V, Renaud B, Suaud-Chagny MF, Gottesmann C. (2005). Variations in extracellular levels of dopamine, noradrenaline, glutamate, and aspartate across the sleep-wake cycle in the medial prefrontal cortex and nucleus accumbens of freely moving rats. *Journal of Neuroscience Research*. **81**: 891-299.

Lewis T. (1942) *Pain*. McMillan, London.

Li YW and Dampney RAL. (1994). Expression of fos-like protein in brain following sustained hypertension and hypotension in conscious rabbits. *Neuroscience*. **61**: 613-634.

Li YW and Dampney RA. (1992). Expression of c-fos protein in the medulla oblongata of conscious rabbits in response to baroreceptor activation. *Neuroscience Letters*. **144**: 70-74.

Lightman SL, Todd K, Everitt BJ. (1984). Ascending noradrenergic projections from the brainstem: evidence for a major role in the regulation of blood pressure and vasopressin secretion. *Experimental Brain Research*. **55**: 145-151.

Lipinska S, Forys S, Lipinska J. (2004). The post-haemorrhage vasopressin release into the blood. *Journal of Physiology and Pharmacology*. **55**: 73-83.

Lipski J, Bellingham MC, West MJ, Pilowsky P. (1988). Limitations of the technique of pressure microinjection of excitatory amino acids for evoking responses from localised regions of the CNS. *Journal of Neuroscience Methods*. **26**: 169-179.

Liu RH and Zhao ZQ. (1992). Selective blockade by yohimbine of descending spinal inhibition from lateral reticular nucleus but not from locus coeruleus in rats. *Neuroscience Letters*. **142**: 65-68.

Lovick TA. (1992). Midbrain influences on ventrolateral medullo-spinal neurons in the rat. *Experimental Brain Research*. **90**: 147-152.

Ludbrook J. (1990). Cardiovascular reflexes from cardiac sensory receptors. *Australian and New Zealand Journal of Medicine*. **20**: 597-606.

Ludbrook J and Graham WF. (1984). The role of cardiac receptor and arterial baroreceptor reflexes in control of the circulation during acute change of blood volume in the conscious rabbit. *Circulation Research*. **54**: 424-435.

Ludbrook J, Potocnik SJ, Woods RL. (1988). Simulation of acute haemorrhage in unanaesthetised rabbits. *Clinical and Experimental Pharmacology and Physiology*. **15**: 575-584.

Ludbrook J and Rutter RC. (1988). Effect of naloxone on haemodynamic responses to acute blood loss in unanaesthetised rabbits. *Journal of Physiology*. **400**: 1-14.

Ludbrook J. (1993). Haemorrhage and Shock. In Hainsworth R., Mark A, (eds.) *Cardiovascular reflex control in health and disease*. Saunders, London, pp. 463-490.

Ludbrook J. (1994). Repeated measurements and multiple comparisons in cardiovascular research. *Cardiovascular Research*. **28**: 303-311.

Ludbrook J and Ventura S. (1994). The decompensatory phase of acute hypovolaemia in rabbits involves a central delta 1-opioid receptor. *European Journal of Pharmacology*. **252**: 113-116.

Ludbrook J, Ventura S. (1996). Roles of carotid baroreceptor and cardiac afferents in hemodynamic response to acute central hypovolemia. *American Journal of Physiology*. **39**: H1538-H1548.

Lumb BM. (2004). Hypothalamic and midbrain circuitry that distinguishes between escapable and inescapable pain. *News in Physiological Sciences*. **19:** 22-26.

MacMillan LB, Hein L, Smith MS, Piascik MT, Limbird LE. (1996). Central hypotensive effects of the α_{2a} adrenergic receptor subtype. *Science*. **273**: 801-803.

Madden CJ. and Sved AF. (2003). Cardiovascular regulation after destruction of the C1 cell group of the rostral ventrolateral medulla. *American Journal of Physiology*. **285**: H2734-H2748.

Madden CJ, Stocker SD, Sved AF. (2006). Attenuation of homeostatic responses to hypotension and glucoprivation after destruction of catecholaminergic rostral ventrolateral medulla (RVLM) neurons. *American Journal of Physiology*. **291:** R751-759.

Mansour A, Khachaturian H, Lewis ME, Akil H, Watson SJ. (1987). Autoradiographic differentiation of mu, delta, and kappa opioid receptors in the rat forebrain and midbrain. *Journal of Neuroscience*. **7**: 2445-2464.

Mansour A, Khachaturian H, Lewis ME, Akil H, Watson SJ. (1988). Anatomy of CNS opioid receptors. *Trends in Neuroscience*. **11**: 308-314.

Mansour A, Fox CA, Burke S, Meng F, Thompson RC, Akil H, Watson SJ. (1994). Mu, delta, and kappa opioid receptor mRNA expression in the rat CNS: an in situ hybridisation study. *Journal of Comparative Neurology*. **350**: 412-438.

Mansour A, Fox CA, Akil H, Watson SJ. (1995). Opioid receptor mRNA expression in the rat CNS: anatomical and functional implications. *Trends in Neuroscience*. **18**: 22-29.

Martin-Schild S, Gerall AA, Kastin AJ, Zadina JE. (1999). Differential distribution of endomorphin 1- and endomorphin 2-like immunoreactivities in the CNS of the rodent. *Journal of Comparative Neurology*. **405**: 450-471.

Martinez V, Wang L, Tache Y. (2006). Proximal colon distension induces Fos expression in the brain and inhibits gastric emptying through capsaicin-sensitive pathways in conscious rats. *Brain Research.* **1086**: 168-180.

McCall RB and Harris LT. (1987). Sympathetic alterations after midline medullary raphe lesions. *American Journal of Physiology.* **253**: R91-100.

McDougall A, Dampney R, Bandler R. (1985). Cardiovascular components of the defense reaction evoked by excitation of neuronal cell bodies in the midbrain periaqueductal gray of the cat. *Neuroscience Letters.* **60**: 69-75.

McKinney MS and Fee JPH. (1998). Cardiovascular effects of 50% nitrous oxide in older adult patients anaesthetised with isoflurane or halothane. *British Journal of Anaesthesia.* **80**: 169-173.

Meller ST and Gebhart GF. (1992). A critical review of the afferent pathways and the potential chemical mediators involved in cardiac pain. *Neuroscience.* **48**: 501-524.

Millan MJ, Bervoets K, Rivet JM, Widdowsin P, Renouard A, Le Marouille-Girardon S, Gobert A. (1994). Multiple *alpha*-2 adrenergic receptor subtypes. II. Evidence for a role of rat $R_{alpha\text{-}2A}$ adrenergic receptors in the control of nociception, motor behavior and hippocampal synthesis of noradrenaline. *Journal of Pharmacology and Experimental Therapeutics.* **270**: 958-972.

Millar RA, Warden JC, Cooperman LH, Price HL. (1969). Central sympathetic discharge and mean arterial pressure during halothane anesthesia. *British Journal of Anaesthesiology.* **41**: 918-928.

Million M, Wang L, Wang Y, Adelson DW, Yuan PQ, Maillot C, Coutinho SV, McRoberts JA, Bayati A, Mattsison H, Wu V, Wei JY, Rivier J, Vale W, Mayer EA, Tache Y. (2006). CRF2 receptor activation prevents colorectal distension induced visceral pain and spinal ERK1/2 phosphorylation in rats. *Gut.* **55**: 172-181.

Milner TA, Morisson SF, Abate C, Reis DJ. (1988). Phenylethanolamine N-methyltransferase containing terminals synapse directly on sympathetic preganglionic neurons in the rat. *Brain Research.* **448**: 205-222.

Minson JB, Llewellyn-Smith IJ, Chalmers JP, Pilowsky PM, Arnolda LF. (1997). c-Fos identifies GABA-synthesising barosensitive neurons in the caudal ventrolateral medulla. *Neuroreport.* **8**: 3015-21.

Morgan MM and Clayton CC. (2005). Defensive behaviours evoked from the ventrolateral periaqueductal gray of the rat: Comparison of opioid and GABA disinhibition. *Behavioural Brain Research.* **164:** 61-66.

Morita H and Vatner SF. (1985). Effects of hemorrhage on renal nerve activity in conscious dogs. *Circulation Research*. **57**: 788-793.

Morita H, Nishida Y, Motochigawa H, Uemura N, Hosomi H, Vatner SF. (1988). Opiate-receptor mediated decrease in renal nerve activity during hypotensive hemorrhage in conscious rabbits. *Circulation Research*. **63**: 165-172.

Morrison SF and Gebber GL. (1982). Classification of raphe neurons with cardiac-related activity. *American Journal of Physiology*. **243**: R49-59.

Morrison SF, Callaway J, Milner TA, Reis DJ. (1991). Rostral ventrolateral medulla: a source of the glutamatergic innervation of the sympathetic intermediolateral nucleus. *Brain Research*. **562**: 126-135.

Morrison SF. (1993). Raphe pallidus excites a unique class of sympathetic preganglionic neurons. *American Journal of Physiology*. **265**: R82-89.

Morton CR, Johnson SM, Duggan AW. (1983). Lateral reticular regions and the descending control of dorsal horn neurons of the cat: selective inhibition by electrical stimulation. *Brain Research*. **275**: 13-21.

Mouton LJ and Holstege G. (1994). The periaqueductal gray in the cat projects to lamina VIII and the medial part of lamina VII throughout the length of the spinal cord. *Experimental Brain Research*. **101**: 253-64.

Mouton LJ, Klop EM, Holstege G. (2001). Lamina I periaqueductal gray (PAG) projections represent only a limited part of the total spinal and caudal medullary input to the PAG in the cat. *Brain Research Bulletin*. **54**: 167-174.

Mudge GH Jr, Grossman W, Mills RM Jr, Lesch M, Braunwald E. (1976). Reflex increase in coronary vascular resistance in patients with ischemic heart disease. *New England Journal of Medicine*. **295**: 1333-1337.

Murphy AZ, Ennis M, Rizvi TA, Behbehani MM, Shipley MT. (1995). Fos expression induced by changes in arterial pressure is localised in distinct, longitudinally organised columns of neurons in the rat midbrain periaqueductal gray. *Journal of Comparative Neurology*. **360**: 286-300.

Nakamura K, Matsumura K, Hubschle T, Nakamura Y, Hioki H, Fujiyama F, Boldogkoi Z, Konig M, Thiel HJ, Gerstberger R, Kobayashi S, Kaneko T. (2004). Identification of sympathetic premotor neurons in medullary raphe regions mediating fever and other thermoregulatory functions. *Journal of Neuroscience*. **24**: 5370-80.

Neutze J, Wyler F, Rudolph AM. (1968). Changes in distribution of cardiac output after hemorrhage in rabbits. *American Journal of Physiology*. **215**: 857-864.

Nishi K and Takenaka F. (1973). Chemosensitive afferent fibres in the cardiac sympathetic nerve of the cat. *Brain Research.* **55**: 214-218.

Ngai SH, Neff NH, Costa E. (1969). The effects of cyclopropane and halothane on the biosynthesis of norepinephrine *in vivo*. *Anesthesiology.* **42**: 143-152.

Novikova L, Novikov L, Kellerth JO. (1997). Persistent neuronal labelling by retrograde fluorescent tracers: a comparison between Fast Blue, Fluoro-Gold and various dextran conjugates. *Journal of Neuroscience Methods.* **74**: 9-15.

Oberg B and Thoren P. (1972a). Studies on left ventricular receptors, signalling in non-medullated vagal afferents. *Acta Physiologica Scandinavica.* **85**: 145-163.

Oberg B and Thoren P. (1972b). Increased activity in left ventricular receptors during hemorrhage or occlusion of caval veins in the cat. A possible cause of the vaso-vagal reaction. *Acta Physiologica Scandinavica.* **85**: 164-173.

Oberg B and Thoren P. (1973). Circulatory responses to stimulation of left ventricular receptors in the cat. *Acta Physiologica Scandinavica.* **88**: 8-22.

Odeh F and Antal M. (2001). The projections of the midbrain periaqueductal gray to the pons and medulla oblongata in rats. *European Journal of Neuroscience.* **14**: 1275-1286.

Odeh F, Antal M, Zagon A. (2003). Heterogeneous synaptic inputs from the ventrolateral periaqueductal gray matter to neurons responding to somatosensory stimuli in the rostral ventromedial medulla of rats. *Brain Research.* **959**: 287-294.

Ong BY, Yarnell R, Tweed WA, Sitar DS. (1984). Foetal responses to acute haemorrhage under halothane anaesthesia. *Canadian Anaesthesia Society Journal.* **31**: 123-129.

O' Conner PJ, Hanson J, Finucane BT. (2006). Induced hypotension with epidural/general anesthesia reduces transfusion in radical prostate surgery. *Canadian Journal of Anaesthesiology.* **53**: 873-880.

Oshima N, McMullan S, Goodchild AK, Pilowsky PM. (2006). A monosynaptic connection between baroinhibited neurons in the RVLM and IML in Sprague-Dawley rats. *Brain Research.* **1089**: 153-161.

Pagel PS, Kampine JP, Schmeling WT, Warltier DC. (1991). Comparison of the systemic and coronary hemodynamic actions of desflurane, isoflurane, halothane, and enflurane in the chronically instrumented dog. *Anesthesiology.* **74**: 539-551.

Palmisano BW, Mehner RW, Stowe DF, Bosnjak ZJ, Kampine JP. (1994). Direct myocardial effects of halothane and isoflurane-comparison between adult and infant rabbits. *Anesthesiology.* **81**: 718-729.

Pan HL and Shen SR. (2004). Sensing tissue ischemia: Another new function for capsaicin receptors? *Circulation*. **110**: 1826-1831.

Pao CS and Benovic JL. (2005). Structure/function analysis of alpha2A-adrenergic receptor interaction with G protein-coupled receptor kinase 2. *Journal of Biological Chemistry*. **280**: 11052-11058.

Patel S, Fernandez-Garcia E, Hutson P, Patel S. (2001). An in vivo binding assay to determine central α_1-adrenoceptor occupancy using [^{3}H] prazosin. *Brain Research Protocols*. **8**: 191-198.

Paterson SJ, Robson LE, Kosterlitz HW. (1983). Classification of opioid receptors. *British Medical Bulletin*. **39**: 31-36.

Peltonen JM, Nyronen T, Wurster S, Pihlavisto M, Hoffren AM, Marjamaki A, Xhaard H, Kanerva L, Savola JM, Johnson MS, Scheinin M. (2003). Molecular mechanisms of ligand-receptor interactions in transmembrane domain V of the alpha2A-adrenoceptor. *British Journal of Pharmacology*. **140**: 347-358.

Peng YJ, Wang N, Gong QL, Li P. (2002). Caudal ventrolateral medulla mediates the depressor response elicited by the greater splanchnic nerve afferent stimulation in rats. *Neuroscience Letters*. **325**: 134-138.

Persson B. and Svennson TH. (1981). Control of behaviour and brain noradrenaline neurons by peripheral blood volume receptors. *Journal of Neural Transmission*. **52**: 73-82.

Pinto M, Lima D, Castro-Lopes J, Tavares I. (2003). Noxious-evoked c-fos expression in brainstem neurons immunoreactive for GABAB, mu-opioid and NK-1 receptors. *European Journal of Neuroscience*. **17**: 1393-1402.

Polson JW, Mrljak S, Potts PD, Dampney RA. (2002). Fos expression in spinally projecting neurons after hypotension in the conscious rabbit. *Autonomic Neuroscience*. **100**: 10-20.

Potas JR, Keay KA, Bandler R. (2003). Spinal afferents to the vasodepressor region of the caudal midline medulla in rat. *European Journal of Neuroscience*. **17**: 1135-1149.

Potts PD, Polson JW, Hirooka Y, Dampney RA. (1997). Effects of sinoaortic denervation on Fos expression in the brain evoked by hypertension and hypotension in conscious rabbits. *Neuroscience*. **77**: 503-520.

Potts PD, Ludbrook J, Gillman-Gaspari TA, Horiuchi J, Dampney RAL. (2000). Activation of brain neurons following central hypervolemia and hypovolemia: contribution of baroreceptor and non baroreceptor inputs. *Neuroscience*. **95**: 499-511.

Recordati GM, Moss NG, Genovesi S, Rogenes P. (1981). Renal Chemoreceptors. *Journal of the Autonomic Nervous System*. **3**: 237-251.

Redfern WS and Williams A. (1995). A re-evaluation of the role of α_2-adrenoceptors in the anxiogenic effects of yohimbine, using the selective antagonist delequamine in the rat. *British Journal of Pharmacology*. **116**: 2081-2089.

Renaud LP. (1996). CNS pathways mediating cardiovascular regulation of vasopressin. *Clinical and Experimental Pharmacology and Physiology*. **23**: 157-160.

Rentero N, Bruandet N, Quintin L. (1997). Absence of evidence for a powerful tonic baroreflex-mediated inhibition on catechol activity in the rat rostral ventrolateral medulla: in vivo voltametric evidence during sino-aortic deafferentation. *Pflugers Archives*. **434**: 599-608.

Richmond FJR, Gladdy R, Creasy JL, Kitamura S, Smits E, Thomson DB. (1994). Efficacy of seven retrograde tracers, compared in multiple –labelling studies of feline motoneurons. *Journal of Neuroscience Methods*. **53**: 35-46.

Rios C, Gomes I, Devi LA. (2004). Interactions between delta opioid receptors and alpha-adrenoceptors. *Clinical and Experimental Pharmacology and Physiology*. **31**: 833-836.

Rodella L, Rezzani R, Gioia M, Tredici G, Bianchi R. (1998). Expression of Fos immunoreactivity in the rat supraspinal regions following noxious visceral stimulation. *Brain Research Bulletin*. **47**: 357-66.

Roozendaal B, Okuda S, Van der Zee EA, McGaugh JL. (2006). Glucocorticoid enhancement of memory requires arousal-induced noradrenergic activation in the basolateral amygdala. *Proceedings of the National Academy of Science USA*. **103**: 6741-6746

Rosin DL, Zeng D, Stornetta RL, Norton FR, Riley T, Okusa MD, Guyenet PG, Lynch KR. (1993). Immunohistochemical localisation of α_{2A}-Adrenergic receptors in catecholaminergic and other brainstem neurons in the rat. *Neuroscience*. **56**: 139-155.

Ross CA, Ruggiero DA, Park DH, Joh TH, Sved AF, Fernandez-Pardal J, Saavedra JM, Reis DJ. (1984). Tonic vasomotor control by the rostral ventrolateral medulla: effect of electrical or chemical stimulation of the area containing C1 adrenaline neurons on arterial pressure, heart rate, and plasma catecholamines and vasopressin. *Journal of Neuroscience*. **4**: 474-494.

Rouzade-Dominguez ML, Miselis R, Valentino RJ. (2003). Central representation of bladder and colon revealed by dual transsynaptic tracing in the rat: substrates for pelvic visceral coordination. *European Journal of Neuroscience*. **18**: 3311-3324.

Ruffolo RR, Nichols AJ, Stadel JM, Hieble JP. (1993). Pharmacologic and therapeutic applications of α_2 adrenoceptor subtypes. *Annual Reviews of Pharmacology and Toxicology*. **33**: 243-279.

Ruggeri P, Ermirio R, Molinari C, Calaresu FR. (1995). Role of ventrolateral medulla in reflex cardiovascular responses to activation of skin and muscle nerves. *American Journal of Physiology*. **268**: R1464-1471.

Ruggiero DA, Tong S, Anwar M, Gootman N, Gootman PM. (1996). Hypotension-induced expression of the *c-fos* gene in the medulla oblongata of piglets. *Brain Research*. **706**: 199-209.

Ruta TS and Mutch WA. (1989). Regional cerebral blood flow following hemorrhage during isoflurane anesthesia in the rabbit: comparison of techniques to support blood pressure. *Anesthesiology*. **70**: 978-983.

Rutter PC, Potocnik SJ, Ludbrook J. (1986). Factors influencing the effects of intravenous naloxone on arterial pressure and heart rate after haemorrhage in conscious rabbits. *Clinical and Experimental Pharmacology and Physiology*. **13**: 383-397.

Rutter PC, Potocnik SJ, Ludbrook J. (1987). Sympathoadrenal mechanisms in cardiovascular responses to naloxone after hemorrhage. *American Journal of Physiology*. **252**: H40-46.

Sabbatini M, Molinaro C, Grossini E, Mary DASG, Vacca G, Cannas M. (2004). The pattern of c-Fos immunoreactivity in the hindbrain of the rat following stomach distention. *Experimental Brain Research*. **157**: 315-323.

Sagen J and Proudfit HK. (1981). Hypoalgesia induced by blockade of noradrenergic projections to the raphe magnus: reversal by blockade of noradrenergic projections to the spinal cord. *Brain Research*. **223**: 391-396.

Samar RE and Coleman TG. (1979). Whole-body response of the peripheral circulation following hemorrhage in the rat. *American Journal of Physiology*. **236**: H206-210.

Sandor P, de Jong W, Wiegant V, de Wied D. (1987). Central opioid mechanisms and cardiovascular control in hemorrhagic hypotension. *American Journal of Physiology*. **253**: H507-511.

Sawchenko PE and Swanson LW. (1982). The organization of noradrenergic pathways from the brainstem to the paraventricular and supraoptic nuclei in the rat. *Brain Research Reviews*. **4**: 275-325.

Sawchenko PE, Swanson LW, Grzanna R, Howe PRC, Bloom SR, Polak JM. (1985). Colocalization of neuropeptide-Y immunoreactivity in brainstem catecholaminergic neurons that project to the paraventricular nucleus of the hypothalamus. *Journal of Comparative Neurology*. **241**: 138-153.

Schadt JC, Shafford HL, McKown MD. (2006). Neuronal activity within the ventrolateral periaqueductal gray during simulated hemorrhage in conscious rabbits. *American Journal of Physiology*. **290:** R715-725.

Schadt J, McKown MD, McKown DP, Franklin D. (1984). Hemodynamic effects of hemorrhage and subsequent naloxone treatment in conscious rabbits. *American Journal of Physiology*. **247**: R497-508.

Schadt J and Gaddis RR. (1985). Endogenous opiate peptides may limit norepinephrine release during hemorrhage. *Journal of Pharmacology and Experimental Therapeutics*. **232**: 656-660.

Schadt J. and Ludbrook J. (1991). Hemodynamic and neurohumoral responses to acute hypovolemia in conscious mammals. *American Journal of Physiology*. **260**: H305-H318.

Schadt JC and York DH. (1981). The reversal of hemorrhagic hypotension by naloxone in conscious rabbits. *Canadian Journal of Physiology and Pharmacology*. **59**: 1208-1213.

Schreff M, Schultz S, Wiborny D, Hollt V. (1998). Immunofluorescent identification of endomorphin 2-containing nerve fibres and terminals in the rat brain and spinal cord. *Neuroreport*. **9**: 1031-1034.

Schreihofer AM, and Guyenet PG. (1997). Identification of C1 presympathetic neurons in rat rostral ventrolateral medulla by juxtacellular labelling in vivo. *Journal of Comparative Neurology*. **387**: 524-36.

Schreihofer AM, and Guyenet PG. (2003). Baro-activated neurons with pulse modulated activity in the rat caudal ventrolateral medulla express GAD67 mRNA. *Journal of Neurophysiology*. **89**: 1265-1277.

Schreihofer AM, Stornetta RL and Guyenet PG. (2000). Regulation of sympathetic tone and arterial pressure by rostral ventrolateral medulla after depletion of C1 cells in rat. *Journal of Physiology*. **529**: 221-236.

Seyde WC and Longnecker DR. (1984). Anesthetic influences on regional hemodynamics in normal and haemorrhaged rats. *Anesthesiology*. **61**: 686-698.

Shen YT, Knight DR, Thomas JX, Vatner SF. (1990). Relative roles of cardiac receptors and arterial baroreceptors during haemorrhage in conscious dogs. *Circulation Research*. **66**: 397-405.

Shioda S, Shimoda Y, Nakai Y. (1992). Ultrastructural studies of medullary synaptic inputs to vasopressin-immunoreactive neurons in the supraoptic nucleus of the rat hypothalamus. *Neuroscience Letters*. **148**: 155-158.

Shioda S, Iwase M, Homma I, Nakajo S, Nakaya K, Nakai Y. (1998). Vasopressin neuron activation and Fos expression by stimulation of the caudal ventrolateral medulla. *Brain Research Bulletin*. **45**: 443-450.

Simerly RB and Swanson LW. (1986). The organization of neuronal inputs to the medial preoptic nucleus of the rat, *Journal of Comparative Neurology*. **246**: 312-342.

Simon JK, Kasting NW, Ciriello J. (1989). Afferent renal nerve effects on plasma vasopressin and oxytocin in conscious rats. *American Journal of Physiology*. **256**: R1240-1244.

Singh RB. (1991). Nonpharmacologic measures for lowering blood pressure. *Cardiovascular Drugs Therapeutics*. **5**: 157-158.

Skarphedinsson JO, Stage L, Thoren P. (1986). Cerebral function during hypotensive haemorrhage in spontaneously hypertensive rats and wistar Kyoto rats. *Acta Physiologica Scandinavica*. **128**: 445-452.

Skofitsch G and Lembeck F. (1980). Visceral Pain mediated by capsaicin sensitive neurons. *Naunyn-Schmiedebergs Archive of Pharmacology*. **313**: R2.

Skovsted P, Price ML, Price HL. (1969). The effects of halothane on arterial pressure, preganglinic sympathetic activity and barostatic reflexes. *Anesthesiology*. **31**: 507-514.

Skovsted P and Price HL. (1972). Sympathetic nervous system depression by halothane during prolonged exposure. *Acta Anaesthesiologica Scandinavica*. **16**: 65-68.

Skoog P, Mansson J and Thoren P. (1985). Changes in renal sympathetic outflow during hypotensive haemorrhage in rats. *Acta Physiological Scandinavica*. **125**: 655-660.

Smith A, Brice C, Nash J, Rich N, Ntt DJ. (2003). Caffein and central noradrenaline: effects on mood, cognitive performance, eye movements and cardiovascular function. *Journal of Psychopharmacology*. **17**: 283-292.

Smith DW, Sibbald JR, Khanna S, Day TA. (1995). Rat vasopressin cell responses to simulated hemorrhage: stimulus-dependant role for A1 noradrenergic neurons. *American Journal of Physiology*. **268**: R1336-1342.

Snowball RK, Dampney RAL, Lumb BM. (1997). Responses of neurons in the medullary raphe nuclei to inpts from visceral nociceptors and the ventrolateral periaqueductal gray in the rat. *Experimental Physiology*. **82**: 485-500.

Soghomonian JJ and Martin DL. (1998). Two isoforms of glutamate decarboxylase: why? *Trends in Pharmacological Science*. **19**: 500-505.

Spike RC, Puskar Z, aqndrew D, Todd AJ. (2003). A quantitative and morphological study of projection neurons in lamina I of the rat lumbar spinal cord. *European Journal of Neuroscience*. **18**: 2433-2448.

Spyer KM. (1994). Central nervous mechanisms contributing to cardiovascular control. *Journal of Physiology (London)*. **474**: 1-19.

Srinivasan J and Schmidt WJ. (2004). Treatment with alpha2-adrenoceptor antagonist, 2-methoxy idazoxan, protects 6-hydroxydopamine-induced Parkinsonian symptoms in rats: neurochemical and behavioural evidence. *Behavioural Brain Research*. **154**: 353-363.

Starke K, Borowski E, Endo T. (1975). Preferential blockade of presynaptic α-adrenoceptors by yohimbine. *European Journal of Pharmacology*. **34**: 385-388.

Staszewska-Woolley J, Luk DE, Nolan PN. (1986). Cardiovascular reflexes mediated by capsaicin sensitive afferent neurons in the dog. *Cardiovascular Research*. **20**: 897-906.

Staszewska-Woolley J, Wooley G, Regoli D. (1988). Specific receptors for bradykinin-induced cardiac sympathetic chemoreflex in the dog. *European Journal of Pharmacology*. **156**: 309-314.

Stella A and Zanchetti A. (1991). Functional role of renal afferents. *Proceedings of the American Physiological Society*. **71**: 659-682.

Stone EA, Lin Y, Ahsan R, Quartermain D. (2004). Role of locus coeruleus α1-adrenceptors in motor activity in rats. *Synapse*. **54**: 164-172.

Stone LS, MacMillan LB, Kitto KF, Limbird LE, Wilcox GL. (1997). The α_{2a} adrenergic receptor subtype mediates spinal analgesia evoked by α_2 agonists and is necessary for spinal adrenergic-opioid synergy. *Journal of Neuroscience*. **17**: 7157-7165.

Szafarczyk A, Gaillet S, Barbanel G, Malaval F, Assenmacher I. (1990). Implication des recepteurs α_2 adrenergiques post-synaptiques dans la stimulation catecholaminergique centrale de l'axe corticotrope chez le Rat. *Comptes rendus des séances de l'Académie des sciences. Série III, Sciences de la vie*. **160**: 81-88.

Taiwo YO and Levine JD. (1988). Prostaglandins inhibit endogenous pain control mechanisms by blocking transmission at spinal noradrenergic synapses. *Journal of Neuroscience*. **8**: 1346-1349.

Talley EM, Rosin DL, Lee A, Guyenet PG, Lynch KR. (1996). Distribution of α_{2A} adrenergic receptor-like immunoreactivity in the rat central nervous system. *Journal of Comparative Neurology*. **372**: 111-134.

Tassorelli C, Greco R, Cappalletti D, Sandrini G, Nappi G. (2005). Comparative analysis of the neuronal activation and cardiovascular effects of nitroglycerin, sodium nitroprusside and L-arginine. *Brain Research.* **1051**: 17-24.

Tavares I, Almeida A, Albino-Teixeria A, Lima D. (1997). Lesions of the caudal ventrolateral medulla block the hypertension-induced inhibition of noxious-evoked c-fos expression in the rat spinal cord. *European Journal of Pain.* **1**: 149-160.

Thoren A, Ricksten SE, Lundin S, Gazelius B, Elam M. (1998). Baroreceptor-mediated reduction of jejunal mucosal perfusion, evaluated with endoluminal laser doppler flowmetry in conscious humans. *Journal of the Autonomic Nervous System.* **65**: 157-163.

Trendelenburg AU, Limberger N, Starke K. (1993). Presynaptic α_2-autoreceptors in brain cortex: α_{2D} in the rat and α_{2A} in the rabbit. *Naunyn-Schmiedebergs Archives of Pharmacology.* **348**: 35-45.

Trendelenburg AU, Philipp M, Meyer A, Klebroff, Hein L, Starke K. (2003). All three α2-adrenoceptor types serve as autoreceptors in postganglionic sympathetic neurons. *Naunyn-Schmiedebergs Archives of Pharmacology.* **368**: 504-512.

Troy BP, Heslop DJ, Bandler R, Keay KA (2003). Haemodynamic response to haemorrhage: distinct contributions of midbrain and forebrain structures. *Autonomic neuroscience: Basic and Clinical.* **108**: 1-11.

Troy BP, Hopkins DA, Bandler R, Keay KA. (2007). The haemodynamic response to blood loss in the conscious rat: contributions of cardiac spinal versus cardiac vagal afferent signals. *In Press.*

Tzavara ET, Bymaster FP, Overshiner CD, Davis RJ, Perry KW, Wolff M, McKinzie DL, Witkin JM, Nomikos GG. (2006). Procholinergic and memory enhancing properties of the selective norepinephrine uptake inhibitor atomoxetine. *Molecular Psychiatry.* **11**: 187-195.

Ueda H, Uchida Y, Kamisaka K. (1967). Mechanism of reflex depressor effect by kidney in dog. *Japanese Heart Journal.* **8**: 597-606.

Van Bockstaele EJ, Aston-Jones G, Pieribone VA, Ennis M, Shipley MT. (1991). Subregions of the periaqueductal gray topographically innervate the rostral ventrolateral medulla in the rat. *Journal of Comparative Neurology.* **309**: 305-327.

Van Leeuwen AF, Evans RG, Ludbrook J. (1990). Effects of halothane, ketamine, propofol and alfentanil anaesthesia on circulatory control in rabbits. *Clinical and Experimental Pharmacology and Physiology.* **17**: 781-798.

Vatner SF. (1974). Effects of hemorrhage on regional blood flow distribution in dogs and primates. *Journal of Clinical Investigation.* **54**: 225-235.

Vatner SF and Smith NT. (1974). Effects of halothane on left ventricular function and distribution of regional blood flow in dogs and primates. *Circulation Research.* **34**: 155-167.

Vatner S. (1978). Effects of anesthesia on cardiovascular control mechanisms. *Environmental Health Perspective.* **26**: 193-206.

Velley L, Milner TA, Chan J, Morrison SF, Pickel VM. (1991). Relationship of Met-enkephalin-like immunoreactivity to vagal afferents and motor dendrites in the nucleus of the solitary tract: A light and electron microscopic dual labelling study. *Brain Research.* **550**: 298-312.

Venugopalan VV, Ghali Z, Senecal J, Reader TA, Descarriers L. (2006). Catecholaminergic activation of G-protein coupling in rat spinal cord: Further evidence for the existence of dopamine and noradrenaline receptors in spinal grey and white matter. *Brain Research.* **1070**: 90-100.

Verberne AJ, Beart PM, Louis WJ. (1989). Excitatory amino acid receptors in the caudal ventrolateral medulla mediate a vagal cardiopulmonary reflex in the rat. *Experimental Brain Research.* **78**: 185-192.

Verberne AJM and Guyenet PG. (1992). Midbrain central gray: influence on medullary sympathoexcitatory neurons and the baroreflex in rats. *American Journal of Physiology.* **32**: R24-R33.

Verberne AJM, Sartor DM, Berke A. (1999). Midline medullary depressor responses are mediated by inhibition of RVLM sympathoexcitatory neurons in rats. *American Journal of Physiology.* **276**: R1054-R1062.

Versteeg DHG, Csikos T, Spierenburg H. (1991). Stimulus-evoked release of tritiated monoamines from rat periaqueductal gray slices in vitro and its receptor-mediated modulation. *Naunyn-Schmiedebergs Archives of Pharmacology.* **343**: 595-602.

Veyrac A, Didier A, Colpaert F, Jourdan F, Marien M. (2005). Activation of noradrenergic transmission by alpha2-adrenoceptor antagonists counteracts deafferentation-induced neuronal death and cell proliferation in the adult mouse olfactory bulb. *Experimental Neurology.* **194**: 444-456.

Viana DML and Brandao ML. (2003). Anatomical connections of the periaqueductal gray: specific neural substrates for different kinds of fear. *Brazilian Journal of Medical and Biological Research.* **36**: 557-566.

Victor RG, Thoren P, Morgan DA, Mark AL. (1989). Differential control of adrenal and renal sympetic nerve activity during haemorrhage hypotension in rats. *Circulation Research.* **64**: 686-694.

Vidal MA, Calderon E, Martinez E, Pernia A, Torres LM. (2006). Comparison of 2 techniques for inhaled anesthetic induction with sevoflurane in coronary artery revascularisation. *Rev. Esp. Anestesiol. Reanim.* **53**: 639-642.

Vissing SF. (1997). Differential activation of sympathetic discharge to skin and skeletal muscle in humans. *Acta Physiologica Scandinavica.* **639**: 1-32.

Wang Q and Limbird LE. (2002). Regulated interactions of the alpha 2A adrenergic receptor with spinophilin, 14-3-3ζ, and arrestin 3. *Journal of Biological Chemistry.* **277**: 50589-50596.

Wang WH and Lovick TA. (1992). Excitatory 5-HT_2 mediated effects on rostral ventrolateral medullary neurons in rats. *Neuroscience Letters.* **141**: 89-92.

Wang WH and Lovick TA. (1992). Inhibitory action of 5-hydroxytryptamine on rostral ventrolateral medullary neurons in anaesthetised rats. *Journal of Physiology.* **446**: 259P.

Wang WH and Lovick TA. (1993). The inhibitory effect of the ventrolateral periaqueductal gray matter on neurons in the rostral ventrolateral medulla involves a relay in the medullary nuclei. *Experimental Brain Research.* **94**: 295-300.

Wang CL, Yu Y, Lai LH, Cui Y, Wang X, Wang R. (2007). Cardiovascular responses to intrathecal administration of endomorphins in anesthetised rats. *Peptides.* **28**: 871-877

Warren DJ and Ledingham JG. (1978). Renal vascular response to haemorrhage in the rabbit after pentobarbitone, chlorolose-urethane and ether anaesthesia. *Clinical Science and Molecular Medicine.* **54**: 489-491.

Webb RL and Brody MJ. (1987). Functional identification of the central projections of afferent renal nerves. *Clinical and Experimental Hypertension- Part A Theory and Practice.* **9**: 47-57.

Wenthold RJ, Altschuler RA, Hampson DR. (1990). Immunocytochemistry of neurotransmitter receptors. *Journal of Electron Microscopy Techniques.* **15**: 81-96.

Westlund KN and Craig AD. (1996). Association of spinal lamina I projections with brainstem catecholaminergic neurons in the monkey. *Experimental Brain Research.* **110**: 151-162.

Yamaguchi N. (1982). Evidence supporting the existence of presynaptic alpha-adrenoceptors in the regulation of endogenous noradrenaline release upon hepatic sympathetic nerve stimulation in the dog liver in vivo. *Naunyn Schmiedebergs Archives of Pharmacology.* **321**: 177-184.

Yamamura T, Kimura T, Furukawa K. (1983). Effects of halothane, thiamylal, and ketamine on central sympathetic and vagal tone. *Anesthesia and Analgesia.* **62**: 129-134.

Yamashita Y, Nagamachi K, Morita H, Nishida Y, Tanaka S, Maeta H, Hosomi H (1996). Intravenously-injected naloxone reverses the decrease in renal sympathetic nerve activity seen during hypotensive haemorrhage in conscious rabbits by acting through central mechanisms. *Journal of the Autonomic Nervous System*. **57**: 57-62.

Yamazato M, Sakima A, Nakazato J, Sesoko S, Muratani H, Fukiyama K. (2001). Hypotensive and sedative effects of clonidine injected into the rostral ventrolateral medulla of conscious rats. *American Journal of Physiology*. **281**: R1868-1876.

Yates JM and Fentem PH. (1975). The effects of lower body negative pressure on the cardiovascular system of the anaesthetised rabbit. *Cardiovascular Research*. **9**: 190-200.

Yu D and Gordon FJ. (1996). Anatomical evidence for a bi-neuronal pathway connecting the nucleus tractus solitarius to caudal ventrolateral medulla to rostral ventrolateral medulla in the rat. *Neuroscience Letters*. **205**: 21-24.

Zhang YM, Li P, Lovick TA. (1994). Role of the nucleus raphe obscurus in the inhibition of rostral ventrolateral medullary neurons induced by stimulation in the ventrolateral periaqueductal gray matter of the rabbit. *Neuroscience Letters*. **176**: 231-234.

-Appendix-

Neuroscience 152 (2008) 1099–1109

HYPOVOLEMIC SHOCK: CRITICAL INVOLVEMENT OF A PROJECTION FROM THE VENTROLATERAL PERIAQUEDUCTAL GRAY TO THE CAUDAL MIDLINE MEDULLA

D. J. VAGG, R. BANDLER AND K. A. KEAY*

School of Medical Sciences (Anatomy and Histology), Anderson Stuart Building, The University of Sydney, NSW, Australia 2006

Abstract—Previous research has suggested that the ventrolateral column of the periaqueductal gray (vlPAG) plays a crucial role in triggering a decompensatory response (sympathoinhibition, hypotension, bradycardia) to severe blood loss. vlPAG excitation triggers also quiescence, decreased vigilance and decreased reactivity, the behavioral response which usually accompanies hypovolemic shock. The aim of this study was to identify, in unanesthetized rats, the main descending pathway(s) via which vlPAG neurons trigger sympathoinhibition and bradycardia in response to severe blood loss. Firstly, immediate early gene (c-Fos) expression was used to identify vlPAG neurons selectively activated by severe blood loss. Subsequently, the specific medullary projections of these vlPAG neurons were defined by combined c-Fos, retrograde tracing (double-label) experiments. It was found that vlPAG neurons selectively activated by severe hemorrhage project overwhelmingly to the vasodepressor portion of the caudal midline medulla (CMM). Previous studies indicate that this CMM region mediates behaviorally-coupled cardiovascular adjustments and the findings described here fit with the idea that CMM neurons are uniquely recruited by salient challenges, the adaptive responses to which require more than reflexive homeostatic cardiovascular adjustments. © 2008 Published by Elsevier Ltd on behalf of IBRO.

Key words: shock, hypotension, heart rate, medulla, periaqueductal gray, hypovolemia.

In conscious mammals (including humans) progressive blood loss triggers a biphasic hemodynamic response. Initially, during moderate blood loss (up to15% total blood volume, tbv), arterial pressure (AP) is maintained within a normal range by a selective increase in sympathetic vasomotor tone in specific vascular beds (skeletal muscles, most viscera). The net effect of this *compensatory response* is to maintain, in the face of falling cardiac output, adequate vascular perfusion of critical structures (brain, heart) (Schadt and Ludbrook, 1991; Ludbrook, 1993). In behaving animals compensation is associated usually with increased vigilance and alertness (Persson and Svensson, 1981). Compensation is triggered by baroreceptor unloading, i.e. it is blocked by barodenervation (Evans and Ludbrook, 1991; Evans et al., 1994a).

If blood loss progresses and becomes severe (e.g. 15–30% tbv) a second or *decompensatory phase* (i.e. *shock*), is triggered. This phase is characterized by a large and sustained fall in AP mediated by a rapid-onset sympatho-inhibition and often a vagally-mediated bradycardia (Schadt and Ludbrook, 1991; Ludbrook, 1993). In behaving animals decompensation is associated with quiescence, decreased vigilance and decreased reactivity (Persson and Svensson, 1981).

Decompensation is thought to be triggered, at least in part, by cardiac mechanoreceptors and/or cardiac nociceptors detecting inadequate ventricular filling and/or myocardial perfusion (Oberg and Thoren, 1970, 1972, 1973; Skoog et al., 1985; Thoren et al., 1988; Victor et al., 1989; Togashi et al., 1990; Evans et al., 1994b). Although life-threatening if prolonged, the potential short-term benefits of a shift from compensation (normotension, tachycardia) to decompensation (hypotension, bradycardia) include: i) an increased likelihood of clotting leading to reduced blood loss; ii) better ventricular filling and a longer diastole leading to improved myocardial perfusion; and iii) reduced coronary afterload reducing myocardial metabolic demand (Troy et al., submitted for publication).

Although it is well established that the baroreceptor circuitry contained within the lower brainstem (pons, medulla) is sufficient to mediate compensation (Schadt and Ludbrook, 1991), the neural structures mediating decompensation have yet to be identified. Recent experiments suggest that decompensation requires the integrity of the midbrain. That is, severe hemorrhage triggers decompensation in pre-collicular decerebrate rats (midbrain and lower brainstem intact), but not in rats decerebrated at the pre-trigeminal level (midbrain absent) (Evans et al., 1991; Troy et al., 2003). Additional data indicate that the critical midbrain region mediating decompensation is the ventrolateral column of the periaqueductal gray region (vlPAG). Specifically: (i) stimulation of the vlPAG with excitatory amino acids evokes cardiovascular (hypotension, bradycardia) and behavioral (quiescence, decreased vigilance and decreased reactivity) responses identical to those characteristic of decompensation (Zhang et al., 1990; Lovick, 1992a; Depaulis et al., 1994; Keay et al., 1997a); (ii) severe hemorrhage preferentially evokes immediate early gene (c-Fos) expression within the vlPAG column (Keay

*Corresponding author. Tel: +61-2-9351-4132; fax: +61-2-9351-6556.
E-mail address: keay@anatomy.usyd.edu.au (K. A. Keay).

Abbreviations: AP, arterial pressure; CMM, caudal midline medulla; CVLM, caudal ventrolateral medulla; DAB, 3,3-diaminobenzidine tetrahydrochloride; dlPAG, dorsolateral periaqueductal gray; FB, Fast Blue; FG, Fluorogold; IR, immunoreactive/immunoreactivity; lPAG, lateral periaqueductal gray; PAG, periaqueductal gray; PBS, phosphate-buffered saline; RVLM, rostral ventrolateral medulla; SNP, sodium nitroprusside; tbv, total blood volume; VLM, ventrolateral medulla; vlPAG, ventrolateral periaqueductal gray.

0306-4522/08$32.00+0.00 © 2008 Published by Elsevier Ltd on behalf of IBRO.
doi:10.1016/j.neuroscience.2007.10.070

et al., 1997b, 2002) and (iii) synaptic blockade or reversible inactivation of the vlPAG significantly delays and/or attenuates the sympathoinhibition, hypotension and bradycardia evoked by severe hemorrhage (Cavun and Millington, 2001; Cavun et al., 2001; Dean, 2004).

The specific aim of this study was to identify the main descending pathway(s) via which vlPAG neurons trigger decompensation in response to severe blood loss. A first set of experiments confirmed that the vlPAG contains a population of vlPAG neurons selectively activated by severe blood loss. Subsequent experiments used a combination of retrograde tracing and immediate early gene expression (i.e. double labeling) to identify the medullary projections of the population of vlPAG neurons whose selective activation triggers decompensation.

EXPERIMENTAL PROCEDURES

All experiments were carried out following the guidelines of the NHMRC "*Code of Practice for the Care and Use of Animals in Research in Australia*" as well as the approval of the Animal Care and Ethics Committee of the University of Sydney. These experiments were conducted with the minimum number of animals and every effort was made to reduce suffering.

Data were obtained from 88 male Sprague–Dawley rats (240–400 g). Prior to surgery all animals were housed in groups of six, kept on a 12-h light/dark cycle, and had access to food and water *ad libitum*. Initially, 47 rats were anesthetized with an i.m. injection of ketamine (Parnell Labs, Sydney, NSW Australia) and xylazine (Troy Labs, Sydney, NSW, Australia) (Ketalar 75 mg/kg; Rompun 4 ml/kg) before being placed in a stereotaxic frame in the "flat-skull" position.

Selection of medullary sites for retrograde tracer injection

Previous anatomical studies indicate that the vlPAG projects to three major medullary cardiovascular region:

(i) *the caudal midline medulla (CMM)* a "vasodepressor" region, which in the rat has a restricted rostro-caudal extent (obex to approximately +1.5 mm) (Cameron et al., 1995; Henderson et al., 1998b);
(ii) *the caudal ventrolateral medulla (CVLM)* a "vasodepressor" region, located at the level of the obex, containing rostral ventrolateral medulla (RVLM) –projecting gamma-aminobutyric acid containing (GABAergic) neurons (Cameron et al., 1995)
(iii) *the RVLM* a "vasopressor" region, which in the rat is coextensive with the C1 (adrenergic) cell group (Lovick, 1992a,b).

Retrograde tracer injections were aimed at each of these vlPAG-recipient, medullary cardiovascular regions. Only those rats in which injections encompassed a single region, with no detectable spread into adjacent regions, were used.

CMM injections

In 29 rats the posterior calvarium and dorsal neck muscles were exposed and reflected, and a small part of the occipital plate was removed exposing the cerebellum and dorsal surface of the medulla. A single barrel glass micropipette (tip diameter 10–20 μm) was lowered 2.25 mm from the midline on the dorsal surface of the medulla (0.5–1.0 mm rostral to the obex) at a 23° caudo-rostral angle. Microinjections (50 nl) of retrograde tracer (Fast Blue: N=7; Fluorogold: N=22) were made via an automated air-pressure system that applied brief air pulses (10 ms.) to the pipette barrel. The tracers FB and FG share similar uptake, spread and labeling efficiencies (Richmond et al., 1994; Novikova et al., 1997; Choi et al., 2002). To determine the volume of injectate, the level of the meniscus in the micropipette was monitored via a calibrated graticule in a dissecting microscope. Each injection was made over a period of 10 min after which time the pipette remained *in situ* for a further 10 min. Following removal of the pipette, the rat was removed from the stereotaxic frame, the neck muscles sutured and the scalp incision closed. Subsequently, each animal was given fluids (2.0 ml, 0.9% saline i.p.) before being returned to its home cage. The mobility, activity level, eating, drinking and grooming of each rat were closely observed each post-operative day. A period of 7 days was allowed for transport of the tracer before further experimental procedures were undertaken.

RVLM and CVLM injections

In 18 rats, the dorsal surface of the cerebellum was exposed by a small craniotomy to allow injection of retrograde tracer to be made into either the RVLM (FB; N=5) or the CVLM (FG; N=13) using stereotaxic coordinates relative to anatomical landmarks (RVLM: 12.5 mm caudal to bregma; 2.0 mm lateral; 10.5 mm below cerebellar surface; and CVLM: obex; 1.8 mm lateral; 2.25 mm below medullary surface). Injection of retrograde tracer and the post-injection recovery period was as described above. A period of 7 days was allowed for transport of the tracer before further experimental procedures were undertaken.

Cannulation procedures

Each of the 47 rats injected with retrograde tracer, plus an additional 18 rats (no tracer injection) were cannulated for subsequent removal of blood. Each rat was anesthetized with halothane (2%) and a cannula was placed into the right external jugular vein. The cannula (PE tubing, OD=0.96 mm, with a 32 mm Silastic tip OD=1.19 mm) was passed s.c. and exteriorized in the interscapular region. Following cannulation, anesthesia was discontinued and each animal was given an injection of antibiotic (Norocillin, 150 mg/kg, i.m.) and fluids (2 ml, 0.9% saline i.p.) and returned to its home cage.

In another 17 rats, in addition to cannulation of the R external jugular vein, an additional cannula was placed in the L carotid artery to record pulsatile AP. These 17 animals were used to validate the cardiovascular responses to: (i) 10% hemorrhage; (ii) 30% hemorrhage; and iii) sodium nitroprusside (SNP) infusion (see Fig. 1).

Experimental protocols

Twenty-four hours following cannulation surgery rats were placed on their own bedding in an opaque plastic cage (30 cm dia.) in a dimly lit experimental room and the venous cannula was connected via heparinized, PE 50 tubing to a 1 ml plastic syringe. Each rat was then left undisturbed for 2 h to habituate to the surroundings. Subsequently, each rat was subjected to one of four procedures:

(i) *Venous cannulation alone (no hemorrhage)*: following the habituation period rats were left for an additional 2 h and then perfused.
(ii) *Ten percent (normotensive) hemorrhage*: following habituation, 10% tbv was withdrawn over a 10 min period after which the rat was left undisturbed for an additional 110 min, followed by perfusion. Ten percent (10%) tbv is equivalent to withdrawal of 8 ml/kg, the range of volumes removed was 1.84 ml to 3.0 ml. A 10% hemorrhage does not alter significantly resting AP (Fig. 1A).
(iii) *Thirty percent (hypotensive) hemorrhage*: following habituation, 30% tbv was withdrawn over 20 min (10% over 10 min, followed

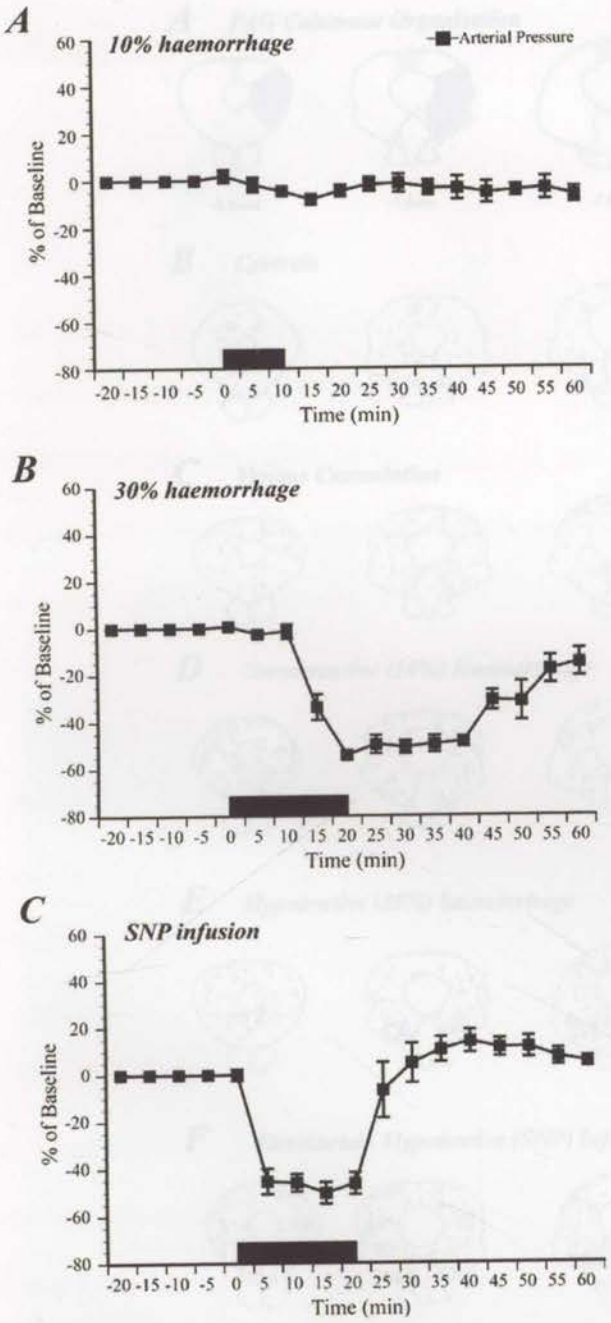

Fig. 1. Graphs illustrating the mean (±S.E.M.) changes in AP (% of baseline) following either: (A) 10% (normotensive) hemorrhage (N=6); (B) 30% (hypotensive) hemorrhage (N=5) or; (C) infusion of SNP (N=6). The bar along the abscissa defines the period of blood withdrawal (A, B) or infusion (C).

by the removal of an additional 20% over the subsequent 10 min). Rats were then left undisturbed for an additional 100 min, followed by perfusion. Thirty percent (30%) tbv is equivalent to 24 ml/kg, the range of blood volumes removed during a 30% hemorrhage was 6.72 ml to 9.6 ml. A 30% hemorrhage evokes a sustained hypotensive response (Fig. 1B).

(iv) *Euvolemic hypotension*: following habituation, SNP, a peripheral vasodilator (1 mg/ml solution) was infused at a rate of 30 μl/min over 20 min. Rats were then left undisturbed for an additional 100 min, followed by perfusion. Infusion of SNP evokes a hypotensive response similar that evoked by 30% hemorrhage (c.f. Fig. 1B and 1C).

(v) *Non-cannulated control*: six additional rats were taken from their home cage, placed in the opaque plastic cage in the experimental room and left undisturbed for the same duration as procedures (i) to (iv) above and then perfused.

Perfusion

Each animal was deeply anesthetized (sodium pentobarbital, 90 mg/kg i.v.) and rapidly perfused transcardially with 500 ml of 0.9% saline followed by 500 ml of ice cold fixative (4% paraformaldehyde in borate-acetate buffer, pH 9.6). The brains were removed, post-fixed for 4 h in the same fixative, then cryoprotected for at least 3 days in 10% sucrose in 0.1 M phosphate buffer. Fifty micron frozen, serial coronal sections of the medulla were cut immediately in order to identify the location and extent of each retrograde tracer injection. Subsequently, frozen, 50 μm serial, coronal sections of the midbrain were cut. Every second section was collected in 0.1 M phosphate-buffered 0.9% saline (PBS, pH 7.4) for immunohistochemical processing.

Immunohistochemistry

Free-floating midbrain sections were washed in PBS, and incubated in polyclonal rabbit anti-c-Fos (Santa Cruz, sc-50:1:2000 for 24 h at 4 °C). Sections were then washed (PBS) and incubated in biotinylated goat anti-rabbit IgG (Vector Laboratories, 1:500, 2 h at room temperature). The sections were washed again and incubated in Extr-Avidin peroxidase (Sigma: 1:1000, 2 h at room temperature). Following a final wash in PBS, chromogenic detection of Fos protein with 3,3-diaminobenzidine tetrahydrochloride (DAB) was performed. The sections were incubated for 20 min in "DAB mix" containing 10 mg DAB, 0.2 ml of 4% ammonium chloride in 0.1 M PBS (pH 7.4), 0.2 ml of 20% D-glucose in 0.1 M PBS (pH 7.4), made up to 20 ml with 0.1 M PBS (pH 7.4). The sections were then placed in a fresh 20 ml of "DAB mix" and 20 μl of glucose oxidase (Sigma: 1000 U/ml) was added to the solution to initiate the chromogenic reaction. The reaction was carried out over ice to control chromogenesis and the reaction stopped when the background staining became visible by rinsing the sections in several changes of 0.1 M

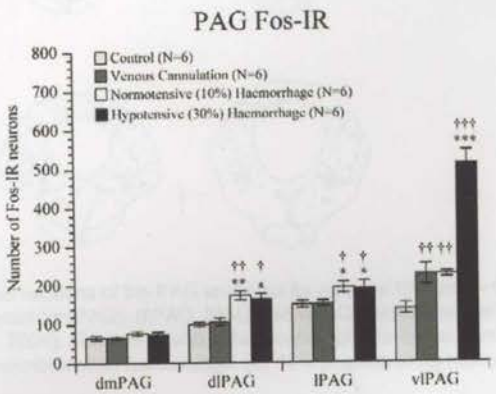

Fig. 2. Bar graphs summarizing the PAG columnar distribution of Fos-IR neurons Each bar represents the mean number (±S.E.M.) of Fos-IR cells in five equi-distant midbrain sections (−6.8, −7.3, −7.8, −8.3 and −8.8 mm caudal to bregma; Paxinos and Watson, 1986) per animal in: (i) control rats (N=6), and following (ii) venous cannulation alone (N=6); (ii) 10% (normotensive) hemorrhage (N=6); and (iii) 30% (hypotensive) hemorrhage (N=6). Significance relative to control (Mann-Whitney U test), † P<0.05, †† P<0.01, ††† P<0.005. Significance relative to venous cannulation alone (Mann-Whitney U test), * P<0.05, ** P<0.01, *** P<0.005.

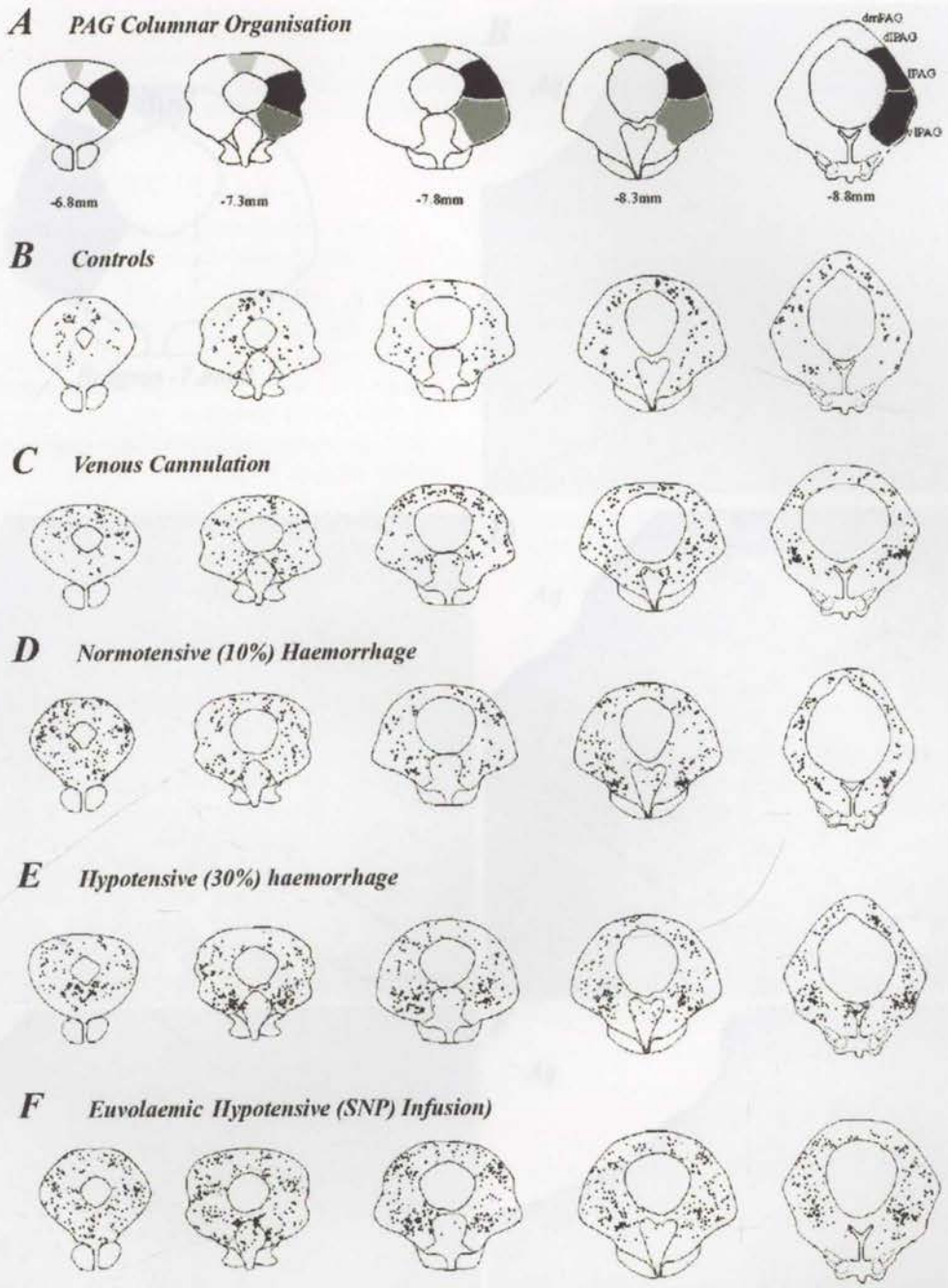

Fig. 3. Rows A to F show camera-lucida reconstructions of the five equi-distant coronal sections of the PAG analyzed for each rat (bregma −6.8 mm to −8.8 mm, rostral to left). The sections in row A indicate the regions of the dorsomedial (dmPAG), dlPAG, lPAG and vlPAG columns as defined by earlier functional-anatomical studies (Bandler and Shipley, 1994; Keay and Bandler, 2004). Rows B–F show the location of Fos-IR neurons (black dots) evoked in: (B) controls (basal Fos-IR); (C) venous cannulation alone; (D) 10% (normotensive) hemorrhage; (E) 30% (hypotensive) hemorrhage; and (F) euvolemic hypotension (i.v. infusion of SNP).

PBS (pH 7.4) (Clement et al., 1996). Sections were mounted onto gelatinized slides, air dried, rapidly dehydrated, cleared and coverslipped with Fluoromount (Gurr).

Analysis

The numbers of single-labeled (Fos-immunoreactive (IR) or retrogradely-labeled) and double-labeled (Fos-IR and retrogradely labeled) periaqueductal gray (PAG) neurons were counted in five equi-distant midbrain sections (−6.8, −7.3, −7.8, −8.3 and −8.8 mm caudal to bregma) (Paxinos and Watson, 1986). Fos-IR neurons were defined under light microscopic conditions by the presence of DAB reaction product clearly visible in the nucleus at 40× magnification (for details see Clement et al., 1996). The presence of retrograde label (FB, FG) in neurons was determined under fluorescence illumination at 100× magnification. Double-labeled neurons were identified by switching between illumination conditions.

The boundaries of each PAG column were defined using anatomical and functional criteria as described previously (Keay

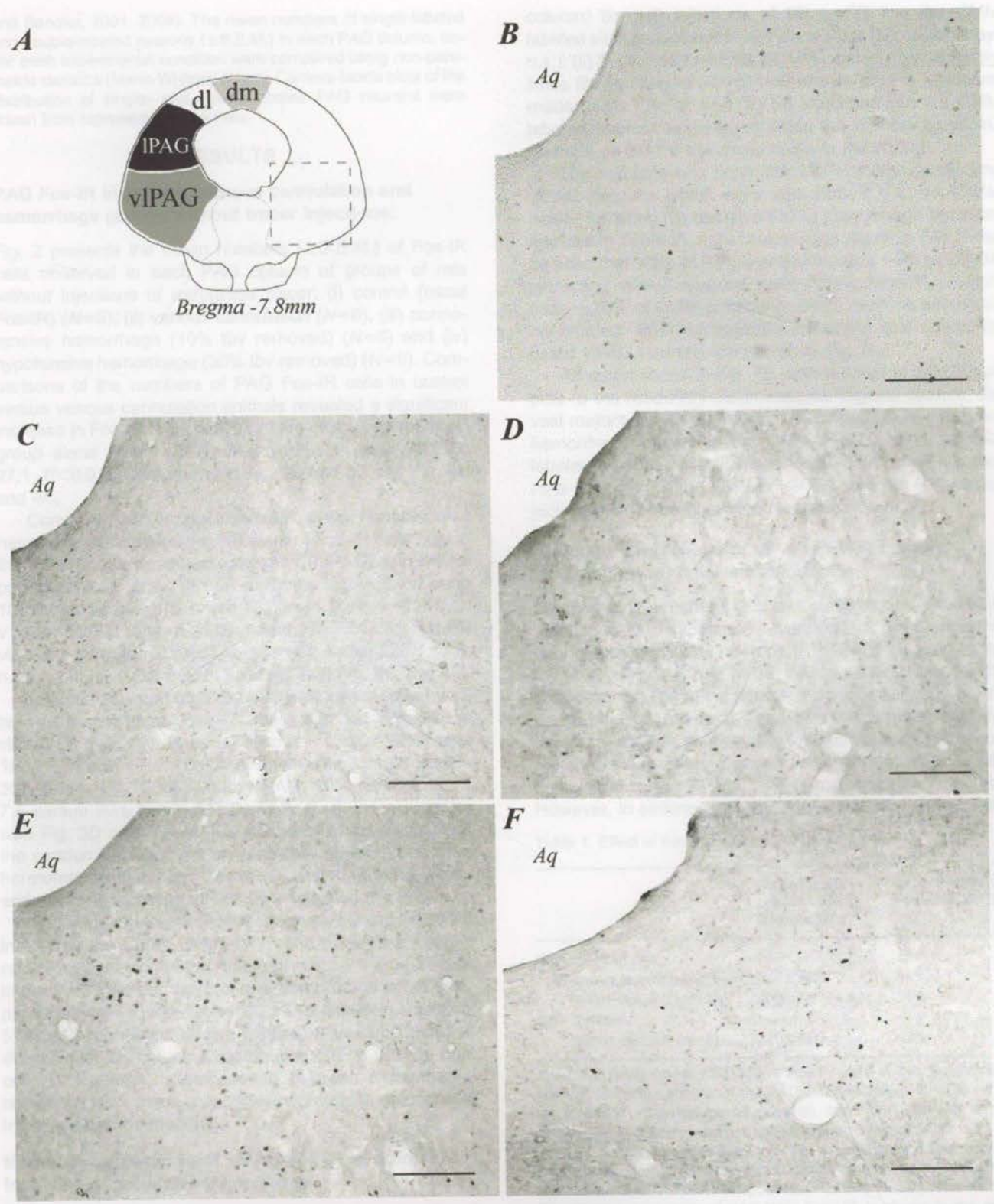

Fig. 4. (A) Coronal section of the PAG (bregma −7.8 mm) illustrating the location of the dmPAG, dlPAG, lPAG and vlPAG columns (Bandler and Shipley, 1994; Keay and Bandler, 2004). (B–F) Low power photomicrographs illustrating Fos-IR in the vlPAG region indicated by the rectangle in (B) control rats; and rats subjected to (C) venous cannulation alone; (D) 10% (normotensive) hemorrhage; (E) 30% (hypotensive) hemorrhage; or (F) euvolemic hypotension (infusion of SNP). Scale bar=200 μm. Aq, cerebral aqueduct.

and Bandler, 2001, 2004). The mean numbers of single-labeled and double-labeled neurons (±S.E.M.) in each PAG column, under each experimental condition were compared using non-parametric statistics (Mann-Whitney *U* test). Camera-lucida plots of the distribution of single- and double-labeled PAG neurons were drawn from representative animals.

RESULTS

PAG Fos-IR in control, venous cannulation and hemorrhage groups without tracer injections:

Fig. 2 presents the mean numbers (±S.E.M.) of Fos-IR cells observed in each PAG column of groups of rats *without* injections of retrograde tracer: (i) control (basal Fos-IR) (N=6); (ii) venous cannulation (N=6), (iii) normotensive hemorrhage (10% tbv removed) (N=6) and (iv) hypotensive hemorrhage (30% tbv removed) (N=6). Comparisons of the numbers of PAG Fos-IR cells in control versus venous cannulation animals revealed a significant increase in Fos-IR in the vlPAG of the venous cannulation group alone (cont, 137.5±14.8 versus v cann, 227.3±27.1, P<0.01). Compare also Fig. 3B and 3C and Fig. 4B and 4C.

Compared with venous cannulation rats, normotensive hemorrhage increased the numbers of Fos-IR cells only in the dorsolateral periaqueductal gray (dlPAG) and lateral periaqueductal gray (lPAG) columns (dlPAG: v cann 105.8±9.9 versus 10% haem 173.3±11.9, P<0.01; lPAG: v cann 151.7±7.3 versus 10% haem 193.3±13.6, P<0.05; vlPAG: v cann 227.3±27.1 versus 10% haem 226.7±7.6, n.s.). Compare also Fig. 3C and 3D and Fig. 4C and 4D.

In contrast, when 30% tbv was withdrawn, i.e. a hypotensive hemorrhage, Fos-IR was increased only in the vlPAG (dlPAG: 10% haem 173.3±11.9 versus 30% haem 163.7±14.2, n.s.; lPAG: 10% haem 193.3±13.6 versus 30% haem 191.0±19.7, n.s.; vlPAG: 10% haem 226.7±7.6 versus 30% haem 512.0±32.9, P<0.001). Compare also Fig. 3D and 3E and Fig. 4D and 4E. To summarize, the sudden transition during progressive blood loss, from normotension to hypotension is associated with a selective and dramatic increase in Fos-IR only within the vlPAG.

Following injections of the retrograde tracers FG or FB into either the CMM, CVLM or RVLM, there was a slight, non-significant increase, in the total number of Fos-IR cells in the PAG following hypotensive hemorrhage when compared with non-injected rats (592±34.7 [tracer injected] vs, 512±32.9 [non-injected] see Table 1). This slight increase did not alter the columnar distribution of Fos-IR (see right column, Table 1). Comparisons between experimental conditions were made only between groups in which tracer injections had been made.

Medullary projections of vlPAG Fos-IR neurons following hypotensive hemorrhage

Camera-lucida reconstructions and photomicrographs of representative sites of retrograde tracer injections made in the CMM (FG N=8, FB N=7), CVLM (N=8) and RVLM (N=5) are shown in Fig. 5. The mean (±S.E.M.) numbers of vlPAG neurons labeled following these tracer injections are summarized in Table 2A. It can be seen (Table 2A, left column) that: (i) injections of FB or FG into the CMM labeled similar numbers of vlPAG neurons (Mann-Whitney, n.s.); (ii) FG injections into the CMM labeled approximately twice the number of vlPAG neurons as did FG injections made in the CVLM; and (iii) FB injections into the CMM labeled approximately three times the number of vlPAG neurons as did FB injections made in the RVLM.

The numbers and proportions of medullary-projecting vlPAG neurons which were also Fos-IR (i.e. double-labeled) following hypotensive (30%) hemorrhage are summarized in Table IA, right column (see also Fig. 7A). It can be seen that ~1% of RVLM-projecting and ~5% of CVLM-projecting vlPAG neurons were double-labeled. In contrast, ~20% of CMM-projecting vlPAG neurons were double-labeled. Photomicrographs of single and double-labeled vlPAG neurons are shown in Fig. 6.

As summarized in Fig. 7B, with respect to vlPAG outputs to the medullary cardiovascular regions studied, the vast majority of vlPAG neurons "activated" by hypotensive hemorrhage project to the CMM (~90% of all double-labeled neurons). Many fewer double-labeled vlPAG neurons projected to the CVLM (~10%), and the RVLM-projecting vlPAG neurons were rarely activated.

Medullary projections of vlPAG Fos-IR neurons following normotensive hemorrhage

To determine whether the above patterns of double-label were specific to hypotensive hemorrhage, the numbers of double-labeled vlPAG neurons (FG/Fos) projecting to the CMM (N=9) and CVLM (N=5) were evaluated also for the normotensive (10%) hemorrhage condition. Firstly, it can be seen (c.f., Tables 2A and 2B, left column) that the numbers of single (retrograde) labeled neurons in the normotensive hemorrhage experiments did not differ significantly from those in the 30% hemorrhage experiments. However, in striking contrast to the proportions of double-

Table 1. Effect of tracer injections of Fos expression

	No of Fos-IR cells in vlPAG (five sections)	% Of total PAG Fos-IR in vlPAG
30% Hemorrhage		
No tracer injection (N=6)	512±32.9	54%
Tracer injected (N=28)	592±34.7 (n.s.)	55%
SNP infusion		
Tracer injected (N=5)	510±16.3	43%

Total number (mean±S.E.M.) of Fos-IR cells in five, equi-distant coronal (50 μm) sections of the PAG (corresponding to −6.8, −7.3, −7.8, −8.3, −8.8 mm caudal bregma), from groups of rats which underwent hypotensive hemorrhage (30% blood loss) either with, or without, a prior intra-medullary injection of retrograde tracer. Significance of comparisons with un-injected animals is shown in brackets in the middle column (ANOVA, post hoc Fisher's PLSD). The vlPAG Fos-IR as a proportion of total PAG Fos- IR is shown in the right column. Total number (mean±S.E.M.) of Fos-IR cells in five, equi-distant coronal (50 μm) sections of the PAG (corresponding to −6.8, −7.3, −7.8, −8.3, −8.8 mm caudal bregma) in rats which underwent SNP infusion following CMM injection of retrograde tracer. The vlPAG Fos-IR as a proportion of total PAG Fos-IR is shown in the right column.

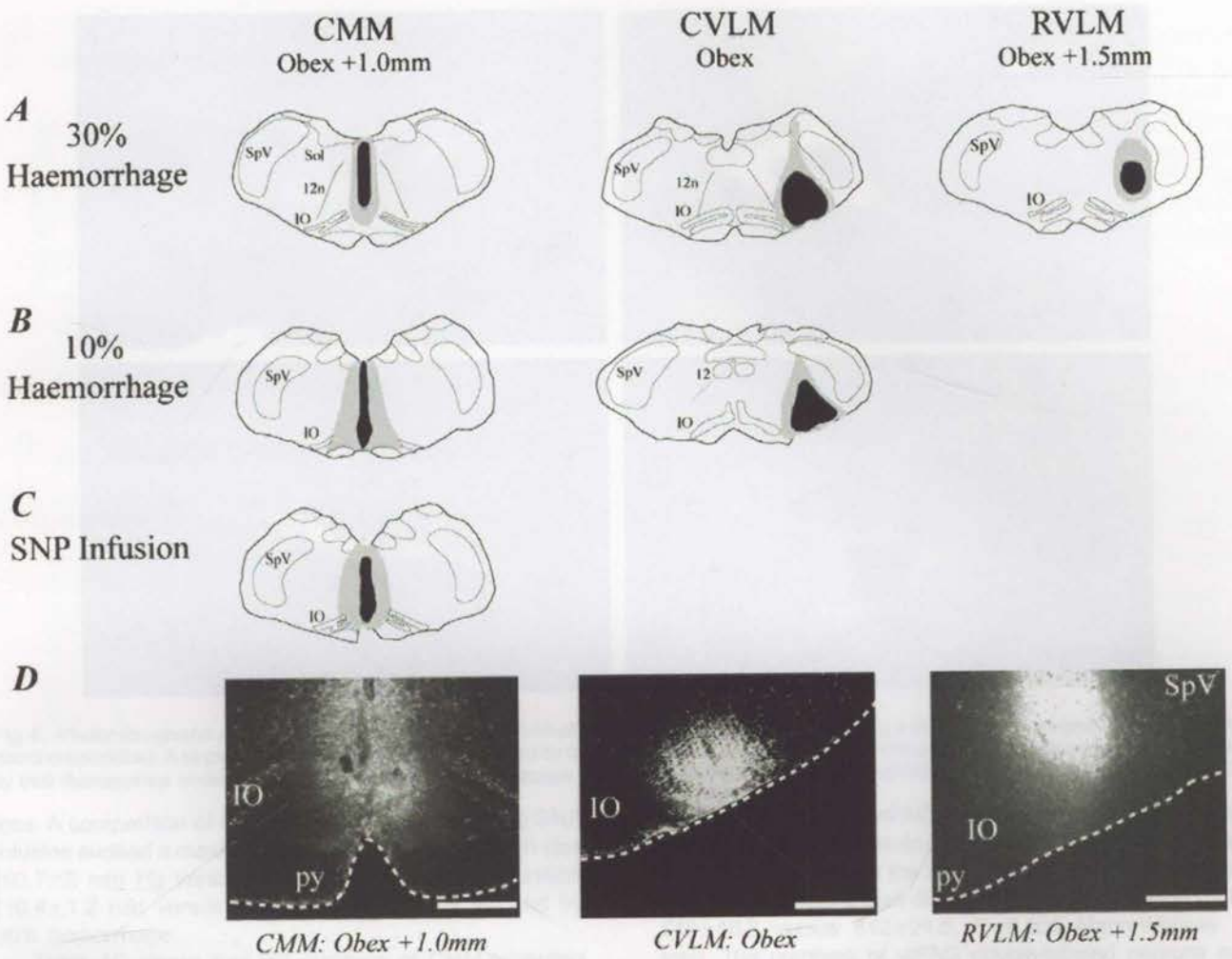

Fig. 5. Rows A–C camera-lucida reconstructions of representative coronal sections of the medulla. (A) Representative sites of retrograde tracer injections made in CMM (FG), CVLM (FG) or RVLM (FB) of rats subjected to hypotensive (30%) hemorrhage. (B) Representative injection sites in CMM (FG) and CVLM (FG) of animals subjected to normotensive (10%) hemorrhage. (C) Representative injection site in the CMM (FG) of a rat subject to euvolemic hypotension (SNP infusion). The sites of tracer injections are shown in black shading and the penumbra of spread in gray stippling. (D) Representative photomicrographs of retrograde tracer injections made in CMM (FG), CVLM (FG) or RVLM (FB). The scale bar=1 mm.

labeled neurons observed after 30% hemorrhage (c.f., Tables 2A and 2B, right column), very few medullary-projecting vlPAG neurons were double-labeled following 10% hemorrhage (CMM-projecting: hypotension, 21% versus normotension, 1%; CVLM-projecting: hypotension 5% versus normotension 2%).

Table 2. Summary of proportions of double-labelled vlPAG neurons

	Retrogradely labeled neurons (vlPAG)	Double-labeled neurons (vlPAG)
A: Hypotensive (30%) hemorrhage		
CMM (FB)	572±28.2	107±16.4 (19%)
CMM (FG)	482±36.5	103±7.8 (21%)
CVLM (FG)	255±54.1	13±2.6 (5%)
RVLM (FB)	178±23.3	2±0.8 (1%)
B: Normotensive (10%) hemorrhage		
CMM (FG)	516±18.7	5±1.5 (1%)
CVLM (FG)	237±31.9	4±1.3 (2%)
C: Euvolemic Hypotension (SNP)		
CMM (FG)	548±22.6	14±1.2 (3%)

To summarize, with respect to vlPAG (medullary-projecting) output neurons "activated" by hypotensive hemorrhage, almost 90% project to the CMM and further the "activation" of these neurons is specific to the decompensatory phase of the response. The relative contribution of CVLM-projecting vlPAG neurons is both smaller and less specific to decompensation.

Fos-IR in CMM-projecting vlPAG neurons following euvolemic versus hypovolemic hypotension

In a final set of experiments the numbers of double-labeled neurons evoked by euvolemic (SNP infusion, $N=5$) versus hypovolemic hypotension ($N=8$) were compared with determine the extent to which the "activation" of CMM-projecting vlPAG neurons was a direct consequence of blood

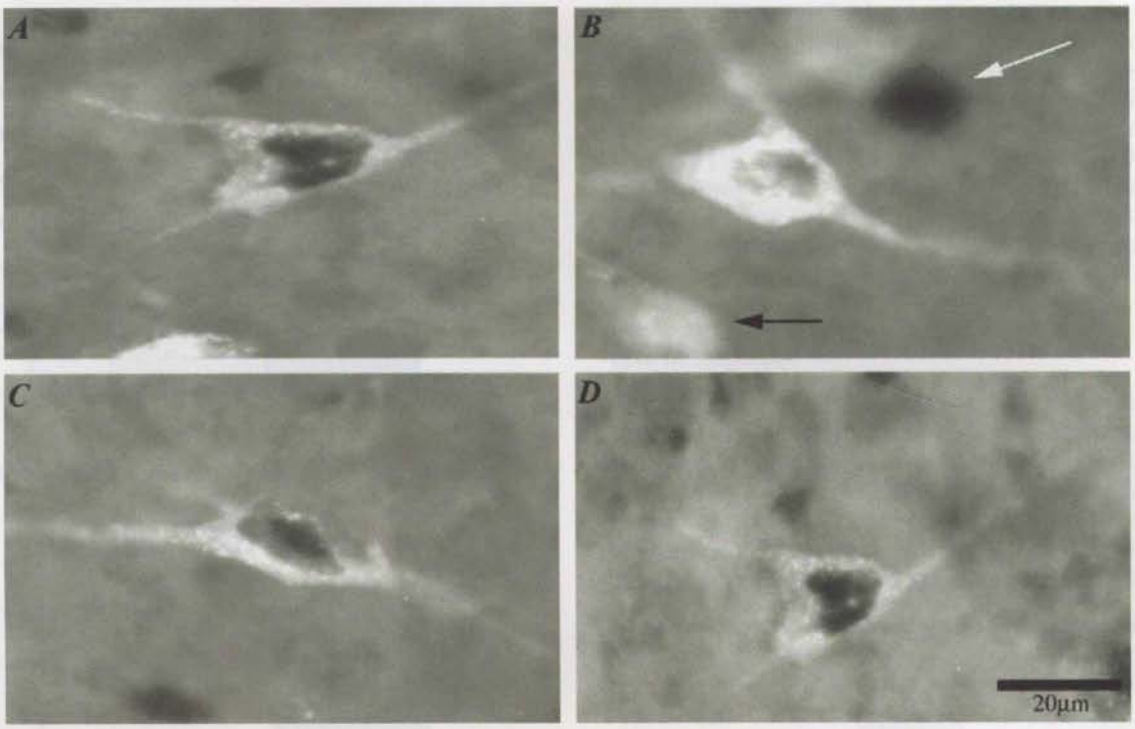

Fig. 6. Photomicrographs A–D show vlPAG neurons in four individual animals. Fos-IR cells are identified by a darkly stained nucleus (nickel-enhanced diamino-benzidine). A single-labeled, Fos-IR nucleus is indicated by the white arrow in B. CMM projecting (retrogradely labeled) neurons are identified by their fluorescence under UV-light. The black arrow in B indicates a single labeled (CMM-projecting) vlPAG neuron. The scale bar=20 μm in D.

loss. A comparison of Fig. 1B and 1C shows that the SNP infusion evoked a maximal fall in AP nearly identical in size (60.7±5 mm Hg versus 62.5±2.7 mm Hg) and duration (16.4±1.2 min versus 16.5±1.4 min) to that evoked by 30% hemorrhage.

Table 1C shows that the numbers of CMM-projecting vlPAG neurons were nearly identical to those of the previous experiments (c.f., Table 2A, 2B and 2C, left column). Figs. 3 and 4 indicate that similar to hypotensive (30%) hemorrhage, SNP infusion also dramatically increased vlPAG Fos expression over and above the levels seen in control, venous cannulation and normotensive hemorrhage animals (c.f., 3B, C, D versus 3F and 4B, C, D versus 4F).

The numbers of vlPAG Fos-IR neurons following euvolemic versus hypovolemic hypotension are compared in Fig. 8A. It can be seen that the SNP infusion evoked significantly less Fos-expression than did hypotensive hemorrhage (SNP 510±16.3 versus 612±24.5. $P<0.005$ Mann-Whitney U test). The numbers of vlPAG double-labeled neurons are compared in Fig. 8B. Note that in striking contrast to the large numbers of CMM-projecting vlPAG neurons double-labeled after a 30% hemorrhage, very few CMM-projecting vlPAG neurons were double-labeled after SNP infusion. In fact, the absolute difference in the numbers of double-labeled vlPAG neurons following 30% hemorrhage versus SNP infusion (103±7.8 versus 14±1.2; a difference of 89 neurons) (see

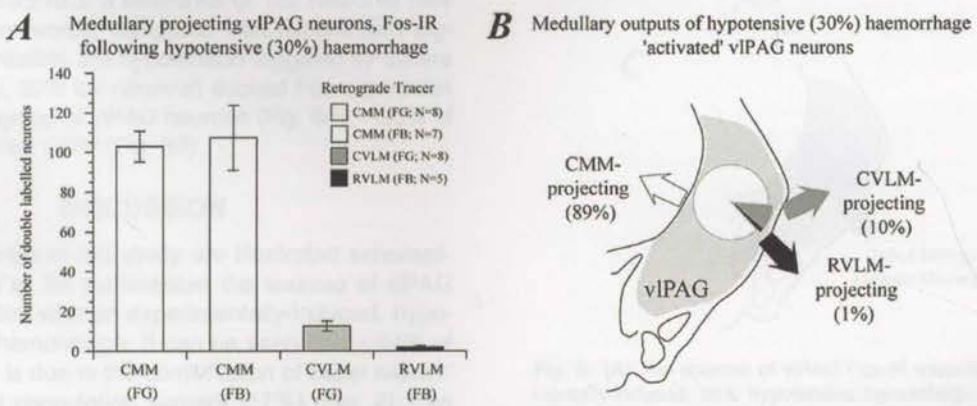

Fig. 7. (A) Bar graphs summarizing the mean number (±S.E.M.) of CMM- (FG: N=8, FB: N=7), CVLM- (FG: N=8) and RVLM- (FB: N=5) projecting vlPAG neurons in five equi-distant midbrain sections (−6.8, −7.3, −7.8, −8.3 and −8.8 mm caudal to bregma; Paxinos and Watson, 1986) which were also Fos-IR (i.e. double labeled) following 30% (hypotensive) hemorrhage. (B) The vast majority (89%) project to the CMM.

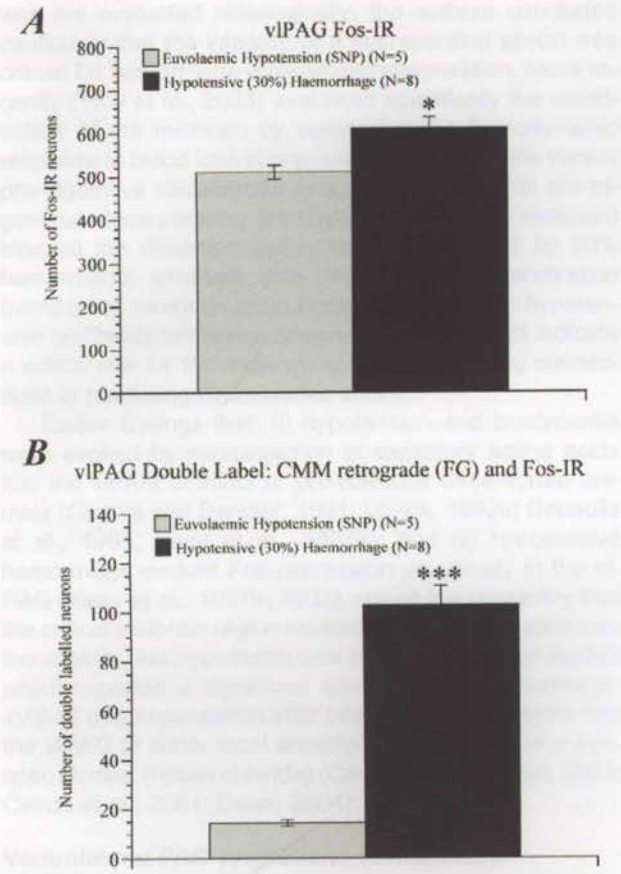

Fig. 8. Bar graphs showing: (A) mean number (±S.E.M.) of single-labeled Fos-IR vlPAG neurons in five equi-distant midbrain sections (−6.8, −7.3, −7.8, −8.3 and −8.8 mm caudal to bregma; Paxinos and Watson, 1986); and (B) the mean number (±S.E.M.) of double-labeled (i.e. CMM-projecting, Fos-IR) neurons in five equi-distant midbrain sections (−6.8, −7.3, −7.8, −8.3 and −8.8 mm caudal to bregma; Paxinos and Watson, 1986) for euvolemic hypotension (infusion of SNP) (N=5) and 30% (hypotensive) hemorrhage (N=8). * P<0.05, *** P<0.005 (Mann-Whitney U test).

Fig. 8B and c.f., Table 2A and 2C, right columns) is remarkably similar to the difference in the numbers of Fos-IR vlPAG neurons following 30% hemorrhage versus SNP infusion (612±24.5 versus 510.0±16.3; a difference of 102 neurons) (see Fig. 8A). In other words, compared with hypotension triggered by SNP infusion, the hypotension triggered by severe hypovolemia (i.e. 30% tbv removal) evoked Fos-expression in an additional group of vlPAG neurons (Fig. 8A), ~90% of which project to the CMM (Fig. 8B).

DISCUSSION

The major findings of this study are illustrated schematically in Fig. 9. Fig. 9A summarizes the sources of vlPAG Fos-IR associated with an experimentally-induced, hypovolemic (30%) hemorrhage. It can be seen that ~44% of the total Fos-IR is due to the combination of basal expression (27%) and cannulation surgery (17%) (Fig. 2). The initial withdrawal of 10% tbv (a normotensive hemorrhage) did not increase vlPAG Fos-IR (Fig. 2). However, the subsequent removal of an additional 20% tbv (sufficient to trigger decompensation) more than doubles the numbers of vlPAG Fos-IR cells (see Fig. 2 and Table 1). As illustrated in Fig. 9B our double-label data suggest that this large increase in vlPAG Fos-expression (+56%) was a consequence of: (i) the removal of additional blood (hypovolemia) (16% of the additional Fos-IR); and (ii) the resultant hypotension (40% of the additional Fos-IR) (see also Fig. 8A). Finally, Fig. 9C illustrates that the vlPAG neurons that project to the CMM are activated almost exclusively by severe hypovolemia and not by hypotension.

Hemodynamic response to hemorrhage: role of midbrain

The first study to address the possible contribution of the rostral brainstem/forebrain to the biphasic hemodynamic response to hemorrhage, reported that decompensation to a simulated hemorrhage (60% reduction in cardiac output evoked by gradual caval occlusion) in the rabbit, was blocked completely by a high mesencephalic decerebration (Evans et al., 1991). As the extent of midbrain damage

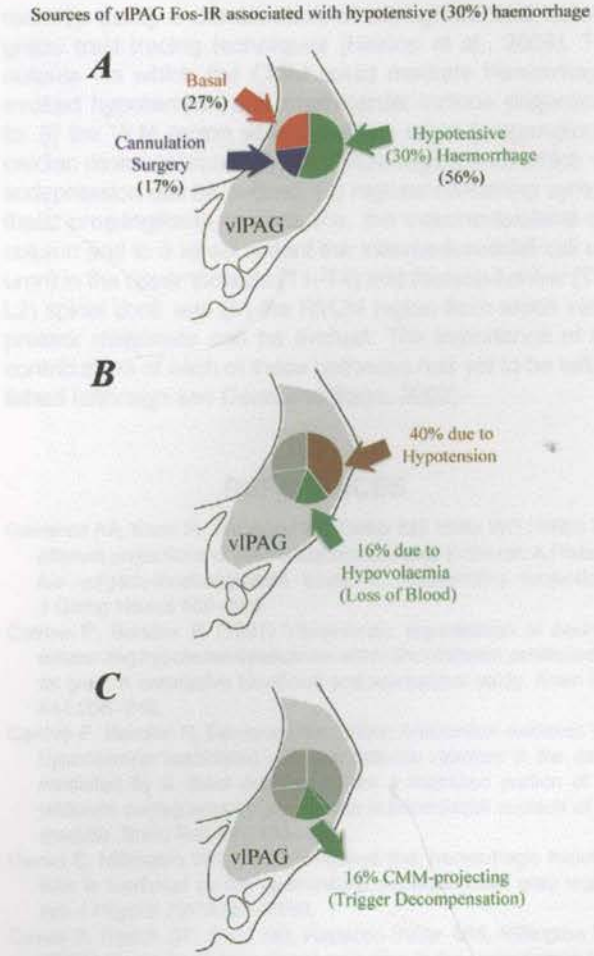

Fig. 9. (A) The sources of vlPAG Fos-IR associated with an experimentally-induced, 30% hypotensive hemorrhage. (B) The increased vlPAG Fos-IR specific to hypotensive hemorrhage (30% tbv removal) is a consequence of both *hypovolemia* and *hypotension*. (C) The vast majority of vlPAG neurons activated by severe *hypovolemia*, but not by *hypotension*, project to the CMM.

was not evaluated histologically, the authors concluded cautiously that the integrity of a suprapontine site(s) was critical for hemorrhage-evoked decompensation. More recently (Troy et al., 2003) evaluated specifically the contribution of the midbrain by comparing the hemodynamic response to blood loss in pre-collicular decerebrate versus pre-trigeminal decerebrate rats. It was found that pre-trigeminal decerebration (removal of forebrain+midbrain) blocked the decompensatory response evoked by 30% hemorrhage; whereas after pre-collicular decerebration (removal of forebrain only) normal hypovolemic hypotension and bradycardia was observed. These results indicate a *critical role for the midbrain and its descending connections* in mediating hypovolemic shock.

Earlier findings that: (i) hypotension and bradycardia were evoked by microinjection of excitatory amino acids into the vlPAG of intact or pre-collicular decerebrate animals (Carrive and Bandler, 1991; Lovick, 1992a; Depaulis et al., 1994; Keay et al., 1997a); and (ii) hypotensive hemorrhage evoked Fos-expression selectively in the vlPAG (Keay et al., 1997b, 2002), raised the possibility that the critical midbrain region mediating decompensation was the vlPAG. This hypothesis was confirmed by later studies which reported a significant attenuation of hemorrhage-evoked decompensation after bilateral microinjections into the vlPAG of either local anesthetic (lignocaine) or a synaptic blocker (cobalt chloride) (Cavun and Millington, 2001; Cavun et al., 2001; Dean, 2004).

Ventrolateral PAG projections to medullary cardiovascular regions

Previous anatomical tract-tracing studies revealed substantial projections from the vlPAG to multiple medullary cardiovascular regions including: rostral ("vasopressor") (Lovick, 1985, 1992b; Carrive et al., 1988; Van Bockstaele et al., 1991; Verberne and Boudier, 1991; Cameron et al., 1995; Henderson et al., 1998b) and caudal ("vasodepressor") parts of the VLM (Van Bockstaele et al., 1991; Cameron et al., 1995; Henderson et al., 1998b), and the vasodepressor part of the CMM (Henderson et al., 1998b). Somewhat surprisingly, given the extensive medullary outputs of the vlPAG, the results reported here indicate that hemorrhage-evoked hemodynamic changes are mediated by only a small subset of these projections. Specifically: (i) almost no vlPAG neurons selectively activated by severe hypovolemia projected to the RVLM; and (ii) only a small number of vlPAG neurons selectively activated by severe hypovolemia projected to the CVLM; whereas (iii) nearly all vlPAG neurons selectively activated by severe hypovolemia (loss of 30% tbv) project to the CMM. In other words, the sympathoinhibition and bradycardia triggered by severe blood loss depend critically on activation of CMM-projecting vlPAG neurons.

Consistent with this conclusion are earlier findings that microinjection into the CMM of either local anesthetic (lignocaine) or a synaptic blocker (cobalt chloride) respectively either blocked, or delayed and attenuated, hemorrhage-evoked decompensation (Henderson et al., 1998a, 2000, 2002; Heslop et al., 2002). Strikingly, such blockade of the CMM altered neither resting AP nor heart rate, nor did it affect cardiovascular reflexes triggered by either baroreceptor-loading (i.v. phenylephrine) or activation of 5-HT_3-sensitive cardiopulmonary afferents (i.v. phenylbiguanide or 5-HT) (Henderson et al., 2000). In this context the dramatic effects on hemorrhage-evoked decompensation suggest that CMM neurons are recruited only under special circumstances (i.e. injury-related/life-threatening challenges), the adaptive responses to which require more than basic homeostatic cardiovascular adjustments (see also Johansson, 1962). Injury-related signals from nociceptors in deep somatic and visceral structures are known to trigger sudden falls in both AP and heart rate (i.e. the so-called *vaso-vagal* reactions). Such signals are likely to be relayed to the CMM, as its major afferents include inputs from: (i) spinal cord (laminae IV, V and X); (ii) spinal trigeminal nucleus, specifically the transition area between n. interpolaris and n. caudalis; and (iii) solitary tract nucleus, particularly ventrolateral and parasolitary subnuclei (Potas et al., 2003).

The efferent projections of the CMM have been studied recently using a combination of retrograde and anterograde tract tracing techniques (Heslop et al., 2004). The outputs via which the CMM could mediate hemorrhage-evoked hypotension and bradycardia include projections to: (i) the VLM region which contains vagal (preganglionic) cardiac motor neurons; (ii) the CVLM region from which vasodepression can be evoked; (iii) regions containing sympathetic preganglionic neurons (i.e. the intermediolateral cell column and to a lesser extent the intermediomedial cell column) in the upper thoracic (T1–T4) and thoraco-lumbar (T9–L2) spinal cord; and (iv) the RVLM region from which vasopressor responses can be evoked. The importance of the contributions of each of these pathways has yet to be established (although see Dean and Bago, 2002).

REFERENCES

Cameron AA, Khan IA, Westlund KN, Cliffer KD, Willis WD (1995) The efferent projections of the periaqueductal gray in the rat: A *Phaseolus vulgaris*-leucoagglutinin study. II. Descending projections. J Comp Neurol 568–584.

Carrive P, Bandler R (1991) Viscerotopic organisation of neurons subserving hypotensive reactions within the midbrain periaqueductal grey: A correlative functional and anatomical study. Brain Res 541:206–215.

Carrive P, Bandler R, Dampney RA (1988) Anatomical evidence that hypertension associated with the defence reaction in the cat is mediated by a direct projection from a restricted portion of the midbrain periaqueductal grey to the subretrofacial nucleus of the medulla. Brain Res 460:339–345.

Cavun S, Millington WR (2001) Evidence that hemorrhagic hypotension is mediated by the ventrolateral periaqueductal gray region. Am J Physiol 281:R747–R752.

Cavun S, Resch GE, Evec AD, Rapacon-Baker MM, Millington WR (2001) Blockade of delta opioid receptors in the ventrolateral periaqueductal gray region inhibits the fall in arterial pressure evoked by hemorrhage. J Pharmacol Exp Ther 297:612–619.

Choi D, Li D, Raisman G (2002) Fluorescent retrograde neuronal tracers that label the rat facial nucleus: a comparison of Fast Blue, Fluoro-Ruby, Fluoro-Emerald, FluoroGold and DiI. J Neurosci Methods 117:167–172.

Clement C, Keay K, Owler B, Bandler R (1996) Common patterns of increased and decreased fos expression in midbrain and pons evoked by noxious deep somatic and noxious visceral manipulations in the rat. J Comp Neurol 366:495–515.

Dean C (2004) Hemorrhagic sympathoinhibition mediated through the periaqueductal gray in the rat. Neurosci Lett 354:79–83.

Dean C, Bago M (2002) Renal sympathoinhibition mediated by 5-HT(1A) receptors in the RVLM during severe hemorrhage in rats. Am J Physiol Regul Integr Comp Physiol 282:122–130.

Depaulis A, Keay KA, Bandler R (1994) Quiescence and hyporeactivity evoked by activation of cell bodies in the ventrolateral midbrain periaqueductal gray of the rat. Exp Brain Res 99:75–83.

Evans RG, Ludbrook J (1991) Chemosensitive cardiopulmonary afferents and the haemodynamic response to simulated haemorrhage in conscious rabbits. Br J Pharmacol 102:533–539.

Evans RG, Ludbrook J, Ventura (1994a) Role of vagal afferents in the haemodynamic response to acute central hypovolaemia in unanaesthetised rabbits. J Auton Nerv Syst 46:251–260.

Evans RG, Ludbrook J, Ventura S (1994b) Role of vagal afferents in the haemodynamic response to acute central hypovolaemia in unanaesthetised rabbits. J Auton Nerv Syst 46:251–260.

Evans RG, Ludbrook J, Woods RL, Casley D (1991) Influence of higher brain centres and vasopressin on the haemodynamic response to acute central hypovolaemic in rabbits. J Auton Nerv Syst 35:1–14.

Henderson LA, Keay KA, Bandler R (1998a) Hypotension following acute hypovolaemia depends on the caudal midline medulla. Neuroreport 9:1839–1844.

Henderson LA, Keay KA, Bandler R (1998b) The ventrolateral periaqueductal gray projects to caudal brainstem depressor regions: a functional-anatomical and physiological study. Neuroscience 82:201–221.

Henderson LA, Keay KA, Bandler R (2000) Caudal midline medulla mediates behaviourally coupled but not baroreceptor mediated vasodepression. Neuroscience 98:779–792.

Henderson LA, Keay KA, Bandler R (2002) Delta- and kappa-opioid receptors in the caudal midline medulla mediate haemorrhage-evoked hypotension. Neuroreport 13:729–733.

Heslop DJ, Bandler R, Keay KA (2004) Haemorrhage-evoked decompensation and recompensation mediated by distinct projections from rostral and caudal midline medulla in the rat. Eur J Neurosci 20:2096–2110.

Heslop DJ, Keay KA, Bandler R (2002) Haemorrhage-evoked compensation and decompensation are mediated by distinct caudal midline medullary regions in the urethane-anaesthetised rat. Neuroscience 113:555–567.

Johansson B (1962) Circulatory responses to stimulation of somatic afferents. Acta Physiol Scand 57:1–91.

Keay KA, Bandler R (2001) Parallel circuits mediating distinct emotional coping reactions to different types of stress. Neurosci Biobehav Rev 25:669–678.

Keay KA, Bandler R (2004) Periaqueductal gray. In: The rat nervous system, 3rd edition (Paxinos G, ed), pp 243–257. San Diego: Elsevier Academic Press.

Keay KA, Clement CI, Matar WM, Heslop DJ, Henderson LA, Bandler R (2002) Noxious activation of spinal or vagal afferents evokes distinct patterns of Fos-like immunoreactivity in the ventrolateral periaqueductal gray of unanaesthetised rats. Brain Res 948: 122–130.

Keay KA, Crowfoot LJ, Floyd NS, Henderson LA, Christie MJ, Bandler R (1997a) Cardiovascular effects of microinjections of opioid agonists into the "depressor region" of the ventrolateral periaqueductal gray region. Brain Res 762:61–71.

Keay KA, Henderson LA, Clement CI, Matar WM, Smith D, Day T, Bandler R (1997b) Different "vasodepressor stimuli" activate distinct regions of the ventrolateral periaqueductal gray of the rat. J Auton Nerv Syst 65:101.

Lovick TA (1985) Ventrolateral medullary lesions block the antinociceptive and cardiovascular responses elicited by stimulating the dorsal periaqueductal grey matter in rats. Pain 21:241–252.

Lovick TA (1992a) Inhibitory modulation of the cardiovascular defence response by the ventrolateral periaqueductal grey matter in rats. Exp Brain Res 89:133–139.

Lovick TA (1992b) Midbrain influences on ventrolateral medullo-spinal neurones in the rat. Exp Brain Res 90:147–152.

Ludbrook J (1993) Haemorrhage and shock. In: Cardiovascular reflex control in health and disease (Hainsworth R, Mark A, eds), pp 463–490. London: Saunders.

Novikova L, Novikov L, Kellerth JO (1997) Persistent neuronal labeling by retrograde fluorescent tracers: A comparison between Fast Blue, FluoroGold and various dextran conjugates. J Neurosci Methods 74:9–15.

Oberg B, Thoren P (1970) Increased activity in vagal cardiac afferents correlated to the appearance of reflex bradycardia during severe hemorrhage in cats. Acta Physiol Scand 80:22A–23A.

Oberg B, Thoren P (1972) Increased activity in left ventricular receptors during hemorrhage or occlusion of caval veins in the cat. A possible cause of the vaso-vagal reaction. Acta Physiol Scand 85:164–173.

Oberg B, Thoren P (1973) Circulatory responses to stimulation of left ventricular receptors in the cat. Acta Physiol Scand 88:8–22.

Paxinos G, Watson C (1986) The rat brain in stereotaxic coordinates. San Diego: Academic Press.

Persson B, Svensson TH (1981) Control of behaviour and brain noradrenaline neurons by peripheral blood volume receptors. J Neural Trans 52:73–82.

Potas JR, Keay KA, Bandler R (2003) Spinal afferents to the vasodepressor region of the caudal midline medulla in rat. Eur J Neurosci 17:1135–1149.

Richmond FJR, Gladdy R, Creasy JL, Kitamiura S, Smits E, Thomson DB (1994) Efficacy of seven retrograde tracers, compared in multiple-labelling studies of feline motneurones. J Neurosci Methods 53:35–46.

Schadt JC, Ludbrook J (1991) Hemodynamic and neurohumoral responses to acute hypovolemia in conscious mammals. Am J Physiol 260:H305–H318.

Skoog P, Mansson J, Thoren P (1985) Changes in renal sympathetic outflow during hypotensive haemorrhage in rats. Acta Physiol Scand 125:655–660.

Thoren P, Skarphedinsson JO, Carlsson S (1988) Sympathetic inhibition from vagal afferents during severe haemorrhage in rats. Acta Physiol Scand 571:97–105.

Togashi H, Yoshioka M, Tochihara M, Matsumoto M, Saito H (1990) Differential effects of hemorrhage on adrenal and renal nerve activity in anesthetized rats. Am J Physiol 259:H1134–H1141.

Troy BP, Heslop DJ, Bandler R, Keay KA (2003) Haemodynamic response to haemorrhage: distinct contributions of midbrain and forebrain structures. Auton Neurosci 108:1–11.

Van Bockstaele EJ, Aston-Jones G, Pieribone VA, Ennis M, Shipley MT (1991) Subregions of the periaqueductal gray topographically innervate the rostral ventral medulla in the rat. J Comp Neurol 309:305–327.

Verberne AJ, Boudier HRS (1991) Midbrain central grey: Regional haemodynamic control and excitatory amino acidergic mechanisms. Brain Res 550:86–94.

Victor RG, Thoren P, Morgan DA, Mark AL (1989) Differential control of adrenal and renal sympathetic nerve activity during hemorrhagic hypotension in rats. Circ Res 64:686–694.

Zhang SP, Bandler R, Carrive P (1990) Flight and immobility evoked by excitatory amino acid microinjection within distinct parts of the subtentorial midbrain periaqueductal gray of the cat. Brain Res 520:73–82.

(Available online 2 February 2008)